In The Name of God
the compassionate, the merciful

Permeability Issues in Pharmacokinetics

Kioomars Nasseri
Pharm D, Iran
M Sc, Great Britain

Department of Pharmacy
The University of Manchester

1996

A thesis submitted to the University of Manchester
for the degree of
Doctor of Philosophy
in the Faculty of Science

TABLE OF CONTENTS

CHAPTER TWO: THEORETICAL

CHAPTER THREE: MATERIALS & GENERAL METHODS

CHAPTER FOUR: STUDIES IN EXPERIMENTAL CIRRHOSIS

CHAPTER SEVEN: STUDIES WITH CREATININE
Section 2: Liver Perfusion Experiments

Abstract

Permeability of solutes through membranes, which influences many pharmacokinetic processes such as absorption, distribution, and elimination, is governed by factors relating to both membrane and solute as well as other factors, such as protein binding. The present project was aimed at characterising the influence of structural and physiological factors on tissue cell membrane permeability of selected model compounds in rat. Two approaches were adopted. In the regional permeability studies, using five established radiolabelled non-eliminated markers (erythrocytes, albumin, sucrose, urea, and water), the permeability and exchange in the isolated perfused control and cirrhotic livers were characterised. Using carbon tetrachloride and phenobarbitone, hepatic cirrhosis was induced experimentally in rats. After injecting into the portal vein of markers and model drugs with different properties (diazepam, DZ, diclofenac, DCL, and salicylic acid, SAL), using the indicator dilution method, outflow data were collected and analysed using moment analysis and the dispersion model (DM). Various parameters, including hepatic volumes of distribution (V_H), mean transit time (MTT), the relative spreading (CV^2), dispersion number (D_N), efficiency number (R_N), intrinsic clearance (CL_{int}), permeability (PS) and membrane permeability (ρ) were calculated. The maximum frequency outflow concentration, $f(t)_{max}$, and the time at which it occurred, t_{max}, were observed parameters. The output profiles of markers in cirrhotic livers, compared to control livers, displayed a sharper appearance (expressed in larger $f(t)_{max}$ and shorter t_{max}). The V_H values of markers were reduced which was reflected in reduced MTT. The reduction was variable among the markers. While the hepatic cellular volume was reduced marginally, the reduction in the sinusoidal and interstitial volumes was severe. While the significant increase in the D_N value of markers in cirrhotic livers was indicative of changes in the hepatic vascular arrangements in cirrhosis, the increase in the CV^2 value indicated that the relative spreading of markers is increased in cirrhotic livers. The described changes implied that due to parenchymal and microcirculatory alterations, the blood-liver exchange is progressively limited in cirrhosis. These findings, which were confirmed by the histological evaluations, were compatible with the literature reports. Data indicated that urea is an acceptable alternative to water as total aqueous space marker; in contrast sucrose did not appear to be a good alternative to albumin as an extracellular marker. For the lipophilic drugs, DZ and DCL, while the values of $f(t)_{max}$, D_N, and CV^2 increased significantly in the cirrhotic livers, the values of t_{max} and V_H reduced compared to those observed in the control livers. The unaltered values of R_N and CL_{int}, and the reduced values of PS and ρ for these two drugs suggest that while the hepatic metabolic activity is not changed notably in experimental cirrhosis, the permeability of hepatocyte membrane to drugs, as a consequence of reduced diffusion in the space of Disse, is reduced substantially. The unaltered CL_{int} value may be due to the initial induction effect of phenobarbitone treatment on the cirrhotic livers. For the relatively hydrophilic drug, SA, the data indicated that the permeability of a non-metabolising permeability limited drug is reduced in systems with reduced permeability (cirrhosis). In the steady-state (SS) experiments, DM provided a better description of the effect of change in protein binding on hepatic extraction of DZ than the other models of hepatic elimination, in control and cirrhotic livers, and demonstrated that larger D_N obtained in cirrhotic livers is caused by increased enzymatic heterogeneity. Studies with creatinine, another potentially permeability rate-limiting model compound, demonstrated that this compound can traverse cellular membranes and is distributed in part and not all of the intracellular space. *In vivo* experiments indicated that although creatinine can enter erythrocytes quickly, its distribution into other tissues is permeability-rate limited. Impulse-response and continuous infusion *in situ* liver perfusion studies demonstrated that creatinine is distributed in the total hepatic aqueous space in a permeability rate-limited fashion which can be described by the two-compartment dispersion model.

Declaration

No portion of the work referred to in the thesis has been submitted in support of an application for another degree or qualification of this or any other university or other institute of learning.

Copyright

Acknowledgements

I would like to acknowledge the Government of Islamic Republic of Iran for financial support and Professor Malcolm Rowland for his guidance.

List of Abbreviations

A	Effective uptake area
A_T	Amount in tissue
AUC	Area under the curve
AUC_P	Area under plasma concentration curve
AUC_T	Area under tissue concentration curve
β	Beta
C	Concentration
C_b	Blood concentration
CL	Clearance
CL_{int}	Intrinsic clearance
CLu_b	Clearance unbound in blood
CLM	Chemiluminescence
cm	Centimeter
C_{ss}	Steady state plasma concentration
C_T	Tissue concentration
C_u	Unbound concentration
CV	Coefficient of variation
CV^2	Relative dispersion
CV_b^2	CV^2 of blood volume marker
CV_P^2	CV^2 of plasma volume marker
D	Diffusion Constant
D_u	Diffusion constant for unbound ligand
D_b	Diffusion constant for bound ligand
D_N	Dispersion number
dpm	Disintegration per minute
E	Extraction ratio
EC	Extracellular
EV	Extravascular
F	Fractional recovery; availability
f_{max}	Maximum frequency
fu	Unbound fraction
fu_b	Unbound fraction in the blood/perfusate
fu_C	Unbound fraction in the cell
g	Gram
hr	Hour
HSA	Human serum albumin
IC	Intracellular
IDT	Indicator dilution technique
IPRL	Isolated perfused rat liver
IS	Interstitial
K_p	Tissue to plasma partition coefficient
k_{12}	Influx rate constant
k_{21}	Efflux rate constant
k_{23}	Elimination rate constant

K_P	Equilibrium distribution ratio
k_T	Distribution ratio constant
logP	Log n-octanol:water partition coefficient
M	Molar
μCi	Micro Curie
min	Minute
mg	Miligram
μl	Microlitre
ml	Millilitre
mm	Millimetres
mM	Millimolar
MTT	Mean transit time
MW	Molecular weight
NA	Not applicable
n	Sample number
nm	Nanometer
NR	Not relevant
°C	Degree centigrade
PBPK	Physiologically-based Pharmacokinetics
PS	Permeability-surface area product
PS_{inf}	Intrinsic influx clearance
Q	Blood/perfusate flow rate
RBC	Red blood cell
R_N	Efficiency number
SD	Standard deviation
sec	Seconds
SS	Steady state
t	Time
t_{mid}	Midpoint time
t_{ss}	Time to steady-state extraction
t_{max}	Time to peak concentration
V	Volume of distribution
V_b	Volume of vascular space
V_C	Volume of cellular space
V_d	Apparent volume of distribution
VTT	Variance of transit times
~	Approximately
λ	Exponential coefficient

CHAPTER ONE: GENERAL INTRODUCTION

1.1 Permeability

The transport of solutes through membranes is a factor that influences many pharmacokinetic processes such as absorption, distribution, and elimination. The difference in ease of penetration of solutes is quantitatively expressed in terms of the permeability. Cellular membranes appear to be composed of an inner, predominantly lipoidal, matrix covered on each surface by a layer of protein[328]. The hydrophobic portions of the lipid molecules are oriented toward the centre of the membrane and the outer hydrophilic regions face the surrounding aqueous environment. Narrow aqueous-filled channels exist between some cells, and cell membranes contain small aqueous-filled pores [16]. Each of the interposing cellular membranes and spaces impede drug transport to varying degrees, and any one of them can rate-limit the overall process. It is this complexity of structure that makes quantitative prediction of drug transport difficult [329].

1.1.1 Factors Influencing Permeability

The rate and extent of penetration of substances through tissue membranes is governed by factors relating to both the membrane (*ie* the structure, surface area and thickness of the membrane) and the substance (*ie* the size, shape and charge of the molecules, and concentration difference in either sides of the membrane)[23,192,105,289]. Other important factors are protein binding and perfusion rate. A major source of variation in permeability is the lipophilicity of the molecule, often characterised by its partition between oil and water. Lipid-soluble compounds tend to penetrate lipid membranes with ease and thus have high permeability. Polar neutral molecules and ionised compounds partition poorly into lipids, and they are either unable to pass through membranes or do so with much greater difficulty than do lipophilic molecules. Water-soluble materials, however, may move through the narrow channels between cells. Drug transport continues toward equilibrium, a condition in which the concentrations of the diffusing species are the same in the aqueous phases on both sides of the membrane. Movement of drug between regions still continues at equilibrium, but the net flux is zero.

Blood flow: With highly lipid-soluble drugs and drugs that pass freely through the aqueous-filled pores, membranes offer no barrier to drug movement and the slowest step controlling the rate of

movement through the membrane is perfusion, not permeability. As membrane resistance to drug increases, the rate limitation moves away from one of perfusion to one of permeability [289].

Ionisation: Most drugs are weak acids or weak bases and exist in solution as an equilibrium between unionised and ionised forms. Only unionised non-polar drug penetrates the membrane, and at equilibrium, the concentration of the unionised species is equal on both sides of the membrane. The unionised form should be sufficiently lipophilic to traverse membranes. The fraction unionised is controlled by both the pH and the pK_a of the drug [105,330]. In biological fluids, some molecules can exist in several chemical forms, thereby changing their charge. Therefore, if the charge is the main determinant of uptake, many organic compounds should be transported by more than one system.

Protein binding: Drug protein binding is reversible and instantaneous. Only unbound drugs are thought to be capable of passing through membranes. The rate of movement of drug through a membrane is affected by protein binding only if the limitation is in permeability. However, protein binding affects distribution of the total concentrations at equilibrium, irrespective of the rate limitation [289].

1.1.2 Mechanisms of Transport

Drug transport occurs by several mechanisms. Most lipophilic drugs pass through membranes by passive diffusion, the natural tendency for molecules to move down a concentration gradient. Movement results from the kinetic energy of the molecules and no work is expended by the system. Many polar substrates pass the membrane by association with a membrane protein which 'carries' the drug across the lipid bilayer [289]. Different carrier systems have been described for organic anions [290], organic cations and uncharged drugs [289]. Two types of specialised transport processes have been proposed; passive facilitated diffusion and active transport. Common characteristics of both systems are saturability, specificity, and competitive inhibition. Active transport is distinguished from facilitated diffusions by the net movement of substance against a concentration gradient.

Drugs that are not taken up by the cells *via* specific transport system, might be slowly internalised along with extracellular fluid as has been described for hepatic uptake of sucrose and

inulin. In addition to discrete, class-specific membrane transport processes, there are a number of systems with a broader spectrum of substrates [20]. In the case of liver, it appears that the hepatic cell plasma membrane contains either multiple distinct transport systems for charged compounds, with overlapping specifities, or multiple binding proteins which represent the acceptor components of a more complex transport machinery.

1.1.3 Transport Properties of Erythrocytes

In order to model the diffusion of organic solutes in blood, it is necessary to have an understanding of those factors which have an influence, such as plasma-erythrocyte solute distribution and diffusive transport through the erythrocyte. Blood is a suspension of formed elements in plasma. The red cells, which comprises 40-45 % by volume in blood, are biconcave disks, 8.4 μm in diameter and 1 and 2.4 μm thick at their narrowest and widest points, respectively. They have a volume of 87 μm3 and a surface area of 163 μm2 [331]. The erythrocyte membrane is arranged as a bilayer, comprising of lipid layer (80%) and integral proteins (20%). In principle, the lipid domain is pervious to all solutes. In practice, this domain does not permit a significant penetration of many hydrophilic and most charged solutes and thus converts the pathway into a barrier.

1.2 Physiological Pharmacokinetics

1.2.1 Advantages and Uses

A common aim of any pharmacokinetic model is to describe, quantitate and interpret the time course of drugs in the body [243]. Based on the objective and the degree of approximation, pharmacokinetic models range from purely mathematical description or empirical models (*eg* sum-of-exponentials function), through conceptual and predictive compartmental models, to physiological models [287]. Empirical descriptionsof data do not allow correlation between events observed *in vivo* and physiological parameters. The compartmental approach is not able to describe the disposition kinetics of drugs within a specific tissue. Physiologically based phamacokinetic (PBPK) modelling has many advantages over these more traditional approaches. It is useful in evaluating the effect of physiological (*eg* protein binding and perfusate flow) [60] and pathological (*eg* hepatic diseases) changes [19] on drug disposition, rationalising drug targeting [57], defining quantitative structure-pharmacokinetic relationships [258], and in scaling of

pharmacokinetic and/or toxicological data between different gender of the same specie or different species [18] and in risk assessment in toxicology [332].

PBPK models, which "define pharmacokinetic processes in terms of physiologically, anatomically and biochemically meaningful parameters"[240], have now become an important and well established branch of Pharmacokinetics [241]. They have been successfully used to describe the whole body disposition of a wide variety of compounds [120,121,63,64,53]. In order to obtain a realistic PBPK model, physiological factors such as tissue weights and volumes, regional blood flows, enzyme activity, membrane permeability, plasma protein and erythrocytes binding, tissue binding and partitioning and the architecture of organ microvasculature must be considered [228].

1.2.2 Whole-body PBPK Models

In whole body models, the tissues and organs are anatomically arranged, with intercompartmental transport occurring by blood flow [22]. These models are characterised by two limiting conditions which can vary between organs within the same model; drug disposition can be perfusion-rate limited or permeability-rate limited. In the first instance, one rate equation describes the distribution in the whole tissue and in the second condition , a rate equation is required for each region within the tissue incorporating membrane permeability [285]. To simplify the mathematics of the model, several assumption are generally made. The most common ones are a) only unbound drug can diffuse into the tissue b) specific organs, such as the liver and kidney, are the only sites of elimination c) all processes are linear. Elimination is generally assumed to be first order; alternatively, Michaelis-Menten kinetics may be incorporated [124].

1.2.3 Regional Pharmacokinetic Studies

Regional pharmacokinetics study the factors affecting drug disposition in specific regions of the body. A region is defined as "any anatomical area of the body between specified afferent and efferent blood vessels"[289]. The main advantage of regional studies is that the relationship between specific molecular and tissue structures in a given organ can be studied without the influence of the rest of the body [289]. One method of studying regional pharmacokinetics is by vascular isolation and artificial perfusion of the region. When the organ is left *in situ*, its integrity and normal anatomical relationships are maintained [289]. Hence, the system can be probed to

elucidate the controlling mechanisms on the exchange process. A number of studies have been performed in perfused organs including rat liver [60].

1.2.4 Lumping

The full model can often be simplified by lumping pharmacokinetically similar tissues which are of no specific interest. Tissues which are generally not lumped are those which act as substantial reservoirs for drug distribution (*eg* adipose, muscle), are involved in excretion or metabolism (*eg* kidney, liver), are sites of drug toxicity (*eg* bone marrow, brain) or are a compartment of special interest (*eg* lung) [18,19]. Tissues which are in parallel, display perfusion-limited distribution and no elimination and have similar distribution rate constants, may be lumped together [22].

1.2.5 Models of Hepatic Elimination

Many PBPK models of the liver have been developed due to its importance in the elimination of drugs. Several models presently exist which relate distribution and hepatic extraction of eliminated solutes to physiological factors [308]. The most commonly used models of hepatic elimination are the ideal-flow models (well-stirred and tube models) [193], and the stochastic models (distributed [12] and dispersion models [227]).

1.2.5.1 Well-stirred and tube models

The well-stirred model assumes that the liver is a single well-stirred homogeneous compartment, in which emergent venous unbound drug is in equilibrium with that throughout the liver [193]. The tube model describes the liver as a set of identical unconnected parallel tubes in which blood moves with constant and equal velocities [73,74]. The average unbound drug concentration in blood within the liver is assumed to be the logarithmic mean of that entering and leaving the organ.[228,229]. A major limitation of these models is their inability to describe experimental data obtained from isolated organ and microsomal systems [73,193,194].

1.2.5.2 Distributed model

The distributed model describes the liver as an array of sinusoids (parallel tubes) each with plug flow [12]. The sinusoids can differ with respect to length, blood flow and enzyme activity; it is the variance of the statistical distributions which represent these factors that defines organ

heterogeneity [14]. The limitation of distributed model lies in its inability to predict adequately drug availability for highly extracted solutes.

1.2.5.3 Axial dispersion model

The dispersion model of hepatic elimination, proposed by Roberts and Rowland [227], implies that the observed spread in solute distribution is dominated by longitudinal or axial dispersion, with only a minor contribution from diffusion [227]. This dispersion is characterised by a dimensionless parameter ., the axial dispersion number, D_N, which increases as the extent of spreading increases. In the liver, dispersion is caused by the branching of sinusoids, together with variations in the velocity and path lengths travelled by elements of blood [227,228,229].

The dispersion model explains the influence of altering blood flow and protein binding on the transient and steady-state elimination of drugs and can accommodate a cellular permeability barrier. However, for parameter estimation, bolus administration of a non-eliminated substance yields the greatest amount of information on dispersion. Two forms of the dispersion model have been used to analyse impulse-response data. The one-compartmental dispersion model assumes that as a substance travels along the liver length, radial movement (by diffusion) into its distribution space is instantaneous and that dispersion due to the heterogeneity of the organ vasculature is the main factor influencing axial spreading [223]. The two-compartmental dispersion model considers radial transport to be non-instantaneous [319]. The major limitation of the dispersion model is that the physiological interpretation of D_N is problematical [65,66].

1.2.6 Estimation of Equilibrium Distribution Ratio (Kp)

Kp is critical in the development and scaling of PBPK models and can be estimated using *in vivo* and *in vitro* methods.

In Vivo methods: There are two common methods of estimating Kp *in vivo*; from constant rate infusion to steady state and after bolus administration during the elimination phase [42,138]. After infusion to steady state, Kp for non-eliminating organs is calculated from the steady-state tissue drug concentration, $C_{t,ss}$, and the steady-state arterial concentration, C_{ss} [18,19,42,26]. In the whole body situation, elimination must occur for steady state to be achieved. However, the above relationship can only be applied to those organs where elimination is negligible. Chen&Cross [42]

also developed an expression to estimate Kp after bolus administration in non-eliminating organs which Igari [125] extended to an eliminating organ (liver), incorporating Michaelis-Menten kinetics. Gallo *et al* [333] proposed the area method for the estimation of Kp as the ratio of the total area under the tissue drug concentration time curve (AUC_t) to the total area under the plasma concentration time curve (AUC_p). A problem common to both estimation after intravenous bolus and area method is the definition of the terminal phase; the steady-state method is not subject to such difficulties [333].

In vitro methods: *In vitro* methods, involving equilibrium dialysis have evolved which consider tissue and plasma binding and the pH difference across the cell membrane in tissue homogenates [334]. These methods appear to correlate with *in vivo* estimates but present problems regarding incorporation into PBPK models [335].

Regional studies: In regional or single organ studies, the method of choice for the estimation of Kp is infusion to steady state with tissue sampling at the end of the infusion period. A single pass system allows stricter control of the inflow conditions and reaches steady state earlier than a recirculating system; in the case of an eliminating organ, it also prevents the accumulation of metabolites [336].

Methods not involving tissue sampling have also been developed. Schary and Rowland [336] determined the Kp, when uptake was perfusion rate-limited, in perfused rat liver using the expression: $Kp = \frac{Q.t_{1/2,ss}}{0.693 \,.\, V_H}$ where $t_{1/2,ss}$ is the half-life for approach to steady state, Q is the perfusate flow rate and V_H the volume of distribution of the liver. Williams and Rivier[309] estimated the volume of distribution in pig skin flaps from the ratio of total radioactivity in the tissue to mean venous concentration at the end of infusion period.

1.3 The liver

The overall pharmacokinetic behaviour of many drugs is influenced by the liver. When the drug disposition kinetics is studied in the context of hepatic insufficiency, a knowledge of the physical and functional properties of the liver is essential.

1.3.1 General Organisation

The liver is the largest internal organ of the body, weighing approximately 2% body weight (1300 g) in adult man and 4% (10 g) in a 250 g rat. The liver has a dual blood supply: a) the hepatic artery (20-25%) carrying oxygenated blood at high pressure and in a pulsatile stream to the liver, and b) the portal vein (75-80%) carrying blood which is relatively desaturated of oxygen at low pressure and in a steady stream to the liver [337]. Venous blood emerging from the liver enters the hepatic veins which join the inferior vena cava.

1.3.1.1 Hepatic acinus

Histologically, the liver is a continuous mass of parenchymal cells, tunnelled by vessels (Figure 1.1). It has a lobular structure. The microcirculatory and microfunctional unit of the liver is the acinus [211], a small parenchymal mass, irregular in size and shape, but mostly berry-like (Figure 1.2). The vascular axis (the portal triad) consists of a terminal portal venule and hepatic arteriole and a bile duct. The periphery of the acinus is formed by terminal branches of the hepatic vein, that drain acinar blood (Figure 1.3). Arterioles and portal venules join somewhere in the acinus. Between the portal triad and hepatic venule, sinusoids are radiating [99].

1.3.1.2 Hepatic sinusoids

The sinusoids are organised into a dense network with extensive anastomoses (Figures 1.1-1.3). The length of a sinusoid varies between 200-500 μm and each is lined by 10-30 hepatocytes. Portal venules end directly in the sinusoids but hepatic arterioles join sinusoids through various pathways [313]. Sinusoidal flow is regulated only by variations in arterial inflow [314]. Sinusoids are not passive channels but represent a very sophisticated network which controls hepatocellular function. Sinusoids contain several types of cells. Endothelial cells, which form the barrier of the sinusoids, are fenestrated [313]. Red blood cells are confined to the inner axial core by the

epithelium, but blood constituents are in direct contact with the plasma membrane of hepatocytes through the space of Disse (Figure 1.4) [313].

1.3.1.3 Space of Disse

This is the space between the hepatocyte cell plates and the sinusoidal wall (Figure 1.4). The dimensions and constituents of the space of Disse are essential in hepatic uptake. The thickness of space of Disse is about 1-2 μm. It is filled with microvilli of hepatocytes and contains the major components of the extracellular matrix such as collagen and glycosaminoglycans. Glycosaminoglycans form a hydrated gel with pores which filter molecules according to their size and charge. Comparison of the pore size for the hepatic interstitium (pore radii of 0.02-0.03 μm) [11], with the size of albumin (0.004-0.008 μm), water (1.2 x 10-4 μm), urea (2.3 x 10-4 μm) and sucrose (4.8 x 10-4 μm)[78] indicates that these solutes may distribute freely into the space of Disse, but the free diffusion of larger molecules may be limited.

1.3.1.4 Hepatocytes

Hepatocytes are organised into unicellular plates in contact with two sinusoids. Hepatocytes are irregular having a mean diameter of 25 μm and occupying a volume of $1x10^{5}$ μm^{3} [145]. They are covered with microvilli which increase their surface area by six-fold [313]. The hepatocyte plasma membrane is a bilayer of 7 x 10-3 μm thick.

1.3.2 Heterogeneity in Liver Structure and Function

Apart from the intracellular heterogeneity, three additional levels of hepatic compartmentalisation exist. Firstly the liver consists of several cell types including various sinusoidal cells. Secondly there are different spaces within the liver; vascular, interstitial, cellular, bile canalicular, and special arterial space. The third is the existence of three zones within each acinus. Zone 1 or the periportal cells, zone 3 or the perivenous cells and the intermediary zone 2 [313]. Many structural differences exist between the zones.

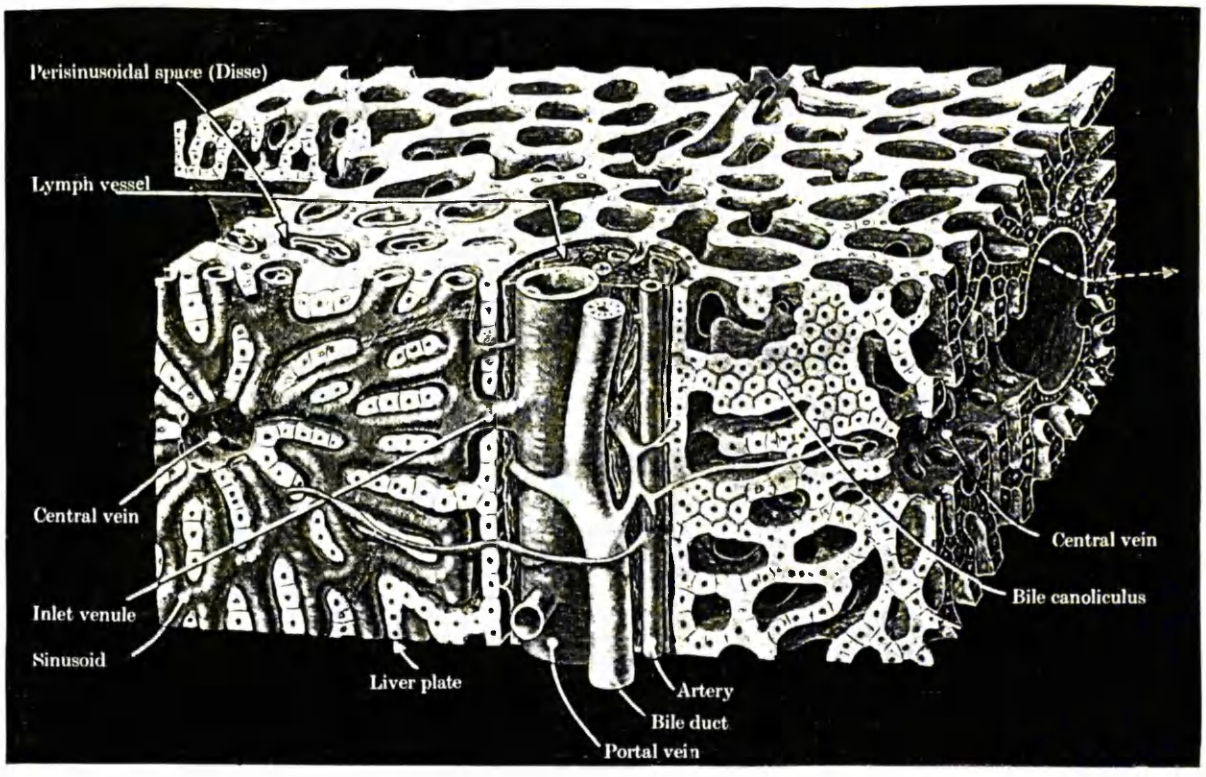

Figure 1.1 A three-dimentional view of liver structure (from reference [107]).

next page

Figure 1.2 Diagram illustrating the concept of liver substance being composed of acini. So that the relation of acini to classic lobules can be visualised. In the acini to the *upper right of centre*, the three zones are indicated in strippling. The shape of the one just *below centre* is indicated by the layout of the trabculae that have been drawn in (from reference [17])

Figure 1.3 Diagram illustrating how blood from branches of the portal vein and hepatic artery flows into the sinusoids that lie between trabeculae and empty into a central vein.

Figure 1.4 Diagram illustrating the relationship between hepatocytes and sinusoids. The numerous microvilli on the sinusoidal surface of hepatocytes extend right across the space of Disse to reach the endothelial cell.

Figure 1.2

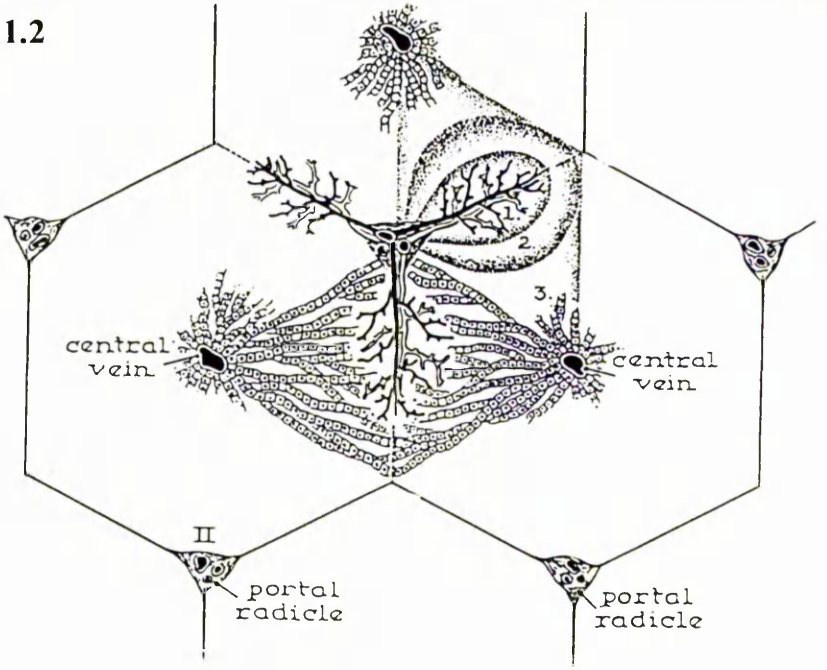

Figure 1.3

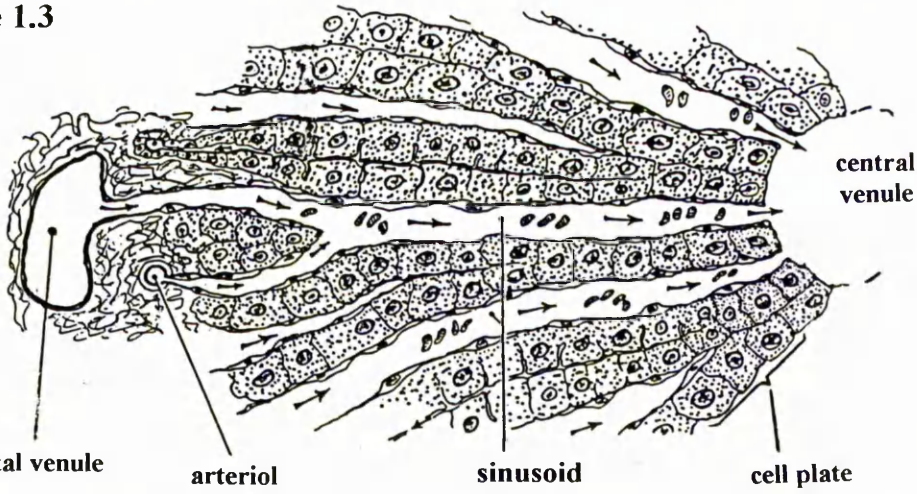

Figure 1.4

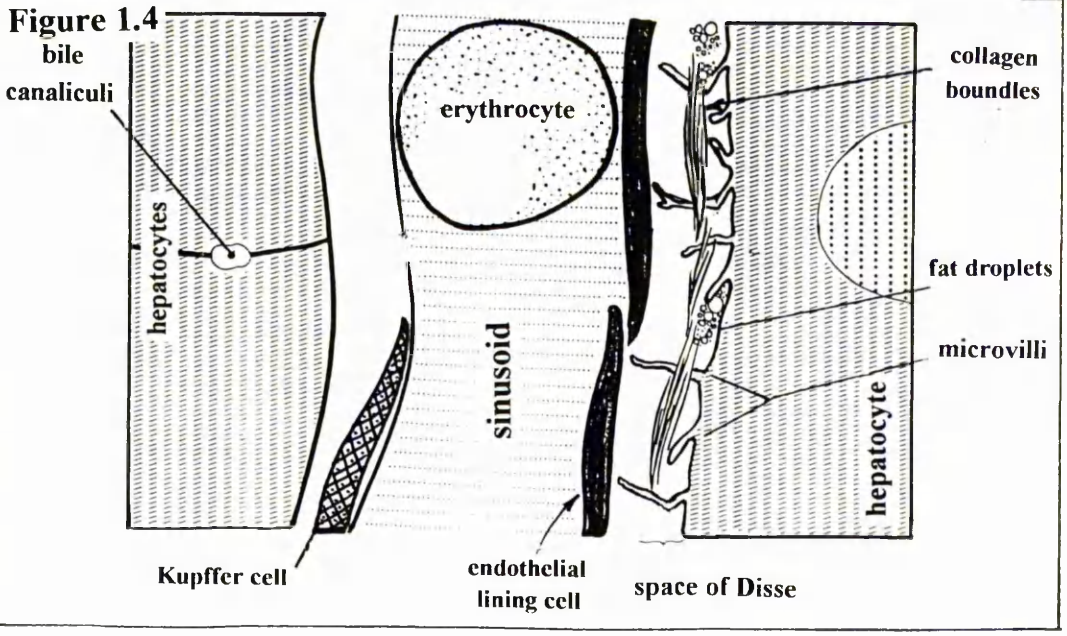

1.4 Hepatic Cirrhosis

1.4.1 Definition

The hepatic cirrhosis is the end stage of many hepatic diseases and presents a similar pathophysiological and clinical picture irrespective of aetiology. The response of the liver to persistent pathological stimulus is repeated cell damage, progressive rearrangement of tissue structure in the form of nodules, formation of fibrous tissue, and massive hemodynamic alterations [32,318,4].

1.4.2 Altered Drug Disposition in Cirrhosis

Cirrhosis influences various determinants of drug disposition simultaneously. Despite extensive clinical reports, the mechanism involved in these changes are still poorly understood [161]. There is a wide variation between the effect of cirrhosis on different drugs. There are also many reports on changes that occur in pharmacodynamic response (*ie* receptor sensitivity) [307].

1.4.2.1 Pharmacokinetic principles

Any assessment of changes in drug disposition caused by hepatic disease requires quantitation according to pharmacokinetic principles. Hepatic drug disposition depends on the relationship between several biological factors such as blood flow, metabolising activity, and binding. This relationship is best described by the concept of clearance [317,239].

1.4.2.2 Hepatic clearance

Hepatic clearance (CL_H) is a quantitative measure of the liver's ability to eliminate a drug [243]. It is the product of hepatic blood flow (Q_H) and hepatic extraction ratio (E_H):

$$CL_H = Q_H \cdot E_H \qquad (1.1)$$

The changes in clearance and extraction ratio may be mediated by the change in the following determinants:

a) Perfusion: For a drug of high extraction ratio, elimination is perfusion rate-limited, *ie* changes in blood flow produce corresponding changes in clearance. In contrast, elimination of a drug with a low extraction ratio is rate-limited by the speed of other processes influencing E_H such as

metabolism, hepatic uptake, diffusion, dissociation of drug from proteins. In this case, the hepatic extraction ratio varies inversely with blood flow when clearance is constant [241].

b) Binding within Blood: For a drug with a high E_H, the rate of elimination depends on the total blood concentration and neither the extraction ratio nor the clearance is affected materially by changes in binding [243]. For a drug with a low E_H, clearance is sensitive to change in plasma protein binding and depends on the unbound concentration, C_u, (except, if binding is dissociation rate-limited). No matter if metabolism or distribution into the hepatocyte is the rate-limiting step, the concentration that determines elimination is always C_u:

$$CL_H = CL_u \cdot f_u \qquad (1.2)$$

where CL_u, the unbound clearance, is a measure of hepatocellular activity or permeability and f_u is the unbound fraction. Protein binding can limit extraction if binding is high enough.

c) Enzyme activity: The measure of enzyme activity is intrinsic clearance (CL_{int}) which indicates the ability of the liver cells to irreversibly remove drug in the absence of other physiological constraints. According to the well-stirred model

$$CL_b = Q.E = \frac{Q.CL_{int}.fu_b}{Q + CL_{int}.fu_b} \qquad (1.3)$$

where fu_b is fraction unbound within blood.

1.4.2.3 The influence of cirrhosis on hepatic clearance

The influence of hemodynamic alterations [97,306] and parenchymal injuries [67] in cirrhosis, depending upon the severity of the injury, varies among the different drugs. Generally, the contribution of altered flow to change in CL_H will be most significant for high E_H drugs and the contribution of parenchymal damage will be most pronounced for low E_H drugs [161].

a) Flow-limited hepatic elimination: The examples of drugs in this category are propranolol and lidocaine. Of the pathological changes in cirrhosis, circulatory change (change in Q_H, relative contribution of portal and arterial flows, shunting, and capillarisation) are expected to influence their elimination to a greater extent [24].

b) Capacity-limited hepatic elimination: The hepatic clearance of low-bound drugs in cirrhosis is unaffected by changes in protein binding or Q but is affected by loss of cell mass, reduction in the level or activity of enzymes per cell, and sinusoidal capillarisation [24]. The overall hepatic clearance of extensively-bound drugs is low and depends on the extent of protein binding as well as the intrinsic clearance of the drug. Restricted access to the space of Disse and the hepatocyte surface for albumin during cirrhosis should not affect the uptake of these drugs. This is because in any case uptake is limited to the unbound fraction [161,39].

1.4.3 Experimental Cirrhosis

Medical literature abounds in reports on experimental cirrhosis [28,107,137,204,267]. Since 1896, when the first report on experimental hepatic damage was published [176,113], more than 30 agent which belong to different chemical and biological categories, have been used in the induction of cirrhosis [272,48,176]. Using different animal species, regimens, and routes of administration, only a few of these agents have met satisfactorily the rigid criteria for cirrhosis [107]. The oldest and most widely used agent is carbon tetrachloride (CCl4) [107, 160,70].

1.4.3.1 CCl4-induced cirrhosis

The original technique of using multiple doses, usually twice-weekly of CCl4, given either subcutaneously or by inhalation over a period of several months in the rat was unpredictable and resulted in low yield of severe cirrhosis and high rate of death. This technique was modified and standardised by Proctor *et al* [208] and now has become the routine method of induction of cirrhosis for biological studies [119,276,106,252,129,48,4]. All these studies are based on acceptance of CCl4-induced cirrhosis of the liver as an adequate experimental model of cirrhosis in man.

1.4.3.2 Experimental versus human cirrhosis

Several excellent reviews have been published that examine the available evidence on the similarity of the CCl4-induced model of cirrhosis with ethanol-induced human cirrhosis [276,259]. The large body of available data is often variant or discrepant. This is because, as in human cirrhosis, according to the degree of hepatic damage and stage of the illness, varying histological and functional changes are observed. It is therefore useful, albeit difficult, to correlate the degree of structural damage to the extent of functional changes. Despite the few differences in the

mechanism of induction of cirrhosis between ethanol and CCl4, the resultant histological and functional alterations in both clinical and experimental cirrhosis are the same [276, 259,208,209].

1.5 Model Substances

1.5.1 Creatinine

Creatinine is an electrically neutral water soluble compound, with an imidazole ring (Figure 1.5) [264]. It is a normal metabolite with a relatively low molecular weight (MW 113.1). It is considered to be relatively inert, although it has been shown that the microflora from the gastrointestinal tract of rats can metabolise creatinine *in vitro*. A change in the plasma level of creatinine at a stable rate of glomerular filtration is reflected in a parallel change of concentration in the filtrate [298]. Creatinine passes freely from the plasma into the glomerular filtrate [29] and although it is thought that it is neither reabsorbed nor secreted in the tubules, there is evidence for some renal tubular reabsorption and secretion, as well as non-renal routes of elimination [95]. Creatinine is considered to bind negligibly with plasma proteins [115]. The renal clearance and serum concentration of creatinine is routinely used to monitor the renal function and dosage regimens adjustment in patients with renal insufficiency [47]. The volume of distribution of creatinine is of interest in connection with its wide spread use for measurements of the renal plasma flow, tubular transport capacity and glomerular filtration rate [94].

1.5.2 Diazepam

Diazepam is highly lipophilic (Figure 1.5) and exhibits a low aqueous solubility of 50 μ g/ml and a pKa of 3.4 [220]. It is extensively protein bound in plasma, and has a volume of distribution of approximately 1 litre/kg of body weight [220]. The transfer characteristics of diazepam across the GI mucosa are consistent with good absorbability (permeability) [128]. Hepatic metabolism is the predominant route of elimination of diazepam [128]. It is thought to be controlled by two separate isozymes of cytochrome P-450 . family [131,132]. Diazepam pharmacokinetic studies, *in vivo* and *in vitro*, in man and in rats [128] are indicative of a pronounced variability in its disposition which depends on gender, age and exposure to other xenobiotics [220]. The pharmacokinetics of diazepam in humans are known to be altered in hepatic disease [61]. When cirrhosis develops, its volume of distribution and plasma half-life increases while plasma clearance and absorption of

the drug after oral administration is diminished [61]. The effect of hepatic diseases on diazepam disposition kinetics is controversial. While some workers believe that the hepatic damage caused by CCl4 in rats does not affect the clearance or elimination kinetics of diazepam but it affects the distribution kinetics of the drug [61], others have shown that more than one step in the metabolic chain of DZ is impaired [131,132]. Diazepam in common with antipyrine and theophyline, has been used as a probe drug to study how various environmental factors influence drug oxidation and thereby modulate drug effects.

1.5.3 Diclofenac

This drug which is widely used for the treatment of rheumatoid arthritis, osteoarthritis, or analgesia, is a weak acid and highly bound to albumin (>99%), which limits its distribution into the extracellular space [292]. It undergoes extensive metabolism *via* acyl glucuronidation and aromatic hydroxylation followed by conjugation. In human liver microsomes, diclofenac is ring hydroxylated by CYP2C9 [149]. In the rat, 4-hydroxydiclofenac and 5-hydrocydiclofenac are metabolites excreted in the urine whereas acyl glucuronide of unchanged diclofenac is the main metabolite in bile [274]. However, the resulting acyl glucuronides are unstable and may lead to formation of covalently bound adducts to hepatocellular proteins [135].

1.5.4 Salicylic Acid

Salicylic acid is a small relatively polar molecule displaying low permeability across the hepatocyte membrane [121] and it binds to cellular constituents of liver cells [325]. It is metabolised in man and animals to salicyluric acid (SU; glycine conjugate), SPG, salicyl acyl glucuronide, gentisic acid and gentusuric acid. In the rat the main metabolite is the glycin conjugate. Available data suggest that SU and possibly SPG can be reversibly transformed back to salicylic acid [179]. Nevertheless, more recent reports support the idea that salicylic acid is not metabolised. [121, 261] or minimally metabolised by the liver during single pass (*ie* 20 min after infusion, the percentage of metabolites in the perfusate was only ~4% [147]). Salicylic acid has been employed for the determination of transport process mechanisms through various systems including RBCs and cell line. Studies suggest two parallel processes responsible for transfer of salicylic acid through the

erythrocyte membrane-one involving band 3 anion transport protein and the other involving passive diffusion of unionised molecule [171].

Figure 1.5 Diagram representing the chemical structure of the studied drugs

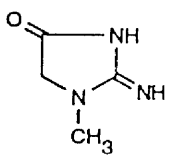

Creatinine

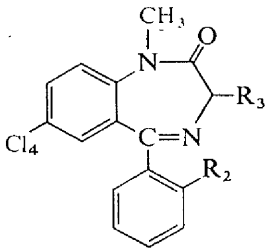

Diazepam

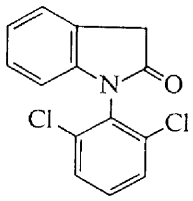

Diclofenac

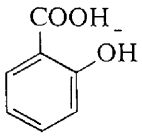

Salicylic acid

1.6 Aims and Objectives of the Project

1.6.1 Aim of the Project

The present project is aimed at characterising the influence of structural and physiological factors on the permeability of selected model compounds in rat.

With regard to the regional permeability studies, hepatic cirrhosis was chosen as a suitable model as it has been shown that due to parenchymal damage and microcirculatory alterations, the blood-liver exchange is progressively limited [119]. Many studies have been carried out in the past to evaluate the relative importance of these alterations on drug elimination [119,32,306,307] but only few studies have been performed so far to investigate the cirrhosis of the liver in view of permeability limitations [119]. Application of the indicator dilution technique in the isolated perfused liver allows us to effectively approach this issue [60]. We aimed to chose model compounds with high lipophilicity or high hydrophilicity to evaluate the role of structure on distribution. With regard to the whole-body pharmacokinetic studies, rat was chosen as this animal has proved very suitable for such studies.

Another aim of the project was to test the applicability of the axial dispersion model to the conditions of altered permeability in experimental cirrhosis. The development of this model not only represents a promising conceptual advance in modelling, it has extended our ability to quantify hepatic drug elimination and distribution as well [228,229]. However, much experimental work is still required to validate this model. This project has been undertaken with such a view.

1.6.2 Specific Objectives

1.6.2.1 Studies on physiological factors

The specific objectives of each study are listed below.

Study 1. Permeability-limited distribution. To characterise the permeability of substances in system with reduced permeability (hepatic cirrhosis). The distribution of five established radiolabelled non-eliminated reference markers is examined in the isolated perfused rat liver using the indicator dilution technique. Comparative studies are carried out in cirrhotic livers as well as non-cirrhotic (control) livers.

Study 2. Permeability-limited uptake. To investigate the dispersion of solutes with different distribution properties in system with reduced permeability in comparison to that of reference markers. Three model drugs, diazepam, diclofenac, and salicylic acid are used in an impulse-response mode.

Study 3. Steady-state extraction. To evaluate the influence of altered protein binding on steady-state hepatic extraction of a drug with high intrinsic clearance. The test compound is diazepam.

1.6.2.2 Studies on Physicochemical properties

Study 4. Permeability-limited uptake. To evaluate the relationship between physicochemical properties and hepatic dispersion of drugs with different membrane permeability. Diazepam (logP=2.8), diclofenac (logP=4.4), and salicylic acid (logP=2.2) are used.

Study 5. Constant-rate infusion. To assess the hepatic distribution and pharmacokinetic parameters of a test substance, whose disposition properties in impulse-response mode is difficult to establish, using conditions after stopping a constant-rate infusion. Creatinine is used as a test substance.

Study 6. The whole-body distribution. To evaluate the distribution kinetics of a test compound in the major tissues of body (*in vivo* experiment) in comparison to an extracellular marker (sucrose). Creatinine is used as test substance.

1.6.3 Plan of the Project

Animal experiments: In regional pharmacokinetic studies, the isolated perfused rat liver preparation in single-pass mode is used. For studies in hepatic cirrhosis, each batch of rats is divided into three groups. The first group is treated with hepatotoxin and the second and third groups serve as normal and phenobarbitone-treated controls. In the whole-body (*in vivo*) pharmacokinetic studies, the carotid artery and jugular vein of normal rats were cannulated for the administration and sampling of substances. To minimise variability and the number of animals required, a multicomponent mixtures of substances is examined in each preparation.

Chemical assay: In the steady-state experiment, diazepam is assayed by HPLC, using modifications of a standard procedure [60]. In all other studies, radiolabelled substances are assayed by radiochemical analysis.

Induction of cirrhosis: An established animal model of hepatic cirrhosis is induced in rat using oral administration of phenobarbitone and carbon tetrachloride. This model is thought to resemble human cirrhosis.

Labelling of erythrocytes: In order to use erythrocytes as vascular markers in the indicator dilution technique, they are radiolabelled using ^{51}chromium.

Protein binding: The degree of protein binding of diazepam in the perfusion medium is determined by equilibrium dialysis [60]. Preliminary experiments are performed to confirm the equilibrium time, the stability of diazepam during analysis and the linearity of diazepam binding. The magnitudes of non-specific binding and volume shift are also estimated. The degree of binding of diclofenac is determined by ultracentrifugation [120].

Data analysis: Estimates of the pharmacokinetic parameters are obtained by fitting the appropriate equation associated with the dispersion model to the experimental data using the non-linear least squares regression programme MULTI-FILT version 3.4 [321] and SIPHAR 3.3 (Simed, France). The statistical moment analysis is also used (MOMENT program; Tanigawara,1992 [277]) in comparison with the dispersion model. All data are reported as mean±standard deviation

Liver evaluation: Histological evaluation is used to verify the state of control and treated livers. The degree of shunting in the isolated perfused livers is assessed using radiolabelled microspheres.

CHAPTER TWO: THEORETICAL

2.1 Data Analysis

In this project, two different approaches were exploited for the analysis of hepatic outflow data;

a) Non-parametric method; this method, using statistical moment analysis [318], emphasises the general behavioural rather than detailed structural or mechanistic properties of the system.

b) Mechanistic approach; here, application of the axial dispersion model [228,229] aims to characterise the behaviour of the system and express it in terms of physiologically meaningful parameters.

2.1.1 Statistical Moment Analysis

For many flow systems, such as liver, usually the only quantities that can be measured are the concentrations of solute in the inflow and outflow of the system. It would be desirable then to describe the transit of drug from inflow to outflow using some general methods that do not depend on the knowledge of the structure of the system. Statistical moment theory views drug disposition as a statistical process, with the transit time distribution (TTD) occurring due to the spread in transit times of molecules on pass through the system [273,103,127,226,164]. The outflow profile can then be expressed in terms of its moments.

$$S_r = \int_0^\infty t^r . C . dt \qquad (r = 0, 1, 2, \ldots m) \tag{2.1}$$

The TTD is most often characterised by the first three moments;

$$AUC = S_0 = \int_0^\infty C . dt \tag{2.2}$$

$$MTT = \frac{S_1}{S_0} = \frac{\int_0^\infty t . C . dt}{AUC} \tag{2.3}$$

$$VTT = \frac{S_2}{S_0} - \left(\frac{S_1}{S_0}\right)^2 = \frac{\int_0^\infty t^2 . C . dt}{AUC} - MTT^2 \tag{2.4}$$

where AUC, MTT and VTT are area under the outflow frequency versus time curve, mean transit time and variance of transit times, respectively. AUC reflects the recovery of the drug in the outflow and hence the hepatic extraction. MTT is the average time taken by a solute molecule to traverse the system; it is an indication of the size of the system and the interaction

between the system and drug. These moments are linked to physiological parameters *via* perfusion flow (Q) using the following equations [226,228,164].

$$F = \frac{AUC}{Dose} \cdot Q \qquad (2.5)$$

when F=1, Dose = Q . AUC (2.6)

V = MTT . Q (2.7)

where F and V are the fractional recovery and the apparent volume of distribution for non-eliminated solute. Equations 2.5 and 2.7 are structure-free in the sense that they do not depend on the physical nature of the system or organ being investigated [226].

VTT is a measure of spreading or dispersion of drug in the liver. By taking into the account the size of the system, the normalised variance, CV^2, gives the relative dispersion of solute within the liver.

$$CV^2 = \frac{VTT}{MTT^2} \qquad (2.8)$$

CV^2 is a more useful parameter than VTT because it is a) independent of flow [16], b) dimensionless, and c) much less affected by extrapolation errors [302].

For an eliminating solute, although MTT, VTT, V and CV^2 are obtainable from the outflow data using moment analysis, as they are influenced by elimination, further evaluation can only be made by applying a parametric model to account for the effect of the hepatic elimination [242]. Furthermore, as global descriptors, parameters estimated from moment analysis are concerned with steady-state properties such as the extent of distribution (V_d) and elimination (E, CL), rather than kinetic aspects of the disposition processes. Therefore, a detailed analysis of the transient kinetics cannot be achieved without recourse to a model.

2.1.1.1 Calculation of moments

The moments of the outflow profile can be calculated by numerical integration using trapezoidal approximation [318]. These numerical methods replace the integrals by finite sums and so introduce an error of approximation. Since the outflow concentration is usually only measured up to a finite time, one has to be aware of the cut-off errors introduced by truncation of data[318]. Usually, it is necessary to extrapolate these calculated moments to time infinity. However, extrapolation beyond the last data point may be a source of large and unpredictable errors, particularly in

estimating higher moments. It is therefore not surprising that the zeroth and first moments are the most frequently used ones in Pharmacokinetics.

2.1.1.2 Correction of catheter distortion

On calculating the moments of a solute, it is important to consider the effect of the non-hepatic region on its TTD [242]. The correction for MTT is

$$MTT_H = MTT - MTT_{NH} \quad (2.9)$$

where MTT_H and MTT_{NH} are the mean transit times in the liver and non-hepatic region, respectively. The effect of catheter distortion can also be accommodated by numerical deconvolution when model equations are used [242].

2.1.2 Axial Dispersion Model

2.1.2.1 Transient considerations

The frequency outflow of a solute injected into the single-pass isolated perfused liver can be described by a series of differential equations which can be solved using Laplace Transform operations.

One-compartment dispersion model: When the radial transfer of drug between the blood and the hepatic spaces into which it distributes is instantaneous (*ie* the liver behaves as a single cylinder with flow-limited distribution), the hepatic transfer function for the solute during a single pass can be adequately described using the one-compartment dispersion model [228], expressed by

$$W(s)_H = \exp\left[\frac{1-\sqrt{1+4D_N.(R_N+V_H.S/Q)}}{2D_N}\right] \quad (2.10)$$

where D_N is the hepatic dispersion number, a measure of relative axial spreading of a solute in the liver. The efficiency number, R_N, is defined as

$$R_N = \frac{fu_b.CL_{int}.\rho}{Q} \quad (2.11)$$

where fu_b is the unbound fraction of the solute in perfusate, and ρ is given by

$$\rho = \frac{PS}{PS + CL_{int}} \quad (2.12)$$

where PS is the permeability-surface area product of hepatocyte membrane to the solute (with units of volume per time). V_H is the apparent volume of distribution of drug within the liver,

$$V_H = V_{b+} \frac{fu_b}{fu_c} \cdot \rho \cdot V_c \qquad (2.13)$$

where fu_c is the unbound fraction of the solute in the cell, V_b is the volume of the central compartment (which physiologically represents the combined volumes of the vascular and Disse spaces in the liver) and V_c is the aqueous volume of the cellular space. If the drug is not eliminated (R_N=0), Equation 2.10 reduces to

$$W(s)_H = \exp\left[\frac{1-\sqrt{1+4D_N \cdot V_H \cdot s/Q}}{2D_N}\right] \qquad (2.14)$$

Two-compartment dispersion model: In the case where a permeability barrier exists within the liver, such that radial distribution of a solute into hepatic tissue is not instantaneous, the hepatic transfer function is described by the two-compartment dispersion model [61,321].

$$W(s)_H = \exp\left[\frac{1-\sqrt{1+\frac{4D_N \cdot V_b}{Q}\left(s+k_{12}-\frac{k_{12}\cdot k_{21}}{s+k_{21}+k_{23}}\right)}}{2D_N}\right] \qquad (2.15)$$

The transfer rate constants, k_{12} and k_{21}, represent the influx and efflux first-order rate constants across the hepatic cellular membrane, respectively, and k_{23} is the first-order rate constant for elimination of drug from the peripheral compartment (which is assumed to represent the cellular space). The influx, efflux and elimination rate constants can be further defined by the following physiological equivalents

$$k_{12} = \frac{fu_b \cdot PS}{V_b} \qquad (2.16)$$

$$k_{21} = \frac{fu_c \cdot PS}{V_c} \qquad (2.17)$$

$$k_{23} = \frac{fu_c \cdot CL_{int}}{V_b} \qquad (2.18)$$

For a non-eliminated solute (k_{23}=0), Equation.. can be reduced further.

$$W(s)_H = \exp\left[\frac{1-\sqrt{1+\frac{4D_N \cdot V_b}{Q}\left(s+k_{12}-\frac{k_{12}\cdot k_{21}}{s+k_{21}}\right)}}{2D_N}\right] \qquad (2.19)$$

The transfer function of the frequency outflow curve obtained from the experimental system without the liver can be described using a rearranged version of Equation 2.14 [63,242].

$$W(s)_{NH} = \exp\left[\frac{1-\sqrt{1+4D_{N,NH}.MTT_{NH}.s}}{2D_{N,NH}}\right] \qquad (2.20)$$

where $D_{N,NH}$ and MTT_{NH} are the dispersion number and mean transit time of the solute in the non-hepatic perfusion system.

2.1.2.2 Steady-state considerations

The availability or fractional recovery (F) of a drug across the liver at steady state is given by the ratio of hepatic outflow to inflow concentrations. In terms of the axial dispersion model [228,229], for closed boundary conditions, F is given by

$$F = \frac{4a}{(a+1)^2.\exp\left[\frac{a-1}{2D_N}\right]-(a-1)^2.\exp\left[\frac{-(a+1)}{2D_N}\right]} \qquad (2.21)$$

where a is defined as

$$a = \sqrt{1+4D_N.R_N} \qquad (2.22)$$

As D_N approaches infinity (extensive axial dispersion), Equation 2.21 becomes

$$F = \frac{1}{1+R_N} \qquad (2.23)$$

which is the expression for the well-stirred model. In contrast, as D_N approaches zero (negligible axial dispersion), Equation 2.21 reduces to

$$F = \exp(-R_N) \qquad (2.24)$$

which is the expression for undistributed parallel-tube model.

2.1.3 Statistical Analysis

All data are presented as mean±standard deviation. Analysis of variance (ANOVA) followed by intergroup comparisons was used to test:

a) in impulse-response experiment: the effect of treatment on the different parameters studied. When a significant F was obtained, a student t test was employed.

b) in steady-state experiment: the effect of fraction unbound on availability.

2.2 The Theory of Indicator Dilution Technique (IDT)

The indicator dilution technique provides a model independent method of comparing the behaviour of a test substrate against a reference substance in a given organ [154,316,119,164]. This behaviour may be expressed in a variety of terms including capillary permeability, metabolic uptake, rates of movement, or volume of distribution. The central idea in the multiple indicator dilution technique (MIDT) is the simultaneous introduction of both a diffusible (tissue permeating) solute and a group of reference markers (including diffusible and non-diffusible tracers) at the inflow to an organ and to deduce from their relationship between the outflow profiles of diffusible and non-diffusible tracers what kind of events have occurred within the organ. By achieving this, a set of outflow indicator dilution profiles are generated allowing an assessment of the compound under study, in the same physiological condition.

In the past, direct analysis of tissue has been used to define the composition of tissue in terms of accessible volumes of distribution for various substances and tissue compartments [83]. By choosing appropriate marker, the IDT technique may similarly be used to estimate the intravascular (IV), extracellular (EC) and intracellular (IC) spaces within a tissue. Generally, radiolabelled markers are used as the concentration required is so low that it does not interfere with any concentration dependent process. However, technical difficulties arise in terms of the selection of non-eliminated markers for use in conjunction with the labelled substrate. For example, use of a tritiated substrate renders the concomitant use of tritiated water highly undesirable. Alternatively, ^{14}C-labelled substrate would exclude the concomitant use of ^{14}C-sucrose. The presence of two or more markers with the same radioisotope would necessitate tedious separation procedure for quantitation of the radiolabelled species in large numbers of samples of small volumes which in turn produce some errors. More often, the choice of a label for the test substrate is dictated by its ease of acquisition and cost. These facts have led to the application of single indicator dilution technique (SIDT) which requires the injection of the markers sequentially. The present study has been designed from this point of view.

CHAPTER THREE: MATERIALS AND GENERAL METHODS

3.1 Materials

Acetonitrile	HPLC grade	BDH Chemical Ltd
^{14}C-Albumin	5μCi/65μl	Sigma Chemicals
Carbon tetrachloride		BDH Chemical Ltd
^{51}Chromium	374mCi/mg	ICN Biomedical Inc
^{14}C-Diazepam	1mCi/ml	ICN Biomedical Ltd
^{14}C-Diclofenac	150μCi/ml	ICN Biomedical Ltd
Chloroform		BDH Chemical Ltd
Dichlorodimethylsilane	99%	Aldrich Chem Ltd
Evans blue		Sigma Chemicals
Halothane (Fluothane)		Zeneca Ltd
Heparin sodium	1000&5000U/ml	CP pharmaceuticals Ltd
HSA (human serum albumin)	20% w/v	Pharmacia,Sweden
Hydrochloric acid (conc)		Fisons Chemicals
Hydrogen peroxide	30%w/v	BDH Chemical Ltd
Hypnorm		Janssen Animal Health
Fentanyl citrate	0.315mg/ml	
Fluanisone	10mg/ml	
Medazolam	10mg/5 ml	Roche Company Ltd
Methanol	HPLC grade	BDH Chemicals Ltd
^{57}Co-Microspheres	9.2mCi/g	NENTrac,Germany.
Pentobarbitone (Sagatal)	60mg/ml	RMB Animal Health
Perchloric acid	60%	BDH Chemicals Ltd
Phenobarbitone		BDH Chemicals Ltd
Propan-2-ol		Fisons Chemicals
^{14}C-Salicylic acid	50μCi/ml	Fisons Chemicals
Scintillation fluid	Hisafe'2	Fisons Chemicals
^{14}C-Sucrose	0.1mCi/ml	SigmaChemicals
^{14}C-Urea	125μCi/ml	Sigma Chemicals
^{3}H-Water	100mCi/ml	ICN,Biomedical Ltd

All other chemicals, mentioned in the methods and analytical assays, were obtained from either Sigma Chemicals or BDH.

3.2 Equipment

3.2.1 General Equipment

Balance	Salter-A&D Ltd
Centrifuge	MSE Scientific Instruments
Micro Centaur	
Mistral 3000i	
Beckman 50Ti	
Dialysis Membrane	Scientific Instrument Centre Ltd
Dianorm®	Diachema AG, Switzerland
Dispensing pipettes (10ul-5ml)	Eppendorf Multipette
Filter	Millipore Corp
various sizes & specifications	
Gas Cylinders95%O_2:5%CO_2; N2; CO_2	BOC Ltd, UK
LKB Liquid Scintillation Counter	Wallac Ltd
Micropipette (50-5000µl)	volac, Boehringer Mannheim
Microscope (standard 35mm cassette film)	BDH
Mixer Rotator	Stuart Scientific Equipments
pH-meter (digital, CD620)	Fisons Scientific Equipments
Scintillation vials (8ml plastic, 20ml glass)	Wallac Ltd
Shaking Water Bath (STATUS 100)	The Northern Media Supply Ltd
UV/Vis Spectrophotometer (Ultrospec II)	LKB, Sweden.
Vortex Mixer	Northern Media Supply Ltd
WhirliMixer®	Fisons Scientific Equipment

3.2.2 HPLC Equipment

Pump (Kontron® LC420)	Kontron Instrument Ltd
Guard Column (NewGuard® RP18,15x3.2mm,15µm)	Brownlee Lab,USA
Column (Spheri-15® RP-18,100x4.6 mm,15µm)	HPLC Technology Ltd
UV Detector (Jasco®100-IV)	Japan Spectroscopic Co Ltd,Japan.

Integrator (HP3392A)	Hewlett Packard Co

3.2.3 Perfusion Equipment

Cabinet	Pharmacy Workshop,Manchester Univ
Cannulae (Medicut® 14&16GA)	Sherwood Medical
Carousel	Pharmacy Workshop,Manchester Univ
Fraction Collector (Redifrac®)	Pharmacia
Injection Port (Venisystem ®)	Abbott Ireland Ltd
Oxygen Meter (Jenway® portable)	Fisons Scientific Equipment
Peristaltic Pump	Watson-Harlow Ltd
pH/Temperature meter (Jenway® portable)	Fisons Scientific Equipment
Syringe (Microliter® 50,100µl)	Hamilton Company,USA
Water Bath	Northern Media Supply Ltd

3.2.4 Surgical Equipment

Dissecting Set	Arnold Horwell Ltd
Hypodermic Needles (12g,16g,20g)	Gillete Surgical Ltd
Syringe Driver (MS 16A)	Graseby Medical Ltd
Metabolic Cages	Lab Care Precision Ltd
Microcentrifuge Tubes (polystyrene, 1-5ml)	Alltech
Plastic Syringes (1-10 ml)	Becton Dickinson Co
Polyethylene Tubing (PE 10,50,90)	Caly Adams,USA.
Surgical Table (with heating block)	CF Palmer Ltd
Timer (digital, 59min,59sec,99/100sec)	BETA Company

3.3 METHODS

In this chapter, only those methods which have general application are discussed. There are several other more specific methods which are located in the pertinent sections.

3.3.1 Induction of Cirrhosis

Drug disposition studies in the context of hepatic deficiency requires application of numerous methods and techniques which are often impossible to perform on human livers. These studies, therefore, are best accomplished on experimental models in laboratory animals. To this end, a rat model of experimental cirrhosis introduced by Proctor and Chatamra [208,209], which closely resembles human cirrhosis [107], was adopted for our studies.

3.3.1.1 Methods

3.3.1.1.1 Animals

Rat was chosen as experimental animal model throughout the project. Male Sprag-Dawly rats, weighing 145-155 g (six week old), obtained from the animal unit, Faculty of Medicine, University of Manchester were used. They were allowed free access to food (stock pellet diet) and water and housed in groups of 3 in temperature-controlled (22±1 °C) rooms under a 12-hr light/dark cycle (8.00-20.00). Rats, in each batch, were randomised into three groups. The first group was used for induction of cirrhosis. The rats in the second group served as phenobarbitone controls and the third group served as normal controls.

3.3.1.1.2 Weighing

Accurate daily weighing of the rats was carried out at the same time (9.00 h) each day using an electronic balance and the weight recorded when the rat remained motionless. The weight changes were measured with an accuracy of ±0.1 g in the 100-800 g range.

3.3.1.1.3 Phenobarbitone

Sodium phenobarbitone was added every day to the fresh drinking water (35 mg/dl). This solution was the only source of drinking water available to the rats.

3.3.1.1.4 CCl4 dosing scheme

After 10 days on phenobarbitone, when the rats were about 200-250 grams in weight, the first intragastric dose of CCl4 was given. The CCl4, mixed in corn oil (as vehicle), was given by gavage after anaesthesia (2 min exposure to halothane/oxygen). The amount of CCl4 administered had to be increased each week. In order to keep the volume of oil administered low, different concentrations of CCl4 in corn oil were prepared. A maximum volume of 2 ml was given to each rat. Rats were not starved before receiving the dose of CCl4.

The cannula for the intragastric intubation was made from a fine intravenous catheter (Portex®; 5FG; od 1.65 mm) cut to 12 cm long, with the end fused into a bullet-nosed shape with a side hole. The dose was given at the same time of day (9.00 h) once a week (on Mondays). The initial dose used was based on that proposed by Proctor *et al.*[208,209] together with an introductory experiment that we did. A batch of twelve rats was divided into three groups of four rats. A single dose of CCl4 was given to each group. The doses were 0.04, 0.08, 0.16 and 0.32 ml CCl4, respectively. The initial dose was defined as half the dose at which death began to occur which. It was 0.08 ml CCl4. Several months later, when additional rats were started on the CCl4 treatment, the initial dose was increased to 0.12 ml CCl4.

Subsequent weekly doses of CCl4 were adjusted depending on body weight responses to previous doses. Each subsequent dose was calibrated based on the response of the previous dose to maintain a critical level of damage, as reflected by the daily body weight fluctuation of each individual rat. The intended change was a weight loss of 6-9% 2-3 days after each CCl4 administration and a weight gain on the 7th day. A total weight loss of approximately 25% was intended in the CCl4-treated animals compared to controls.

In rats achieving the intended weight changes, weekly doses of CCl4 were increased by 1.5-, 2-, 3-, 4-, *etc.*, times the initial dose (standard scheme). In rats with a weight loss of less than approximately 6% on days 2-3 after CCl4 administration, the dose was increased by twice the initial dose. In rats with a weight loss of 6-9%, the dose was increased by 1.5-times the initial dose. If the body weight loss was more than 9%, the dose was maintained when there was a clear weight gain on the 7th day. Doses were reduced by the initial dose if the body weight was

just regained or increased a little on the 7th day. Doses were reduced by half the initial dose if the body weight was not regained.

After some time, a clinical impression of the animals' condition also helped to determine the adjustment of dosage. The doses of CCl4 ranged from 0.04 to 0.96 ml. The duration of treatment varied between 12-16 weeks. A minimal delay of 7 days after the last dose of CCl4 and phenobarbitone administration was allowed before *in situ* perfuion studies were carried out. The cirrhotic rats, therefore, at the time of *in situ* perfusion were approximately 6-7 months old.

The second group of rats only received phenobarbitone in drinking water and vehicle without CCl4. The third group of rats received no treatment. The second and third groups of rats served as weight matched control rats, *ie* when their body weight reached the mean value of that for cirrhotic rats they were used for liver perfusion experiment (~ 4 months old). This permitted a basis for comparison of data between the two groups of controls and cirrhotic rats. A few normal rats, however, were kept alive to serve as age-matched controls. This allowed comparison of the overall growth pattern between the two groups. CCl4-treatment was performed on a total of 9 batches of 12 rats. Each batch had a normal control and a phenobarbitone-treated (PT) control group each containing 4 rats. Suitable animals were selected from each group and used in the isolated liver perfusion experiments.

3.3.1.1.5 Measurement of pressure

Perfusion pressure in perfused liver preparation was measured using a purpose built mercury manometer. The zero reference for each flow rate was established while inflow and outflow cannulae were connected together (without the liver). The intrahepatic resistance was calculated using the following equation [295]:

$$\mathbf{R}\ (\text{mmHg/ml/min/g liver weight}) = \frac{P}{Q}\ \frac{mmHg}{ml\ /\ \text{min}/\ g.liver.weight} \qquad (3.1)$$

3.3.1.1.6 Prediction of cirrhosis

In the final weeks of treatment, most of the rats developed some degree of transient ascites. When the ascites persisted it was assumed that cirrhosis had developed [209] and the treatment was stopped. Bleeding from the nose, which is a sign of esophageal varices and occurs in parallel with the development of portal hypertension and onset of cirrhosis also occurred. Plasma levels

of albumin were measured in most cirrhotic and control rats at the end of the treatment. No other invasive test was performed to verify the status of the treated livers.

The cirrhotic rats as well as rats in the control groups were used for single-pass and steady-state experiments. The *in situ* perfused rat liver studies was 'blindly' accomplished on the treated livers. After the conclusion of each experiment, histology evaluation was obtained in all cases on biopsy specimens fixed for light and electron microscopy examination. Only results from rats showing histologic cirrhosis were used in the data analysis.

3.3.1.1.7 Ultrastructural Examination

Histology provides important information about morphological changes. Anatomical changes are usually indicative of functional alterations and information so obtained are often subsequently used in the interpretation of data. This approach was made in the present project and histologic evaluation was extensively performed with the collaboration of a pathologist. Below are the practical procedures adopted.

Preparation of the liver: At the end of each *in situ* experiment, while the liver was still being perfused with the perfusate, the medium was switched to the following fixative solution [188]:

Formaldehyde 4% v/v
Sodium phosphate 0.65% w/v
Sodium-acid phosphate 0.4% w/v
Distilled water to 100%

The liver was perfused with the above medium for 5 min, removed and two 1 cm^2 samples (for light and electron microscopy) from the large lobe were cut and stored in phosphate buffer (pH 7.4) solution.

Light microscopy: The first sample was embedded in paraffin. 5-μm slices were prepared from paraffin-embedded blocks and stained with haematoxylin and eosine for light microscopy. The area selected for analysis was remote from the portal triads and scarred areas in livers. In cirrhotic livers, because of the differences that occur depending on whether the sample is at the middle or at the edge of a 'regeneration' nodule or whether it is close to a portal tract or terminal

hepatic vein, an attempt was made to minimise the sampling problem by analysing similar sites at the centre of nodules in each specimen.

The evaluation began with a review of all tissue present on the light microscopic section at a relatively low magnification in order to assess the adequacy of the specimen and to identify any major abnormalities. This was followed by a systematic evaluation of the overall condition of the hepatic architecture and connective tissue, the presence and distribution of nodules and the type and the severity of necrosis. Some areas from micronodules were randomly selected and pictures were taken.

Electron microscopy: The second sample from the same pefused liver was postfixed in osmium tetroxide, dehydrated with alcohol, and embedded in Epon 812. Regenerative areas of parenchymal tissue were randomly selected by phase-contrast light microscopy. Thin sections of these areas were stained with lead citrate and uranyl acetate for electron microscopy and 35-mm pictures were taken with an Hitachi H300.

3.3.1.2 Results

3.3.1.2.1 The yield of cirrhosis

The CCl4-phenobarbitone treatment procedure produced cirrhosis in 81% of (72 out of 89 rats) surviving animals with a mortality of 17.6% (19 out of 108 rats). The result of CCl4-treatment for each of 9 batches of rats and the number of surviving and dead animals are presented in Table 3.1.1.

3.3.1.2.2 Gross observations

It was found that when sustained ascites occurred, under the calibrated conditions, it was associated with micronodular cirrhosis. On opening the abdomen, several abdominal organs were observed to be involved. The liver was tan or orange-yellow with fine to gross nodularity (Figure 3.3.3); small and large lobes were involved to the same extent. Both the consistency and fragility of the liver were increased. Increased mesenteric fat lobulation and lymph node hyperplasia frequently occurred. Splenomegaly, testicular atrophy, and alopecia were also observed in most cirrhotic (CR) rats.

3.3.1.2.3 Histologic observations

From every 12 rats in the cirrhotic group, eight rats had a complete picture of micronodular cirrhosis (Table 3.3.2). The remaining four rats showed varying degree of fibrosis, steatosis and hepatic damage which were considered as early stages of fully developed cirrhosis [188].

By gross and microscopic examination, the **control livers** revealed no pathologic alteration. In general the size of hepatocytes was normal and normal architecture of lobules was preserved (Figure 3.3.3). The hepatic sinusoids were relatively narrow and were lined by cells with long, thin, attenuated processes (Figure 3.3.4). The sinusoidal lining cells frequently overlapped but did not exhibit tight intercellular connections. In some areas there were gaps between contiguous segments of the lining cells and no continuous barrier was interposed between the sinusoidal lumens and the parenchymal cells. Thin microvilli extending from the hepatic paranchymal cells and occasionally collagen bands were present in the narrow spaces of Disse.

CCl4-treated livers showed a completely different picture from normal livers. The livers appeared grossly micronodular and icteric. By microscopic examination they revealed complete distortion of lobules and appearance of nodules (Figure 3.3.3). Hepatic cells often exhibited distorted, sometimes swollen, or blunted microvilli. In some areas the paranchymal microvilli were reduced in number (Figure 3.3.4). Signs of cell infiltration were frequently present. In some areas, fenestrations were rarely observed. In some instances, the vessels appeared contracted so that the lumens were collapsed, whereas in other vessels the lumen was patent. While many of the sinusoids remained normal, many were slightly widened or narrowed. In severely cirrhotic livers, sinusoids occasionally were lined by somewhat thickened and continuous cells. In some specimens the space of Disse was widened in part because of retraction of altered hepatocytes and in part as a result of an increase in the amount of material in the space. In other samples, the space of Disse was normal.

3.3.1.2.4 Physiological analysis

In most cirrhotic rats the portal vein showed signs of inflation and hypertension. Perfusion pressure and estimated intrahepatic resistance were significantly elevated in cirrhotic livers. Perfusion pressure, corrected for background value (mean±SD), was 8±4, and 7±4 and 26±14 mmHg/liver in normal, PT, and CR rats, respectively. The calculated intrahepatic resistance was

21±10, 4±1 and 4±1mmHg/ml/min/g in the three groups respectively. Measurement of plasma albumin revealed that cirrhotic rats had lower levels of plasma albumin compared to control rats (3.9±0.4, 3.8±0.4 and 2.5±0.8 g/dl, respectively). Measurement of fraction unbound of diazepam to albumin in serum obtained from normal and cirrhotic rats showed that binding ability of plasma albumin decreased in cirrhotic animals (fu=0.32±0.05 in cirrhotics compared to fu=0.1±0.02 in normals).

A slight difference was observed between gross liver weight of normal (23.2±3.5), PT (23.5±2.5) and CR rats (27.2±4.3), which just reached statistical significance. The value of liver weight to body weight ratio was significantly larger in PT and CR rats compared to normals. Body weight was significantly lower in CR rats (88% of control value) at the time of cessation of treatment (436, 440 and 387 g in CR, PT and normal rats). Body weight in all three groups continue to increase afterwards. At the time of the liver perfusion experiment there was still a noticeable difference in the mean value of body weight between normal and cirrhotic groups (Tabel 3.3.3).

3.3.1.2.5 Growth pattern

Normal- and PT-control rats showed a normal progressive growth pattern (Figures 3.3.1, 3.3.2). The increment in the body weight of cirrhotic rats was slower. At the end of treatment period, the rats in cirrhotic groups had a considerably lower mean value of body weight compared to normal rats.

Table 3.3.1

Yield of production of experimental cirrhosis on rats of different batches using Proctor's method (Ref 208).

	CR	NC	D
Batch Number			
1	6	3	3
2	7	3	2
3	6	3	3
4	7	2	3
5	9	1	2
6	8	1	3
7	9	1	2
8	10	2	0
9	10	1	1
Number that survived	72	17	NA
Percent survival	67.70%	15.70%	NA
Total number that died	NA	NA	19

CR: rats responded to the treatment and showed signes of cirrhosis

NC: rats who did not develop cirrhosis

D: rats who died during the treatment

NA: not applicable

Table 3.3.2

Diagnostic findings of histology evaluation observed for rat livers served in the isolated liver perfusion studies.

	Diagnostic Observations
Untreated Rats	Normal structure
Phenobarbital-treated Rats	Some slight fatty changes
CCl4-treated rats	Grading of Cirrhosis
Number 1	Grade 1
Number 2	Grade 2
Number 3	Grade 1
Number 4	Grade 1
Number 5	Grade 3
Number 6	Grade 2
Number 7	Grade 2
Number 8	Grade 2
Number 9	Grade 3
Number 10	Grade 3
Number 11	Grade 1
Number 12	Grade 3

Grade 1: severe cirrhosis

Grade 2: mild cirrhosis

Grade 3: presence of some nodules with subendothelial fibrosis, steasosis, bridging, hyperplasia

Table 3.3.3

Physiological data in rats served in the isolated liver perfusion studies.

	Normal-control Rats n=10	PT- control Rats n=5	CCl4-treated Rats n=12
Body Weight (g)			
at the end of CCl4-treatment	436+44	440+45	387+39
on liver perfusion experiment	526+79	528+86	479+57
Liver Weight			
g	23.2+3.5	23.5+2.5	27.2+4.3
% body weight	0.04+0.005	0.04+0.004	0.056+0.013
Perfusion Flow (ml/min)			
per liver	34+4.4	27.5+3.7	39.6+5.7
per g liver	1.39+0.3	1.14+0.1	1.47+0.3
Albumin Blood Concentration (g/dl)	3.9+0.4	4.1+0.4	2.5+0.8
Perfusion Pressure (mmHg)	8+3	7+3	26+9
Intrahepatic Resistance (mmHg/ml/min/g)	4+1	4+2	21+8

PT: phenobarbitone-treated
CCl4:carbon tetrachloride

Values are mean+SD

Figure 3.3.1 Body weight change response to the initial dose of intragastric CCl4. Rat 1 and Rat 2 illustrate the extent of the variation in response within a group of 12 rats. Rat 1 indicates the minimum response and Rat 2 the maximum response starting with the right initial dose. Each subsequent dose calibrated by response of previous dose. Note fourfold difference in dose by second dose and threefold difference by third dose. By dose A and B the weight response (compared with control) has been matched by change in dose. Note sustained departure in weight (dashed line) from control weight as critical damage level is maintained. Control is the growth curve (without standard errors for clarity) of a group of similar phenobarbitone-treated rats without CCl4.

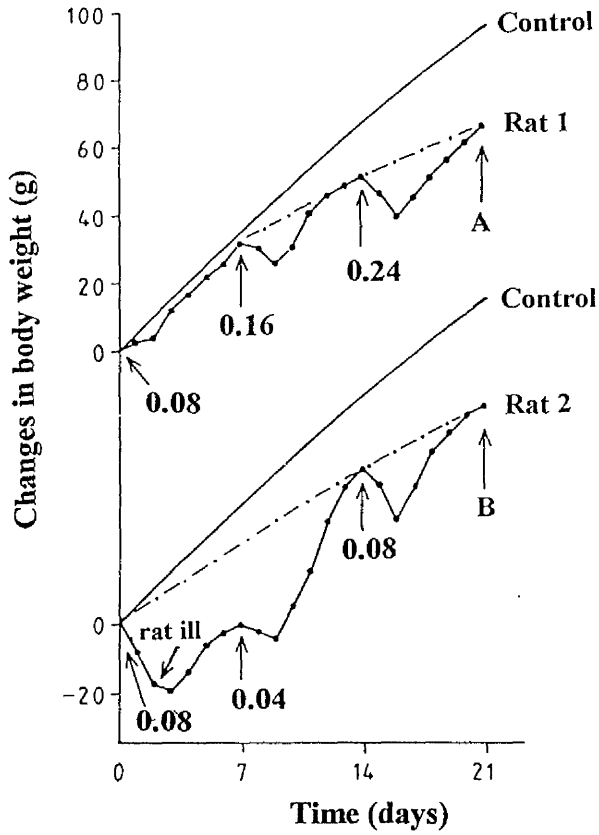

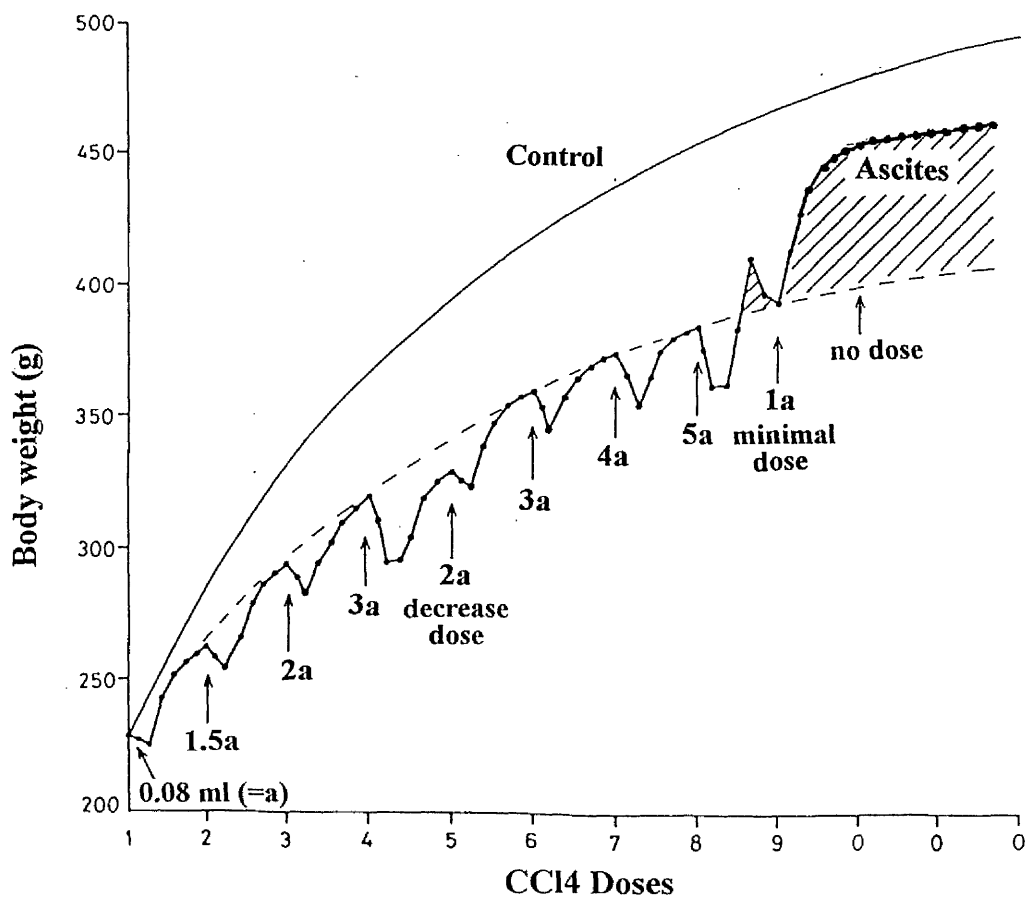

Figure 3.3.2 Typical weight change pattern for individual rat from dose 1 to dose 10 of intragastric CCl4, between the extremes of Rat 1 and Rat 2 in Figure 3.3.1. The doses are recorded in terms of the initial dose (0.08 ml=X). Note the sustained departure in weight (dashed line) of cirrhotic rat from control.

Illustrations

Figure 3.3.3 Light Microscopy:
Illustrations A-L show various sections of rat livers served in isolated perfused liver experiments (stains and magnifications in parenthesis).

Livers from normal control rats
A: central vein (CV) with adjacent part of the parenchyma. Two openings of sinusoids (S) into the lumen of the vein are seen in the right side of the wall (stained with hematoxyline and eosin (H&E) x270).

B: hepatocytes (H) arranged in normal plates (CP). Plates are one cell thick. The arrow shows a sinusoidal lining cell (H&E x400).

C: capsular and sub-capsular area of a sample. Note the thickness of the capsule and the structure of its connective tissue (H&E x30).

D: part of normal liver lobule with a portal tract (P), including an arteriol (A) and a bile ducti (arrow), and a central vein (CV) (H&E x30).

E: a section, as shown in Picture A, shows the condensed reticulin fibers in the wall of central vein (CV) and small bundles of collagen fibers (stained with reticulin (R x270).

F: a section, as shown in Picure D, illustrates the liver cell plates which radiate from the central vein (CV) (R x110).

Livers from phenobarbital-treated rats
G: central vein area (H&E x30).

H: part of centrilobular area. The sinusoids are of normal width and lining cells are to be found. There is no atrophy of the liver cell plates (H&E x270).

Livers from carbon tetrachloride-treated rats
I: overal appearance of cirrhotic liver (the right lobe cut in half).

J: nodules with both slender and broad connective tissue septa (H&E x24).

K: a small nodule is surrounded by broad connective tissue septa with bile duct proliferation. A few fat droplets are visible (stained with van Gieson).

L: micronodules with collagen bundles (stained with Masson trichrome).

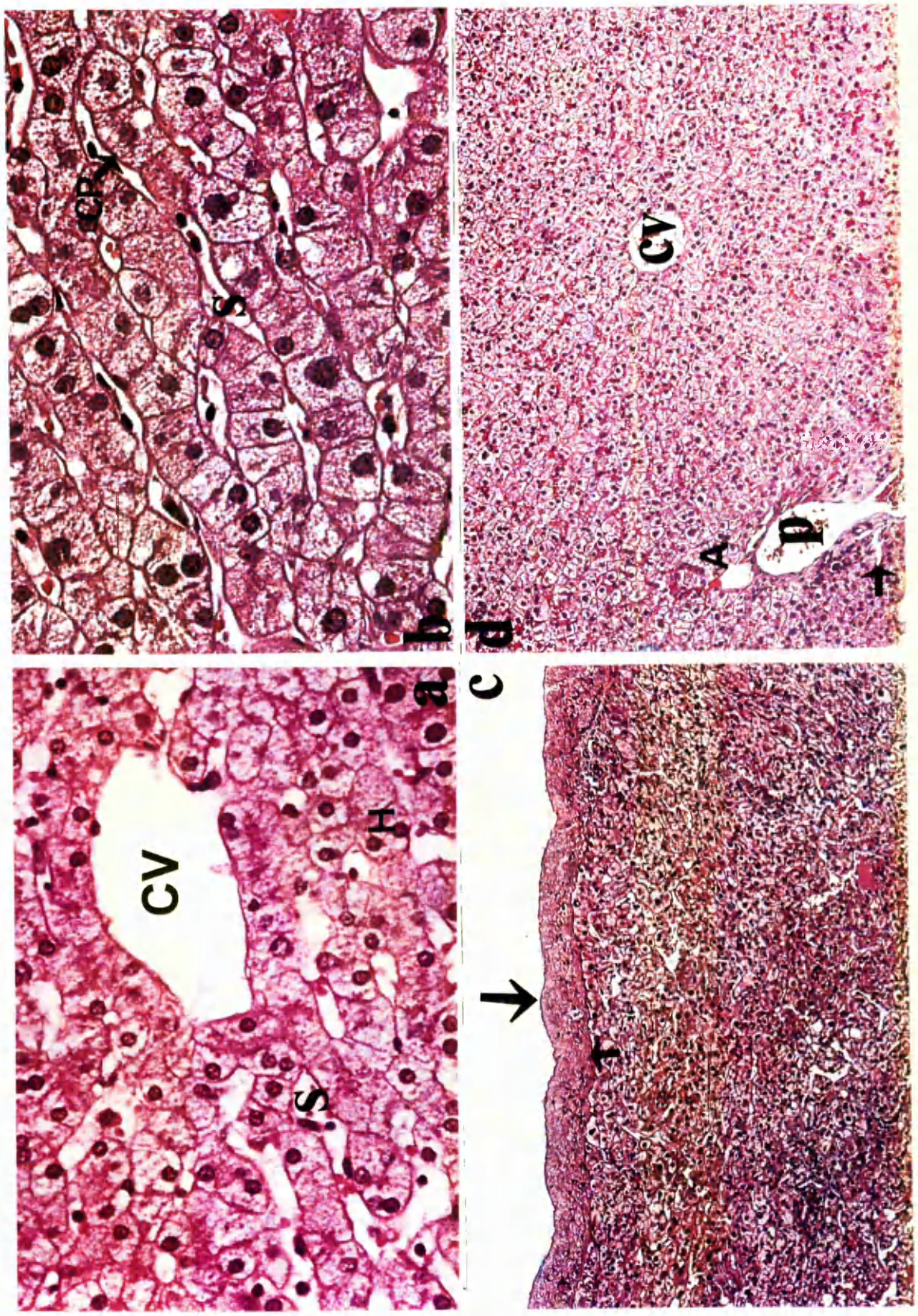
a
CV
H
S
b
CR
S
c
CV
A
D
T
c
T

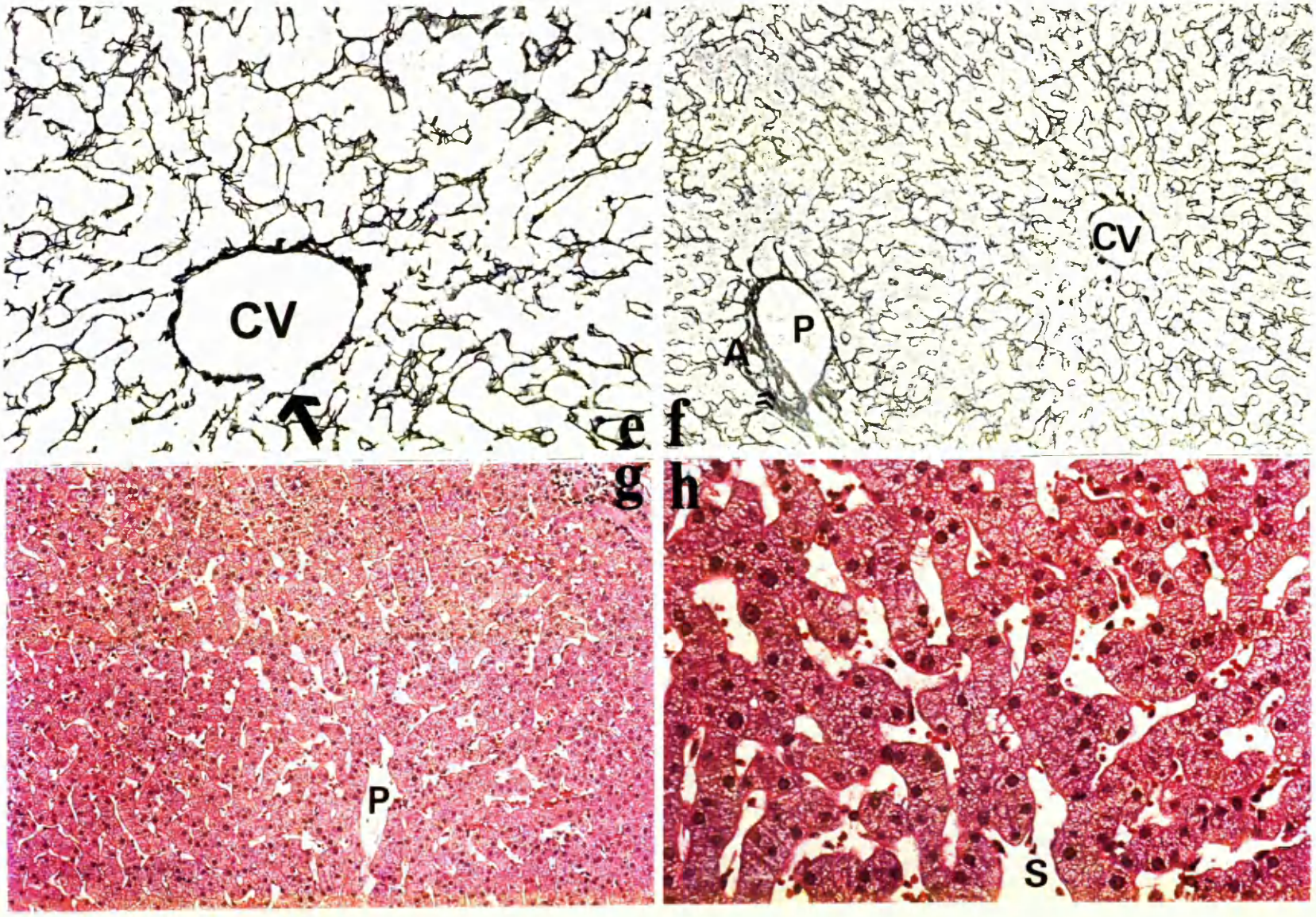
CV
e
CV
P
A
f
g
P
h
S

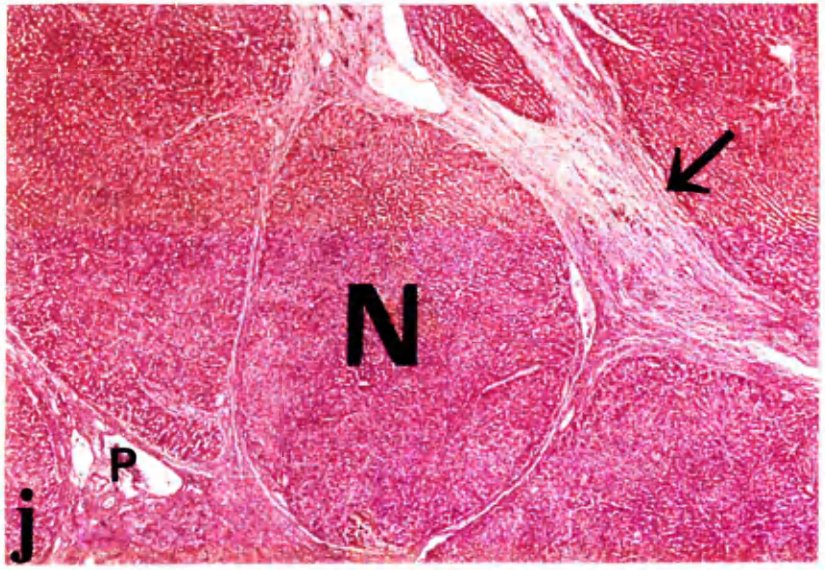

i j

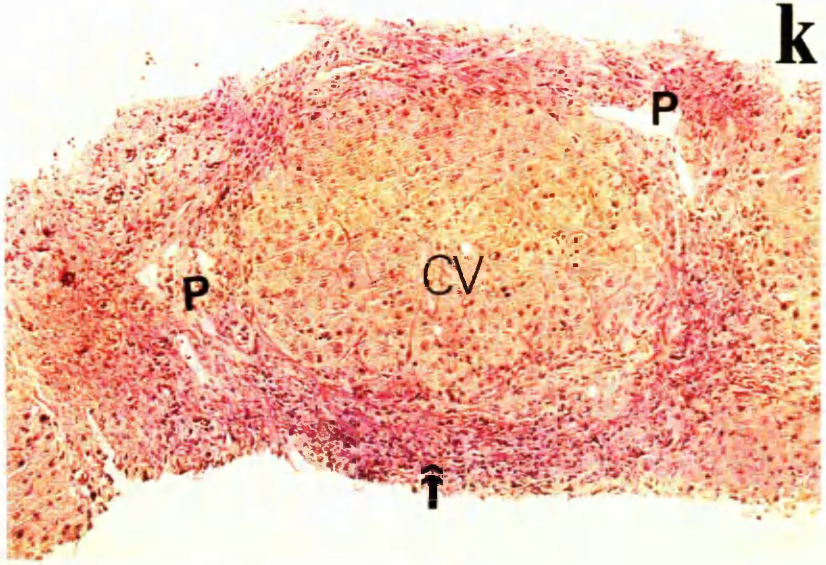

k l

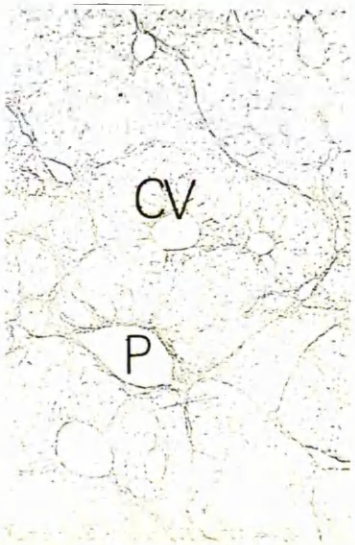

Figure 3.3.4 Electron Microscopy:
Illustrations A-F show various sections of rat livers served in isolated perfused liver experiments (magnifications in parenthesis).

A: sinusoid in a control rat liver. The lumen is delimited at each side by attenuated segments of sinusoidal lining cells (S). At one point, a gap between continuous cells is probed by a process extending from an underlying cell (arrow). At upper right, a small sector of the adjecent hepatic cell is depicted. At lower left is a larger segment of hepatic parenchymal cell cytoplasm (x27,150).

B: a capillarised sinusoid in the cirrhotic liver of a CCl4-treated rat. The empty lumen is delimited by thickened cells. At one point, the tapered ends of two adjoining cells barely make contact (arrow). In the space between the thickened lining cells and the continuous parenchymal cells (the space of Disse), a discontinuous basement membrane-like structure is seen (upper portion of the micrograph) (x24,700).

C: a cross-sectioned vessel along a fibrotic band in the liver of a CCl4-treated rat. Tight intercellular junctions between apposed cells may be seen at several points (long arrow). At one site, however, two adjoining endothelial cells appear barely to make contact (short arrow). In the attenuated portion of one endothelial cell, a fenestration (open arrow) is bridged by a thin diaphragm. Segments of perivascular cells incompletely embrace the vessel. At extreme upper right is the edge of a flanking hepatic parenchymal cell (H), exhibiting decreased number of microvilli (x21,150).

D: a normal liver sample. Note gap in lining cell (L) layer with hepatocellular microvilli (arrow) exposed to the sinusoid (S) (x17,000).

E: active cirrhosis. The space of Disse is widened and many fiber bundles (F) are present. The microvilli of the sinusoidal border of the hepatocyte are almost completely absent (x9000).

F: advanced cirrhosis. Sinusoid appears as a typical capillary surrounded by a continuous basement membrane (arrow) (x8000).

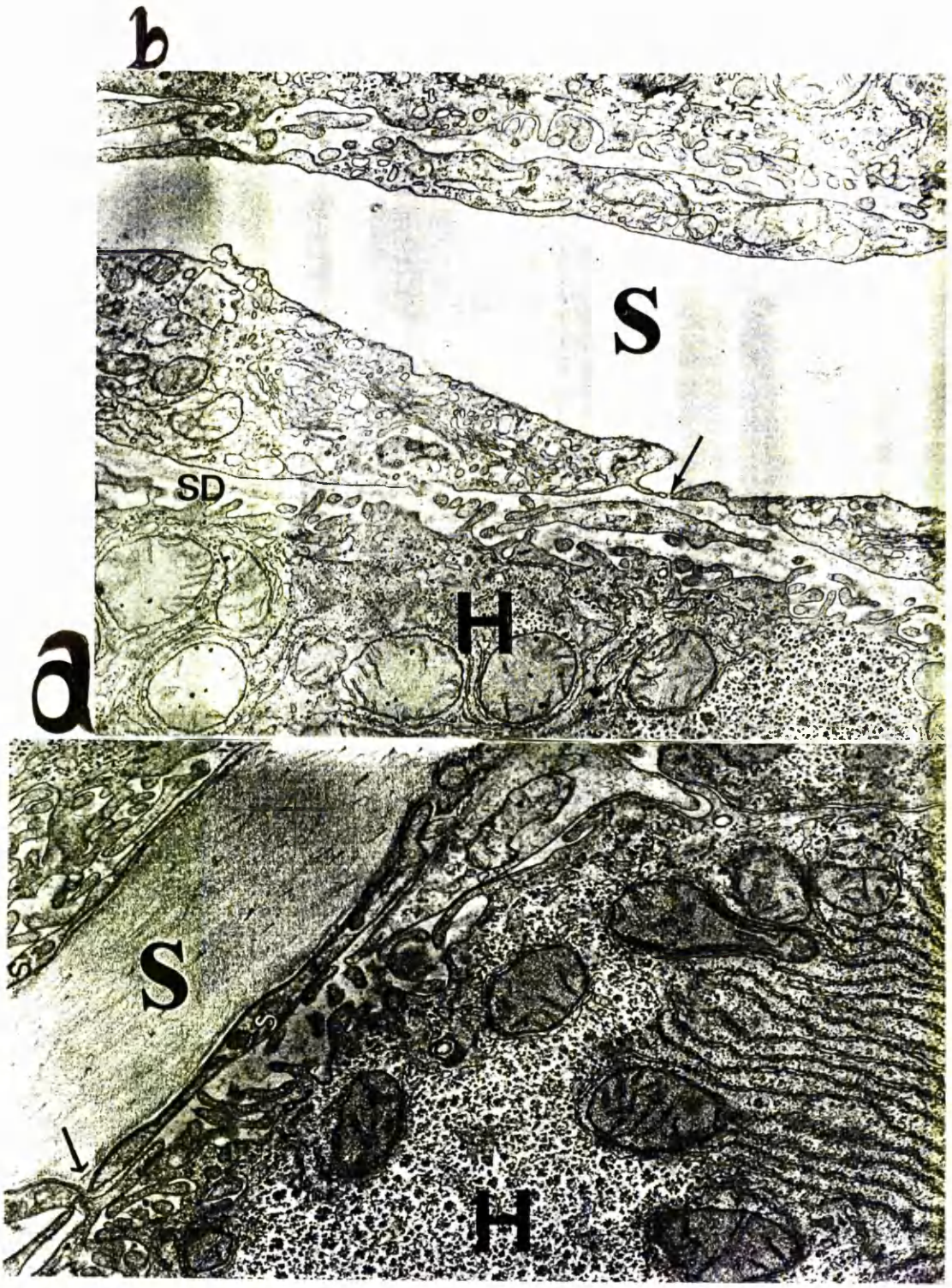
b
S
SD
H
a
S
H


d
H
S
T
e
S
F
f
S
HEPATOCYTE
MC
c

3.3.1.3 Discussion

3.3.1.3.1 Induction of cirrhosis

Providing an experimental model of human cirrhosis in rat is a delicate task. As the hepatotoxin used is not that causing the clinical disease, the subject is not a human but an animal, and the duration of the procedure is long and many variables are involved, the model must be comprehensively examined and sharply defined. This task has been conducted extensively in this project.

Historically, induction of cirrhosis is associated with the problem of unpredictability which arises from two sources: the mechanism of development of cirrhosis by CCl4, and the variation of hepatic response to hepatotoxin, both between the rats of a group and within the individual rat as the effect of the doses of CCl4 accumulate. The problem with respect to the mechanism was clearly stated by Cameron [40] who stressed that "the production of cirrhosis by CCl4 depends upon inflicting repeated damage to the liver, and that each episode of damage must be confined within a narrow and critical range between a reversible hepatitis on the one hand and death from acute liver failure on the other". Proctor's model is a simple approach to this problem, in which both the variation in response to CCl4 and the maintenance of a critical level of damage are monitored by the daily weight change of the rat in response to doses of CCl4. This is then used to calibrate the subsequent doses of CCl4 until a standard level of severe decompensated cirrhosis is reached.

3.3.1.3.2 The rate of success

A considerable amount of time was spent at early stages of the work to learn the optimal conditions for induction of cirrhosis in the rat. Administration of right dose of CCl4, handling of the diseased animals, recognising the stage of the disease, duration of anaesthesia and development of the skills to increase the rate of production and decrease the number of deaths, needed time and experience.

The results clearly show that, using CCl4 and phenobarbitone, it was succeeded to produce micronodular cirrhosis in most (81%) of the rats. A more or less similar rate of production has been reported by most other workers [209]. Fischer-Nielsen *et al*[188] claimed that they produced cirrhosis in all their animals despite using a lower dose of CCl4. They mentioned that the

produced cirrhosis in their experiment was not severe but did not define exactly the type of damage to the liver they produced.

The rate of success in terms of production of cirrhosis and reduction in mortality in the present project improved from the first batch (25% mortality and 33% failure in production) to the final batch (8% mortality and 8% failure in production) (Table 3.3.1). The presence of some rats with only moderate lesions even after 16 dosings with CCl4 probably reflects the insufficiency of the CCl4 dose used in the dosing schedules, particularly in the early stages of the development of the scheme. As the dose was increased by 20% for the next series, more severe cirrhosis was produced indicating that an optimal level of repeated damage to the liver was maintained.

Another possible reason for increasing the severity of liver damage was the reduction in the amount of oil administered. Administration of oil as vehicle to the rats is controversial. While some claimed that administering CCl4 without oil (and CO_2 as anaesthetic) produced cirrhosis in all treated rats, others reported that the hepatotoxicity of CCl4 on mice liver was enhanced when corn oil was employed as the gavage vehicle compare to Tween-60 aqueous emulsion [51]. It was found that excess amounts of oil delayed the onset of the disease. Thus, different concentrations of CCl4 in corn oil were prepared and 1 ml was administered. This was particularly useful during the final weeks of treatment, as the amount of CCl4 had to be increased every week.

The death of animals occurred early either on administration of the anaesthetic or a few days after CCl4 administration, due to acute toxicity. Skilful handling of the anaesthesia and the dose administration reduced the rate of mortality dramatically. This is because the basal levels of cytochrome P450 and the ability of the liver to respond to phenobarbitone are impaired in severely cirrhotic animals [157]. Such animals are in short supply of enzymes and liable to die even after cessation of CCl4 dosage.

3.3.1.3.3 Weight changes

The profile of change in body weight with respect to time in the present work (Figure 3.3.2) is similar to that reported by Proctor *et al* [208], who observed a progressive curve for both groups with a sustained departure in weight of cirrhotics from controls. This is a typical pattern observed in experimental pathology indicating the response of body to the hepatotoxin.

Morphometric and histological studies have demonstrated that liver enlargement is caused by an increase in the size, and not the number, of hepatocytes [10]. Orrego [191] demonstrated that the increase in liver weight observed in alcohol-fed rats was due to an increase in total water (about 60%), fat and protein (30%) and extracellular matrix (10%) [158, 217].

There appears to be a discrepancy in the literature regarding body and liver weight variations in normal and cirrhotic rats. Theoretically, lower body weight of cirrhotic animals compare to normals is expected. This was found in this work (Figure 3.3.2 and Table 3.3.3) and has been demonstrated by many others [188,209]. This is due to the suppressive effect of CCl4 as its effect is not limited only to the liver but it affects the whole body [209]. After the cessation of treatment, all animals including the cirrhotics showed a normal growth pattern, although the mean body weight value of the cirrhotic group never reached that of the normals. This shows that the diseased animals regained their ability to put on weight but could not compensate for the original weight loss during the treatment. This is in contrast to the findings of Proctor *et al* [208] who reported that 3 weeks after stopping CCl4 administration, cirrhotic rats had the same weight as normal control rats. This means that diseased animals were able to grow faster than normal subjects. They did not offer an explanation for their observation.

It has been reported [188] that after 13 weeks of treatment, cirrhotic rats were 260 g compared to 330 g control litter-mates and at 24 weeks post-treatment (8 months old) they were 350 g compare to 370 g control litter-mates. On the other hand, the livers from the same groups of cirrhotic and normal rats both weighed 28 g, or nearly 8% of body weight, which is surprisingly high, as the normally quoted value is closer to 4%. These relatively low values for body and liver weight are in contrast with those that have been found in this work and by other workers [208,295,96,188].

3.3.1.3.4 Variation in response to CCl4

In addition to the variation in response to CCl4 between the rats in a series, there appears to be a variation in response within the individual rats with respect to time, as indicated by the variation in increment of doses. This may be due to I) the increasing age of each rat, which reduces the

sensitivity to CCl4 [40], and II) the increasing damage to the liver with each dose of CCl4, which decreases the ratio of the cytochrome P450/CCl4 effect [160]. Both these factors act in the same direction to reduce the sensitivity of the rat liver to CCl4, and require that the dose be increased with time. Because CCl4 was more hepatotoxic to the 200-250 g rats than to the 300-350 g rats it was found that care must be taken in applying doses to younger rats, as has been confirmed by others [37].

3.3.1.3.5 Prediction of cirrhosis

A general problem associated with the induction of cirrhosis is the prediction of onset of the disease. Many tests have been proposed as markers of liver injury but are not widely available, developed or evaluated. Laboratory tests also lack sensitivity and specificity in differentiating between the various stages of liver disease [153]. Not only is no information yet available regarding the natural history of changes in quantitative function tests in chronic liver disease [96], but also the implication of using these tests in animals has not been demonstrated.

In the case of cirrhosis, laboratory tests such as enzymatic tests or measurement of thrombin or plasma albumin often are not especially indicative of the disease, as they change in most acute and chronic liver failures. Transient ascites also does not denote a fully developed cirrhosis as the liver usually returns to normal after cessation of toxin administration. It was found that relatively more sustained ascites, together with the overall clinical impression of the animal, can lead to a reasonable diagnosis. Otherwise, until the abdomen is opened and the liver inspected, a final decision can not be made. Histology plays a vital role in evaluating the architecture at the ultrastructural level and relating the structural alterations to data analysis. The present histological findings, which are in agreement to the literature data, confirm this fact [252,191,202,142]

3.3.1.3.6 Ascites

Chronic administration of CCl4 resulted in the appearance of ascites in the rat. The onset of ascites in the rats varied from 8 to 12 weeks. With the appearance of a transient ascites (lasting one day), the subsequent dose was reduced. If ascites was sustained (for a week or more), then the liver was considered to be cirrhotic and the administration of CCl4 was stopped. The

combination of assessing the ascites and evaluating the weight changes is a non-invasive method to determine when the cirrhotic process has become micronodular and decompensated [208].

3.3.1.3.7 Physiological parameters

The change in plasma albumin was used as a diagnostic in this project. The level of plasma albumin was lower in cirrhotic rats than in control rats. This shows that, despite the long duration of treatment, the liver could not adapt itself to the chronic injury and recover its ability to maintain a normal serum albumin level. The plasma albumin concentrations in normal and cirrhotic rats in this work were similar to most values reported for rat [188] and human [131], although some different values have been reported by some other workers [61].

The increased consistency and fragility of the liver and fat lobulation in cirrhotic rats had an impact on the surgical procedure in the in situ liver perfusion experiment. This increased the duration of the surgery, made the liver more sensitive to handling and increased the overall percentage of failed surgical operations. On the other hand, the limited number of animals showing a complete picture of cirrhosis added to the practical difficulty associated with the perfusion technique.

Despite the higher total flow rate of perfusate in cirrhotic than normal livers, flow rate per gram of liver was approximately the same for both groups indicating the validity of the "perfusion-rate-estimation" procedure. The perfusion flow rate was calculated according to the body weight measured before surgery. Body weight was lower in cirrhotic rats but this was compensated for by the larger proportionality factor that was multiplied by body weight to calculate the perfusate flow rate used. The reason for this higher value was that with respect to literature data, a higher liver weight was predicted for a given body weight in the cirrhotic animals.

The perfusion pressure which is an indirect measure of *in vivo* portal pressure was measured in the present work . This gave an indication of intrahepatic resistance. A great deal of discussion exists in the literature regarding the nature of portal pressure and resistance. Portal hypertension in cirrhosis has been attributed to a) increased portal vein inflow from the splanchnic region[295] and b) increased intrahepatic resistance [295]. Elevated intrahepatic resistance, either of presinusoidal or sinusoidal origin is the result of a) stiffness and therefore loss of compliance of

the intrahepatic vasculature [25], b) change in the hepatic architecture including sinusoidal compression [271,272] and decreased communication between sinusoids and the space of Disse [25]. In cirrhotic patients a significant inverse correlation exists between hepatocyte size (and surface area) and sinusoidal area [293]. Ethanol fed rats in which liver enlargements of 36% to 42% were observed, had a significant reduction in both extracellular space and blood space per unit liver weight [293]. Increased intrahepatic resistance in most cirrhotic rats in this work was in accordance with the above theory and available reports in the literature [295]. It should be mentioned that while there is a link between these factors and cirrhosis, there are reports of cirrhotic subjects with normal portal pressure and resistance [25].

The severity of the disease determines the reversibility of the histological and physiological alterations in the liver. If the disease is severe enough, *ie* fully developed cirrhosis, the cirrhosis is irreversible. Even after 24 weeks post-treatment, histology evaluation and various hepatic function tests are indicative of a persistent micronodular cirrhosis [271,272,37]. Less severe hepatic lesions, *ie* limited parenchymal damages with some fatty changes, usually recover after 2-3 weeks. As we normally performed the *in situ* liver perfusion experiment on rats 1-2 weeks after cessation of CCl4-treatment, we avoided the problem of using recovered rats.

3.3.1.3.8 Conclusion

The experimental model of cirrhosis appears to reproduce the major features of the human disease: the liver is grossly nodular, there are signs of portal hypertension, and the normal architecture is replaced by nodules of regenerating liver cell plates surrounded by connective tissue septa with proliferated bile ducts. A large body of data exists in the literature [276,271,272,37,106,252] that support these findings.

3.3.2 Isolated *in situ* Perfused Liver Preparation (IPLP)

An established [240,66,64] surgical and perfusion technique suitable for drug distribution studies using impulse-response and steady-state methods was applied to the rat liver.

3.3.2.1 Perfusion System (Figure 3.3.5)

The apparatus was housed in a purpose-built cabinet (1.5×1×1 m) with metal frames and glass walls and windows at the front. The temperature was thermostically controlled by a fan heater and maintained at 37 °C.

Pump: A Minipuls 6 finger pump was used as means of perfusion and was based on the sequential compression of a flexible tube by 'fingers'. A forward peristaltic flow resulted. By arranging two channels in parallel the wave was damped out. Output from 4 to 60 ml/min was linear with changing rate of pumping. The pump was checked daily.

Gas supply: The gas used was 95%O_2:5%CO_2, the concentration required to provide a pH of 7.4 with 25 mM bicarbonate buffer used in the system. It was saturated with water before entering the bubble trap, by bubbling through a bottle fitted with a sintered-glass distributor.

Perfusion medium: Krebs-Henseleit bicarbonate (KHB)[60] was used as perfusion medium containing the following components (in mM): NaCl 118, KCl 4.74, $CaCl_2.6H_2O$ 2.5, KH_2PO_4 1.86, $MgSO_4.7H_2O$ 1.86, $NaHCO_3$ 24.9 and D-glucose 8.3. Taurocholate (10 mg/L) was also added for the maintenance of normal bile flow [60]. A concentrated solution of each component of the medium was separately prepared. A specific amount of each solution was mixed and made up to the required volume with distilled water. The buffer was prepared and filtered (0.22 μm membrane filter) daily. A high pH occasionally led $CaCl_2$ to sediment and make the medium turbid. Hydrochloric acid or CO_2 was used to lower the pH and clear the solution. The perfusate was continuously oxygenated and magnetically stirred for 30 min before and also throughout the perfusion period. Its pH was monitored continuously and adjusted to pH 7.4 using 0.1 M sodium hydroxide or hydrochloric acid, as appropriate. When albumin was required in the system (as the binding protein), a previously prepared concentrated solution of purified HSA (6%) was added. The volume added depended upon the required final albumin concentration in the perfusate. This solution was added to the perfusate just before the perfusion system was switched from KHB to albumin-perfusate. This prevented denaturation and foaming of albumin caused by oxygenation.

Since the albumin solution was acidic, the pH was again adjusted to 7.4. All experiments were carried out in the enclosed, thermostatically controlled cabinet maintained at 37±0.5°C.

Bubble trap: The formation of gas bubbles was prevented by incorporating a bubble trap in line just before the pump.

Cannulae: Transparent vinyl tubing cannulae were used throughout, size 16 for the portal vein and size 14 for the vena cava.

3.3.2.2 Operating Procedure (Figure 3.3.6)

The rat was anaesthetised by intraperitoneal injection of pentobarbitone (50 mg/kg body weight). Sodium heparin, 250 U, was injected intraperitoneally to prevent blood clotting. The abdomen was opened through a mid-line incision, and mid-transverse incisions to right and left of the mid-line were made avoiding the larger vessels. Bleeding was minimised by clamping the major vessels of the abdominal wall with forceps. The intestines were then placed to the animal's left, between layers of tissue wetted with saline so that the liver, portal vein, right kidney, inferior vena cava and the bile duct became exposed. The thin strands of connective tissue between the right lobe of the liver and vena cava were cut and a loose ligature of silk (Ligature 1), size 3/0 was placed around the cava above the right renal vein. First, the bile duct was cannulated by a length of Portex tubing size PP10 cut at an angle to provide a sharp point. The bile duct was cut across half its diameter with fine scissors and the cannula was inserted and pushed to the point where the duct arose from its branches. Here it was secured with a ligature (Ligature 2). Two loose ligatures (Ligatures 3 and 4), were passed around the portal vein at intervals of 3-4 mm below the point where the vein divides to enter the separate lobes of the liver, and a third ligature (Ligature 5) was placed around the vein at a point distal to the liver. The portal vein was then cannulated with a 16 gauge Frankis-Evans needle, a double cannula, from which the sharpened central metal cannula could be withdrawn after insertion into the vein. This cannula usually became filled with blood. With care blood loss was negligible. The two loose ligatures were tied, securing the cannula in place; the third ligature was then tied, shutting off the blood supply from the viscera to the portal vein. The inside metal needle was removed leaving the cannula in position. Perfusion of the medium was then started, while care was taken to avoid air entering the portal vein. The hepatic artery remained open to supply the liver with blood throughout the surgical procedure. The thorax was quickly opened by a transverse incision just above and along the line of the insertion of the diaphragm and by two longitudinal incisions towards the head from the two ends of the transverse incision. The chest wall was flapped back towards the head and a

large pair of artery forceps was placed along the base of the flap and locked in position. The flap was then cut off. The vagus nerve and oesophagus were cut about 1 cm above the diaphragm in order to paralyse the diaphragm and to eliminate possible vasomotor effects of the vagus. A loose ligature was placed around the inferior vena cava close to the heart (Ligature 6).

The cannula which was placed in the inferior vena cava consisted of a 5-cm length of Portex tubing which had been heated in a gas flame, drawn out to an outside diameter of 2 mm and cut off at an angle to form a sharp tip. This was sharp enough to penetrate the right atrium; it was pushed down the vein towards the diaphragm and tied in position. The outflow fluid (consisting of blood and perfusion medium) was discarded. At this stage the loose ligature around the abdominal vena cava was tied. The whole operation took about 10 min. There was an interval of about 30 sec from the introduction of the cannula into the portal vein during which the circulation was maintained by the hepatic artery alone. The admission of an air bubble to the portal vein or extended interruption of the liver circulation may cause an uneven perfusion, indicated by uneven colouring, from which the liver may not completely recover. Such preparations were rejected. An indication of the success of the operation was a uniform brown colour of the perfused liver. After cannulation, the preparation was moved into the cabinet and allowed to stabilise at 37°C for 15min during which time blood was washed out from the liver.

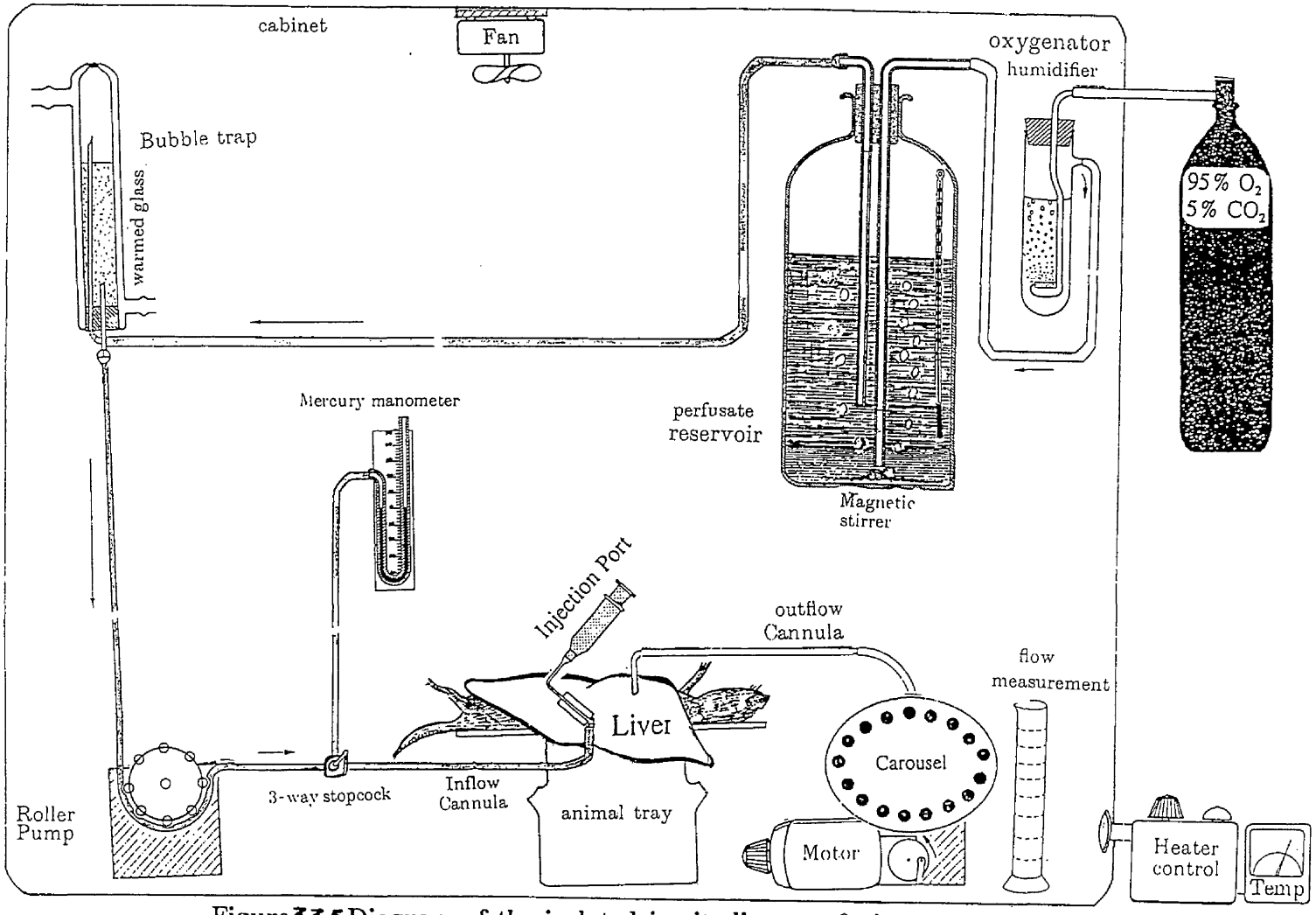

Figure 3.3.5 Diagram of the isolated *in situ* liver perfusion system

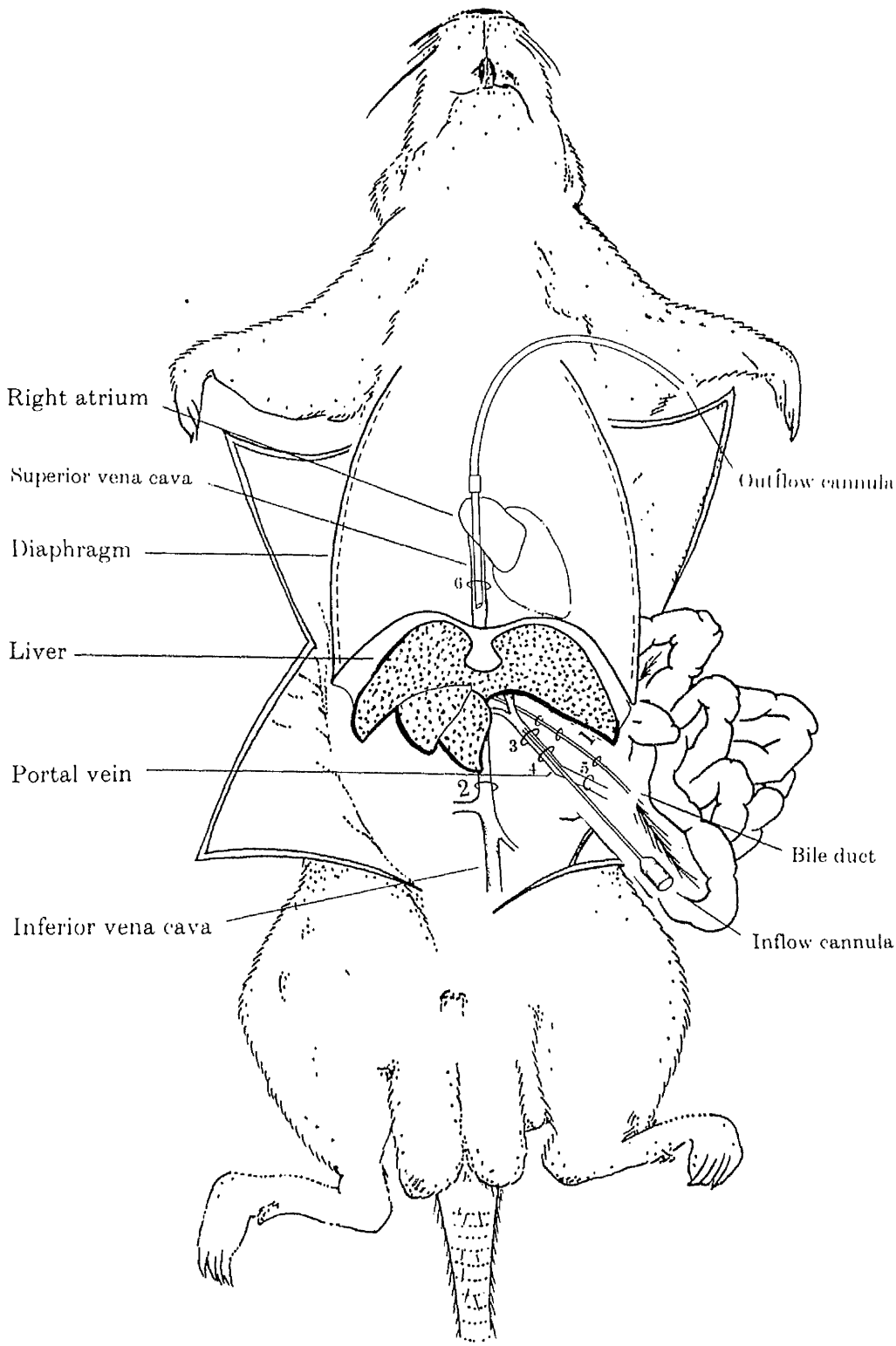

FIG. 3.3.6 Operative preparation for liver perfusion *in situ*. The abdomen and thorax are exposed as described in the text. Ligatures 1–6 are placed and the portal vein and inferior vena cava cannulated.

3.3.2.3 Viability of the liver preparations

The viability of the liver was assessed by several means; (a) gross appearance of the liver including its colour, (b) measurement of bile flow, (c) regular measurements of temperature, pressure, flow recovery and pH of the outflow perfusion medium, and (d) measurement of oxygen consumption of the liver. A dye (Evans blue) was also used to examine whether all parts of the liver were perfectly perfused. A concentrated bolus of dye was injected into the portal vein after the equilibrium period and the extent of perfusion to the isolated liver was visually verified. Only those liver preparations which were perfusing thoroughly were accepted. The removal of the dye from the liver was subsequently accelerated using 1% albumin solution.

3.3.2.4 Results

The success rate for the surgical procedure was 90%. The failed attempts included those preparations which failed one or more of the viability tests (*eg* unidentifiable perfusate leaks in the preparation), or to coming out of outflow cannula from vena cava in repositioning the preparation, or to liver ischemia owing to delay in cannulating the portal vein. The rate of failure increased in cirrhotic livers due to the following reasons.

a) Technical difficulties. Cirrhotic livers were more sensitive to pressure. They also showed a greater resistance to perfusion flow making the retaining of the inflow cannulae for portal vein more difficult.

b) Establishment of a cirrhotic liver. The treatment procedure for induction of cirrhosis results in some animals dying and some animals failing to meet the criteria of a fully developed cirrhosis. A willingness to limit the number of animals receiving CCl4 treatment and yet achieve a sufficient number of cirrhotic liver preparations placed great demands on this component of the procedure.

The probe dye proved to be an early and significant indicator of the state of perfusion. In control livers, it coloured the liver thoroughly and gradually washed away. Its dispersion within the cirrhotic livers was less uniform. The bile flow was normal and steady towards the end of dilution experiment and no difference was detected between the control and cirrhotic livers. The pH of outflow perfusate, compared to that in the reservoir, was reduced (about 7.1 compare to 7.44, respectively) indicating an active metabolism with no significant difference between control and cirrhotic livers.

3.3.2.5 Discussion

3.3.2.5.1 A review of techniques of liver perfusion

The first reports on liver perfusion techniques are as early as 1903 when Brodie [33] explained methods of perfusion for several organs. Since then, perfusion techniques have been developed. The emphasis in recent years has been upon simplifying techniques in order that they become more reproducible.

The numerous methods offered in the literature for liver perfusion may be reduced to those introducing differences in principle. There are four main methods and represent what most experiments require from an isolated perfused rat liver. These methods including a) Isolated liver perfusion technique (using either diluted rat blood[102,168] or semi-synthetic liquids[254] as medium), b) Reverse perfusion technique (through vena cava)[281], c) Perfusion of hepatic artery [237,238], and d) Liver *in situ* [111]. The *in situ* liver perfusion technique has the following advantages:

1) The operative technique is simpler and less liable to error. It may be readily performed by a single operator. Once set up, the preparation requires only minimal attention and may continue to function for the desired length of time without further adjustment.

2) The liver is not handled and is therefore not exposed to mechanical damage. The degree of trauma caused by excessive handling of the liver in the first method may influence the results of the experiments [102].

3) The operative time and anoxic period is much shorter.

4) Perfusion through hepatic artery or vena cava is not desirable because the metabolic and circulatory behaviour in perfusion *via* these routs is different to that of portal vein. Furthermore, perfusing the liver through the portal vein is sufficient and the liver functions normally without perfusion of the hepatic artery.

The "liver *in situ*" method, developed and modified by different workers [168,180,254], implies that the liver, although isolated from the rest of the animal, remains *in situ*. The perfusion medium enters the liver through the portal vein and leaves it through the vena cava. This method has been applied successfully over a period of years for permeability studies, drug distribution studies within the liver and physiologically-based phrmacokinetic modelling [60,231,228,229,230]. In this model, physiological conditions and rates of as many reactions as possible are reproduced.

3.3.2.5.2 The perfusion system

Apparatus: An apparatus and cabinet designed and built in the Department of Pharmacy were used throughout the studies. A number of advantages of a purpose built cabinet and apparatus has been discussed elsewhere [237]. The pump we used allowed us to well maintain the flow and pressure. The total output of the pump covered the required range of flow for perfusion experiments.

A pump with maximum fingers was used to minimise the effect of pulse perfusion on the steadiness of portal flow. In all indicator dilution experiments, typical unimodal patterns were obtained, indicating uniform mixing at the inflow and homogenous perfusion of the portal vascular bed. This procedure avoided a transient sharp increase in portal flow, as observed by Zeigler and Goresky [327], and the biphasic pattern of some dilution curves reported by Reichen [218] after hepatic artery injection of tracers, which can be best explained by a similar phenomenon.

Perfusion medium: It should provide an environment near to the state existing *in vivo*, *ie* of constant pH and temperature, a physiological concentration of the principal ions, and a suitable oxygen and carbon dioxide tension. It is desirable to use a perfusion medium which is defined and of reproducible composition. Thus, the medium may differ from the physiological 'ideal' [238,110]. The perfusion can be successful even if blood is omitted from the medium [109]. Today, perfusion with defined semi-synthetic medium has become a standard procedure and has been applied to many organs including the liver. Krebs-Henseleit bicarbonate is a reasonable medium for most studies involving liver perfusion and fulfils the requirements of a perfusion medium [254].

The duration of perfusion: Workers using semi-synthetic media have suggested an experimental time of up to 4 hours, although the liver does not 'fail' at this time [238]. When some of the components of the medium which allows prolongation of perfusion time (such as erythrocytes and albumin) are missing, the viability of the liver for the required duration of an experiment should be confirmed. Several viability tests were conducted in the present studies and the conditions of liver preparations (up to 2 hrs) were closely examined.

Gas supply: One of the requirements of an organ perfusion apparatus is that the medium reaching the organ contains sufficient oxygen to exceed the maximum requirements of the tissue under investigation. Thus, some form of oxygenator is used. A sintered-glass bubbler type oxygenator was used in this work which has been shown to be very efficient in saturating and maintaining the medium with the gases [238]. The oxygen content of the medium in the reservoir was 35mg/L, which reduced to 7mg/L in the outflow perfusate indicating a sufficient oxygen tension and normal liver function.

Bubble trap: Bubbles of gas could be troublesome in liver perfusion. Obstruction to capillaries results in uneven perfusion, so the extrapolation of distribution studies to weight of functioning tissue becomes inaccurate. This was prevented by incorporating a bubble trap in line just before the pump and was monitored throughout the perfusion experiment.

Cannulae: The cannulae were chosen to have as large an internal diameter as can be inserted into the required vessel. A large outflow cannula was chosen, in particular, to provide little resistance to flow, because 'back' pressure could affect perfusion. The material of the cannulae was strong enough to prevent its lumen being occluded by the ligature used to hold it in place.

Materials: Care was taken for the materials of the perfusion apparatus that come directly into contact with the perfused liver or the perfusion medium to be non-toxic to animal tissues. Translucent materials were chosen since gross appearance of cleanliness, the detection of bubbles, or simply changes in colour of the perfusion medium could be observed directly.

3.3.2.6 Optimisation of experimental design

Throughout the development of the surgical technique, improvements were continuously made to the system design. The perfusion pressure was measured at the start of each perfusion period using a mercury manometer connected by a side-arm anterior to the portal cannula; preparations which remained viable for the 2 hr perfusion period were readily identified, as the initial perfusion pressure was approximately 8 mmHg. Oxygenation originally involved direct gassing of perfusate with humidified oxygen and carbon dioxide. However, with albumin containing perfusate, this produced frothing of the perfusate which caused a reduction in the perfusate albumin concentration. Adding albumin at the final stage just before the impulse (administration

of diazepam and diclofenac) allowed for enough oxygenation without the problems of frothing. The length of the outflow tubing was reduced to 15 cm by placing the animal on a perspex platform suspended 5cm above the fraction collector. Over the course of the work, total surgery time has been reduced from 20 min to 10 min.

3.3.2.7 Criteria for acceptance

For a preparation to be considered successful, the following criteria need to be fulfilled:

1. The temperature of the perfusate should remain within 37±1°C.
2. The perfusate should remain within pH 7.44±0.05.
3. The oxygen content of the perfusate should remain above 25 mg/l.
4. The surgery should be neat and efficient and quick.
5. Upon cannulation, perfusate flow should be interrupted for less than 10 sec.
6. The initial perfusion pressure in control livers should be about 8 mmHg.
7. The colour of the whole liver should be uniformly light brown.
8. The initial volumetric recovery should not be less than 98%.
9. The end volumetric recovery should not be less than 95%.
10. Upon dye injection, the liver should be uniformly and thoroughly coloured.

The experiments reported had all adequate viability.

3.3.3 Microsphere Studies

It has been suggested that the percentage of shunted flow *via* the liver is increased in cirrhosis [148]. As shunting may have a significant impact on hepatic drug disposition, it was decided to investigate this matter using the microsphere technique.

3.3.3.1 Preparation of microsphere suspension

Microspheres (15 μm diameter, labelled with ^{57}Co, with specific activity of 56 dpm/microsphere) were obtained dry. All procedures were performed behind a lead shield using lead lined gloves and long tongs to minimise exposure. The microspheres were suspended in 5 ml 0.9% NaCl. After vortexing and sonicating, each for 10 min, a working solution of 33.3 mCi/ml (1.3×10^6 microspheres) was prepared. The surface-active agent tween-80 was added no more than three days before use to give a final concentration of 0.01%. The appearance of the microspheres was verified microscopically.

3.3.3.2 Application of microspheres

At the end of each liver perfusion experiment, whilst the liver was still being perfused by the perfusion medium, 100 μl of the microsphere suspension, which had previously been sonicated for 10 min and vortexed for 1 min, was injected into the portal vein over 15 sec. The hepatic outflow was collected from just before the injection until 5 min after. The samples were transferred into the scintillation vials and counted for 1 min. All possible sources of loss of microspheres such as the cannulae, stopcock, pipette tip and so forth were also washed and counted. The dose administered and background were estimated in triplicate. All samples were corrected for background. To assure that injected radioactivity was truly bound to the microsphere particles, an aliquot of stock microspheres was centrifuged, and the pellet and supernatant separately counted. It was found that 99.9% of the counts were present in the pellet, indicating negligible leaching of radioactivity from the microspheres.

3.3.3.3 Estimation of shunting

The total outflow gamma emission radioactivity was divided by the radioactivity of the dose administered multiplying by 100. The result represents the fraction of microspheres that bypasses the microcirculation in the sinusoids, a measure of shunting.

3.3.3.4 Results

Upon injection of microspheres into the normal livers, only trace amounts of microspheres were recorded in the outflow. The mean value was 0.76±0.6% ranging from 0.25% to 1.8% (n=5). In cirrhotic livers, the recovery was variable, ranging from 0.45% to 4.1% with a mean value of 2.1±1.4% (n=8). However, there were two cirrhotic livers having microsphere recovery of 7% and 11%. Because the indicator dilution experiment in these two livers were not complete and consequently their data were not analysed, the results of their microsphere recovery were not included here. The recovery of microspheres in both normal and cirrhotic livers never produced the profile of a dilution curve (Figure 3.3.7).

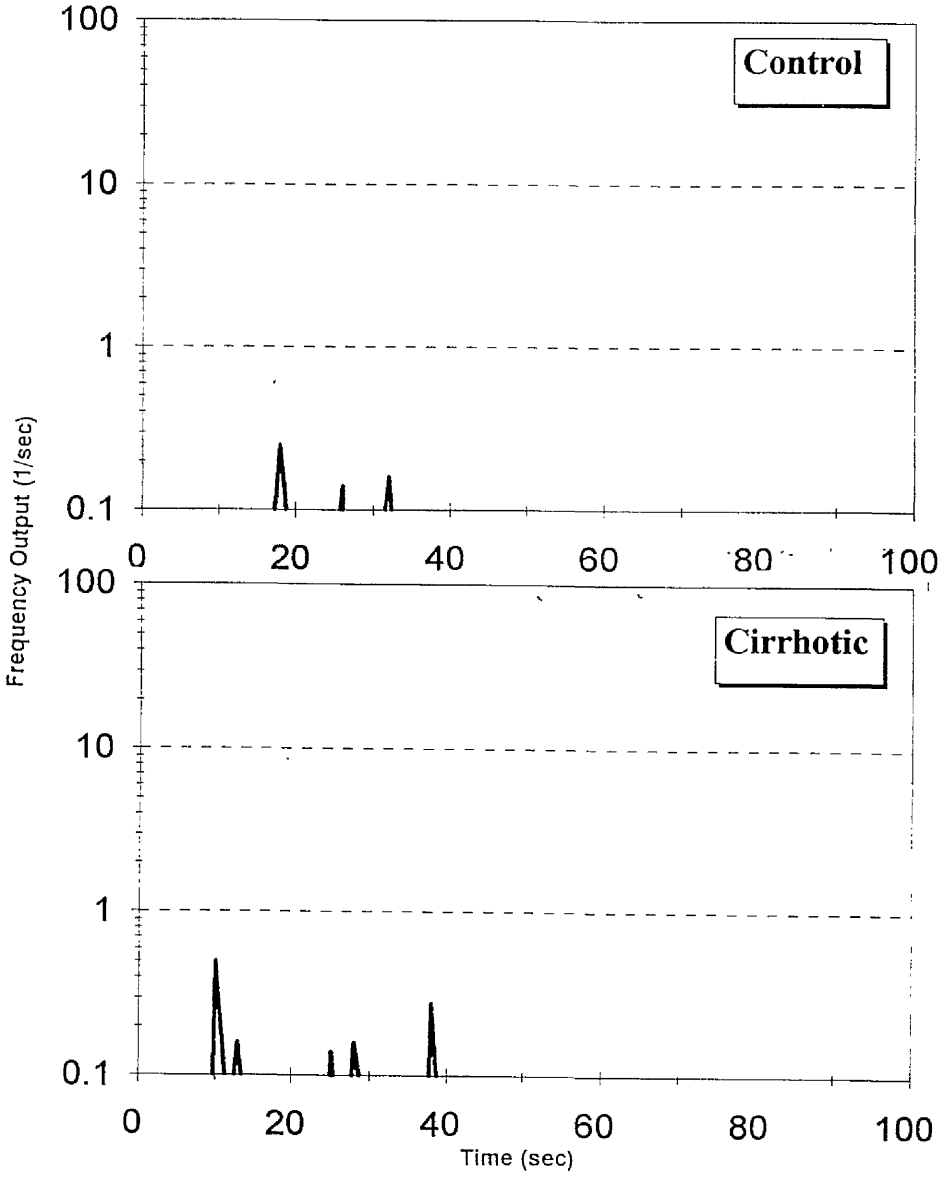

Figure 3.3.7 Typical outflow patterns of radiolabelled microspheres in isolated perfused rat livers. A) control livers: recovery=0.2%, B) cirrhotic livers: recovery 1%.

3.3.3.5 Discussion

Radiolabelled microspheres are widely used for studies of circulatory activity in experimental animals [248]; microspheres provide a momentary picture of the circulation. In employing microsphere techniques, a number of assumptions are made: their flow properties are similar to erythrocytes; the spheres reach their final destination within a 'few' seconds, 15 μm diameter spheres lodge in capillaries, once lodged their location is permanent; embolization has an insignificant effect on the microcirculation. Use of microspheres in measurement of shunting, particularly in experimental cirrhosis, is well established (27,300) and is based on the fact that due to their larger diameter (~15 μm) compare to sinusoids (~10 μm) they are entrapped inside the sinusoids but pass through the shunts (larger diameter). Their presence in the outflow, therefore, is an indicative of shunting.

The presence of anastomoses between hepatic artery-portal vein, between hepatic artery-hepatic vein and between portal vein-hepatic vein in normal livers have been shown by means of latex cast electron microscopy [203]. These vessels carry only a small fraction of total organ blood playing a protective role in its physiology. During the course of cirrhosis, the diameter and number of these anastomoses increases forming portal-systemic shunts. This partially counteracts portal pressure [296] but greatly reduces the flow perfusing the sinusoids. The question arising is whether this increase in diameter is high enough to divert a large volume of blood away from the liver and make a significant impact on hepatic extraction.

The extent of shunting varies according to the species, cause, and severity of portal hypertension [48,129,296,203]. While models of prehepatic portal hypertension, such as partial portal vein ligation in the rat, are characterised by a maximal portal-systemic shunting (up to 90%) [296], CCl4-induced cirrhosis in the rat is usually associated with low degrees of portal-systemic shunting, ranging from 0.2 to 30% in several studies [218,148]. Some workers [129] have not been able to find any shunting in CCl4-induced cirrhotic rats. The extent of shunting in cirrhotic patients with developed oesophageal varices may be as high as 60%. In the present experiments, from 8 cirrhotic rats who developed oesophageal varices, 5 died before being used for perfusion experiment. From the remaining three, only 1 (4% shunting) was included in the analysis. The

high variability in the extent of shunting in cirrhotic rats has been similarly observed in patients with portal hypertension[48].

The presence of considerable portal-systemic shunting would result in the appearance of an early peak in the indicator dilution curve. This is because the portion of flow travelling in the short straight collaterals will emerge faster in the outflow than the portion travelling inside the hepatic vascular network. Such a double peak was not observed for any of the model substances. In fact, the microsphere recovery in these experiments did not exceeded 4% and never attained the profile of a dilution curve. These results confirm the earlier findings published by others[291].

The amount of shunting may be considered in modelling studies by two methods. One possible way is to estimate the shunting in each individual liver and allow for it in modelling studies (Equations 2.14 and 2.19) when the outflow profiles of dilution curves are described in that liver. Another way is basically to consider the collaterals as a separate parallel compartment of distribution for tracer and incorporate a new term in the above mentioned equations. As the estimated shunting in perfused livers in the present work was not substantial, no attempt was made to model shunting.

There is a potential error in estimating the amount of hepatic shunting. That is the use of defective microspheres. If microspheres are too old or are handled excessively, their radiolabelled cover may be separated from the core hence acting like a plasma soluble substance. This will overestimate the fraction of shunted flow. On the other hand, if the suspension of microspheres is not sonicated properly or a surface acting agent (*eg* Tween-80) is not used, there will an error in the dose administered and the fraction of shunted flow will be underestimated. In none of the studies reported in literature are these issues addressed. Thus, the validity of the estimation of shunting is unclear.

The existence of large intrahepatic shunts (10-200 μm diameter) shown in vascular corrosion-cast studies[8], may be explained by the fact that cast preparation requires high-pressure injection for satisfactory penetration of all vascular systems. At very high perfusion flow rates, the number and diameter of perfused collaterals are increased allowing for more microspheres to bypass the sinusoids. Thus, the perfusion flow plays an indirectly important role in estimating shunting.

Using high flow rates in *in situ* perfused liver preparations may lead to similar situations. The perfusion flow rates used in the current studies were in the range of physiologic values making the estimation of shunting closer to the physiologic situation.

3.3.4 Protein Binding Determination

The purpose of this study is to estimate the unbound fraction (fu) of diazepam which was used as model drug in the isolated perfused liver studies (Chapters 4 and 5). The degree of binding of diazepam to human serum albumin (HSA) was determined by equilibrium dialysis. All concentrations were measured in a 0.2 ml aliquot by radiochemical analysis. All glassware were silainised. The degree of binding of diclofenac was also estimated using ultracentrifugation technique, which is briefly explained at the end of this section.

3.3.4.1 Dialysis apparatus

Equilibrium dialysis was performed using two chambered Teflon dialysis cells, each of 1mL capacity. Cellulose (size 32/32) was used as the dialysis membrane and all measurements were at 37oC. Visking tubing, cut into 1 inch squares, was soaked in distilled water for 15 min and then in 30% v/v aqueous ethanol for a further 20 min. The membranes were rinsed in distilled water for 30 min, soaked in buffer (Krebs-Henseleit bicarbonate, ph 7.4) for 15 min and finally allowed to soak overnight in fresh buffer. The dialysis system was rotated at a fixed rate of 20 rpm.

3.3.4.2 Preliminary experiments

3.3.4.2.1 Stability: The stability of diazepam was assessed using a drug solution of 1 mg/ml, prepared in buffer. The solution placed into a 37°C water bath and aliquot samples were taken at 1, 2, 3, 4, 5, 6 hrs during the experiment and measured. The concentration of diazepam did not change noticeably during the experiment (from 1.00 to 0.97) indicating that it is stable for at least 6 hr under the conditions studied.

3.3.4.2.2 Equilibrium and adsorption: To investigate the time to reach equilibrium and non-specific absorption of diazepam, the dialysis procedure (see below) was performed on diazepam using spiked buffer. Duplicate samples were withdrawn at 15 min intervals for the first hr, at 30 min intervals for next 2 hr and then hourly for the final two hr, a total of 5 hr in all. In five of the dialysis cells, no membrane was used so that adsorption of drug onto the cells could be estimated. Equilibrium was achieved when diazepam concentration in the buffer side was equal to that in albumin side. From experiment, this ratio at 1, 2, 3, 4, and 5 hr were 0.71, 0.94, 1.01, 0.98, and 1.00, respectively. Thus, equilibrium was reached within 3 hr. Binding of diazepam to the experimental system was negligible, as indicated by high total recovery of the drug (95±2%).

3.3.4.2.3 Volume shift and unbound fraction: To assess the magnitude of volume shift, 1 ml of diazepam (1 mg/l in 0.05, 0.1, 1, and 2% HSA-buffer solution) was dialysed against 1 ml buffer. Four cells were prepared for each concentration. After equilibrium, the solutions from each chamber were expelled by pushing air through the cells, using a one-ml pipette, and collected into pre-weighed test tubes. The postdialysis HSA and buffer volumes were obtained assuming the density of both solutions to be equal to 1. The ratio of HSA-volume to buffer-volume for the albumin concentrations used were 1.05±0.0.08, 1.11±0.07, 1.02±0.06, and 1.02±0.05, indicating that the magnitude of volume shift was small. Therefore, the unbound fraction of diazepam was taken to be the ratio of the concentration of ^{14}C-diazepam in the buffer chamber to that in the albumin-containing chamber at the end of dialysis (*ie* at equilibrium).

3.3.4.2.4 Effect of drug concentration: The effect of drug concentration on protein binding was investigated as follows. Four different solutions of ^{14}C-diazepam were prepared in buffer containing 1 mg/l diazepam and 1% HSA. The diazepam activity ranged from 0.005 to 0.1 μCi. Four cells were prepared for each concentration. The degree of binding was concentration independent over the range studied for diazepam (Table 3.3.4).

Table 3.3.4 Unbound fraction of diazepam at different drug radioactivity (mean±SD; n=4)

Diazepam Radioactivity (μCi)	*f*u
0.005	0.066±0.003
0.01	0.070±0.003
0.05	0.072±0.003
0.1	0.077±0.003

3.3.4.2.5 Effect of liver perfusion: To assess whether the binding of diazepam was influenced by passage through the liver, the fraction unbound of diazepam was determined in a set of perfusate samples collected from the venous effluent, including protein-free samples. At each HSA concentration, the binding of diazepam in hepatic outflow samples was almost identical to that determined in fresh perfusate suggesting that binding was not influenced by passage through the liver (Table 3.3.5). The unbound fraction of diazepam in protein-free perfusate collected from the effluent of different liver preparations (n=5) was 0.98±0.03, indicating that the drug did not bind to material escaping from the liver into the perfusate during the experiment.

Table 3.3.5 Unbound fraction of diazepam at different HSA concentration (mean±SD; n=4)

HSA(%)	*f*u	
	Fresh Perfusate	Hepatic effluent
0.1	0.402±0.022	0.415±0.030
0.5	0.115±0.004	0.116±0.004
1	0.070±0.003	0.081±0.004
2	0.035±0.004	0.041±0.004

3.3.4.3 Determination of fraction unbound

Stock solution (10 mg/ml) of diazepam was prepared in methanol. A 1 mg/l solution of diazepam was prepared in varying concentrations of HSA (0.1, 0.5, 1, and 2 g/dl, %; 1%=0.14 mM) solution in buffer. One ml of this perfusate containing 0.01 μci of ^{14}C-diazepam [60] was pipetted into one chamber of dialysis cell. One ml of buffer was pipetted into the other chamber. Four cells were prepared for each concentration. The apparatus was placed in water bath and rotated for 4 hr. Duplicate samples were withdrawn. The concentration of ^{14}C-diazepam in both chambers was determined. The association binding constant (ka) was calculated as

$$ka = \frac{1 - fu}{fu.Pt} \qquad (3.2)$$

where Pt is the total HSA concentration [376].

The estimated value of ka (13.95±1.25) indicates the high affinity of diazepam to HSA (Table 3.3.5). The data showed a progressive increase in binding (reduction in *f*u) with increase in HSA concentration. The relationship between unbound fraction of diazepam and HSA concentration is depicted in Figure 3.3.8.

3.3.4.4 Discussion

Loss of drug during equilibrium dialysis (due to decomposition or binding to experimental system) may lead to an underestimation of *f*u [117]. On the other hand, adsorption of drug to the dialysis cells may significantly increase the equilibrium time [162]. Because diazepam is highly bound to HSA, any considerable loss to the system might not be immediately apparent. Therefore, non-specific binding of diazepam to the system was determined in the absence of HSA. The complete recovery of diazepam, within the experimental error, indicated that diazepam binding to the apparatus was negligible. These results confirm earlier observations of other workers in this laboratory [60].

The significance of volume shift has been addressed by several workers [30,56]. Based on theoretical considerations [118], when the volume shift is less than 10%, the associated error is insignificant. However, when the volume shift is greater than 10% and *f*u is less than 0.1, the error is significant and should be corrected. Using varying concentration of HSA, the degree of volume shift in the current experiments ranged between 2 to 11% (1.05±0.04). Thus, no correction step was considered.

The concentration of diazepam in the steady-state perfusion studies (Chapter 5) was 1 mg/l. Due to the strong affinity of diazepam to HSA, it is technically difficult to estimate *f*u at this low concentration. This made the use of radiolabelled diazepam necessary. The extent of binding in the current work is in good agreement with previous reports [60].

3.3.4.5 Diclofenac binding to HSA

Radiolabelled diclofenac was added to perfusate solutions (5 ml) to produce a final concentration of 1 mg/l, and incubated at 37°C for 45 min. After ultracentrifugation (50,000 rpm at 37°C for 15 h), an aliquot (500 µl) of the protein-free solution was withdrawn in duplicate and measured radiochemically (Section 3.3.6). The *f*u of diclofenac within the perfusate was calculated as the ratio of the average concentration of ^{14}C-diclofenac in the protein-free solution to that in the precentrifuged perfusate sample. At HSA concentration of 1% (the HSA concentration used in bolus experiment; Chapter 4), the estimated *f*u was 0.008±0.001 which is similar to the values estimated for diclofenac in this laboratory previously [120].

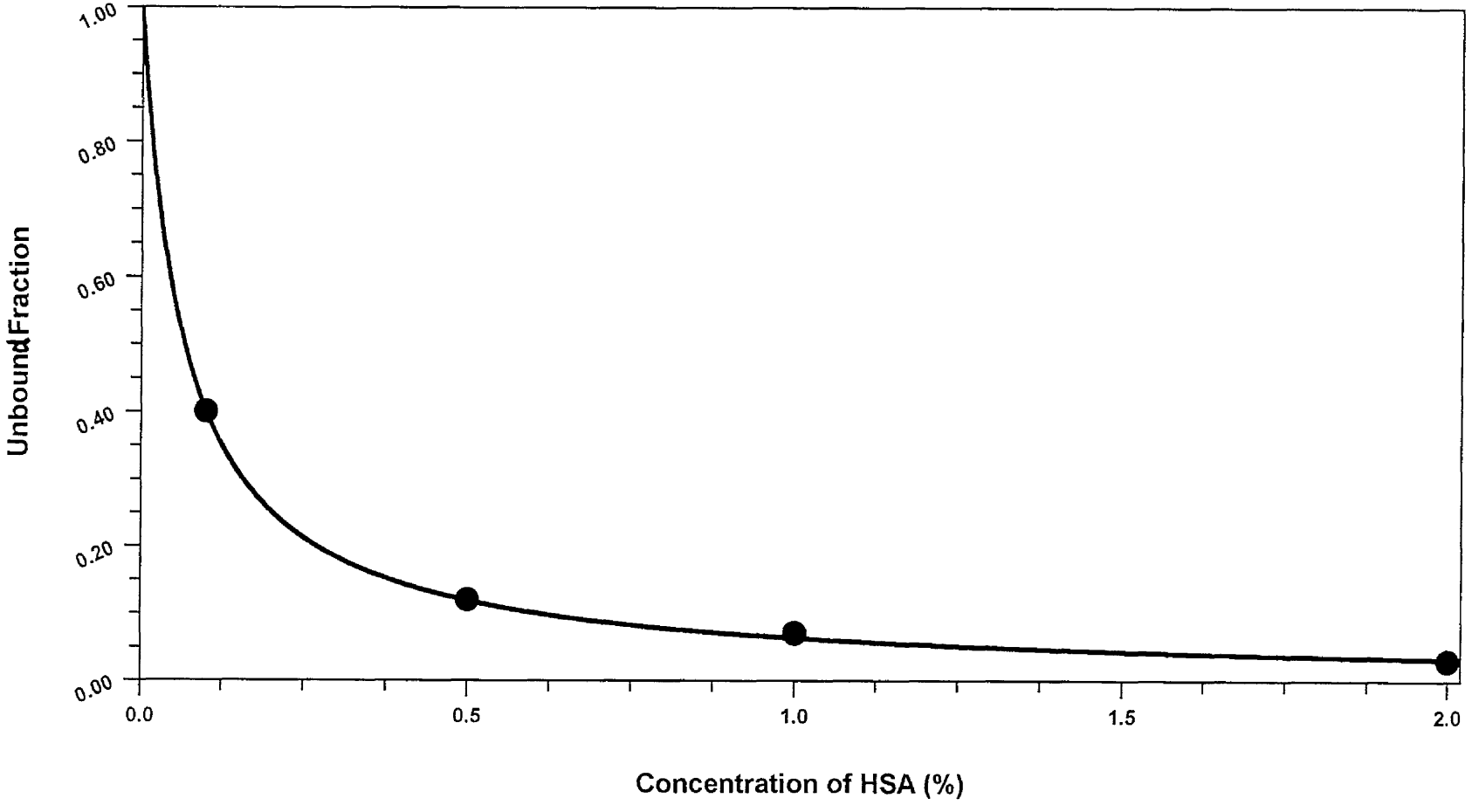

Figure 3.3.8 Relationship between unbound fraction of diazepam and albumin concentration. The solid line is the fitted curve.

3.3.5 Purification of Serum Albumin

Human serum albumin (HSA) was used as binding protein in the perfused liver preparations (Chapter 4). It was necessary to purify albumin from impurities which reduce its binding efficiency. The method of Chen [41], based on charcoal treatment, was used for this purpose.

3.3.5.1 Method

HSA (40 g) is dissolved in 400 ml of distilled water and the solution placed in an ice bath at 0°C. Charcoal (20 g) is added and the solution titrated to pH 3.0 using 1M HCl. The solution is stirred magnetically for 1 hr, maintaining the temperature at 0°C. After 1 hr, the charcoal is diluted to 4 gram percent and centrifuged down at 0°C for 20 min at 20,000 rpm. Some losses occurs during this process but much charcoal remains in suspension. The residual charcoal is removed by filtration through a millipore 0.22 μm filter. The albumin solution is then titrated to pH 7.4, at 0°C using 1M NaOH. Final traces of charcoal are removed by filtration through a bed of BDH Kieselguhr.

3.3.5.2 Measurement of albumin

Albumin concentrations were measured using a commercial diagnostic kit (Sigma Chemicals). The principle is that bromcresol green binds with HSA to form an intense blue-green complex with an absorbance maximum at 628 nm. The intensity of the colour produced is directly proportional to the albumin concentration in the sample.

3.3.5.3 Results

The commercial albumin solution used had an initial concentration of 20 g/l. After the purification procedure, the concentration of albumin was reduced to 6.5 g/l. This latter solution was then used for the preparation of various concentrations of albumin in perfusion medium. The purification procedure resulted in the binding capacity of HSA to increase substantially (judged by the fu of diazepam). The results are presented in Table 3.3.6.

Table 3.3.6 Unbound fraction of diazepam in different albumin concentrations before and after albumin purification (mean±SD, n=4)

Albuminconcentration(%)	*fu*	
	Before	After
1	0.433+0.085	0.070+0.003
2	0.376+0.086	0.035+0.004
6	0.203+0.021	0.018+0.001

3.3.5.4 Discussion

Serum albumin preparations contains variable amounts of lipid impurity [41,49]. The bulk of the impurity appears to consist of free fatty acids, saturated fatty acids and ketones. In many past studies, using albumin as binding protein, not enough attention has been paid to such contaminations [75] and is not clear whether albumin impurities have influenced the results of such studies. Binding studies involving albumin could be drastically altered depending on whether the ligand of interest competes for a site occupied by fatty acid contaminants; an example of such a situation is the binding of tryptophan [41] by HSA. As the present work aimed to study the influence of protein binding on the hepatic dispersion and extraction of diazepam over a wide range of fraction unbound in the perfusate (Chapters 4 and 5), it was desirable to purify the albumin from such impurities. Various procedures have been described for this purpose [41,339,340]. As the method of Chen is quicker, more efficient and does not entail the risk of denaturation than other methods, it was chosen for removing fatty acid impurities and other contaminants.

Based on the original method, it was anticipated that centrifugation followed by one step filtration was needed to remove charcoal from solution. However, ultra-centrifugation, even at very high speed, was not enough to efficiently remove charcoal from the solution. One step filtration also resulted in traces of charcoal being left in the solution. This was not acceptable, as it resulted in erroneous estimation of fraction of drug bound to albumin. The measure undertaken to overcome this problem was to omit the centrifugation step and incorporate step-by-step filtration, using a series of different size filters. This filtration, when combined with Kieselguhr filtration, was found to be more efficient and quicker than the original method. The resultant albumin solution was perfectly clear and no traces of charcoal was observed under light microscopy. It should be mentioned, however, that application of Kieselguhr causes some degree (~10%) of albumin loss.

3.3.6 Radiochemical Analysis

3.3.6.1 Introduction

The elements Hydrogen and Carbon form the basis of all organic compounds. Tritium and Carbon-14 are the radioactive isotopes of Hydrogen and Carbon that decay with the emission of Beta radiation. Substitution of an active isotope for the stable nuclei does not change the chemical or biological properties of the organic compound. These isotopes are, therefore, ideal for labelling and tracing studies [200].

In the analysis of β-labelled samples, energy transfer is not perfectly efficient and immune to the nature of the immediate environment. There are two potential problems in this regard; quenching and chemiluminescence.

3.3.6.2 Quenching

This term is applied to any factor that reduces the light output in the system. Most samples exhibit variations in counting efficiency which is caused by the non-uniformity of the vials, the amount of oxygen dissolved in the solvent, and the variable absorption of photons by the sample itself. Three types of quenching can be defined [62].

1. Impurity quenching (chemical quenching): This arises when the yield of energy is decreased by the presence of other molecules which compete with the solute molecules for the excitation energy of the solvent molecules.

2. Colour quenching: Coloured samples can arise from either chemical or photochemical reactions in the scintillator solution promoted by the labelled material, or the incorporation of coloured materials (*eg* haemoglobin). The effect is to diminish the path of fluorescence photons with a resultant impairment of light collection efficiency at the photomultipliers.

3. Photon quenching: The incorporation of intractable substances into a cocktail may result in a heterogeneous counting mixture. In these cases the maximum interaction between the β energy and the solvent plus solute is not achieved, which is a type of self-absorption effect [76].

It is often impossible to avoid quenching but by applying simple rules its effect can be minimised [62]. These are a) by keeping the concentration of quencher low; b) by increasing the concentration of primary solute; c) by cooling to reduce the diffusion coefficients of quenching molecules and hence the probability of a quench collision. There are several methods for quench correction. In

our work, we applied the most common and efficient method, referred to "Internal Standardisation Method" [200]. In this method, spikes of the isotope, in an unquenched form, are added to the sample which is then recounted. Comparison of the count rate before and after the spike is added enables a correction for quenching to be made.

3.3.6.3 Chemiluminescence (CLM)

The liquid scintillation spectrometer has been designed to measure even small quantities of light. This means that the counter readily responds to light from sources other than the emission of the scintillator [326]. These light sources are plastic caps, any impurity, static charges from movement of the vials, and the production of a CLM reaction in the sample. Light-producing chemical processes can arise in a variety of ways during sample preparation; a) from the presence of oxygen in the sample, b) from the presence of peroxides, c) alkaline solutions, and d) from any kind of contamination such as tissue samples.

The cures for chemiluminescence are many and varied. The most obvious is to avoid strongly coloured samples. The others include optimisation of pH, flushing the scintillator with nitrogen, addition of an antioxidant, reduction in temperature of the counting chamber, and a period of storage in the dark [62]. Modern instruments are fitted with photon monitoring which can distinguish between true sample counts and the single photon events caused by other light-producing processes and correct for it.

3.3.6.4 Sample Analysis

3.3.6.4.1 Beta emitters

The scintillation counter used throughout the project has an in-built spectrum and a Wallac quench library. By defining factors such as vial type, type of scintillation cocktail and count time required, this can be fine-tuned for individual requirements. By comparison with an external standard, the spectral quench parameter [62] is estimated. This is able to correct for the extent of quenching, assuming equal quench for the external standard and samples. Protocols capable of counting ^{3}H and ^{14}C individually and ^{3}H &^{14}C simultaneously were set up on the scintillation counter and verified by standards. It is possible to count these pairs of isotopes due to the differences in their photopeaks and the small degree of overlap in the energy spectra.

For all liquid outflow samples, 5 ml scintillation fluid were added and vortexed and left for 1 hr. The samples were then counted on the appropriate channel. Tissue samples required dissolution (Chapter 6), after which 12 ml scintillation fluid were added, vortexed and left for a week in cool-dark place. The samples were counted on ^{3}H &^{14}C dual channel. Efficiency was corrected for all samples and all results were obtained as disintegration per minute (dpm).

3.3.6.4.2 Gamma emitters

Erythrocyte gamma-emitting samples containing ^{51}Cr were counted on the gamma counter. A program was set up which incorporated the photopeak with minimum inclusion of background. All results were obtained as count per minute (cpm). Although ^{51}Cr is a gamma emitter, its decay is detectable and quantifiable at equal efficiency in a liquid scintillation counter.

3.3.7 Radiolabelling of Red Blood Cells

Red blood cells (RBC) have been used throughout this project as vascular reference marker. There are two methods for the measurement of RBC concentration. The first method involves attachment of a radionucleotide to the cells with measurement of radioactivity. The second method is a simple colourimetric method which involves haemolysis of erythrocytes and subsequent measurement of the colour using a spectrophotometer.

3.3.7.1 First method

This method is based on that of Kuehl *et al* [136]. Fresh blood (10 ml) is collected *via* the vena cava from normal rats into lithium heparin tubes and sodium heparin (5 U/ml blood) and neutral citrate (prepared by titrating 80 mM citric acid and 80 mM trisodium citrate to a pH of 7.4 at 22°C; this solution is mixed with 1 M NaCl and H_2O in a ratio of 95:4:1 v/v/v; its pH is 7.27 at 22°C) is added. One ml of this anticoagulant is mixed with an equal volume of blood. After thorough mixing, the red blood cells are concentrated by centrifugation at 1400 *g* for 10 min at 4°C. Plasma and buffy coat are carefully removed by aspiration, leaving 4-5 ml of packed red blood cells.

The packed erythrocytes are preincubated for 5 min at 37°C, after which time 1 ml (100 mCi) ^{51}Cr-sodium chromate is added with thorough and gently mixing. The mixture is incubated for 30 min at 37°C, 5 volumes of ice-cold normal saline are added and the cells concentrated by centrifugation. This washing step is repeated twice. The red blood cells are then resuspended in normal saline (50:50, v/v). The activity of the suspension is determined by gamma spectrometry (Section 3.3.6). 100 µl of this is injected into the portal vein of rat.

The extent of ^{51}Cr binding to RBCs was investigated by centrifuging three aliquots (1 ml) and determining the activity in the supernatant and the cells; in all experiments less than 2% of the total radioactivity after washing was extracellular.

3.3.7.2 Second method

Fresh blood is collected *via* vena cava from normal rats into lithium heparin tubes and sodium heparin and neutral citrate are added (as previously described). After thorough mixing, the red blood cells are washed twice and suspended in normal saline. 100 µl aliquot is used for injection

into the portal vein of rat. The outflow samples collected. 1 ml water is added to 200 µl aliquot from every sample. The mixture is then left overnight to allow for complete hemolysis of the erythrocytes and release of haemoglobin. On the following day, the samples are vigorously stirred and measured in 1 ml spectrophotometer cells set at 415 nm. The same procedure is performed on 200 µl outflow perfusion medium from the *in situ* perfused liver before the injection of RBC and the solution served as blank.

Both methods were tested in several preparations. Briefly, a bolus of ^{51}Cr-labelled erythrocytes with known activity was injected into the portal vein of perfused liver and the outflow samples were collected. This was followed by another bolus containing normal erythrocytes with known absorbance and the outflow samples were collected and counted. The normalised outflow profiles of erythrocytes counted by the two method were then compared. In another experiment, suspensions of normal erythrocytes with different concentration and suspensions of labelled erythrocytes with different activity were prepared and measured with the pertinent method. Concentration versus absorbance (or activity) profiles (*ie* standard curves) of the two methods were obtained and the correlation was compared.

3.3.7.3 Results

Figure 3.3.9 demonstrates the frequency outflow profiles of erythrocytes obtained by application of the first and the second methods into the same liver preparation. The shape of the curves and calculated vascular volume obtained from the two methods were similar. As presented in Figure 3.3.10, there was a good correlation between the two methods of measurement of erythrocytes.

3.3.7.4 Discussion

Measurement of vascular volume in a given organ requires a probe which is accessible to the vascular spaces of the organ. This is usually performed using erythrocytes. For isolated organ preparations, such as the perfused liver, erythrocytes may be simply administered into the stream perfusing the organ and the outflow samples are collected and measured by an spectrophotometer. However, measurement of vascular volume in the whole body (*in vivo*) studies, requires prior labelling of erythrocytes. This allows tracing the cells within the vasculr network of the body and its blood content. Thus, for *in vivo* studies the first method and for *in situ* studies both methods are applicable.

One potential problem of handling of erythrocytes is hemolysis. The idea of using erythrocytes is based on the fact that as they remain within the vasculature, they give an estimate of vascular volume. If however they lyses, the released haemoglobin gains access to some extravascular volume. This results in the overestimation of the vascular volume. This problem could be minimised using fresh blood, a proper washing procedure, and use of precisely made isotonic solutions.

The second method is quicker and requires less handling of RBCs than the first method. This ensures that the erythrocytes are better preserved and less susceptible to hemolysis. This advantage, together with safety considerations, favour the second method when it is applicable. In this project, the first method was originally adopted for the measurement of erythrocytes prior to the knowledge of the second method. A good correlation was observed between the two methods in several liver preparations. As only the first method was used in all liver preparations, the results of the estimated vascular volumes measured by this method are presented in Chapter 4.

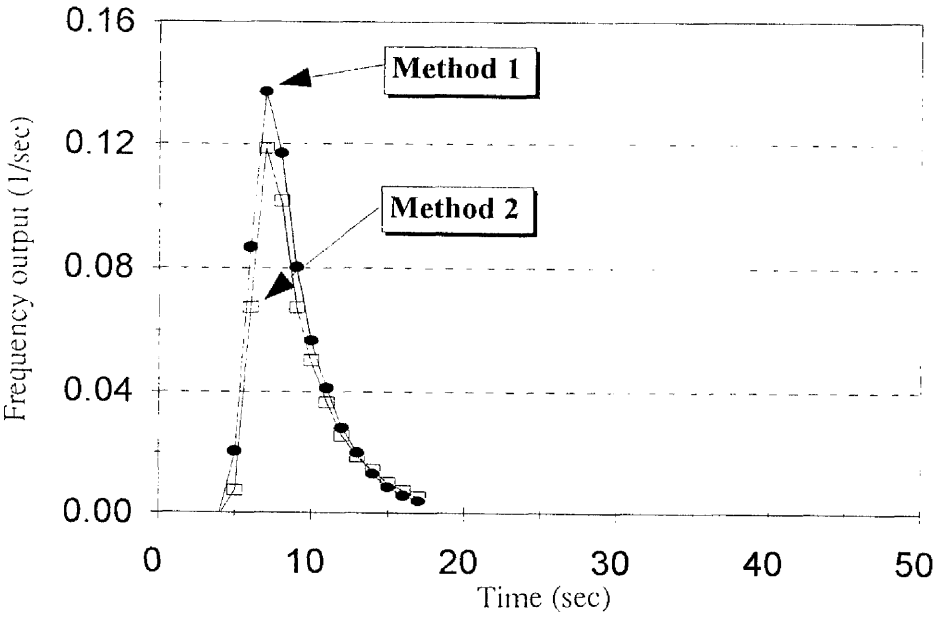

Figure 3.3.9 Frequency output profiles of erythrocytes in a representative normal rat liver measured by the first and second methods of analysis.

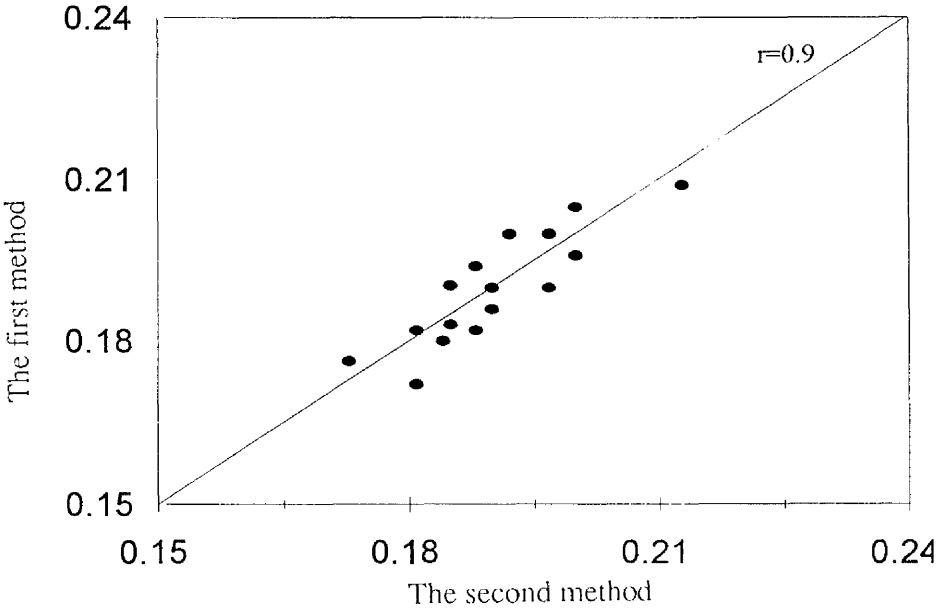

Figure 3.3.10 Diagram illustrates the correlation between the first and second methods of measurement of erythrocytes for the estimation of vascular volume in normal rat livers..

CHAPTER FOUR: STUDIES IN EXPERIMENTAL CIRRHOSIS

Section One: Bolus Considerations

4.1 Introduction

In contrast to other organs where the capillary presents a substantial barrier between the vascular and interstitial space, the first barrier encountered by a substance entering the liver is the hepatocyte membrane [313]. In hepatic cirrhosis, the normal structure and function of the liver is disturbed and blood-tissue exchange is thought to be altered. This make the hepatic cirrhosis an attractive model for permeability studies in the context of drug disposition.

Several approaches have been used to estimate the membrane permeability of a compound in the liver [167]. The initial uptake rate method is a common approach used to obtain the permeability of the isolated hepatocytes. However the extrapolation of such *in vitro* data to the organ level should be taken with care. This is because the dynamic architecture of the liver is absent. The single-pass isolated perfused liver is a suitable preparation in which the permeability in an intact organ can be estimated while maintaining the normal architecture of liver. This system is particularly useful coupled with the "impulse-response technique". When a drug is injected in the form of a bolus into the blood supply of the liver, the observed concentration versus time profile in emerging blood can provide valuable insight into the processes that act on a drug during passage through the liver. In this manner factors such as perfusate flow rate and drug binding to perfusate components are readily controlled [60,63,64,65,242].

Although the impulse-response technique has been used to characterise the microcirculation in hepatic cirrhosis [291], no study has been conducted to specifically investigate the influence of permeability alterations associated with cirrhosis on the parameters of drug distribution and elimination. The present study, which was designed for this purpose, also provides an opportunity to examine the dispersion model which has been used to describe the residence time distribution (RTD) of non-eliminated tracers [223] but has not been extensively applied to substances for which membrane permeability, perfusate and cellular binding and hepatic extraction may influence the shape of the RTD.

4.2 Experimental Design

In this study, the "indicator dilution technique" was used to investigate the influence of hepatic cirrhosis on hepatic drug disposition kinetics. Three drugs, salicylic acid, diclofenac and diazepam were chosen as model substances. To define the hepatic spaces and transport processes and have a basis for interpretation of drug profiles, five established markers of hepatic circulation (erythrocytes as vascular marker, albumin and sucrose as extracellular markers, water and urea as total hepatic aqueous space marker) were used in the study. The three model drugs together with reference markers were injected in the form of an impulse to several cirrhotic and control liver preparations and their dispersion in the liver was characterised. A single-pass isolated *in situ* perfused rat liver system was employed.

Note: All reference markers and drugs employed in this study were radiolabelled materials. To avoid wordiness, each radiolabelled substance is referred to by its name, *eg* albumin to mean radiolabelled albumin.

4.3 Experimental procedure

After the stabilisation period (see Section 3.3.2), eight injections (three drugs and five markers) were administered into the portal vein of each liver in a randomised order. A rapid bolus of the tracer (50 μl) was introduced into the injection port using a 50 μl Hamilton syringe, the tip of which was placed after the inflow of the perfusate to ensure adequate mixing. The total hepatic venous outflow was automatically collected at 1-sec intervals using a motor-driven carousel with 57 sampling holes at the rate of 1 hole/sec for 1 min, and thereafter (into serial silanised test tubes) at 5-sec intervals for up to 4 min. The collection period was set for each tracer so that the activity measured in the last sample was always less than 0.5% dose. This was 1 min for erythocytes (RBC), albumin (ALB) and sucrose (SUC), 3 min for water (WAT), urea (URA) and salicylic acid (SAL), and 5 min for diclofenac (DCL) and diazepam (DZ). The effluent collection was started immediately after injection of the bolus with time zero being set as the time of injection. A washout period of 4 min was allowed after each bolus. An aliquot (250 μl) from each tube was used for the determination of gamma and beta activity, as appropriate, and processed as described in Section 3.3.6. At the end of each experiment, the liver was removed and weighed.

4.4 Data Analysis

In order to provide a basis for comparison between the tracers, the concentration of radioactivity (dpm/ml) of each tracer in the hepatic outflow at time t, C(t), was expressed as a fraction of the dose appearing per second, f(t), and plotted against the mid-point time of the collection period yielding a pattern expressed in terms of the frequency output. The expression

$$f(t) = \frac{C(t).Q}{Dose} \qquad (4.1)$$

was used, where Q is the perfusate flow rate (ml/sec), measured volumetrically, which was maintained constant throughout each experiment.

The above equation assumes that the solute is not eliminated so that the areas under the fractional outflow curves for all substances completely recovered from the outflow are the same and is denoted as=1. For model drugs which are eliminated, dose was multiplied by the fraction recovered. Two approaches were used for the analysis of the outflow data.

4.4.1 Model Independent Analysis (statistical moment)

Using an analytical software (Moment, version 1.2), the following parameters were calculated directly from experimental data (Equations 2.2-2.7, Section 2.2.2).

a) The total area under output concentration versus time profile (AUC) was calculated using the trapezoidal rule. As the activity in latter samples for reference markers was very low and to minimise artefact in data analysis, a cut-off point of 4 times the background level (at time tend) was chosen. In the case of the test drugs, all samples remained above that level hence a cut-off point was not required. Linear extrapolation of the downslope to infinity was carried out using a semilogarithmic plot. The maximum f(t) value, $f(t)_{max}$, and the time at which it occurred, t_{max}, were observed values.

b) Availability (F); two types of availability (recovery) were determined. Firstly, for all solutes availability was taken to be the total AUC from frequency profiles. For non-eliminated substances it should be equal to 1. A second type of availability was also determined for drugs. It was expressed as the ratio of the AUC to that of the non-eliminated albumin and/or water.

c) Mean transit time (MTT) and variance of transit time (VRT).

d) Hepatic volume of distribution (V_H or V); was expressed in terms of absolute (ml) and relative (ml/g liver weight) values.

e) The mean catheter transit time; the distortion of tracers inside the catheters was determined and all dilution curves obtained were duly corrected [121]. The catheter transit time was measured by the following methods:

I. The transit time through the combined injection device and collection catheter was determined for each liver perfusion experiment by using the volume (weight/density ratio) of perfusate (density=1.0) in the inflow and outflow cannulae, which were summed and divided by the flow rate.

II. In a separate perfusion experiment, the inflow and outflow cannulae (in the absence of the liver) were connected and an impulse was introduced into the inflow. Various parameters of this system (including MTT, V, D_N, F) were calculated. This procedure was conducted at various flow rates. The MTT values obtained from both methods were compared and were assumed to apply equally to all solutes.

The values obtained above were used to account for delay and distortion in non-hepatic regions of the perfusion system. Two methods were applied. In the first method, the catheter transit time was subtracted from the total observed tracer transit time. This method was used for the estimation of MTT and V of the solutes. In the second method, which was used for modelling, the MTT and D_N of the catheter were incorporated into the dispersion model.

4.4.2 Dispersion Model Analysis

Both one- and two-compartmental forms of the axial dispersion model (Chapter 2) were fitted to the frequency output data of the tracers. The outflow curves were constructed using a numerical inversion program (MULTI-FILT version 3.4; written in Fortran IV) [60,64,66,320,321,224,225,282], with a weighting scheme of $\frac{1}{y(t)_{observed}}$. Data for all solutes were analysed individually. The following parameters were subsequently calculated:

The volume of distribution (V) of tracers, the dispersion number (D_N), the rate constants of influx (k_{12}), efflux (k_{21}), and sequestration (k_{23}).

4.5 Results

4.5.1 Recovery

Table 4.1 lists the estimated recovery for all test substances in control and cirrhotic livers. For the reference markers in both control and cirrhotic livers, more than 96% of the administered dose was recovered, except for albumin in cirrhotic livers from which around 90% of the dose was recovered. As illustrated in the cumulative outflow profiles (Figure 4.1), each of the curves rises to a near constant value (complete recovery), but the time to reach this value varied. RBC was the first to be fully recovered followed by albumin, sucrose, urea and water. The extrapolated area for the markers was very small (3.2% in control livers and 4.2% in cirrhotic livers). The fraction for the test drugs was more variable. For diclofenac, it corresponded to around 9% in control livers and 4% in cirrhotic livers. For salicylate, the corresponding values were 5% and 8%, respectively, while for diazepam the values were greater, at 22% and 29% respectively. The relative recovery of drugs, when calculated with reference to the markers, was greater than values based on nominal dose administration.

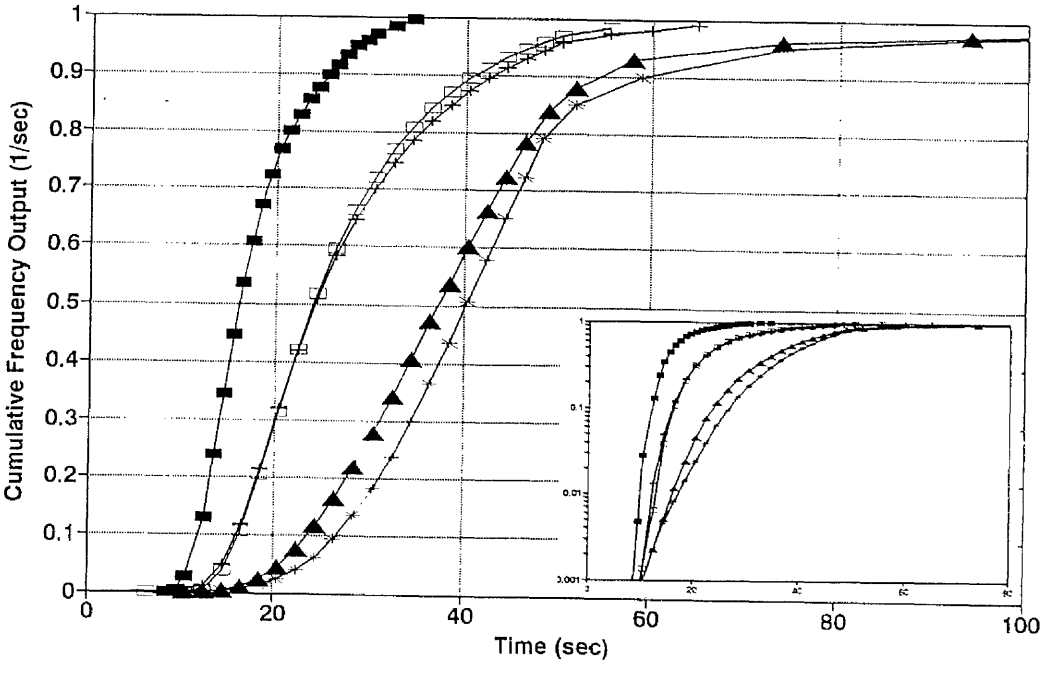

Figure 4.1 Typical tracer cumulative outflow profiles, following bolus administration of RBC (■), albumin (□), sucrose (+), urea (▲) and water (-) from the isolated perfused rat liver. Profiles are from an individual liver and expressed as the cumulative outflow of marker as a percentage of total recovered against its own midtime (min).

Table 4.1

Recovery (%) for various markers and drugs following bolus administration into the hepatic portal vein in situ perfused rat liver preparations.

		RBC		Albumin		Sucrose		Urea		Water		Diclofenac				Salicylate				Diazepam			
		Total	Ex	Total	Ex	Total	Ex	Total	Ex	Total	Ex	Total	Ex	to ALB	to WAT	Total	Ex	to ALB	to WAT	Total	Ex	to ALB	to WAT
Normal	mean	**101**	**3**	**96**	**2**	**100**	**4**	**98**	**3**	**96**	**4**	**78**	**8**	**81**	**81**	**83**	**5**	**87**	**88**	**60**	**17**	**63**	**63**
livers	±S.D.	2		3		2		5		3		5		7	5	7		7	7	10		10	12
n=10	C.V.(%)	2		3		2		5		3		6		8	5	8		8	8	15		16	17
PT*	mean	**100**	**3**	**95**	**3**	**99**	**4**	**98**	**4**	**96**	**4**	**73**	**9**	**77**	**77**	**81**	**7**	**84**	**84**	**57**	**21**	**60**	**60**
livers	±S.D.	2		3		4		4		3		6		8	5	7		7	6	11		12	12
n=5	C.V.(%)	2		3		4		4		3		8		10	6	8		8	7	14		18	18
Cirrhotic	mean	**100**	**2**	**90**	**6**	**98**	**5**	**100**	**3**	**93**	**5**	**89**	**4**	**100**	**100**	**91**	**8**	**100**	**99**	**58**	**24**	**65**	**63**
livers	±S.D.	2		4		4		3		2		5		10	3	5		9	3	12		10	10
n=12	C.V.(%)	2		4		4		3		2		5		10	3	3		9	3	19		14	14

*: phenobarbital treated
RBC: erythrocytes

Ex: fraction eluting beyond the last experimental point (estimated by extrapolation)
to ALB: ratio of drugs'recovery to the recovery of albumin
to WAT: ratio of drug's recovery to the recovery of water

4.5.2 Outflow Profiles

4.5.2.1 Profiles of reference markers in control livers

Figure 4.2 illustrates a typical set of dilution curves for reference markers from representative normal and phenobarbitone-treated (PT) control livers. In general, after an initial delay, the frequency outflow per second for each substance rose to a peak and then diminished mono-exponentially with time. Erythrocytes emerged first, their frequency outflow rose rapidly to form the highest peak, and then diminished the fastest. This was followed by albumin, which exhibited a peak that was slightly later and lower in magnitude and produced a more delayed downslope. Sucrose emerged later with a lower and wider peak. Urea peaked much later and the curve was of a much lower magnitude decaying in a much more prolonged fashion. Water was the last marker to emerge and the curve produced the lowest magnitude decaying in a more prolonged fashion. Dilution curves for urea and water were associated with a tailing-off appearance.

Table 4.2 lists the observational parameters including $f(t)_{max}$ and t_{max} for the reference marker curves and expresses frequency outflow pattern in a numerical fashion. The $f(t)_{max}$ decreased (mean values in parenthesis; 1/sec) from RBC (0.11) to ALB (0.053), SUC (0.05), URA (0.02), and WAT (0.018). The t_{max}, on the contrary, increased from 11.5 sec for RBC to 16.5 sec for ALB, 18.5 sec for SUC, 30.5 sec for URA, and 39 sec for WAT. The outflow patterns of reference markers in PT livers were similar to those observed in normal livers (Figure 4.2) and the slight differences in their $f(t)_{max}$ and t_{max} values were not significant.

4.5.2.2 Profiles of model drugs in control livers

Although all three drugs eluted in a prolonged mono-exponential fashion, notable differences were observed between their output curves (Figure 4.3). The output profile of diclofenac was associated with a relatively late peak ($f(t)_{max}$ = 0.035) occurring at approximately 17 sec followed by a slower eluting flat tail. The frequency outflow of salicylate rose slowly to a maximum ($f(t)_{max}$ =0.017) and after a greater amount of time had elapsed (55-75 sec) then began to diminish. The frequency output of diazepam rose more slowly to give a lower maximum ($f(t)_{max}$ =0.0065) and eluted over a longer period of time. The maximum outflow, which did not display the shape of an identifiable peak, eluted from the experimental system over approximately 50 sec. Among the three drugs, diclofenac was the first curve to display a decrease with an elution that was completed within 3 min. Next it was salicylate which decreased, taking approximately 250 sec to be completely eluted. The elution of diazepam was not completed within the perfusion

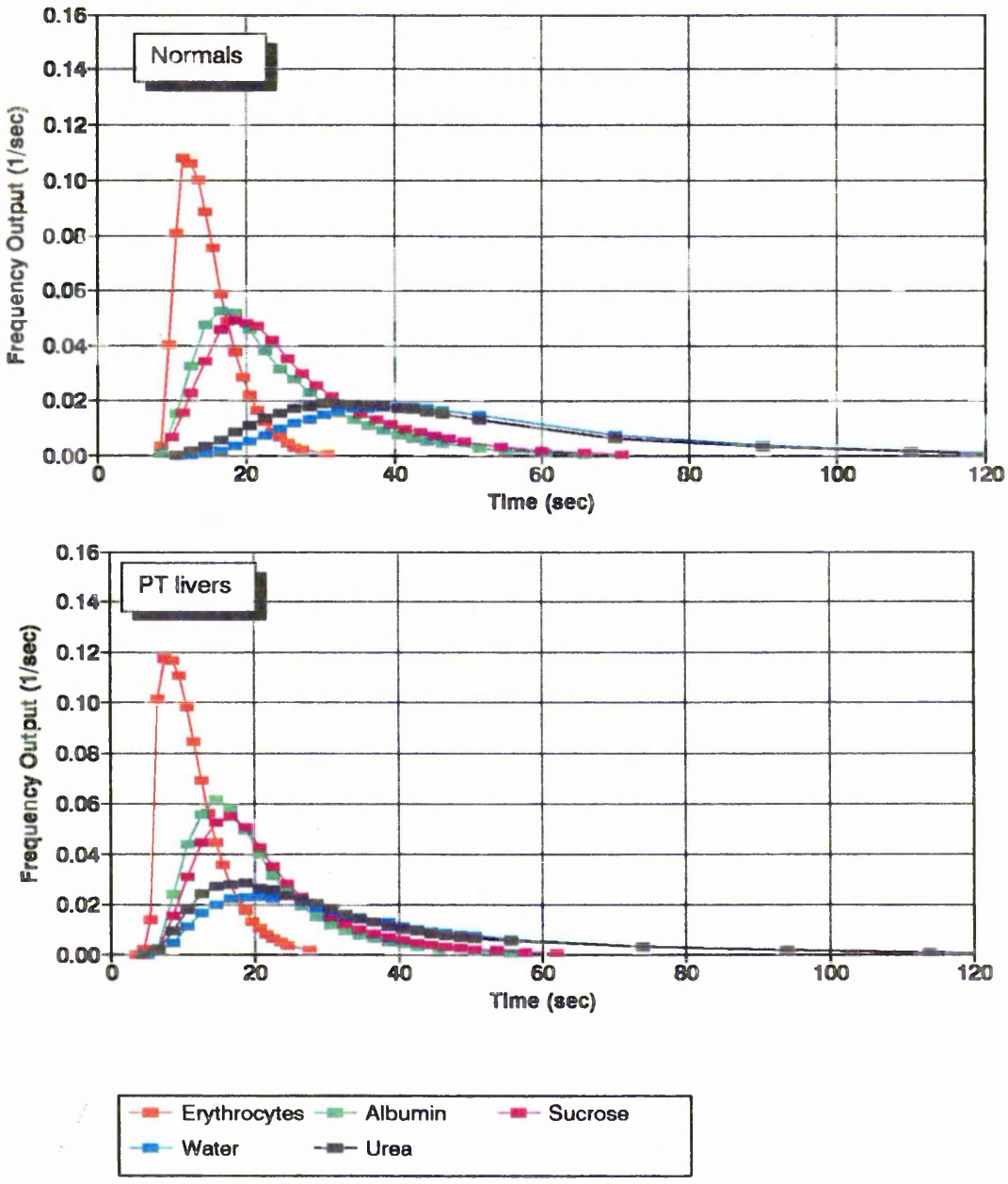

Figure 4.2 Typical frequency output profiles of reference markers in isolated perfused rat liver preparations.

Table 4.2

Observational parameters for various markers and drugs in the isolated perfused rat liver preparations.

		f(t)max (1/sec)								t-max (sec)							
		RBC	ALB	SUC	URA	WAT	DCL	SAL	DZ	RBC	ALB	SUC	URA	WAT	DCL	SAL	DZ
Normal livers	**Mean**	**0.110**	**0.053**	**0.050**	**0.020**	**0.018**	**0.019**	**0.009**	**0.002**	**12**	**17**	**19**	**31**	**39**	**12**	**47**	**40**
n=10	±S.D.	0.022	0.015	0.012	0.004	0.003	0.005	0.002	0.0006	1.9	3	4.2	6	6	2.9	11.5	9
	C.V.(%)	20	28	24	20	16	26	22	30	16	18	22	19	15	26	24	22
PT* livers	**Mean**	**0.110**	**0.054**	**0.050**	**0.021**	**0.018**	**0.020**	**0.009**	**0.002**	**11**	**16**	**17**	**31**	**40**	**13**	**54**	**39**
n=5	±S.D.	0.021	0.014	0.012	0.004	0.004	0.005	0.0016	0.0008	1.2	3.3	4.1	6.3	6	2.7	13	8
	C.V.(%)	19	25	24	19	22	25	17	40	10	20	24	19	15	24	24	20
Cirrhotic livers	Group 1	0.244	0.147	0.110	0.042	0.035	0.110	0.048	0.028	6.5	6.6	8.5	11	17.5	6.5	9	8
n=12	Group 2	0.132	0.107	0.070	0.031	0.028	0.080	0.038	0.019	7	8	8.5	12.5	18	8.5	10	9
a	Group 3	0.110	0.055	0.051	0.026	0.025	0.040	0.029	0.012	7.5	10.5	14.5	18.5	22.5	15	12	12
	Overal Mean	**0.166**	**0.120**	**0.070**	**0.030**	**0.028**	**0.074**	**0.041**	**0.022**	**7.1**	**9**	**11**	**15.3**	**21.1**	**11.0**	**11.3**	**10.4**
	±S.D.	0.030	0.030	0.020	0.007	0.006	0.026	0.008	0.007	0.5	2	3	3.5	2.5	4	1.4	1.8
	C.V.(%)	18	25	28	23	21	34	19	31	7	21	28	23	12	34	12	17

*: phenobarbital treated

a: The value in each group of cirrhotic livers is the mean of 4 livers

experiment time frame. As for the markers, the frequency outflow profiles of the three drugs from PT-control livers were similar to those observed for the normal control livers.

4.5.2.3 Profiles of markers in cirrhotic livers

Unimodal curves with smooth exponentially decreasing slopes were obtained (Figure 4.4). In comparison to data in control livers, there was a dramatic difference, with all output profiles emerging and declining more rapidly. While the $f(t)_{max}$ of RBC, ALB, SUC, URA, and WAT were increased by 50%, 130%, 40%, 50%, and 56%, respectively, their t_{max} were reduced by 40%, 45, 40%, 50%, and 45%, respectively. However a large variation was observed in the above values between the cirrhotic livers. While in some livers the degree of change was great, several other livers demonstrated near to normal values. Therefore, according to the degree of change in the observational parameters of markers, cirrhotic livers were sub-divided into three categories. Those livers in which the values of parameters were around the mean value of the whole cirrhotic population, were denoted as category 2. Livers demonstrating maximum and minimum change in the parameters were grouped as category 1 and category 3, respectively (Table 4.2). The number of livers in each category was four. No bimodal curves were observed for any of the reference markers in the cirrhotic livers. The profiles in PT-control livers were similar to those observed in the normal control livers.

4.5.2.4 Profiles of model drugs in cirrhotic livers

The frequency outflow profiles of the three drugs in the cirrhotic livers were noticeably different from the controls (Figure 4.3). All three drugs eluted in a bimodal fashion showing an early sharp peak followed by a long flat tail. The incline of the curves for all three drugs was much steeper compared to that of the control livers. Over the initial 20-sec period, the elution profiles of diclofenac and diazepam were similar to that of albumin, followed by slowly eluting components that continued well after most of the albumin had been recovered. However, the times taken for all three drugs to be completely eluted from the system were considerably shorter compared to the control values. While the $f(t)_{max}$ of salicylate, diclofenac, and diazepam were increased by nearly 3-, 3.6-, and 10-fold, respectively, their t_{max} were decreased by 8%, 75%, and 75%, respectively.

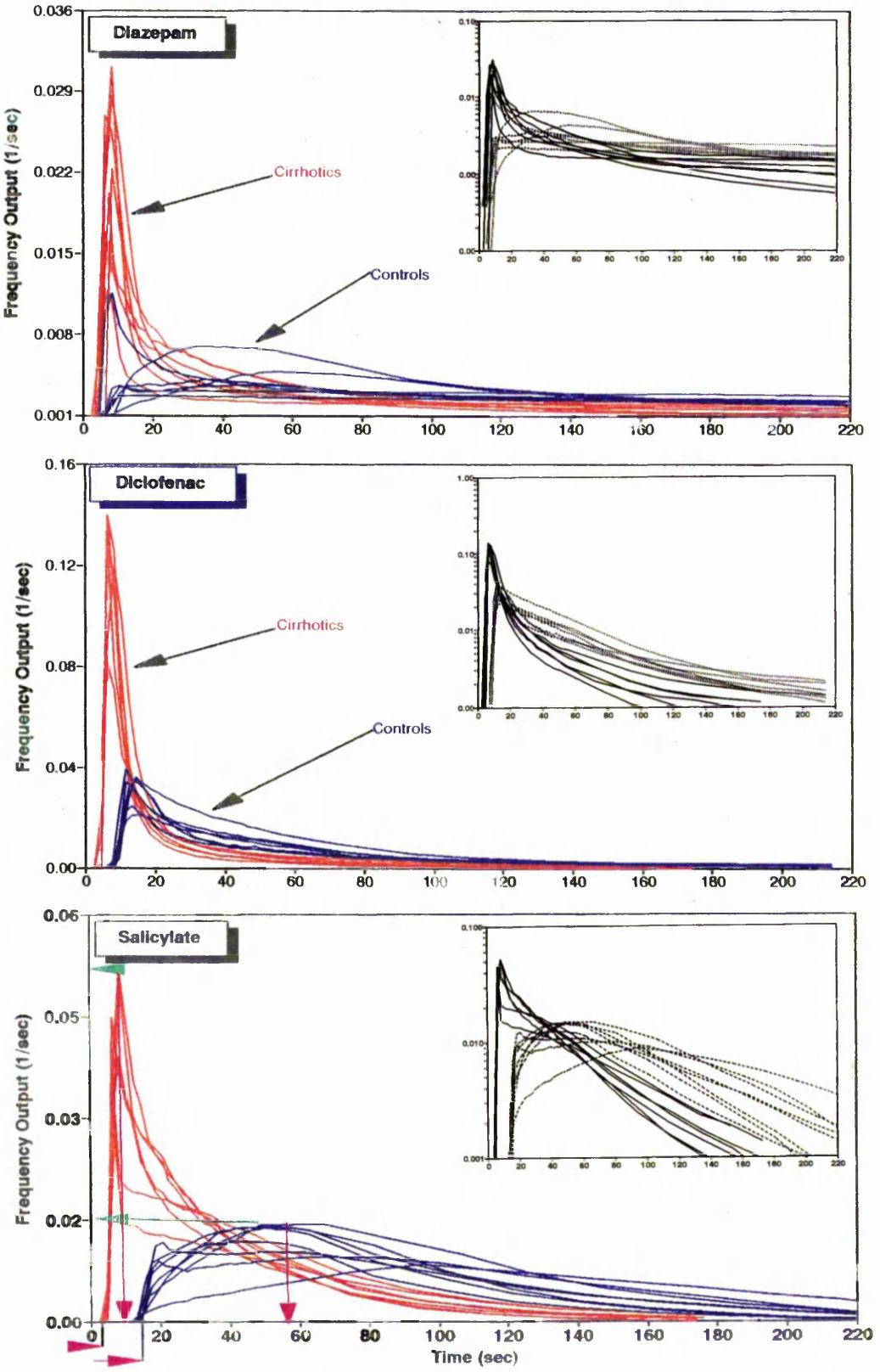

Figure 4.3 Frequency output profiles of model drugs in all control and cirrhotic liver preparations in isolated perfused liver studies.The insets are the logarithmic plots of the same profiles. The $f(t)_{max}$, t_{max} and lag time have been shown for salicylate.

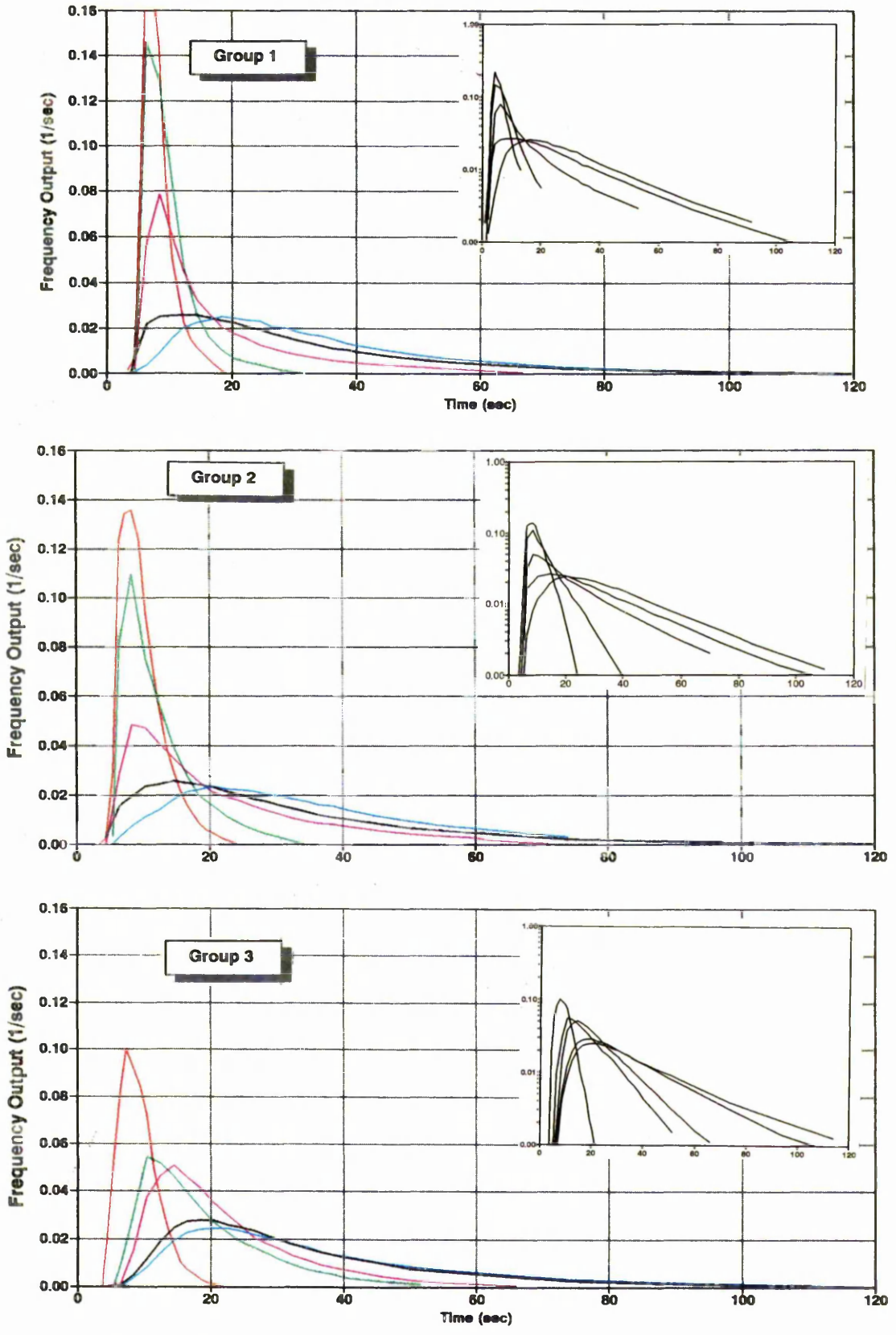

Figure 4.4 Typical frequency output profiles of reference markers in different categories of isolated perfused cirrhotic rat liver preparations. The insets are the logarithmic plots of the same profiles.

4.5.3 Mean Transit Time (MTT)

In control livers, the MTT of markers (mean values in parenthesis) was in the order of RBC (10.1 sec) <ALB (16 sec) < SUC (18.5 sec) < URA (36 sec) < WAT (37.2 sec) (Table 4.3). Among the model drugs, the MTT of diazepam was the largest (595 sec), followed by salicylate (86 sec) and diclofenac (73 sec) (Table 4.4). In cirrhotic livers, while the above relationship was preserved, the MTT of each test substance (except SUC) was significantly reduced compared to the control values. The reduction for RBC, ALB, URA, WAT, SAL, DCL, DZ was 24%, 31%, 12%, 5%, 43%, 36%, and 45%, respectively. The classification of cirrhotic livers proved to hold for MTT and the other statistical moment parameters (*ie* V and CV^2) of the markers, the reduction in MTT being most pronounced in category 1.

4.5.4 Volume of Distribution (V)

In the control livers, the volumes of distribution of reference markers were in the order of total aqueous space marker > extracellular marker > vascular marker. Sucrose showed a slightly larger V than albumin and V of water was slightly larger than that of urea. The V value of erythrocytes approximated 6 ml, representing ~23% of liver weight. Albumin and sucrose had a volume of about 10 ml representing ~40% of liver weight. Water and urea had a volume of more than 20 ml, representing greater than 90% of liver weight (Table 4.5). The vascular and extracellular volumes of the distribution of various labels were similar in PT and normal livers when the data were expressed per gram of liver weight.

In the cirrhotic livers, the volumes of distribution of RBC, ALB, URA, and WAT were decreased by 35%, 42%, 22%, and 23%, respectively (Table 4.5). The V value of sucrose did not change significantly. As for the other parameters of moment analysis, the degree of reduction in volume was greater in category 1 than in the other categories. In this first category, the volumes of distribution of RBC, WAT and URA were reduced to nearly half of the control values. The V value of ALB was reduced to nearly one third of its control value resembling that of RBC in this group. The reduction in V for SUC was less dramatic compared to other markers reaching 85% of the control value. The volume of distribution of SUC in categories 2 and 3 of the cirrhotic livers was slightly larger than its control values. This was not observed for the other markers. In category 3 cirrhotics, the volume of distribution of all markers approached the control values except that of ALB, which remained lower. In this last category, a

Table 4.3

Mean transit times (MTT) for markers in the isolated perfused rat livers.

		RBC	Albumin	Sucrose	Urea	Water
Normal livers	mean	10.1	16	18.5	36	37.2
n=10	±S.D.	0.8	2.1	3.7	5.3	5.4
	C.V.(%)	8	13	20	15	14
PT* livers	mean	9.2	16.5	16.2	37.7	39.1
n=5	±S.D.	1.2	3.1	3.8	6.1	6.7
	C.V.(%)	13	18	22	16	17
Cirrhotic livers	mean	7.6	11	19.4	31.7	35.7
n=12	±S.D.	0.7	2.3	2.7	3.2	5.1
	C.V.(%)	9	20	14	10	14

*: phenobarbital treated The values have been corrected for MTT of non-hepatic region.
RBC: erythrocytes

Table 4.4

Parameters of moment analysis for model drugs in isolated perfused rat liver preparations.

		Diazepam				Diclofenac				Salicylate			
		MTT	CV2	V		MTT	CV2	V		MTT	CV2	V	
		sec		ml	ml/g	sec		ml	ml/g	sec		ml	ml/g
Normal livers	Mean	595	1.08	472	20	73	1.4	41	1.9	86	0.58	53	2.6
n=10	±S.D.	215	0.07	187	3	10	0.4	8	0.4	15	0.12	10	0.5
	C.V.(%)	36	6	39	15	14	28	19	21	17	20	18	19
PT*livers	Mean	498	1.32	241	9.7	70	1.7	33	1.4	128	0.43	59	2.5
n=5	±S.D.	150	0.17	118	2	13	0.43	7	0.3	22	0.1	11	0.5
	C.V.(%)	30	13	48	20	18	25	21	21	17	23	18	20
Cirrhotic livers	Group 1	140	1.06	102		35	3.4	20.6		41	0.77	26.7	
n=12	Group 2	291	1.49	194		47	2.33	27.3		46	0.93	31.3	
	Group 3	485	1.87	368		59	1.59	38.5		63	1.07	45.2	
	Overal Mean	328	1.53	215	7.9	47	3.13	30	1.2	49	0.96	33	1.3
	±S.D.	145	0.35	98	2	11	0.82	8	0.3	7	0.11	8	0.3
	C.V.(%)	44	22	45	25	23	26	26	25	14	11	24	23

*: phenobarbital treated V: hepatic volume of distribution

2-fold difference was found between the volumes of ALB (0.2 ml/g liver weight) and SUC (0.4 ml/g liver weight).

The volumes of distribution of model drugs were substantially larger than that of reference markers. Diazepam had the largest V value (470 ml; 19.3 ml/g) followed by salicylate (53 ml; 2.6 ml/g) and diclofenac (41 ml; 1.9 ml/g) (Table 4.4). In cirrhotic livers, the volumes of distribution of the drugs were reduced by 55%, 38%, and 27% for diazepam, salicylate, and diclofenac, respectively.

4.5.5 Coefficient of Variation (CV^2)

The values of CV^2 of the vascular marker (RBC), the extracellular markers (ALB and SUC), and the total aqueous space markers (URA and WAT) lay within the range of 0.3 to 0.5 (Table 4.6). The values of CV^2 of the drugs were greater than those calculated for markers. Among the drugs, salicylate had a relatively small CV^2 (0.56) (Table 4.4). Diclofenac had the largest CV^2 (1.4), followed by diazepam (1.08). In cirrhotic livers, the values of CV^2 of markers were significantly increased ($p<0.005$), except RBC for which no change in CV^2 was observed. However the degree of change among the test substances was variable. While the value of CV^2 of WAT increased by 12%, the increase in CV^2 of other markers was greater ranging from 42% and 71% for ALB and URA to twofold for SUC. There was also an increase in the values of CV^2 for the model drugs, reaching statistical significance ($p<0.005$). This increase was more pronounced for diclofenac (> twofold), followed by salicylate (65%), and diazepam (42%).

4.5.6 Dispersion Model Parameters

The one-compartment dispersion model adequately described the outflow data for markers in both control (Figure 4.5) and cirrhotic (Figure 4.6) livers, providing estimates for V (Table 4.5) and dispersion number (D_N) (Table 4.7). In contrast, the one-compartment form of dispersion model could not adequately describe the outflow profiles of the drugs and the two-compartment form of the model was needed to describe the data in both control (Figure 4.7) and cirrhotic (Figure 4.8) livers, providing estimates for D_N, k_{12},k_{21}, and k_{23} (Tables 4.8, 4.9, 4.10). In cirrhotic livers, the fit of the two-compartment model to the outflow data of the drugs tended to underestimate the peak and terminal portion.

Table 4.5

Volumes of distribution (ml/g liver weight) of reference markers in isolated perfused rat livers estimated by applying momentan alysis and dispersion model to their frequency outflows.

		RBC		Albumin		Sucrose		Urea		Water	
		Moment	Modeling	Moment	Modeling	Moment	Modeling	Moment	Modeling	Moment	Modelin
Normal livers	mean	0.23	0.23	0.38	0.43	0.41	0.48	0.94	0.78	1	0.81
n=10	≠S.D.	*0.05*	*0.03*	*0.07*	*0.04*	*0.09*	*0.06*	*0.2*	*0.33*	*0.2*	*0.4*
	C.V.	*0.21*	*0.13*	*0.18*	*0.09*	*0.2*	*0.12*	*0.21*	*0.42*	*0.2*	*0.49*
PT* livers	mean	0.23	0.23	0.39	0.44	0.43	0.5	0.96	0.78	1.04	0.82
n=5	≠S.D.	*0.05*	*0.04*	*0.06*	*0.05*	*0.08*	*0.06*	*0.18*	*0.28*	*0.18*	*0.32*
	C.V.	*0.21*	*0.17*	*0.15*	*0.11*	*0.18*	*0.12*	*0.18*	*0.35*	*0.17*	*0.39*
Cirrhotic livers	mean	0.15	0.14	0.22	0.21	0.43	0.37	0.73	0.77	0.77	0.81
n=12	≠S.D.	*0.03*	*0.03*	*0.06*	*0.05*	*0.09*	*0.08*	*0.18*	*0.09*	*0.19*	*0.11*
	C.V.	*0.2*	*0.21*	*0.27*	*0.23*	*0.2*	*0.21*	*0.24*	*0.11*	*0.24*	*0.13*

RBC: erythrocytes
* : phenobarbital treated

Table 4.6

Relative spreading (CV2) values obtained for reference markers in isolated perfused rat livers.

		RBC	Albumin	Sucrose	Urea	Water
Normal livers	mean	0.29	0.29	0.31	0.42	0.51
n=10	±S.D.	0.07	0.06	0.04	0.06	0.08
	C.V.(%)	24	20	12	14	15
PT* livers	mean	0.29	0.3	0.32	0.43	0.52
n=5	±S.D.	0.06	0.07	0.04	0.06	0.09
	C.V.(%)	20	23	12	14	17
Cirrhotic livers	mean	0.27	0.43	0.64	0.72	0.57
n=12	±S.D.	0.04	0.1	0.1	0.1	0.09
	C.V.(%)	14	23	15	13	15

*: phenobarbital treated RBC: erythrocytes

Table 4.7

Dn values of reference markers in isolated perfused rat livers estimated by applying moment analysis and dispersion model to their frequency outflows.

		Erythrocytes		Albumin		Sucrose		Urea		Water	
		Moment	Modeling	Moment	Modeling	Moment	Modeling	Moment	Modeling	Moment	Modeling
Normal livers	mean	**0.1**	**0.1**	**0.1**	**0.1**	**0.11**	**0.1**	**0.18**	**0.18**	**0.2**	**0.21**
a	*S.D.*	*±0.01*	*±0.03*	*±0.02*	*±0.02*	*±0.01*	*±0.02*	*±0.03*	*±0.03*	*±0.03*	*±0.03*
	C.V.	*0.1*	*0.33*	*0.2*	*0.2*	*0.09*	*0.2*	*0.16*	*0.16*	*0.15*	*0.14*
PT* livers	mean	**0.1**	**0.1**	**0.1**	**0.1**	**0.11**	**0.1**	**0.18**	**0.18**	**0.2**	**0.2**
b	*S.D.*	*±0.01*	*±0.02*	*±0.02*	*±0.02*	*±0.01*	*±0.01*	*±0.03*	*±0.03*	*±0.03*	*±0.03*
	C.V.	*0.1*	*0.2*	*0.2*	*0.2*	*0.09*	*0.1*	*0.16*	*0.16*	*0.15*	*0.15*
Cirrhotic livers	mean	**0.08**	**0.08**	**0.14**	**0.14**	**0.25**	**0.3**	**0.28**	**0.31**	**0.24**	**0.3**
c	*S.D.*	*±0.01*	*±0.01*	*±0.013*	*±0.013*	*±0.04*	*±0.08*	*±0.02*	*±0.05*	*±0.02*	*±0.02*
	C.V.	*0.13*	*0.13*	*0.09*	*0.09*	*0.16*	*26*	*0.07*	*0.16*	*0.08*	*0.06*

*: phenobarbital treated

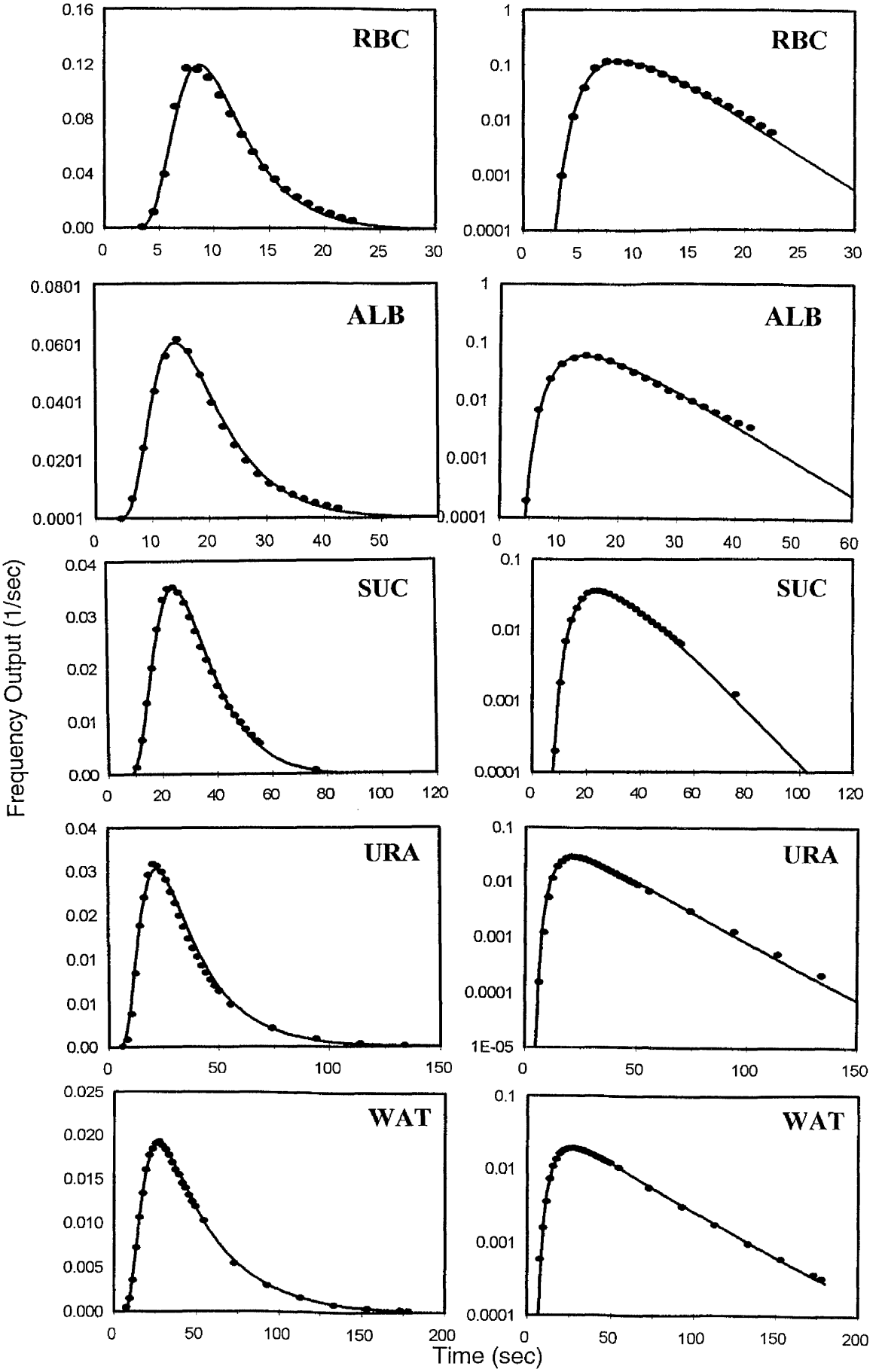

Figure 4.5A Fit of one-compartment dispersion model to the frequency output of reference markers in a representative normal rat liver. The points are the observed data and the lines are the calculated data. RBC:erythrocytes; ALB:albumin; SUC:sucrose; URA:urea; WAT: water. Right panels are the semilogarithmic plots.

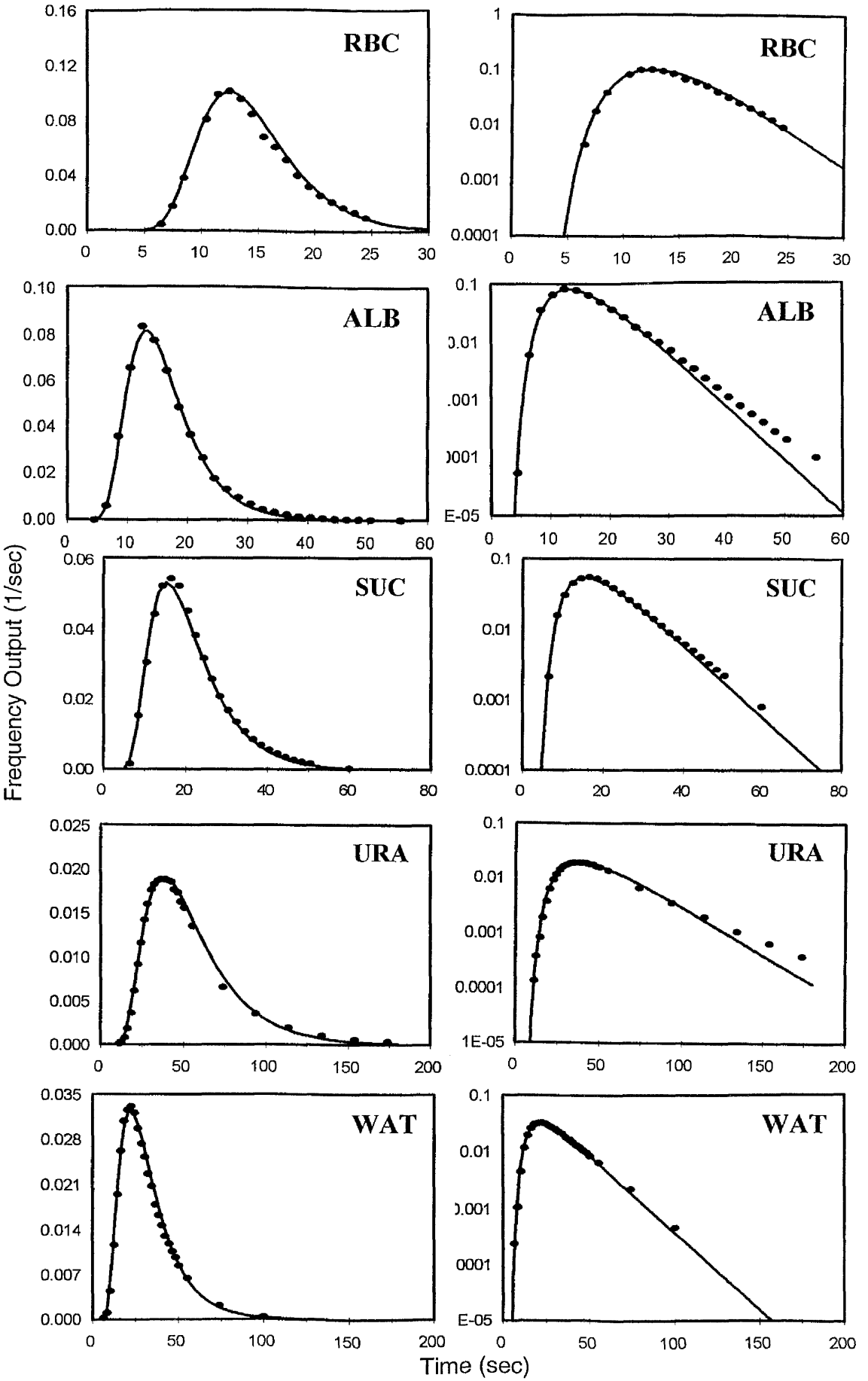

Figure 4.5B Fit of one-compartment dispersion model to the frequency output of reference markers in a representative phenobarbitone-treated liver. The points are observed data and the lines are calculated data. For abbreviations see Figure 4.5A

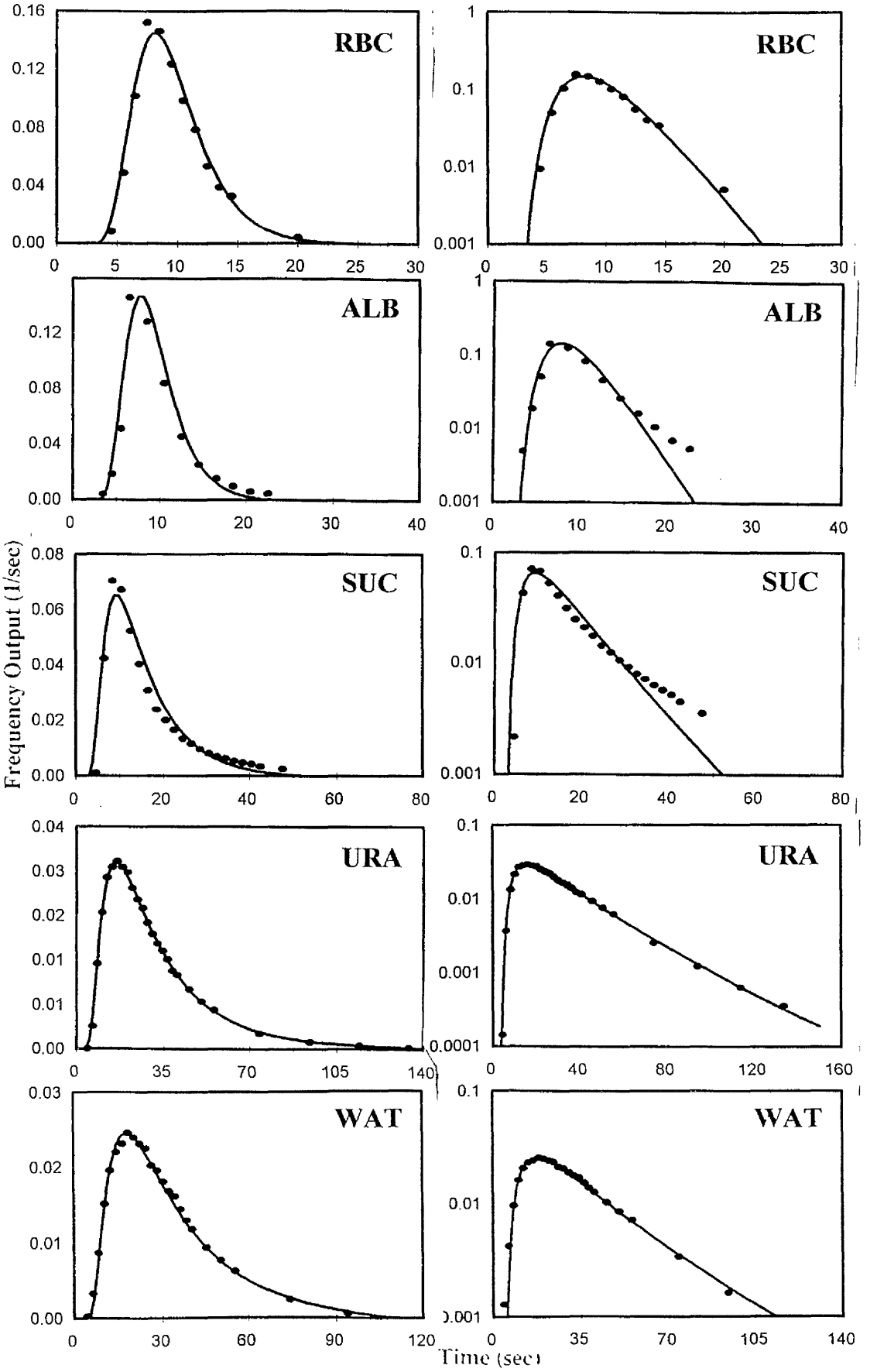

Figure 4.6 Fit of one-compartment dispersion model to the frequency output profiles (•) of reference markers in a representative isolated perfused cirrhotic rat liver. The lines are calculated data. For abbreviations see Figure 4.5A.

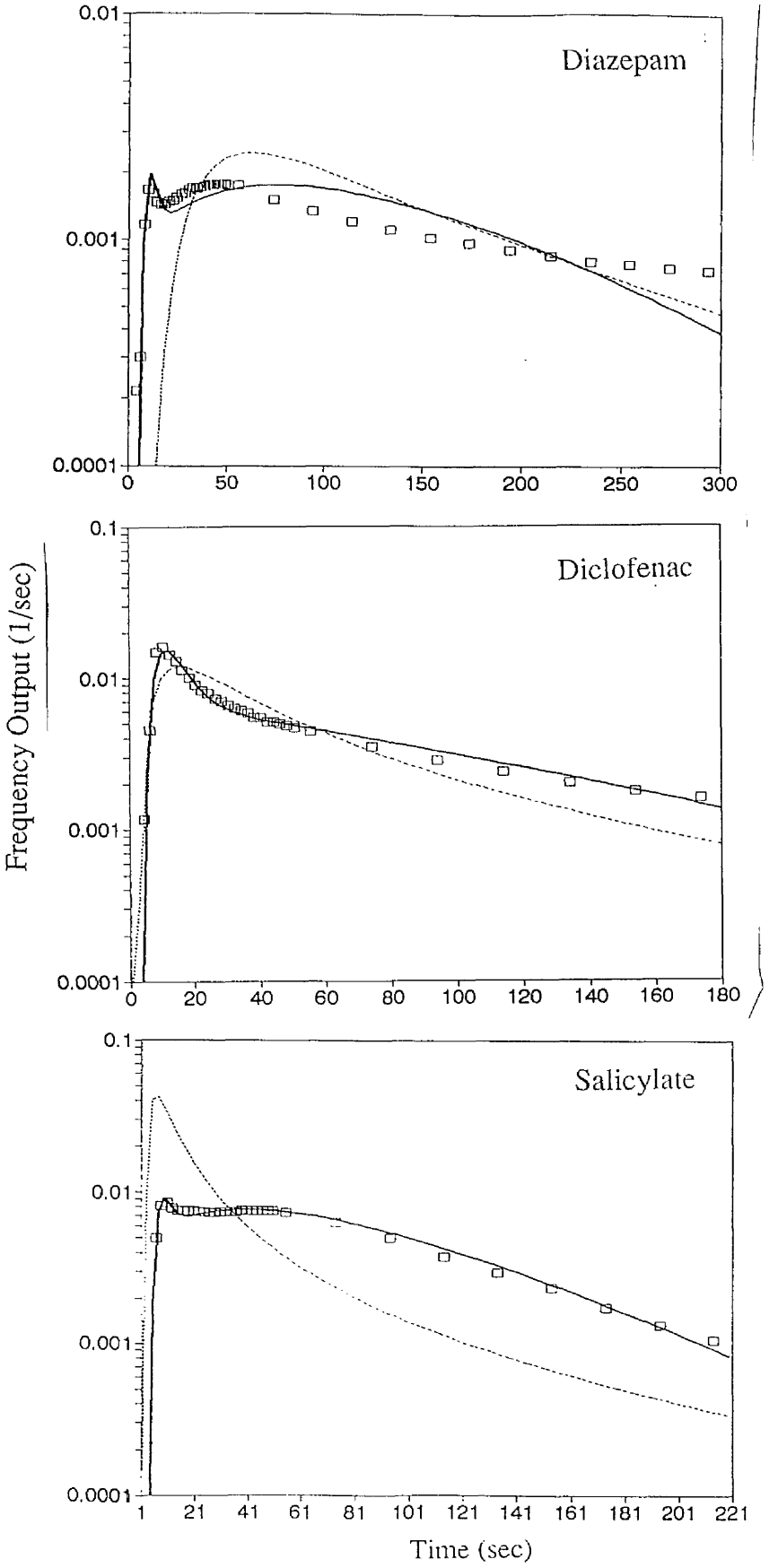

Figure 4.7a Semilogarithmic plots of observed frequency output profiles (□) of model drugs in a representative isolated perfused normal rat liver. The solid and dotted lines are the fit of one- and two-compartment dispersion model, respectively.

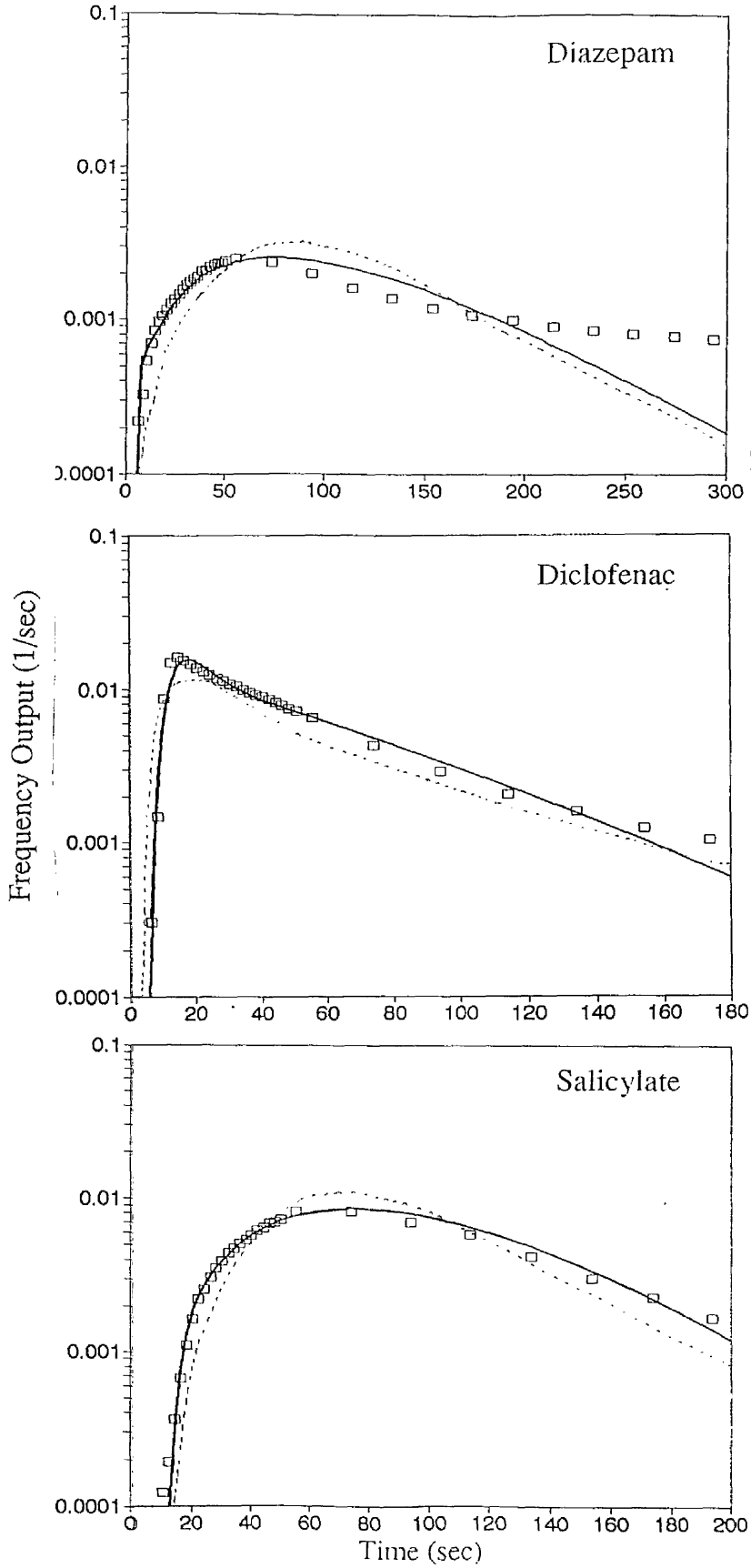

Figure 4.7b Semilogarithmic plots of observed frequency output profiles (□) of drugs in a representative isolated perfused phenobarbitone-treated rat liver. The solid and dotted lines are the fit of one- and two-compartment dispersion model, respectively.

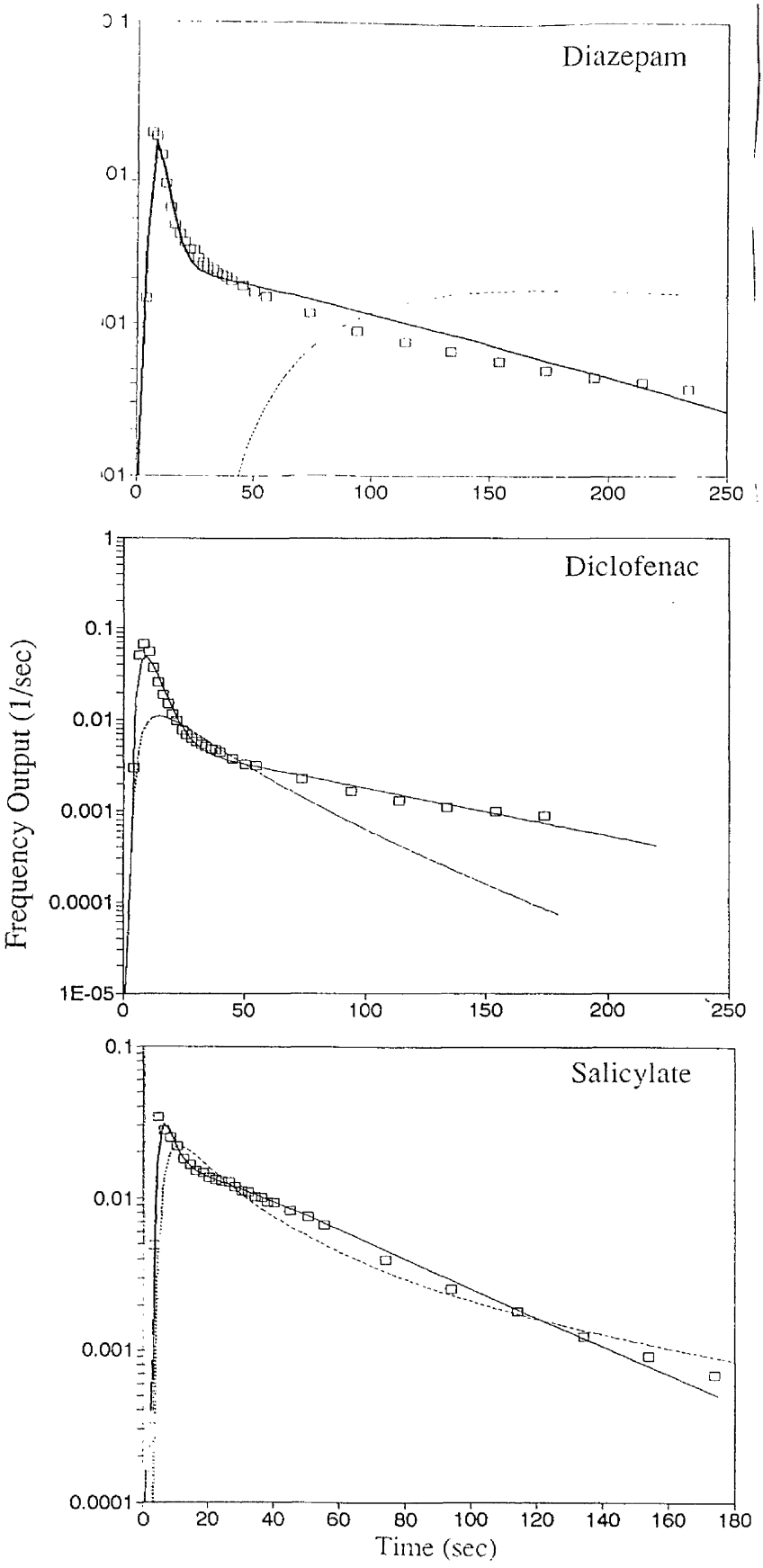

Figure 4.8 Semilogarithmic plots of observed frequency output profiles (□) of model drugs in a representative isolated perfused cirrhotic rat liver. The solid and dotted lines are the fit of one- and two-compartment dispersion model, respectively.

The D_N values for markers in control livers estimated from the dispersion model approximated to those estimated using moment analysis (Table 4.7). However, in the cirrhotic livers, these estimates were slightly different. While the value of D_N in cirrhotic livers increased by 40, 300, 72, and 40% in the case of ALB, SUC, URA, and WAT, respectively, it still remained in the range of 0.1 to 0.3.

4.5.7 Non-hepatic Region

The frequency outflow data for labelled urea and albumin (with or without albumin as binding protein in the perfusate) in the non-hepatic region of the experimental system were equivalent. The recovery in each case was 100%. The estimated values of V, MTT, and D_N of this system were 1.85 mL, 2 sec, and 0.055, respectively. These values were similar to the values previously reported by Rowland *et al* [60,63,64,65].

4.6 Discussion

The unique anatomical and physiological features of the liver, together with numerous methods of experimentation available for it, has made this organ a suitable tool for permeability studies. Due to the central role of the liver in processing of the drugs, hepatic diseases are often associated with altered drug disposition [61,131,132,216,217]. One important issue that may be influential, and should be studied in these circumstances, is the potential change in the permeability of hepatic membranes in relation to the passage of substances. Application of the indicator dilution method with the *in situ* perfused liver [60,63,64,65,119,198,144,218,219,97,123,156] where experimental conditions could be manipulated has made it possible to study permeability in the context of hepatic cirrhosis. To this end, three model drugs for which a considerable body of data associated with various conditions, including impulse-response and steady-state conditions, exists were chosen for the study. It was also necessary to include established reference markers in the study. These markers allowed standardisation and characterisation of the liver preparations, thereby providing a clearer picture of the numerous changes which can take place in cirrhosis as well as helping in the evaluation of the experimental data obtained for the model drugs. Therefore, given their significance, the reference markers are considered first followed by the drugs.

4.6.1 Reference Markers

Erythrocytes, albumin and water are well-known non-eliminated markers used routinely by most workers in microcirculation and permeability studies [83,119,129,130,291]. Sucrose was also included in the study with a view to comparing albumin with an alternative (smaller) extracellular marker that would allow more insight into the potential changes in hepatic microanatomy during the course of cirrhosis. Urea was adopted as alternative cellular marker to water in order to extend the existing limited experimental data of this cellular marker.

4.6.1.1 Definition of the outflow appearance in normal livers

Erythrocytes are confined to the vascular compartment and their dimensions, together with the occurrence of mixing motion within the sinusoids, ensures cross-sectional equilibration there [89]. Beyond the vascular lumen the depth of the space of Disse is such that immediate lateral equilibration would be expected within this space. In the absence of an effective barrier between the vascular space and the Disse space, immediate communication between vascular and interstitial spaces would be expected, with lateral diffusional equilibration between vascular and interstitial spaces occurring as rapidly as labelled materials are introduced. An effective diffusional barrier across the hepatocytes is also absent for substances such as water which equilibrate so rapidly within the cellular space that total hepatic uptake is perfusion rate-limited. This phenomenon of so called "flow-limited distribution" governs the passage through the liver of all the reference markers mentioned.

The cross-sectional area accessible to erythrocytes (the sinusoid) is smaller than the cross-sectional area of the whole space accessible to the diffusible label (the sum of the sinusoidal space plus the interstitial and/or cellular spaces) (Figure 4.9). If ω is the velocity of flow along a sinusoid, then the erythrocytes will be carried from input to output at the velocity of flow. The diffusible substance will in contrast flow along the sinusoid with a velocity $\frac{\omega}{1+y}$ where y is the ratio of the extra-sinusoidal space of distribution : the intra-sinusoidal space of distribution. The diffusible label will travel along the sinusoid as if it is distributed in a larger space, (1+y) times the sinusoidal space of distribution. Accordingly, it will be propagated as a wave travelling more slowly than the erythrocytes and emerging delayed (and lower in magnitude) with respect to it. The decrease in velocity of the concentration wave for the diffusible substance will result in a lag

in the appearance of the wave at the outflow and a proportionate delay in all parts of the concentration wave.

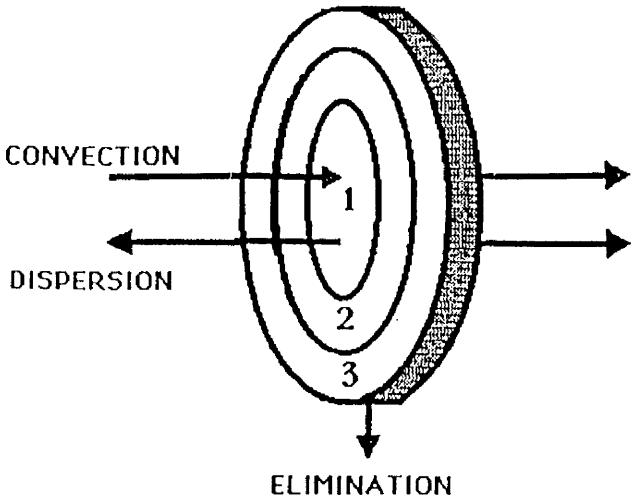

Figure 4.9 Schematic of events in a cross section of the liver, represented as a cylinder. (1) The blood, (2) the space of Disse, (3) the hepatocyte.

In organs other than the liver, the increment in time of distribution for diffusible substance is generally related to the rate at which it leaves and re-enters the capillary, to the size of the extravascular compartment related to each capillary, and to the total number and length of the capillaries across which exchange takes place. The rate of exchange across the capillary in turn is related to the diffusion coefficient for the substance in the capillary wall and extravascular space and to the rate of presentation of materials for exchange (perfusion flow rate) [89]. In the liver, as the diffusion takes place rapidly in comparison to the perfusion rate, the time of transit is limited only by the rate of perfusion and the volume of extravascular space. Thus, for a given flow, a larger volume of distribution is manifested in a larger mean transit time. This explains the finding that the volumes of distribution of cellular markers (WAT and URA) were larger than those of extracellular markers (ALB and SUC) and is in accordance with the literature data [83,119,291].

4.6.1.2 Definition of outflow appearance in cirrhotic livers

The observed change in the outflow profiles of markers in cirrhotic livers is indicative of a progressive alteration in exchange of material between blood and liver. Numerous structural and circulatory alterations that take place in cirrhosis [288,181,310,270,272,203] may explain this change of

behaviour. The change in the profile of each test substance may have been caused by one or more of the following mechanisms.

The general decrease in vascular space in cirrhotic livers (Figure 4.10), the enlargement of the hepatocytes (those that have escaped destruction) and the interstitial space which leads to the compression of sinusoids [158], may account for the sharper and faster elution and longer lag time of erythrocytes emerging from the cirrhotic livers.

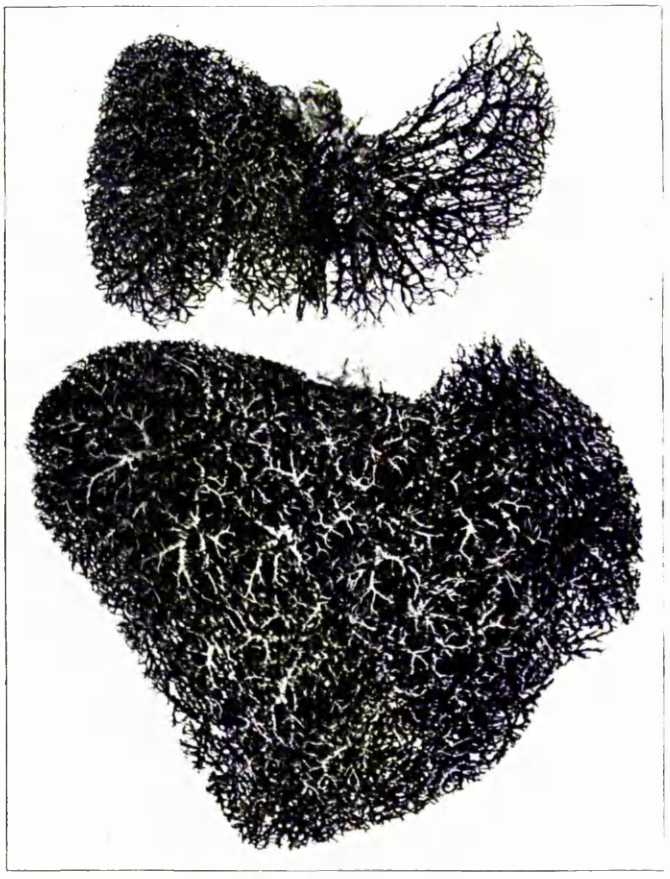

Figure 4.10 Colloidin casts of portohepatic venous trees in normal liver (lower) and in advanced cirrhosis (upper). Note the marked reduction in total vascular bed (from reference 159).

Ultrastructural alterations, including collagenisation of the space of Disse, capillarisation of the sinusoids with the formation of a basement membrane, and a decrease in the number and total areas of endothelial fenestrae, have been demonstrated in cirrhotic rats and humans [155,252]. These changes cause the diffusible substances to be excluded from a part of their original spaces and distribute in a smaller space in a fashion that is still related to the rate of perfusion. On the other hand, development of channels with poor permeability [202] and intrahepatic shunts results in a greater fraction of substance passing through the liver without getting access to its normal distributional space. The implication of the above mechanisms for albumin and albumin-bound compounds (diazepam and diclofenac) is a faster elution and a sharper peak.

Morphometric analysis indicates that the number of hepatocytes in cirrhotic livers is decreased (Table 4.8). This reduction in yield of hepatocytes is compensated for by an increase in other liver cells.

Table 4.8 Morphometric analysis in experimental cirrhosis (% of total tissue volume).

	liver mass (g)	hepatocytes	nonhepatocytes	bile ducts	connective tissue
Normal liver	16.6	85.1	10.2	0.2	1.4
Cirrhotic liver	32.5	51.5	7.8	21.4	15.2

from references 96 and 217

Histological examinations and tracer studies in this and other work confirmed that the volume of hepatocytes is reduced in cirrhotic livers. Regarding the theoretical considerations (Section 4.6.1.1), reduction in the volume of distribution for water and urea and model drugs would imply a steeper appearance and shorter MTT as was observed in the present studies.

From the behaviour of the markers in the cirrhotic livers it is conceivable that their distribution is still compatible with a flow-limited diffusion. Unimodal outflow curves were obtained for the markers. This is in contrast to other findings [119,291] indicating a bimodal outflow pattern for sucrose and water in cirrhotic livers. However, due to technical reasons (the recirculation nature of the experiments and very low level truncation of the outflow data), it is difficult to interpret the results from those reports.

4.6.1.3 Normalisation

In order to provide a basis for comparison among the group of markers used, it was necessary to normalise the primary curves (outflow concentration versus time). For modelling purposes, the outflow concentration was transformed into frequency outflow by simultaneously correcting for perfusion flow rate and administered dose. For all other purposes, the output curves were transformed into the fractional outflow curves by dose normalisation, *ie* the total amount of material injected was defined as 1 unit, and the concentration of material in the outflow was expressed as a fraction of the injected mass per ml of perfusate. Since for non-eliminated substances, the recovery (including the extrapolated fraction) should equal the administered mass, the results for both methods are expected to be the same.

The true value of the administered dose is important in the normalisation procedure and since the volume injected was small (50 μL) it could be associated with some degree of error. Therefore, it may be argued that application of AUC, which is an actual experimental finding, leads to more precise normalised data. However, on using AUC care must be taken. When unextrapolated AUC is used as the correction factor, the value may be variable among the different preparations. On the other hand, sometimes the recovery is not complete and dividing the outflow concentration by AUC produces inter-preparation artefacts. As the recovery of markers in the experiment was virtually complete, and the sampling time for each marker throughout all liver preparations was the same, AUC was used to normalise the data.

4.6.1.4 Superimposition

The definition of the outflow appearance implies that normalisation of outflow concentration for dose and volume, and normalisation of time for MTT results in a dimensionless plot with an area equal to 1 [83]. The superimposible curves for three reference markers (RBC, ALB, WAT) in all liver preparations is shown in Figures 4.11 and 4.12. Each profile showed a normal symetrical distribution, having a dimensionless $f(t)_{max}$ around 0.55. The t_{max} value however was different between the three profiles. While t_{max} of WAT plot centred on the value of 0.7 albumin and erythrocytes profiles shifted to the right having a t_{max} of 0.85 and 1, respectively. In the cirrhotic livers, the shape, $f(t)_{max}$ and t_{max} of albumin and erythrocytes curves were similar. They had a

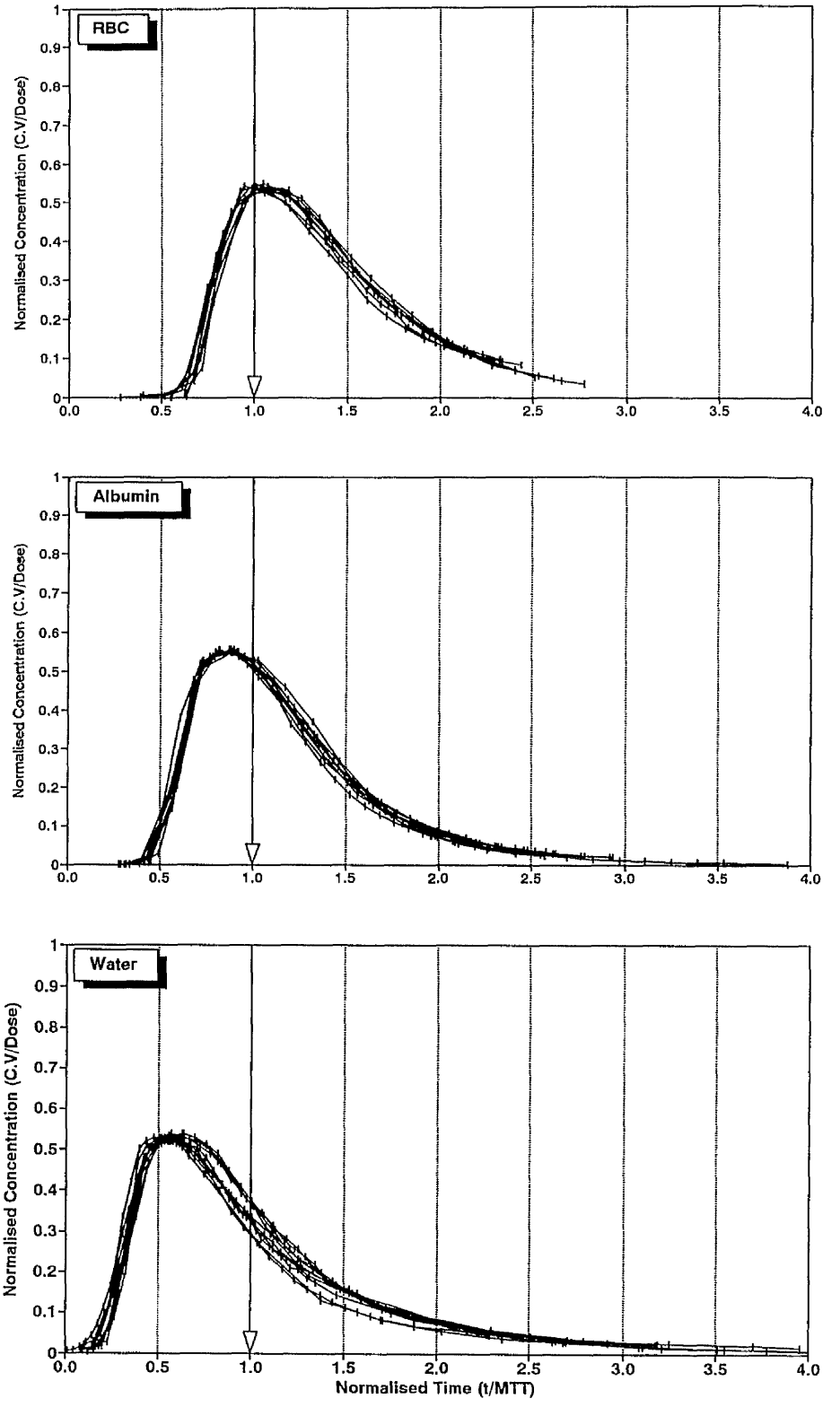

Figure 4.11 Dimensionless plots of output concentrations versus time for various markers in all control liver preparations in isolated perfused rat livers.

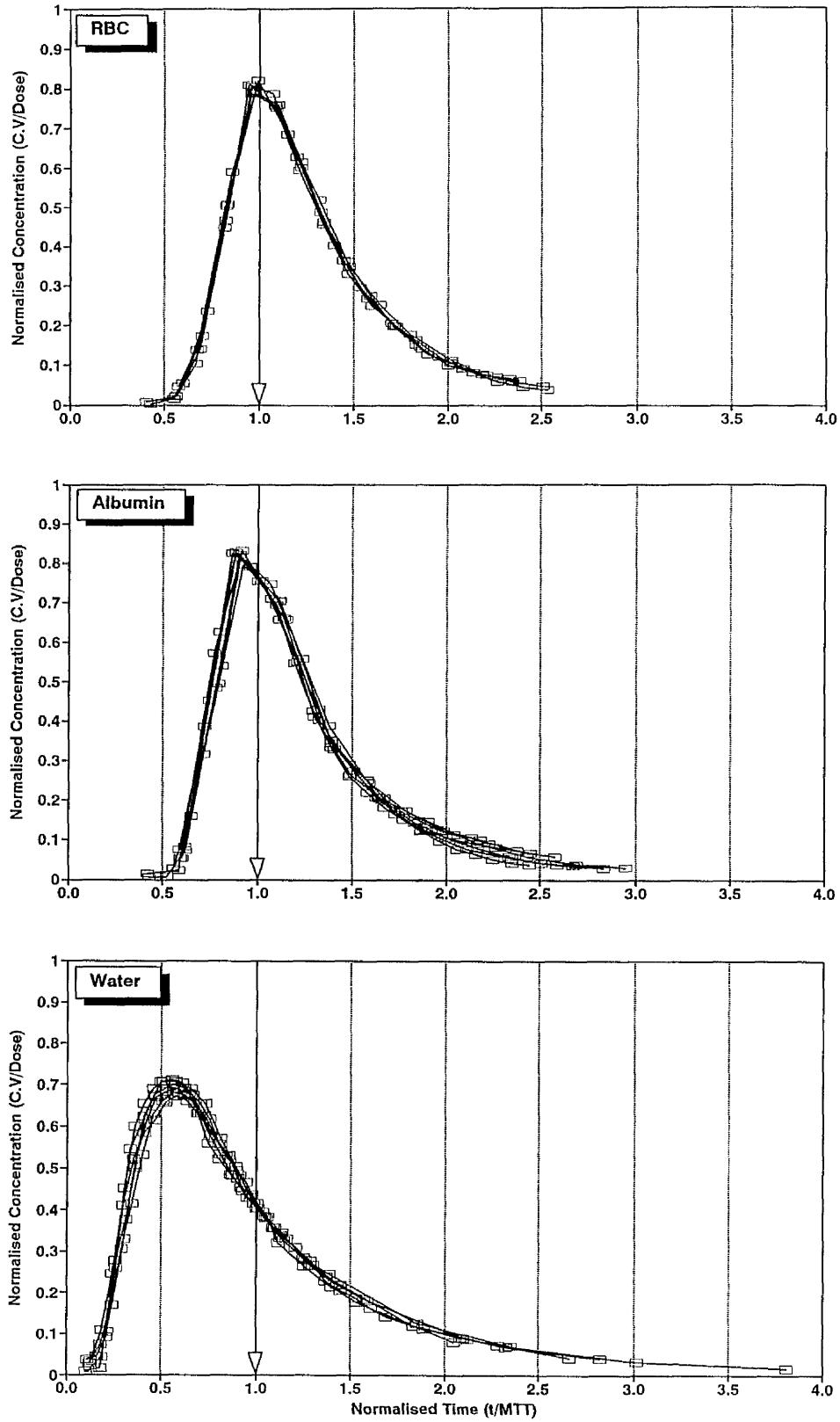

Figure 4.12 Dimensionless plots of output concentrations versus time for various markers in all cirrhotic liver preparations in isolated perfused rat livers.

sharper peak with a greater $f(t)_{max}$ (0.8). The normalised plots for water was less sharp, had a lower peak ($f(t)_{max}$ = 0.7), and became more skewed. The ability to obtain such plots for the vascular, extracellular and cellular markers with high precision may be interpreted as achieving the following: Complete recovery, precision in the estimation of Dose and V, sufficient perfusion to the livers, correct theoretical considerations, and flow-limited distribution of markers.

The shape of the superimposition curve for water was a distribution peaking at dimensionless time=0.65. Similar plots were obtained for erythrocytes and albumin which were only slightly differed in time and shape. The deviation in time could be explained by the large vessel effect. Large vessels (non-exchanging areas) contribute to the estimation of volume of all intrahepatic spaces. The magnitude of this contribution was variable among the various markers, being larger for those restricted to the vascular space followed by extracellular space and cellular space markers. If the erythrocyte and albumin curves were shifted by 0.4 and 0.3 in time to the left, respectively, they become superimposable on the water curve. In cirrhotic livers, where the relative volume of the large vessels was increased, a similar pattern was observed.

Another normalisation method has been proposed [54,83] in which the outflow concentration is expressed as a fraction of maximum concentration (C_{max}) producing plots in which the $f(t)_{max}$ and t_{max} are centred around a value of unity. Compared to the first method where estimated values of the dose and V are used for normalisation, in the second method the normalisation depends only on the C_{max} (the actual observed data). However, as the value of C_{max} is greatly influenced by sampling-time intervals, theoretically the second method is not better. The normalised water outflow data, analysed using this method is depicted in Figure 4.13.

An important parameter that influences the shape of the curves is D_N [54]. Figure 4.14 illustrates simulation of changes in frequency data following a change in D_N for a hypothetical compound. As the value of D_N increases from zero, the peak time decreases from T=1 towards T=0, the shape becomes more skewed and the sensitivity of the shape of the curve to a change in D_N decreases. Therefore, substances demonstrating similar dilution curves should possess similar D_N values. Figure 4.15 depicts the normalisation plots of water in all control liver preparations. The profile indicates that the D_N values for the superimposition curves were in the range of 0.15 to 0.28.

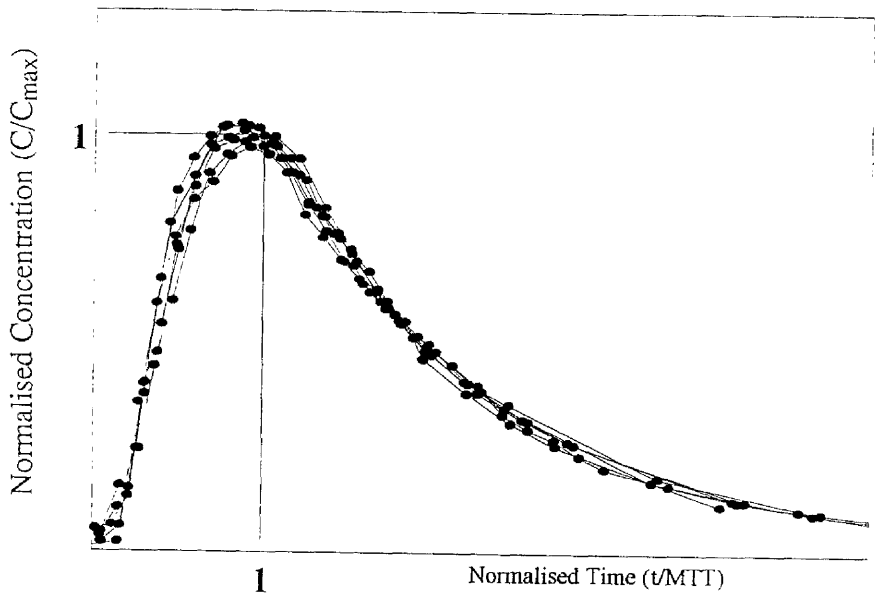

Figure 4.13 Dimensionless plots of output concentrations (normalised for C_{max}) versus time (normalised for MTT) for water in all control liver preparations in isolated perfused rat livers.

D_N is primarily determined by the heterogeneity of hepatic vasculature [228]. In the control livers, there was little variation in hepatic architecture among different livers. Therefore, the D_N values of reference markers were similar and the difference in their superimposible curves was negligible. In cirrhotic livers, as the response of the treated livers to hepatotoxin (in terms of structural changes) was variable, the difference in D_N of diffusible substances became more noticeable. Therefore, the difference between the dimensionless curves of the markers in cirrhotic livers was slightly larger. Visual analysis of the curves also showed that the peak of each of the three markers in cirrhotic livers was higher compared with that of the control but not as much as the tail. Given this situation, it was not possible to obtain adequate fits of cirrhotic curves on top of the control data points (Figures 4.11 and 4.12). The difference in D_N may explain the observed systematic deviation of the normalised cirrhotic curves from the control data points.

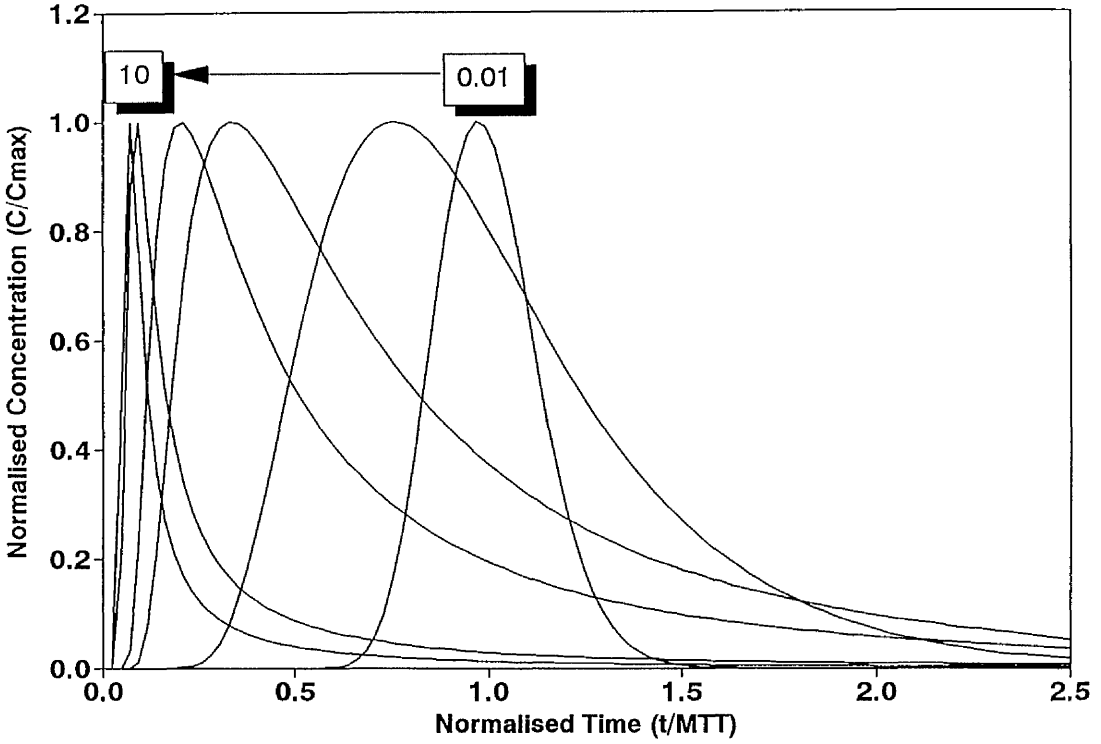

Figure 4.14 Effect of dispersion number on the shape of the normalised output profile for a non-eliminated solute (D_N=0.01, 0.1, 0.5, 1, 5 and 10, from right to left).

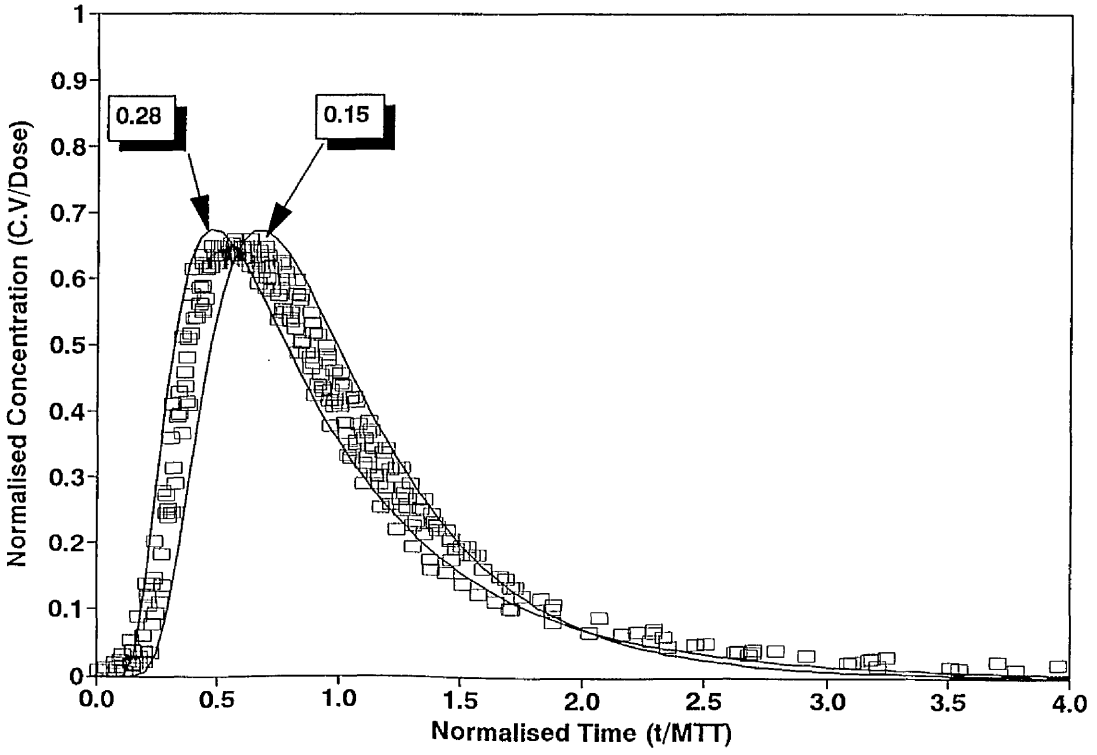

Figure 4.15 Plots of normalised output concentrations versus normalised time for water in all control livers. The figure shows the relationship between D_N and the shpe of the curve.

4.6.1.5 Recovery

Figure 4.4 illustrates the use of linear extrapolation to account for the fraction eluted beyond the last experimental collection point. Extrapolation can greatly influence the results of recovery, MTT and V. The correction for the most rapidly travelling indicator (erythrocytes) was attainable, whereas that for the most slowly travelling substances (urea, water and drugs) was less certain. The sampling schedule plays an important role in reducing the error associated with the estimation of AUC [121,54,47].

The complete recovery of RBC in control and cirrhotic livers (Table 4.1) is demonstrated by the cumulative outflow curves (Figure 4.1). The recovery of sucrose and urea was complete (more than 98%) with no difference between control and cirrhotic livers indicating that neither of these substances was lost during single passage through the liver. The recovery of both albumin and water was complete in controls (96%) but is slightly reduced in cirrhotic livers (91%). Accumulated extracellular matrix in the space of Disse may have contributed to albumin's reduced recovery in cirrhotic livers. The non-recovered fraction of water may be trapped within the preparation and so plays no role in the exchange process and is not associated with a volume. The fact that only a small fraction of the administered dose (3.5%) of markers was eluted beyond the last experimental sampling point indicated that the sampling schedule had been long enough to reduce the potential error involved in extrapolation.

4.6.1.6 Mean transit time (MTT)

The larger MTTs of ALB and SUC, compare to that of RBCs, is indicative of their access to a greater volume of distribution (the extracellular volume). The access of markers of total hepatic aqueous space (URA and WAT) to a still larger volume is manifested in even larger MTT values compare to the other markers. The reduction in the MTTs of markers (except sucrose) in cirrhotic livers indicated that the space in which they were distributed was reduced. The calculated MTT_{RBC} in control livers (10 sec) was in accordance with literature data (Table 4.9). A small inter and intra-species variation was observed. In cirrhotic livers, the value of MTT_{RBC} was reduced. In one study [291], using IDT in CCl4-induced cirrhotic livers, a 10% increase in the value of MTT of erythrocytes was observed. In the same study, the total time needed for the elution of erythrocytes and also vascular and sinusoidal spaces were decreased. The workers did not offer any explanation for this discrepancy. Other clinical studies report only descriptive data, and in the absence of appropriate data analysis, comparison is limited.

A wide inter- and intra-species variation in the MTT values of albumin and sucrose was observed in the literature. From virtually similar MTT values [291] to values with 50% difference [83] have been reported for these two markers. This variation becomes more pronounced in cirrhotic livers.

In the current study, the MTT values of albumin and sucrose in cirrhotic livers differ. While the MTT of albumin, similar to the other markers, was decreased by 45% in the cirrhotic livers, that of sucrose was increased by 5%. This different MTT and outflow profile has been observed by the others [83,291]. The unaltered or slightly increased MTT of sucrose indicated that this marker, unlike albumin, had no major difficulty on distributing into the extracellular space. A 93% increase in MTT of sucrose in cirrhotic livers has been reported by others [318].

Compared to the vascular and extracellular markers, the MTT of cellular markers decreased very little (water 4% and urea 14%). While a part of this diminution was attributable to the reduction in vascular and interstitial spaces, changes at the cellular levels cannot been ignored.

4.6.1.7 Volume of Distribution

4.6.1.7.1 Vascular volume

As erythrocytes are confined to the vasculature, their volume of distribution approximates the vascular space. The vascular space in the cirrhotic livers was reduced by 35% (Figure 4.16). Similar findings have been reported by other workers [291]. Two potential mechanisms may account for the reduction in vascular space. Both mechanisms have received support from histological studies. First, the total hepatic vascular bed is significantly reduced in cirrhotic livers (Figure 4.10). Second, due to hepatocellular expansion and hepatic fibrosis, the vascular space is stretched longitudinally with an overall reduced transversal diameter [203,245]. In cirrhotic patients a significant inverse correlation between hepatocyte size (and surface area) and sinusoidal area has been observed, indicating that larger hepatocytes are associated with sinusoidal compression [293]. Ethanol-fed rats in which liver enlargements of 36 to 42% were observed, had a significant reduction in blood space per unit liver weight [293].

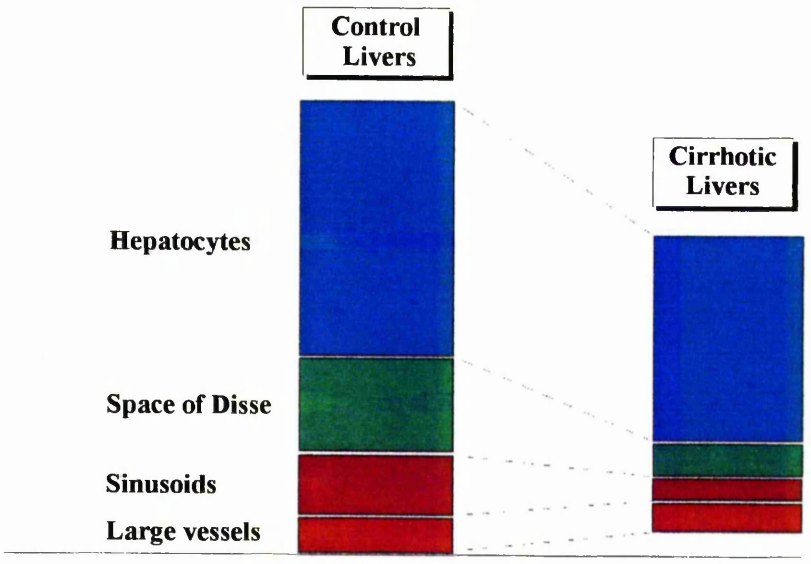

Figure 4.16 Reduction in the estimated volume of hepatic spaces in cirrhosis. The diagram has been drawn using the mean values of data in Table 4.10.

A marked difference in vascular volume between the control and cirrhotic livers was observed. A group of workers, using a similar IDT and IPRL approach, were not able to observe such difference [215]. However, the values of vascular volume in control livers (0.081 ml/g) reported by these workers appear to be much lower than their previously reported values [316,214] or values obtained in the control livers in the current study.

The intrahepatic vasculature comprises large (non-exchanging) vessels and sinusoids which effectively participate in the diffusion. Not much attention has been paid in the past to the effect of large vessels on the dispersion of elements in the liver. The volume of the large vessels and sinusoids can be estimated. Assuming that the observed lag time (time of appearance of first element) is the time spent by an erythrocytes in three separate regions (the non-hepatic region, the large vessels, and the sinusoids) the MTT_{NH} can be easily estimated. If it is subtracted from the total MTT_{RBC}, the MTT_{RBC} in the hepatic region is obtained. Considering the length of a single sinusoid (200-500 μm; [313] and velocity of erythocytes [201,227], the time spent by an erythrocyte to pass through a single sinusoid (0.007 sec for Q=1.3 ml/min/g) can be ignored compared to the MTT of RBC (10 sec). Hence on subtraction of MTT_{NH} from the lag time, the MTT of large vessels (MTT_{LV}) and subsequently the MTT of sinusoids (MTT_{SIN}) can be

determined. These times are then translated into the large vessel and sinusoidal volumes by appropriately multiplying to Q.

$$V_{LV} = MTT_{LV} \times Q \quad (4.2)$$

$$V_{SIN} = MTT_{SIN} \times Q \quad (4.3)$$

The volume of the space of Disse (V_{DIS}) and cellular volume (V_{CELL}) may also be calculated.

$$V_{DIS} = V_{DIFF} - V_{RBC} \quad (4.4)$$

$$V_{CELL} = V_{WAT} - V_{DIFF} \quad (4.5)$$

where V_{DIFF} denotes the volume of distribution of diffusable extracellular markers (albumin and sucrose).

As the time spent by an RBC in a single sinusoid is very short, and every erythrocyte enters into only one sinusoid, it may be concluded that the overall MTT spent by RBCs in the sinusoids is very little compared to the time they spent in the large vessels. But it should be noted that because a greater resistance to the flow exists inside the sinusoids [116,112], sinusoidal volume has a considerable share of the vascular volume. Indeed it was found that the sinusoidal MTT (63% of total MTT) for erythrocytes in normal livers was larger than that in the large vessels (37%) (Table 4.10). These MTT values, and consequently the sinusoidal volume values, are in accordance with data obtained by another group of workers who used a different method of analysis [83,291]. In control livers, the large vessels volume was estimated to be 0.092 ml/g, comprising 37% of hepatic vascular volume. The sinusoidal volume was estimated to be 0.15 ml/g liver weight, approximating 63% of hepatic vascular volume. In PT livers, the volume of large vessels, sinusoids, and the space of Disse were slightly smaller, approximating to 0.09, 0.15, 0.18 and 0.21 ml/g liver weight, respectively.

The ratio of V_{LV}/V_{SIN} was increased substantially from control (0.6) to cirrhotic livers (1.45) (Table 4.10). A review of the data in Table 4.6 shows that this change in ratio was primarily due to reduction in the sinusoidal space rather to an increase in large vessel volume. These observations are in agreement with the ultrastructural morphometric analysis of rat livers with CCl4-induced cirrhosis published recently [245], in which hypertrophy was attributed mainly to an increase in connective tissue with an increased quantity of blood vessels in the septa. It should be noted that the blood vessels in the septa are in fact the large vessels. However the proportion of the large vessels in the septa to the whole liver has not been determined. Others [291], using similar

Table 4.10

Volumes of hepatic spaces in isolated perfused rat livers (ml/g liver weight).

		Large vessels (Vlv)	Sinusoids Vsin	Space of Disse		Hepatocytes				Vlv/Vsin
						Water		Urea		
				Albumin	Sucrose	Albumin	Sucrose	Albumin	Sucrose	
Normal livers	mean	**0.092**	**0.15**	**0.19**	**0.23**	**0.62**	**0.55**	**0.51**	**0.44**	**0.6**
n=10	±SD	*0.02*	*0.03*	*0.03*	*0.03*	*0.11*	*0.09*	*0.09*	*0.07*	*0.1*
	CV%	*21*	*20*	*15*	*13*	*17*	*16*	*17*	*15*	*16*
PT* livers	mean	**0.09**	**0.148**	**0.18**	**0.21**	**0.66**	**0.58**	**0.53**	**0.47**	**0.6**
n=5	±SD	*0.02*	*0.02*	*0.02*	*0.02*	*0.1*	*0.1*	*0.07*	*0.06*	*0.1*
	CV%	*22*	*13*	*11*	*9*	*15*	*17*	*13*	*12*	*16*
Cirrhotic livers	mean	**0.074**	**0.051**	**0.05**	**0.26**	**0.56**	**0.37**	**0.47**	**0.3**	**1.45**
n=12	±SD	*0.015*	*0.015*	*0.02*	*0.04*	*0.09*	*0.06*	*0.05*	*0.08*	*0.23*
	CV%	*20*	*28*	*36*	*15*	*16*	*16*	*10*	*26*	*15*

*: phenobarbital-treated

values have been estimated using moment analysis

method of analysis, similarly found that the sinusoidal volume is decreased in cirrhosis. However, the large vessels volume in their experiment was increased (in contrary to the present findings). This increment in large vessels volume should therefore compensate for a decrease in sinusoidal volume and produce a more or less unchanged vascular volume in cirrhotic livers, as was shown in their even larger MTT_{RBC}. In contrast they reported a 40% decrease in vascular volume. Examination of their method of analysis and their discussion did not reveal any clue for this contradiction.

4.6.1.7.2 Extracellular volume

The larger volume obtained for albumin and sucrose, compare to that of erythrocytes, indicates that these markers have distributed into a larger space (extracellular space). The value calculated for albumin space was similar to those reported by others in *in situ* liver preparation [214,316]. The volume of distribution of sucrose is of the same order of magnitude as those reported in normal dog liver[83,90]. A 20% difference was observed between the volumes of distribution of albumin and sucrose. Since both of these markers share the same vascular volume, the difference in their total volume of distribution is due to a difference in their interstitial volumes (Table 4.6). It is evident that albumin had been excluded from a part of the space of Disse. This exclusion phenomenon is caused by the microanatomical properties of the space of Disse which is filled with an extracellular matrix that limits the free movement of large molecules, such as albumin (MW=66,000). The presence of this kind of phenomenon has been documented *in vitro* for hyaluronic acid gels [61] and collagen [304] and similar properties of the ground substance in the Disse space were being demonstrated in this (Figure 3.3.4) and other work [83].

The apparent exclusion phenomenon increases with an increase in molecular weight [83]. In the liver, the available interstitial space to albumin is 64% of the volume accessible to the small molecular weight extracellular probes such as sodium [83,11]. This indicates that the diffusion of albumin in this space is reduced by one-third of the velocity in water due to the fractional interaction between albumin and the matrix [50]. The exclusion phenomenon implies that, in the design of uptake experiments, it is necessary to use a specific type of second extracellular reference which describes the behaviour the uptake substance will have if it did not enter liver

cells. Of the possible second extracellular markers, sucrose was chosen as its molecular weight (230) is close to that of the drugs (around 300).

A wide range of outflow dilution patterns obtained for albumin. At one extreme, the albumin curve approached that for RBC, and at the other end a pattern similar to that expected in the normal liver was found, with a large separation between the RBC and albumin curves. The experimental data suggest that in the first group of cirrhotic livers, virtually all albumin remained in the vascular compartment along with the erythrocytes. This kind of profile was close to those observed in a circulatory bed which was impermeable to the albumin over a single passage time (*eg* in the pulmonary circulation at low flows) [88,87,122]. The labelled albumin curves obtained in the first category of cirrhotic livers may well have resulted from a similar phenomenon, with the diffusion being limited across capillarised sinusoids [272]. In the second and third categories of cirrhotic livers, the access of albumin to the interstitial space had been limited. This kind of profile is close to those observed in capillary circulations with poor permeability to albumin, such as the coronary circulation [236]. In the heart, where the collagen fibre matrix in the interstitial space is denser, the proportion of the space accessible to albumin was found to decrease to 33% [59]. The proportional exclusion in the liver thus may be expected to increase for albumin, with increasing fibrosis of the Disse space [252].

The behaviour of sucrose was no longer flow limited in the first category of cirrhotic livers. This behaviour may have been caused by the following conditions: a) the passage of a fraction of the sucrose molecules through small intrahepatic shunts (less than 15 μm in diameter); b) extensive capillarisation of sinusoids which would render diffusion of sucrose barrier-limited. Similar profiles have been observed in capillaries with poor permeability to sucrose such as the coronary circulation in the dog[236]. In this capillary system there is a non-linear dissociation of sucrose molecules and albumin because sucrose molecules cross the capillary membrane in a barrier-limited manner to diffuse in the extravascular space. Thus, when sucrose molecules reach the outflow they emerge at a later time than albumin.

In cirrhotic livers the interstitial space accessible to albumin decreased and that of sucrose slightly increased, thus the ratio between extravascular albumin and sucrose space was larger in cirrhotic

livers (1.92) compare to controls (0.83). This observation is in agreement with literature data [130,198].

The ratio of extracellular space (V_{ALB}) to vascular space (V_{RBC}) in control livers was found to be 1.7. However when both spaces are expressed in terms of their effective diffusible space (without the volume of large vessels), this ratio was increased to 2.1. The significance of this ratio is that it determines the area available for exchange; the bigger this ratio, the more effective the exchange would be. In cirrhotic livers, the ratio of total and effective extracellular to vascular space (V_{ALB} / V_{RBC}) was decreased to 1.25 and 1.5, respectively. This indicates that the area available for exchange of albumin and protein bound substances had been reduced by 35 %.

4.6.1.7.3 Cellular volume

The greater volume of distribution of water and urea, compare to those of albumin and sucrose, is indicative of distribution of these markers into a bigger space (*ie* vascular plus interstitial plus cellular spaces). The value found for the intracellular water space corresponds closely to that found (0.635) in other studies [83,90,198,197]. A biexponential barrier-limited distribution, as described by some workers [291,119], was not found for water in cirrhotic livers in this study. In PT livers, the specific cellular volume was relatively greater.

In cirrhotic livers, less difference was found between the values of $V_{CELL\text{-}WAT}$ and $V_{CELL\text{-}URA}$ compared to the control values, whereas the V_{CELL} estimated based on the V of SUC showed more depression than the V_{CELL} based on the V of ALB. The reason lies on the extent of alteration of volume of distribution of markers.

Assuming similar physicochemical properties, similar distribution behaviour may be expected for water and urea. Indeed the volume of distribution for these two cellular markers are similar. However a 10% difference was calculated. Water, as one may expect from its physiochemical properties and behaviour in other organs, is distributed thoroughly into the whole space accessible to a substance in the liver. Therefore, it is the urea that has been limited from access to a part of the cellular space. For non-eliminated cellular markers such as water and urea, uptake by the hepatocytes is expected to be complete by the first pass through the liver. From the

slightly larger $f(t)_{max}$ and smaller t_{max} of urea compare to that of water it is evident that a small fraction of urea was not able to enter the cells and travelled directly to the outflow.

The difference in distributional behaviour of the two cellular markers is further illustrated in Figure 4.17, where the ratio of urea to water is plotted. For the first 16 sec time period of the curve (the ratio of upslope values), the ratio was larger than 1 indicating a bigger uptake for water than urea. The diffusion coefficient for water is slightly more than twice that for urea [79] implying a greater throughput component for urea than water. Therefore, the rate of influx for urea is slightly smaller than that of water and as $PS=k_{12}.V_b$, permeability through the cell membrane is different for the two markers.

The ratio of urea to water after 16 sec was 1:1, and the slope and intercepts were zero and unity, respectively. After 60 sec, this ratio became progressively smaller than 1, which reflected the elution of larger proportion of water in the outflow compared to that of urea. It should be noted however that in the early and final parts of the ratio plot, as the concentration of both urea and water is low, so is the precision of the ratio. In the cirrhotic livers, the ratio plot is systematically different to that observed for control livers. In the first portion of the curve (ratio of inclines), a greater ratio was observed, indicating a bigger throughput component and permeability barrier for urea. The second portion of the curve (ratio of peaks) was short lasting only 8 sec. The final part of the plot (ratio of tails) was relatively longer (starting from 30th sec) and progressively decreasing.

The difference in the profiles of water and urea may alternatively be explained by the analysis of convection and diffusion during indicator transport through the liver [201]. A more rapidly diffusing molecule is, in the delayed wave, expected to exhibit a dispersion along the single pathway, proportional to the square root of the product of the diffusion coefficient and the transit time, divided by the entrance-exit length. As the diffusion coefficient for water is slightly more than twice that for urea [79], a longitudinal diffusional phenomenon thus appears to account for the small scale increase in dispersion of the water curves, in relation to the urea curves.

It has been reported that the volume of distribution of water displays a tendency to increase slightly with increasing flow rate [121]. The reason seems to stem from inadequate perfusion. At

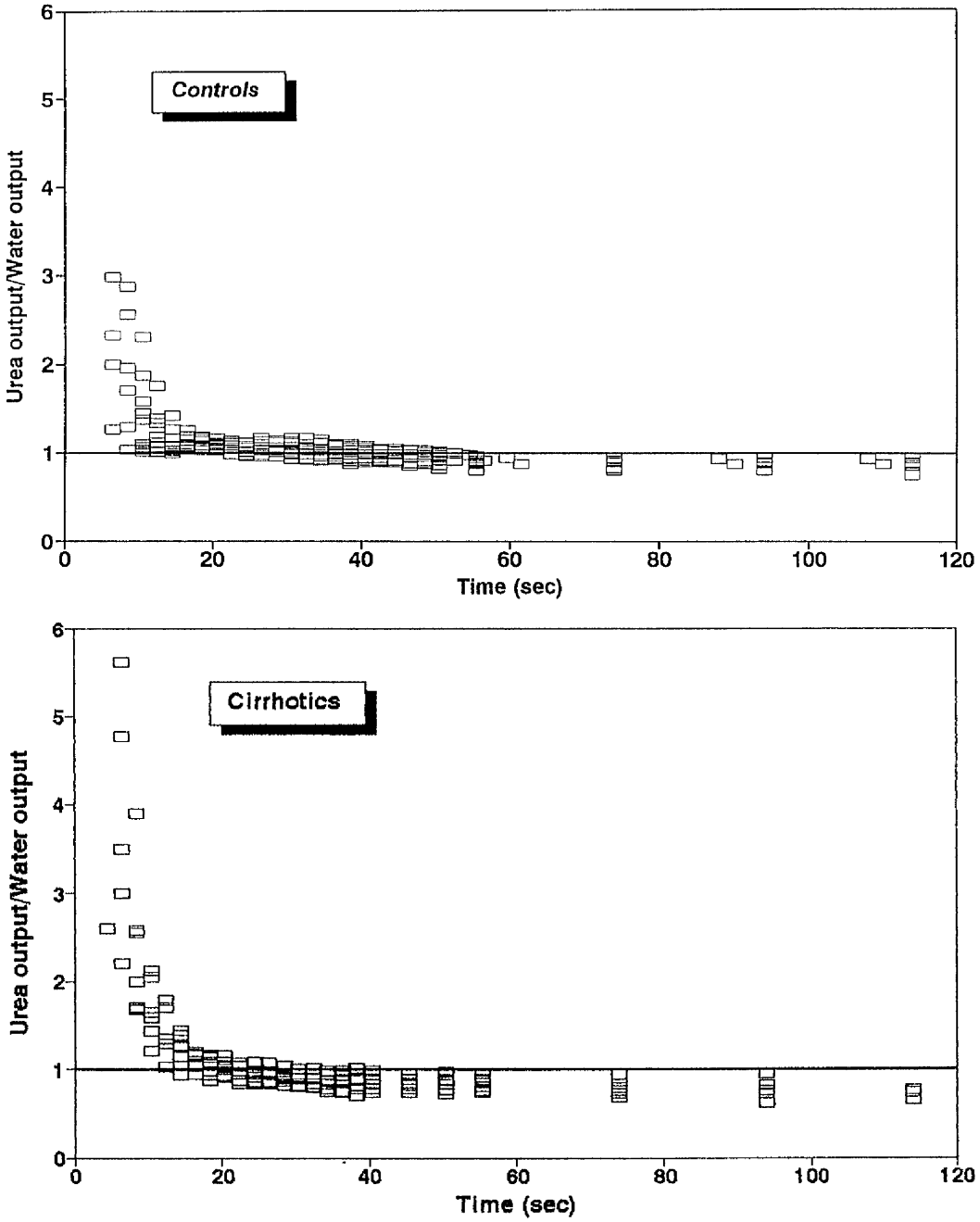

Figure 4.17 Ratio of the frequency output of urea to the frequency output of water obtained in all liver preparations in isolated perfused rat liver.

low perfusion flow rates, perfusate may not take access to all parts of the liver whereas with increasing flow rate, all liver mass is adequately perfused, giving a larger MTT. Indeed a good correlation has been described between perfusion flow rate and specific hepatic spaces [92,197]. As such, as a correlation has not been found for intracellular water space [55], it is conceivable that this reported correlation may have been due to sinusoidal dilation, as has been described by some workers [2].

The estimation of total aqueous space depends on the marker used for the analysis. When ALB and WAT were used, larger volumes were obtained than when URA and SUC were used. Furthermore when ALB and URA were used for the estimation of cellular space, a smaller change was observed between control and cirrhotic livers (0.04 ml/g), whereas using SUC and WAT, indicated larger changes (0.18 ml/g). The finding that cellular space was slightly reduced in the cirrhotic livers is in agreement with literature data. However, in contrast to these findings, a group of workers [291] (using sucrose for analysis) reported a 30% increase in the volume of cellular space. Although they were not able to offer any physiological reason for their observation, their control value for cellular volume was lower compared to literature data. This group of workers also reported an unchanged total water volume suggesting a decrease in the extracellular space in cirrhotic livers. This is in contrast to their observation of a 10% increase in the extracellular volume.

Comparative studies: The outflow profiles may be analysed using another method of analysis called the Peak-Time method [83,291]. In this method, the volume of the accessible space to diffusible markers (DIFF) is estimated from the displacement of outflow curves in relation to that of erythrocytes (RBC). This approach depends on the symmetry in the time-concentration changes of the diffusible label curve shape when compared with that of the erythrocyte curve. The transit time and volume of markers are calculated using the following equations:

$$T_0 = \frac{[T_P RBC(1+y) - T_P DIFF]}{y} \qquad (4.6)$$

$$y = \frac{f(t)_{max} RBC - f(t)_{max} DIFF}{f(t)_{max} DIFF} \qquad (4.7)$$

where T_0 is the time spent by markers in the large vessels, T_PRBC and T_PDIFF are the transit time at the peak of the erythrocyte and diffusible marker profiles, respectively, and $(1+y)$ is the ratio of $\frac{\text{peak RBC}}{\text{peak DIFF}}$; thus:

$$MTT_{SIN} = MTT_{RBC} - T_0 \quad (4.8)$$

$$V_{SIN} = MTT_{SIN} \cdot Q \quad (4.9)$$

When the outflow concentrations and elution time of diffusible markers are adjusted by the factor y (*ie* $\frac{C}{1+y}$ and $t\times[1+y]$), superimposible curves should be obtained. It has been suggested [291] that in cirrhotic liver, if conditions for a flow-limited distribution were no longer fulfilled, the extravascular volume measured by the peak-time method [83] would depart from the volume measured by the transit-time method [44,45]. This disparity can result either from shunting, in which both reference and diffusible labels pass through the vasculature with little difference in their transit times, or from collagenisation and capillarisation, in which the development of a new barrier limits diffusion in the extravascular space.

In order to test this hypothesis, the peak-time method of analysis along with the transit-time method was applied to the outflow data of albumin and sucrose. As illustrated in Figure 4.18, a good correlation was observed for the volume of albumin estimated using the two methods ($r=0.95$), indicating that the distribution of albumin was compatible in a flow-limited kind of behaviour in cirrhotic as well as in control rats, as previously reported in cirrhotic patients [119]. In contrast, in the cirrhotic livers ($n=4$) where the sucrose dilution curves were no longer compatible with flow-limited distribution, the peak-time volume differed from transit-time volume (Figure 4.19).

Volume correction: The control values for the hepatic volume of distribution of markers obtained in the current study (Table 4.5) are similar to the values reported by several other workers [83,316,214,90]. In one study, a total aqueous volume of 0.93 ml/g was reported [291]. However, these values are considerably larger than those reported by most workers (Table 4.9). Thus, for comparative purposes, a modification step was performed on the experimental data. The relative volume of distribution of water was considered as reference and assumed to be 70% of liver weight [65]. As overestimation of volume is reflected in overestimation of MTT,

Table 4.9

Literature values for mean transit times and volumes of distribution of markers in liver, and estimated volumes of hepatic spaces

Mean Transit Time (sec)					Volumes of Hepatic Spaces (ml/g)									REFERENCE	
RBC	ALB	SUC	URA	WAT	Vascular Volume	Sinusoidal Volume	Extracellular	Disse ALB	Space SUC	ALB/SUC	TOTAL WAT	Intracellular URA	Intracellular WAT		
7.7	10.5	11.7						0.07	0.1	0.7				129,130	*rat liver*
		29.1	40	44			0.33		0.13			0.52	0.55	198	*rat liver*
					0.19			0.065	0.085		0.68			218	*rat liver*
					0.08		0.2							218	*rat skin*
7.9	11.4													2	*rat liver*
9.5	11.5	17.5	40	45		0.15		0.07	0.1					83	*dog liver*
					0.152			0.06						341	*dog liver*
					0.194			0.07						342	*rat liver*
					0.19			0.05	0.07					218,219	*rat liver*
9.5	13	15		36	0.2			0.07	0.09		0.52			291	*rat liver*
		8		30			0.15				0.6			54	*rat liver*
							0.18							3,224 225,283	*rat liver*
				25							0.65			121	*rat liver*
	13	12		44			0.17				0.6			291	*rat liver*
													0.55	198	*rat liver*
			42	48				0.08				0.55	0.65	197	*rat liver*
							0.15							63	*rat liver*

RBC: erythrocytes SUC: sucrose WAT: water

ALB: albumin URA: urea values are in normal livers

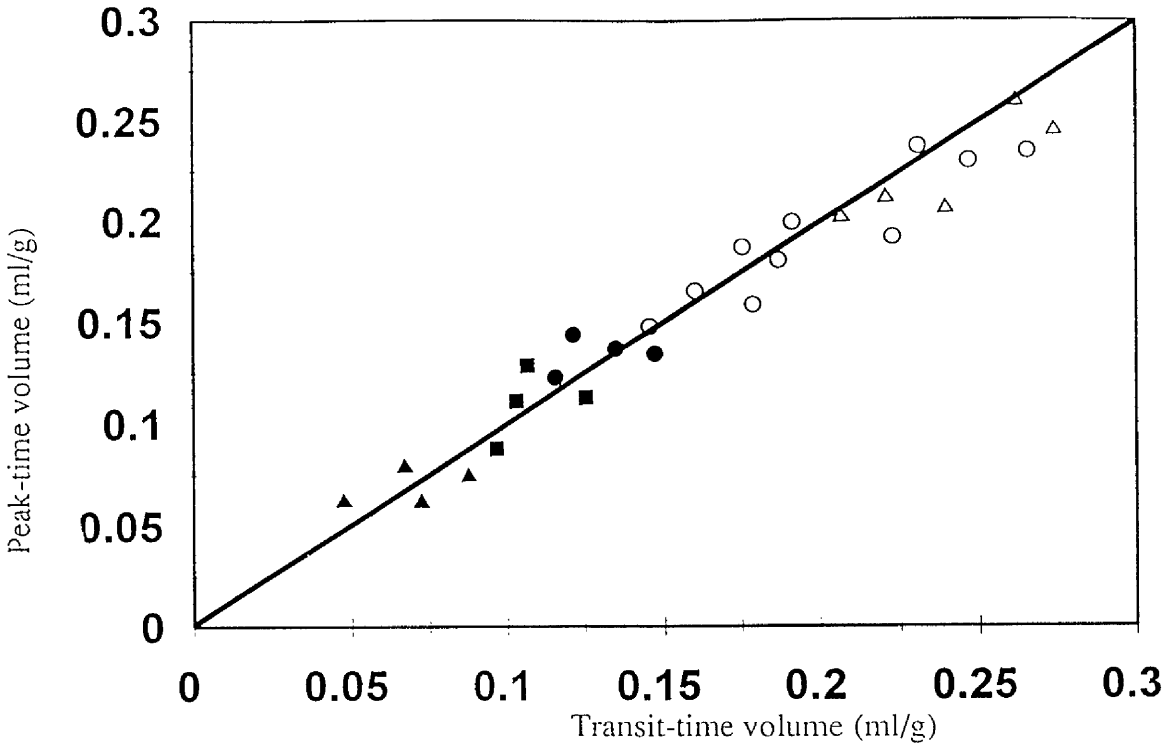

Figure 4.18 Plots of the extracellular volume of distribution of labelled albumin calculated using the peak-time method (abscissa) and the mean-transit method (ordinate). The solid line is the straight-line regression through the data obtained in cirrhotic livers: ▲, category 1; ■, category 2; ●, category 3. The correlation coefficient for the data is 0.92 (n=12). Values obtained in 10 normal livers (○) and 5 phenobarbitone-treated livers (△) are also shown.

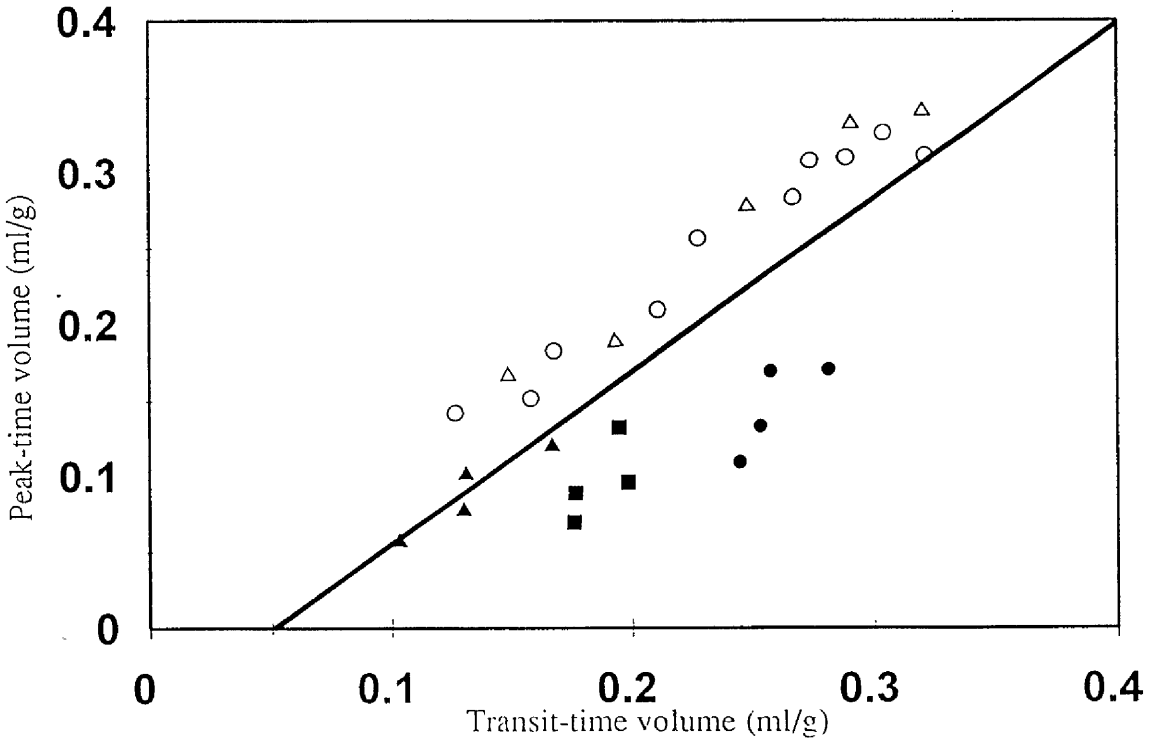

Figure 4.19 Plots of the extracellular volume of distribution of labelled sucrose calculated using the peak-time method (abscissa) and the mean-transit method (ordinate). The solid line is the straight-line regression through the data obtained in cirrhotic livers from category 1(▲).The correlation coefficient for the data is 0.91 (n=4). Values obtained in 10 normal livers (○), 5 phenobarbitone-treated livers (△), and cirrhotic rats from category 2 (■) and category 3 (●) are also shown.

correction of MTT would then result in correction of corresponding volume. Therefore, the correct value of MTT was estimated using the following equations.

$$V_1 = MTT_1 \times Q \quad (4.10)$$

$$V_2 = MTT_2 \times Q \quad (4.11)$$

where V_1 is the assumed value of volume of distribution of water (70%), V_2 is the value obtained experimentally, MTT_1 is the mean transit time of water which was to be estimated, and MTT_2 is the MTT of water observed experimentally. Thus:

$$MTT_1 = (V_1 / V_2) \times MTT_2 \quad (4.12)$$

The ratio of V_1/V_2 of water in each set of experiments was used as a basis for the recalculation of MTT and V of other markers in that experiment, assuming that the magnitude of delay in MTT was the same for all markers. The mean values of MTT and V for all reference markers, estimated in this manner, is presented in Table 4.11.

Table 4.11
Corrected values of Mean Transit Time and Volume of Distribution for radiolabelled reference markers in control livers.

	Mean Transit Time (sec)	Volume of Distribution (ml/g)
Erythrocytes	7.5 ± 0.7	0.19 ± 0.05
Albumin	13.3 ± 1.1	0.31 ± 0.05
Sucrose	14.3 ± 1.6	0.35 ± 0.07
Urea	29.8 ± 1.5	0.68 ± 0.07
Water	32.8 ± 1.9	0.75 ± 0.07

For method of correction see the text
Values are mean ± SD. n=10

Although the cause of overestimation of MTT presumably existed in the cirrhotic preparations as well, the correction technique was not used. This was due to the fact that changes in the hepatic spaces is naturally associated with the disease processes and approximation of the degree of changes in the volume related to each part (disease or experimental error) is very difficult. Hence the uncorrected values of both control and cirrhotic livers used for the comparison of the two groups.

Comparison of methods on volume estimation: There were slight differences between the values of V obtained by moment analysis and those obtained by modelling (Table 4.5). These differences may be explained by considering the moment and modelling procedures. Generally, the values obtained by modelling were similar to those obtained by moment analysis when the following conditions were met:

a) on modelling, calculated data closely approximated the observed data.

b) on moment, the sampling time was adequate, so that the error involved in extrapolation was minimal.

The dispersion model did not provide for any change in the values of volume of distribution of water and urea from control to cirrhotic livers, whereas moment analysis indicated a reduction of 23% for this parameters. With regard to the physiological properties of water, a major change in the volume during the disease process is not expected. However, there are several possibilities that may account for the observed reduction in water volume estimated by moment analysis. It may well be due to hepatic fibrosis. Fibrosis of the liver may lead to inadequate perfusion and thus an underestimation of MTT. In contrast, the cirrhosis process results in the alteration of the liver composition, increasing the volume of connective tissue (inaccessible to water) [217]. Another possibility was the effect of large vessels. As the volume of large vessels is relatively reduced in cirrhotic livers, their bias effect on the estimation of volumes showed also to be reduced.

4.6.1.8 Relative spreading (CV2)

On calculating CV^2, variance is normalised for the mean value. When the variance of transit (statistical distribution) of elements of an injected label is normalised for the size of the system (MTT), then comparison between two populations is possible. For non-eliminated labels showing flow-limited distribution, similar values of CV^2 (normalised measure of spreading) should be obtained. This was the case for the vascular and extracellular markers in the control livers. Despite the large difference between their volume of distribution, the estimated CV^2 for RBC, ALB and SUC was found to be in the range of 0.285 to 0.3. The value of CV^2 for cellular markers was slightly larger than that for the vascular and extracellular markers.

In the cirrhotic livers, a greater relative spreading was estimated for the reference markers. Numerous structural changes which take place in cirrhosis may have caused this increase. However, it should be noted that calculation of MTT and particularly VTT involves some

extrapolation which renders some error in the estimation of CV^2. The RBC was the only marker whose CV^2 slightly decreased in cirrhotic livers, indicating a lesser spread in the liver. As the sinusoidal volume was decreased and large vessels volume remains relatively unchanged, it may be concluded that the sinusoids were the major site of spread for RBCs within the liver. The extent of increase in CV^2 of sucrose to that of cellular markers suggests that it may even have penetrated into the hepatocytes. The marginal change in the relative spreading of water is compatible with its physicochemical properties. The noticeable change in the relative spreading of a small molecule such as urea (60% increase in CV^2) clearly indicated some permeability changes at the membrane level.

4.6.1.9 Dispersion number

There was good agreement between the D_N values of markers obtained in the control livers and those reported by the others [54,121]. The D_N values calculated using moment analysis also closely approximated those estimated by modelling. The D_N values for the markers in the control livers were similar as it might be expected. The D_N values of the markers in the cirrhotic livers changed markedly which indicated a change in the hepatic microstructure[228] and the diffusional properties of the space of Disse and increased resistance to permeability. Comparison between the D_N of water and slightly decreased D_N of erythrocytes and distribution properties of these two markers reveals that altered dispersion of markers has primarily been caused by change in the diffusional characteristics of the space of Disse.

4.6.1.10 Classification of cirrhotic rats

The difference in the observational parameters between the reference markers was the basis for classification of cirrhotic livers (Table 4.12). This classification proved to hold also for the moment parameters of the markers and the model drugs (Table 4.13). This classification matches the categorisation of cirrhotic livers according to the histological observations. This finding illustrates that a good correlation exists between the degree of structural damage and functional alteration in cirrhosis. An example of such correlation for MTT values of urea is depicted in Figure 4.20.

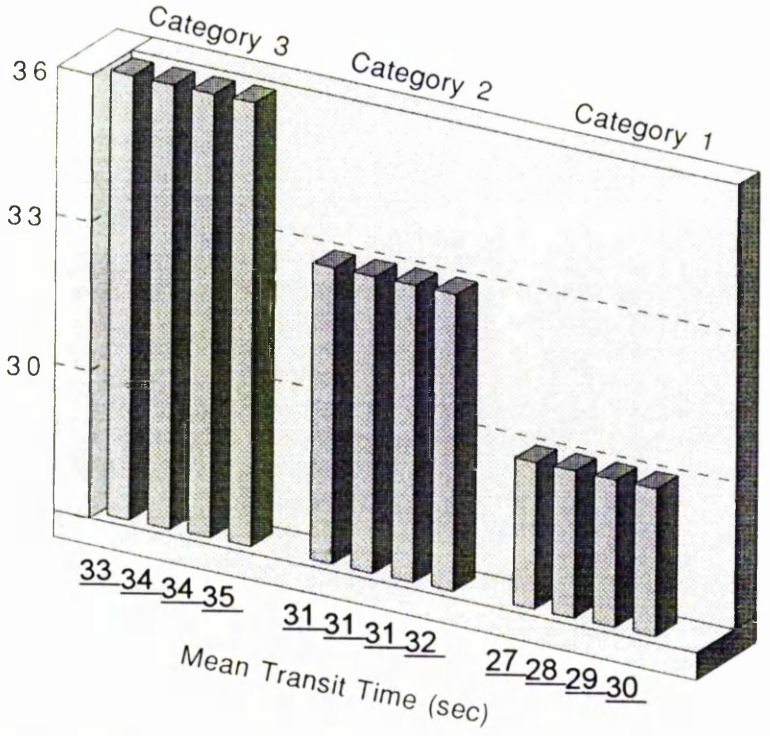

Figure 4.20 Relationship between the MTT of urea (the numbers) obtained in different cirrhotic liver preparations and the categories of cirrhotic livers based on the histological evaluation.

Table 4.12

Classification of cirrhotic livers served in the isolated perfused liver studies based on the extent of change in the parameters of moment analysis of model compounds and histology.

	Albumin and Sucrose		Urea and Water		Diazepam		Diclofenac		Salicylate		Histology	
Category 1	3	4	3	4	3	4	3	4	3	4	3	4
	7	8	8	10	7	10	7	8	7	8	7	8
Category 2	2	6	1	2	2	6	2	6	2	6	2	6
	9	10	7	10	8	9	9	10	9	10	9	10
Category 3	1	5	5	6	1	5	1	5	1	5	1	5
	11	12	11	12	11	12	11	12	11	12	11	12

The numbers in each box are the numbers of cirrhotic livers.
Category 1 contains the cirrhotic livers with the maximum changes.

Table 4.13

Parameters of moment analysis of reference markers in various categories of cirrhotic livers in isolated rat liver preparations.

		MTT (sec)					V (ml/g liver weight)					CV2				
		RBC	ALB	SUC	URA	WAT	RBC	ALB	SUC	URA	WAT	RBC	ALB	SUC	URA	WAT
Category 1	mean	7.0	8.9	16.1	29.3	31.8	0.11	0.13	0.35	0.54	0.59	0.37	0.58	0.80	0.85	0.69
	≠S.D	0.4	2.4	2.9	2.9	4.6	0.02	0.02	0.07	0.11	0.13	0.06	0.12	0.12	0.14	0.09
	CV%	5	26	18	10	14	20	20	17	22	21	15	20	15	15	12
Category 2	mean	7.8	11	18	33	39	0.16	0.22	0.45	0.74	0.68	0.25	0.36	0.55	0.64	0.58
	≠S.D	0.5	2.9	3.8	0.8	2.1	0.03	0.04	0.05	0.13	0.15	0.04	0.10	0.10	0.11	0.08
	CV%	10	30	20	2	10	15	20	10	18	21	13	25	16	18	13
Category 3	mean	8.2	16.0	22.5	36.1	40.3	0.21	0.24	0.55	0.84	0.93	0.21	0.26	0.45	0.58	0.47
	≠S.D	0.8	2.8	2.6	3.2	5.5	0.03	0.06	0.10	0.15	0.18	0.03	0.08	0.07	0.07	0.07
	CV%	10	20	10	10	10	15	30	16	18	20	15	26	14	11	14
Overal Mean		7.5	11.1	19.4	31.7	35.7	0.15	0.22	0.43	0.73	0.77	0.27	0.42	0.64	0.72	0.57
	≠S.D.	0.7	2.3	2.7	3.2	5.1	0.03	0.06	0.09	0.18	0.19	0.04	0.10	0.10	0.10	0.09
	C.V.	10	20	10	10	10	15	30	22	25	23	13	25	16	14	15

MTT: mean transit time
V: volume of distribution
mean value in each cirrhotic group is the men of 4 subjects

The Model Drugs

In the previous section, radiolabelled reference markers were used to characterise the hepatic distribution and reveal the effect of cirrhosis on hepatic resistance to solute exchange. A knowledge of distribution properties of normal and cirrhotic livers, obtained in the previous section, would help to closely examine the influence of permeability alterations on the distribution of model drugs. As all the test substances (markers and drugs) are studied under similar controlled experimental conditions, many related issues including membrane permeability, hepatic dispersion, distribution, and structure-activity relationship can be defined for model drugs.

The selection of model drugs was based on the theoretical considerations. Studies show that small, lipophilic, unionised molecules readily diffuse through cell membranes and often show perfusion rate-limited distribution [129,344,90]. Many polar, hydrophilic and ionised compounds penetrate cell membranes with difficulty showing permeability rate-limited distribution [196,257,172,343]. Diazepam and diclofenac are examples of the first type and salicylic acid is an example of the second type of substances. Since the hepatic disposition of these drugs has been previously studied in this laboratory [121,60,120], they were selected as model solutes. This provided an opportunity to conduct a comparative study.

4.6.2 Salicylic Acid

To study the influence of altered membrane permeability on the distribution kinetics of a relatively poorly permeable solute, salicylate is a suitable choice based on published findings:

1-Its clinical pharmacokinetics and metabolism are well established [297,325,21,121,115,146,147,150].

2-The low extraction allows the examination of drug distribution in IPRL.

Despite the attractive characteristics of salicylate as a model compound, a limited number of reports exist in the literature on its application for the evaluation of hepatic drug distribution per se. A group of workers [122] reported the use of salicylate in IPRL in single-pass mode. That data, however, due to the short duration of outflow collection time in their experiments cannot be clearly interpreted. Another series of experiments conducted in this laboratory by Hussein *et al* [121] studying tissue binding of salicylate in isolated perfused livers. The present work which

extends the previous knowledge on salicylates was the first to study the hepatic dispersion of a poorly extracted compound under the conditions of altered permeability.

4.6.2.1 Salicylate output profile in control livers

The shape of the salicylate frequency outflow in studies performed by Hussein *et al* [121] can be resolved in two parts: The rapidly eluting peak represented the throughput component, the fraction of the total outflow that passes through the liver without entering hepatic cells due to poor cellular membrane permeability and rapid flow washout from the vascular compartment. The more slowly eluting fraction of the output, corresponding to the "returning component", represents salicylate that has entered cells and returns to the vascular compartment. The return is impeded by intracellular binding and limited permeability [323].

The absence of an early sharp peak in the control curves in this study indicated that there was no obstacle for salicylate to leave the vascular space, *ie* high cellular permeability. A very small throughput component still existed which was not due to a permeability barrier at the membrane level (Figure 4.22). This component, which could not be visualised, was the material that did not have time to exchange. The CV^2 value of salicylate (0.55) approximated to that of water (0.5) indicating the existence of equilibrium distribution for salicylate between vascular and cellular spaces, and instantaneous radial influx of salicylate into hepatic cells. However the fraction of salicylate that entered the cells was subjected to intracellular binding. As most of the injected salicylate had been taken up by the liver the returning component was much more pronounced. Using simulation studies, it has been published[228,122] that this kind of output profile is characteristic of solutes that distribute freely through intra and extracellular spaces and bind to hepatocyte components.

The observed difference in output curves in the two studies was not due to a variation in flow rate. The experimental conditions including perfusion flow rate per g liver weight in both studies were similar (1.5 ml/g). However the liver populations used in the two studies were different. Normal livers in these experiments were approximately 7 months old weighing 23.5±3.5 g. Normal livers in the study of Hussein *et al* would have been less than 2 months old weighing 12.2g. The difference in the outflow profiles would not stem from weight difference since the data were either free from weight consideration (*eg* MTT) or were normalised for weight (*eg* V).

It is possible that the difference in the profiles is caused by the age difference. It has long been recognised that ageing is associated with alterations in physiological and pharmacological variables, and an age-related decline in the metabolism of a number of xenobiotics has been observed in old rats [5,169,262]. Several physiologic processes such as biliary function decline at greater ages (>1 year) [256]. Cardiac output and tissue perfusion are both reduced with age [35,132], although drug distributional changes due to these alterations may well be offset by changes in the tissue distribution of the cardiac output, as well as decreases in tissue and lean body masses [34,36]. In addition to these reports, several systematic studies have been conducted to evaluate the influence of age on pharmacokinetic parameters. The influence of age on rat liver plasma membrane enzymes has also been demonstrated [1]. The life span of a laboratory rat is normally 2 years. Although control rats in these experiments did not reach that age, these were much older than other rats used in experimental pharmacology. To examine whether the outflow profile was different in younger livers, a separate dilution experiment was carried out on three two-months-old livers weighing 15 g using three different flow rates (20, 30 and 40 ml/min). The observed frequency output profiles obtained in the young livers (Figure 4.21) were different from those described for older control livers, but were similar to those obtained by Hussein *et al* [121].

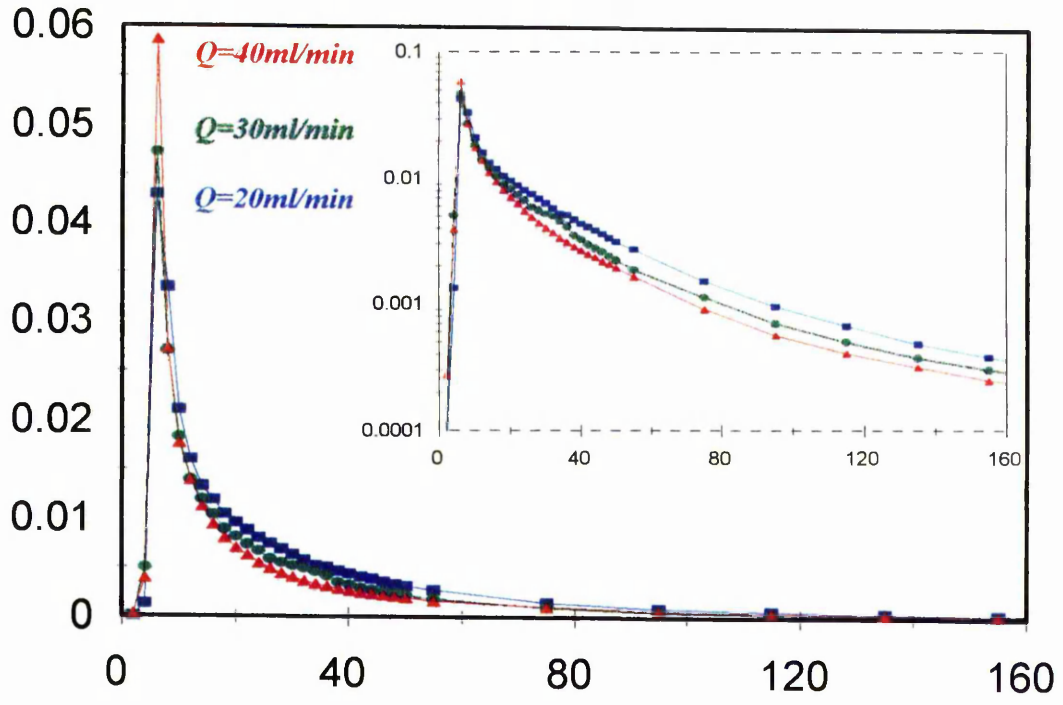

Figure 4.21 Linear and semilogarithmic plots of frequency output concentration of salicylate in a representative normal liver, from a 2-month old rat, perfused at different perfusion flow rates.

4.6.2.2 Salicylate outflow profiles in cirrhotic livers

The profound change in the outflow profiles of salicylic acid (Figure 4.3) in cirrhotic livers is indicative of change in the distribution to non-equilibrium conditions. This is confirmed by the increased CV^2 value compared to the control value and that of water. The appearance of a fast eluting sharp peak suggests that the hepatic uptake of salicylate has been decreased. The permeability barrier that has caused this reduction in uptake may have been formed at various levels. The formation of some sort of basement membrane in the sinusoids as well as collagen deposition in the space of Disse and structural changes at hepatocyte membranes can lead to progressive limitation in sinusoid-tissue exchange. Since salicylate is a small molecule (MW 138) and unbound in the perfusate, the permeability barrier should be mainly at the level of the cell membrane. Comparison of the salicylate profiles in the cirrhotic livers to those obtained by Hussein *et al* [121], where a permeability barrier at membrane level was described for salicylate hepatic distribution, confirms this idea.

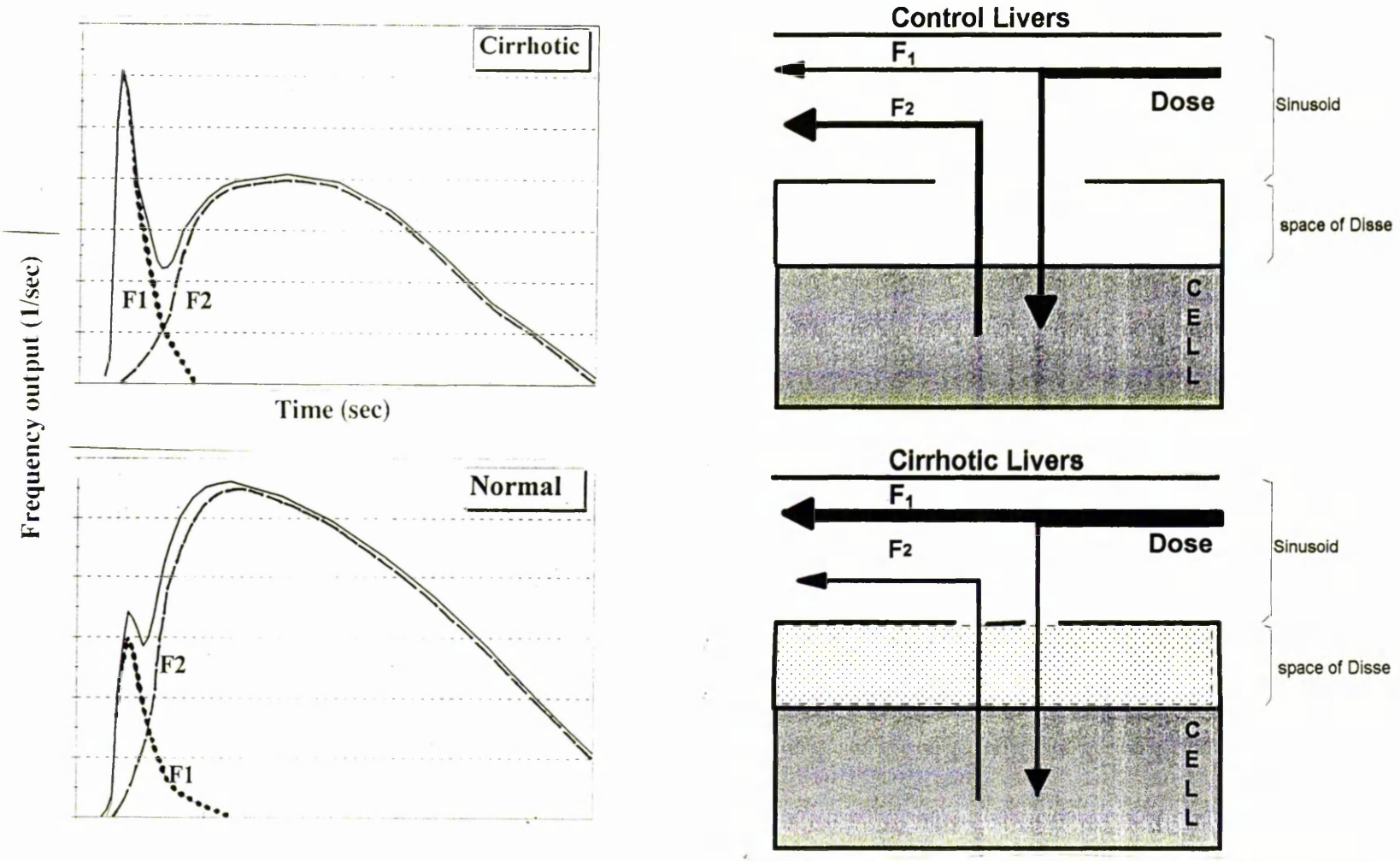

Figure 4.22 Simulation of throughput (F_1,.....) and returning (F_2, - - - -) components, and the complete profile (—) of frequency output of salicylate in representative normal and cirrhotic livers. Diagram illustrates the effect of cirrhosis on the hepatic distribution of salicylate.

4.6.2.3 Recovery

In this work only total ^{14}C radioactivity was measured and assumed to be equivalent to the ^{14}C-salicylate, given that salicylate is not eliminated when administered as a bolus into the single-pass perfused liver [147,186]. This assumption was based on results from the HPLC analysis of unlabelled salicylate perfusate concentrations from previous studies in this laboratory [121]. These studies indicated that the steady-state output was achieved within 15 min and the recovery of unchanged salicylate was between 94% and 99%. This was in agreement with the very low hepatic extraction ratio (0.05) of salicylate in the rat [186,115]. The relatively higher recovery of radiolabelled salicylate reported by Hussein *et al* [121], compared to the values found in the current experiment, was probably due to the presence of cold salicylate in the perfusate in those experiments. The increase in the recovery of labelled salicylate in the presence of cold drug has been observed by another worker [246]. Another possibility is the greater influx of the drug leads to more extensive and stronger intracellular binding. In cirrhotic livers, where the rate of influx has been decreased, an increase in recovery was observed.

4.6.2.4 Volume of distribution in control livers

The much larger volume of distribution of salicylate (53 ml) (Table 4.4) compared to that of sucrose (10.9 ml) indicated that salicylate permeated through the hepatocyte membrane and distributed into the cellular space. A larger normalised volume of distribution (2.6 ml/g) compared to that of water (1 ml/g) indicated that this compound had a significant affinity for hepatic tissue. The normalised volume in this work was considerably larger than that obtained by Hussein *et al* (1.5 ml/g) [121] but the corrected value (Table 4.11) was less different (1.8 ml/g). From the non-parallel change in the volume of distribution of salicylate (50% reduction), cellular markers (20% reduction) and intracellular space (10% reduction) it was thought that the structural changes that occurs either at the cellular membrane level (new permeability barrier) or inside the cells (influencing tissue binding) may have contributed to the salicylate decreased volume. The decrease in k_{12} (Table 4.14) and unchanged k_{21} favour the first potential mechanism (Equation 2.16). Conversely reduced k_{12} and increased V_b would imply an unchanged membrane permeability.

Table 4.14

Pharmacokinetic parameters for salicylic acid in isolated perfused rat liver obtained by fitting the dispersion model equations to its frequency outflow.

		k_{12}	k_{21}	D_N	K_P	*fuc*	TC%	RC%	PS
Normal Livers	Mean	0.29	0.075	0.082	3.7	0.29	5	78	8.2
n=10	±S.D.	0.051	0.013	0.023	0.64	0.05	1.4	12	1.3
	C.V.%	17	17	26	17	17	28	15	15
PT* Livers	Mean	0.29	0.073	0.084	3.9	0.3	4	78	8.5
n=5	±S.D.	0.058	0.015	0.023	0.7	0.05	1.2	12	1.5
	C.V.%	20	20	26	17	16	30	15	17
Cirrhotic Livers	Mean	0.12	0.084	0.29	1.5	0.58	18	73	3.2
n=12	±S.D.	0.02	0.015	0.08	0.34	0.07	3.3	13	1.1
	C.V.%	16	17	26	22	12	18	17	34

* phenobarbital treated
k12: influx rate constant
k21: efflux rate constant

Dn: dispersion number
Kp: perfusate-tissue distribution coefficient
fuc: fraction unbound in tissue

TC: throughput component
RT: returning component

It was possible to calculate a cellular volume accessible to salicylate, extra to that of water. Assuming salicylate occupies total hepatic water space,

$$V_{wat}=V_b+V_c \quad (4.13)$$

$$V_{sal}=V_b \cdot (1+K_p) \quad (4.14)$$

where K_p is the ratio of k_{12} to k_{21}. Therefore,

$$V_{sal} - V_{wat} = K_p \cdot V_b - V_c \quad (4.15)$$

The value of k_{12} is greater than k_{21} which indicates a considerable cellular influx and slow cellular efflux (compatible with the salicylate outflow profile), and also a greater volume of distribution compare to water. The estimated specific cellular volume accessible to salicylate in control livers was 1.15 ml/g which was similar to the values calculated from the data reported by Hussein *et al* (1.1 ml/g) [121]. This volume was reduced to very low values in cirrhotic livers indicating limited access of salicylate to the hepatocytes in the cirrhotic livers.

4.6.2.5 Dispersion Model analysis

Although the isolated perfused rat liver preparation is useful for determining the distribution of transit times after a bolus injection of the drug into the hepatic portal vein, the events occurring within the liver are difficult to describe with any precision without the use of a physiologically based model. Nevertheless, it is important to test the applicability of any model by assessing its ability to describe the kinetic behaviour of different compounds under a variety of test conditions.

In the present project, the two-compartment dispersion model was capable of adequately describing the frequency outflow profiles of salicylate in both control and cirrhotic livers (Figures 4.7 and 4.8). The modelling analysis allowed for the estimates of kinetic parameters such as k_{12}, k_{21}, D_N, fu_c and K_P. Unlike the two-compartment model, the one-compartment dispersion model could not adequately describe the temporal profile of salicylate in both groups. This finding, supported by the observations of others [121,122], suggested that the overall distribution of salicylate in the liver, unlike water (cellular marker) is influenced by: a) intracellular binding, in normal livers; b) intracellular binding plus permeability barrier at cellular level, in cirrhotic livers.

The values of D_N determined for salicylate in this and other studies [121,122] were consistently lower than those have been observed for other solutes [63,60,65,242,228,84]. A possible explanation for this low estimates of D_N lies in the sensitivity of this parameter to the fitting procedure used to describe salicylate dilution curves. The model tended to underestimate the peak and end stage tailing portions of the salicylate outflow curve. This appeared to be independent of the weighting scheme employed. Simulations using dispersion model parameter estimates obtained in this study confirmed that failure to accurately characterise the throughput portion, especially the upcurve and $f(t)_{max}$, could lead to underestimation of the true value of D_N. In practice, this problem arises when the collection interval of liver effluent is relatively large compare to the time taken for the throughput component to eluent. More frequent sampling times, particularly at the beginning of collection, may improve the fit. Simulating experimental data by manipulating the sampling times (using a D_N value in the range 0.15 to 0.2, observed for water 2-5&20/34a) over 1.5 sec intervals it was possible to produce an outflow curve that was identical to the profile simulated using a D_N of 0.08. Hence, the consistently lower value of D_N observed in the present study appears to have arisen from a limitation in the outflow fraction collection procedure relative to the very rapid flux of salicylate from the IPRL

The D_N values in Table 4.14 have been calculated using modelling procedure. The dispersion number could also be calculated by moment analysis using the following equation [228-230]:

$$CV^2 = 2D_N - 2D_N^2 \times [1 - \exp^{(-1/D_N)}] \qquad (4.16)$$

The D_N of salicylate in both liver populations estimated using the dispersion model (0.082 and 0.29) was consistently lower from that obtained using moment analysis (0.25, and 0.43). This gave some indication of the goodness of fit and confirmed the previous theory that imperfect fitting leads to underestimation of D_N. It may appear that the magnitude of potential error involved in the estimation of D_N value using moment analysis was less than that of modelling. However D_N is always being estimated using model equations and CV^2 could be readily estimated by moment analysis.

4.6.2.6 Throughput and returning components

To assess the relative influence of the throughput and returning components on the shape of the outflow profiles, two profiles were simulated. Based on the estimated mean values for k_{12}, k_{21} and D_N (Table 4.14), the complete profile for salicylate was first simulated using Equation 2.15.

In the second simulation, all parameters remained the same except k_{21}, which was set to zero (*ie* no return of salicylate from the cellular space) [323]; this profile depicted the throughput fraction (Figure 4.22). The difference between the AUCs of complete and throughput profiles represents the returning component [85,90]. Based on these simulations, it was estimated that the throughput and returning components comprise 5% and 78% of the injected material, respectively. An increase of > threefold in the throughput component (to 18%) in cirrhotic livers (Table 4.14) was another indication of the reduced permeability of salicylate in cirrhosis.

4.6.2.7 Fraction of salicylate bound in hepatic tissue

The presence of salicylate in the perfusate results in a concentration-dependent decrease in the volume of distribution [121]. This ability would suggest that salicylate undergoes considerable binding to the tissue. The absence of protein in the perfusate (fu=1) in these experiments provided an opportunity to investigate the extent of binding of salicylate within the hepatic tissue. An estimate of fraction unbound in the cells, f_{u_c}, could be obtained from the two-compartment dispersion model parameter estimates by rearranging and combining Equations 2.16 and 2.17 to give,

$$f_{u_c} = \frac{k_{21} \cdot V_c}{k_{12} \cdot V_b} \qquad (4.17)$$

where V_c is the aqueous cellular volume (the difference between volume of water and extracellular volume). This calculation assumes that salicylate is distributed into the total water space within the liver, the influx and efflux permeability-surface area are equal ($PS_{in} = PS_{out}$) and that there is no binding in the perfusate.

An agreement was found between the f_{u_c} value calculated in the control livers (0.29) and that calculated by Hussein *et al* (0.37)[121]. This was despite the fact that the calculated k_{12} in these experiments was smaller than that found by these workers. The reason lies in the ratio of V_c/V_b, which was smaller in these experiments (1.6) than that experiment (2.8). In cirrhotic livers, the value of f_{u_c} was increased to 0.58, which may be considered as an indication of decreased intracellular binding capacity in cirrhosis.

The intracellular binding of salicylate was further supported by a larger K_P (liver-to-perfusate partition coefficient) of 3.7 compare to that for water (K_P =1). The value of K_P obtained in the present experiments was in good agreement with the *in vivo* unbound Kp (K_Pu) presented in the literature. The estimate of K_Pu for liver, calculated based on data supplied by Hirate *et al*[115], was 6.4 following a dose of 10 mg/kg salicylate. This parameter was reduced to 1.7 when a higher salicylate dose was administered (173 mg/kg). This was in accordance with the fact that the K_P value estimated in this work (3.7) was lower than that reported by Hussein *et al* (Kp=6), who administered a smaller dose in the absence of cold salicylate. A similar value for liver (K_Pu =2) was calculated from data presented by Yoshikawa *et al* [325], obtained in studies on the tissue distribution of salicylate in normal and pregnant rats. It has been suggested that both albumin and other proteins in the hepatic cytosol have a role in binding salicylate within the liver [325].

Adding salicylate to the perfusate results in a concentration-dependent decrease in hepatic tissue binding [121]. A concentration- and flow rate-dependence change in salicylate volume has also been described for salicylate. In the current work, unlabelled salicylate was absent from the perfusate, and the perfusion flow rate was fixed. Therefore, any change in fu_c and volume between control and cirrhotic livers was due to the structural alteration caused by cirrhosis.

The intracellular volume of distribution of salicylate (2.2 ml/g) was much larger than that of the estimated volume of cytoplasmic ground substance (0.26 ml/g, [299]). In previous studies in this laboratory, where the estimated salicylate volume of distribution was smaller compared to the present study, the intracellular volume of distribution of salicylate (1.2 ml/g) was much larger than the estimated cytoplasmic volume (0.4). This confirms that salicylate not only penetrates the intracellular components (such as nuclei, mitochondria and endoplasmic reticulum) but binds to them as well.

Some aspects of salicylate distribution could be explained in the light of comparison with other compounds. The steady-state volume of distribution of the most poorly permeable member of the 5-ethyl-barbituric acid family (C0) is greater than that obtained from bolus experiment [54]. Conversely, the volume of distribution of labelled salicylate in the absence of cold salicylate in the perfusate is greater than that in the presence of cold salicylate. These apparently contradicting

observations from two poorly permeable compounds can be explained by different mechanisms. For C0, the explanation lies in the low membrane permeability. In the bolus experiment, the fraction of C0 that may have permeated into cells is much less than the throughput component and hence the distribution volume associated with returning component reflects largely the volume of cytoplasmic ground substance and does not include all the available water space of hepatocytes. Therefore the distribution volume estimated from a bolus injection would be less than that calculated from steady-state study. For salicylate, the presence of cold drug in the perfusate will lower the binding capacity of the liver and decrease the volume of distribution of labelled salicylate. This explains the reduction of salicylate volume parallel to the increase in the concentration of cold salicylate in the perfusate [121]. This comparison indicates that caution should be taken when evaluating the volume of distribution of a drug with low membrane permeability.

4.6.2.8 Flow rate and salicylate kinetics

A lack of dependence of model parameters (*eg* D_N) on perfusate flow rate has been described for compounds that display one- and two-compartment characteristics [323,224]. Furthermore, D_N is determined primarily by the hepatic microvasculature, with the values of D_N the same for all compounds and equal to that of erythrocytes [228,242]. These findings are in contrast to that presented by Yano *et al* [323] for cefixime, whereby both the D_N and V_H in the isolated perfused liver tended to increase with increased flow rate, while K_P was reduced. One explanation for the apparent sensitivity of D_N of cefixime to changes in perfusate flow rate was a failure by the investigators to adequately correct for dispersion in the non-hepatic region of the experimental system [231,90].

In the present study, where the flow rates calculated were based upon liver weight and were uniform among liver preparations, the computed D_N for salicylate (0.08) was similar to that obtained by Hussein *et al*[121]. In cirrhotic livers, with relatively similar flow rates, a higher D_N (0.2) was obtained. The change in D_N then may have reflected an increase in heterogeneity of hepatic vasculature. This fact was confirmed by histologic observations and analysis of markers distribution (see earlier).

4.6.2.9 Salicylate membrane permeability

The marked reduction in PS value (mean permeability-surface area product) from 8.2 ml/min/g in control livers to 3.2 ml/min/g in the cirrhotic livers clearly demonstrated that the permeability of salicylate was reduced during cirrhosis. Permeability estimates are independent of flow rate and of the concentration of salicylate in the perfusate [121]. Interestingly, the data obtained from *in situ* experiments were similar with the literature estimates of the permeability-area product of salicylate determined in isolated hepatocyte uptake experiments (6.4 ml/min/g)[325]. These findings confirm that salicylate has a major permeability limitation in the liver and suggest that this is most likely to be at the hepatocyte membrane site. The relationship between membrane permeability and relative spreading for salicylate in cirrhotic livers can be described using the following equation [321]:

$$CV^2 = CV_b^2 + \frac{2Q\,(V_b + V_c)^2}{PS\,(V_b + V_c)^2} \qquad (4.18)$$

This relationship indicates that when membrane permeability is decreased, relative spreading is increased, as was observed in these experiments. While the PS value was lower in cirrhotic livers, their value of CV^2 was increased (0.98 compare to 0.55 in controls).

4.6.2.10 Barrier and relative spreading

According to the two-compartment dispersion model, the effect of a permeability barrier on the CV^2 of a non-eliminating solute can be described by the following equation [321]

$$CV^2 = CV_b^2 + [(2Q/f u_b.PS) \cdot (1 - V_b/V_H)^2] \qquad (4.19)$$

where CV_b^2 is the CV^2 of a blood marker.

Therefore, in addition to CV_b^2, the CV^2 is influenced by the flow rate, membrane permeability, and binding of drug. When the exchange between vascular and cellular compartment is very rapid ($f u_b.PS >> Q$), CV^2 will equal CV_b^2. When a barrier exists between the two compartment or due to low permeability the transport is non-instantaneous ($f u_b.PS << Q$), CV^2 will be greater than CV_b^2, as shown for salicylate.

4.6.3 Diazepam and Diclofenac

In the previous section, the dispersion of a relatively hydrophilic compound (salicylate) in cirrhotic liver was investigated. The present section evaluates the influence of cirrhosis on the dispersion of two lipophilic solutes in the liver. Linear systems analysis and a two-compartment dispersion model were used to quantify the relative roles of distribution and elimination events on the extraction of diazepam and diclofenac and to identify the manner in which these processes are influenced by altered permeability.

4.6.3.1 Recovery

Diclofenac and diazepam output concentrations were measured non-specifically by total ^{14}C activity. Thus, it was important to ensure that radioactive metabolites did not contribute significantly to the outflow radioactivity over the 4-min sampling period. For Diclofenac, previous investigations, where radiochemical estimates of output concentrations were compared with those determined specifically by HPLC, showed that regardless of albumin concentration, more than 90% of the ^{14}C-related product in the hepatic effluent was diclofenac. The control values for diclofenac availability in this study (Table 4.1) are in excellent agreement with those reported by others who used a similar approach [60,66,130].

The identical availability estimates for diazepam (F=78% in 10g/L albumin concentration) determined using non-specific (radiochemical; Chapter Three) and specific (HPLC; Chapter Five) methods suggests that the metabolites of ^{14}C-diazepam did not contribute significantly to the total radioactivity in hepatic outflow. In experiments conducted by Diaz-Garcia *et al* [60], where a radiolabelled bolus of diazepam was injected into the portal vein during a constant infusion of unlabelled diazepam, the same findings were noted.

4.6.3.2 Impact of protein binding on drug distribution

In the case of salicylate, where no binding protein was present in the perfusate, the throughput and returning components were influenced by Q, k_{12}, and D_N. For protein-bound drugs such as diclofenac and diazepam, both components are additionally influenced by the presence of albumin, despite a virtual equilibration between drug-protein complex and unbound drug. Thus, both the height of the initial peak and the slope of the terminal phase decrease in magnitude as perfusate albumin concentration is lowered [66].

The perfusate HSA concentration selected (1%) ensured that most of the drugs (>98% of diclofenac and 95% of diazepam) were bound. Under these conditions, their availabilities were about 80%. For labelled albumin, D_N and V are independent of perfusate protein concentration [66]. This would suggest that any changes in the output profiles of diclofenac and diazepam (discussed here) are not due to changes in the disposition of its binding protein per se.

As albumin is confined to the extracellular compartment, of the various physiologic parameters influencing k_{12}, k_{21}, and k_{23}, the only one sensitive to changes in albumin concentration would be fu_b, which operates on k_{12}. This fact is confirmed by the excellent agreement for diazepam and diclofenac k_{12} values (0.33 and 0.11 1/sec, respectively) found in this work (Tables 4.15 and 4.16) and experiments conducted by others [120,66,60], at similar albumin concentrations (1%).

The "true" unbound fraction of diazepam and diclofenac within the liver sinusoids may be greater than that estimated from *in vitro* experiments. Passage through a capillary bed may enhance the dissociation rate of protein-ligand complexes [72,300]. Enhanced dissociation could arise from a change in the conformation of the protein-ligand complex in the microenvironment surrounding the cell membranes, due to factors such as specific or non-specific protein-surface interactions or local pH changes. Numerous alterations take place in the microenvironment surrounding the cell membranes in cirrhotic livers. Thus, it may be argued that reduced membrane permeability in cirrhotic livers may be obscured by an increased fu. But it should be noted that any change in fu would lead to a parallel change in k_{12} and thus the ratio k_{12}/fu would be expected to remain unchanged.

Table 4.15

Effect of hepatic cirrhosis on the disposition kinetics of diazepam in the isolated perfused rat livers.

		F	E	CL ml/min	CL ml/min/g	k_{12} 1/sec	k_{21} 1/sec	k_{23} 1/sec	Kp	k_{21}/k_{23}	D_N	PS ml/min/g	f_{uc}	p	R_N	CLint ml/min/g
Normal Livers	**Mean**	**0.6**	**0.4**	**13.5**	**0.59**	**0.32**	**0.028**	**0.0059**	**13.5**	**4.75**	**0.13**	**149**	**0.021**	**0.83**	**1.3**	**9.8**
n=10	*SD*	*0.11*	*0.07*	*1.6*	*0.07*	*0.06*	*0.006*	*0.0011*	*3.2*	*0.9*	*0.03*	*29*	*0.0033*	*0.18*	*0.29*	*2.5*
	CV%	*18*	*17*	*12*	*11*	*18*	*21*	*18*	*23*	*18*	*23*	*19*	*15*	*21*	*22*	*25*
PT Livers	**Mean**	**0.55**	**0.45**	**12.4**	**0.53**	**0.33**	**0.028**	**0.0068**	**13.7**	**4.11**	**0.14**	**160**	**0.022**	**0.81**	**1.84**	**11.8**
n=5	*SD*	*0.1*	*0.08*	*1.9*	*0.08*	*0.07*	*0.007*	*0.0016*	*3.3*	*0.9*	*0.04*	*31*	*0.0035*	*0.21*	*0.41*	*2.5*
	CV%	*18*	*17*	*15*	*15*	*21*	*25*	*23*	*24*	*21*	*27*	*19*	*15*	*25*	*22*	*21*
	ANOVA	NS	NS	NS	NS	NS	NS	NS	NS	NS	NS	NS	NS	NS	p<0.005	NS
Cirrhotic Livers	**Mean**	**0.58**	**0.42**	**16.8**	**0.61**	**0.22**	**0.018**	**0.0075**	**14.4**	**2.4**	**0.16**	**78**	**0.021**	**0.75**	**1.13**	**10.2**
n=12	*SD*	*0.14*	*0.08*	*2.6*	*0.14*	*0.04*	*0.004*	*0.0017*	*3.6*	*0.4*	*0.04*	*22*	*0.0041*	*0.18*	*0.3*	*2.4*
	CV%	*20*	*19*	*15*	*22*	*18*	*22*	*22*	*25*	*16*	*25*	*28*	*19*	*24*	*26*	*23*
	ANOVA	NS	NS	p<0.005	NS	p<0.005	p<0.005	p<0.005	NS	p<0.005	NS	p<0.005	NS	NS	NS	NS

Parameters obtained by applying the two-compartment dispersion model to the outflow profiles. Perfusate contained 1% HSA.

F, E, and CL calculated using moment analysis. fu=0.07

Table 4.16

Effect of hepatic cirrhosis on the disposition kinetics of diclofenac in the isolated perfused rat livers.

		F	E	CL ml/min	CL ml/min/g	k12 1/sec	k21 1/sec	k23 1/sec	Kp	k21/k23	DN	PS ml/min/g	fuc	p	RN	CLint ml/min/g
Normal Livers	**Mean**	**0.78**	**0.22**	**7.5**	**0.32**	**0.11**	**0.03**	**0.0057**	**4.1**	**5.6**	**0.18**	**422**	**0.0025**	**0.86**	**0.35**	**69**
n=10	*SD*	*0.07*	*0.03*	*1.5*	*0.06*	*0.017*	*0.007*	*0.001*	*0.7*	*1.1*	*0.04*	*89*	*7E-04*	*0.14*	*0.06*	*18*
	CV%	*8*	*12*	*20*	*18*	*15*	*21*	*17*	*17*	*19*	*22*	*21*	*28*	*16*	*17*	*26*
PT Livers	**Mean**	**0.71**	**0.28**	**8**	**0.34**	**0.11**	**0.03**	**0.0065**	**4**	**4.4**	**0.2**	**456**	**0.0026**	**0.84**	**0.53**	**90**
n=5	*SD*	*0.07*	*0.04*	*1.5*	*0.07*	*0.02*	*0.007*	*0.001*	*0.7*	*1*	*0.05*	*98*	*7E-04*	*0.14*	*0.08*	*14*
	CV%	*9*	*13*	*17*	*20*	*22*	*22*	*15*	*17*	*22*	*25*	*21*	*28*	*16*	*15*	*15*
	ANOVA	NS	NS	NS	NS	NS	NS	p<0.005	NS	NS	NS	NS	NS	NS	p<0.005	p<0.005
Cirrhotic Livers	**Mean**	**0.9**	**0.1**	**4**	**0.15**	**0.07**	**0.02**	**0.0065**	**3.8**	**2.6**	**0.2**	**220**	**0.0022**	**0.71**	**0.27**	**69**
n=12	*SD*	*0.05*	*0.02*	*0.6*	*0.03*	*0.016*	*0.005*	*0.001*	*0.8*	*0.4*	*0.05*	*62*	*7E-04*	*0.12*	*0.05*	*14*
	CV%	*5*	*20*	*15*	*20*	*22*	*26*	*15*	*20*	*15*	*25*	*28*	*31*	*17*	*18*	*20*
	ANOVA	p<0.005	p<0.005	p<0.005	p<0.005	p<0.005	p<0.005	p<0.005	NS	p<0.005	NS	p<0.005	NS	p<0.005	NS	NS

Parameters obtained by applying the two-compartment dispersion model to the outflow profiles. Perfusate contained 1% HSA.

F, E, and CL calculated using moment analysis. fu=0.008

4.6.3.3 Throughput and returning components

In both control and cirrhotic livers, the initial peak of diclofenac output profiles took a shape similar to that for albumin, ie it is steeper and elutes faster in cirrhotic livers. The initial peak, the throughput component, represents the material that is bound to albumin and has escaped extraction. The flat tail, the returning component, continues to elute well after most of the injected albumin has been recovered.

The total availability of an injected dose of substance (F) can be viewed as the sum of the throughput component (denoted F1) and the returning component (denoted F2). The ratio of the returning component to the fraction of material that initially left the central compartment, *ie* $\frac{F_2}{1-F_1}$, provides an index of the survival of material that enters the peripheral compartment, "the survival fraction" [66].

Upon examination of the simulated "complete" and "throughput" profiles (Figure 4.23), the reason for the distinctive change in the shape of diazepam and diclofenac output profiles from control to cirrhotic livers becomes apparent. In control livers, when k_{12} is higher, a larger portion of injected material accesses the peripheral compartment, where it will either be eliminated or ultimately appear in the venous output. In this group, F1 and F2 are 0.09 and 0.7, respectively, such that the returning component comprises the major portion of the output profile. The survival fraction in this group is 0.77.

In cirrhotic livers, as k_{12} decreases (as a consequence of decreased permeability), a relatively smaller amount of injected material can access the peripheral compartment during organ transit. Therefore, a large fraction appears in the hepatic outflow without having left the central compartment. In fact, the throughput component (F1) is 0.69, and the returning component (F2) is 0.24. Hence, in cirrhotic livers, the output profile is composed mainly of the throughput component (Figure 4.23) and the shape of the profile is similar to that of a non-eliminated tracer that is confined to the extracellular space such as labelled albumin (Figure 4.4). Of the fraction (1-F1=0.31) that enters the peripheral compartment on at least one occasion, most (78%) escapes hepatic elimination (*ie* the survival fraction is 0.78). Thus the survival fraction has hardly been changed.

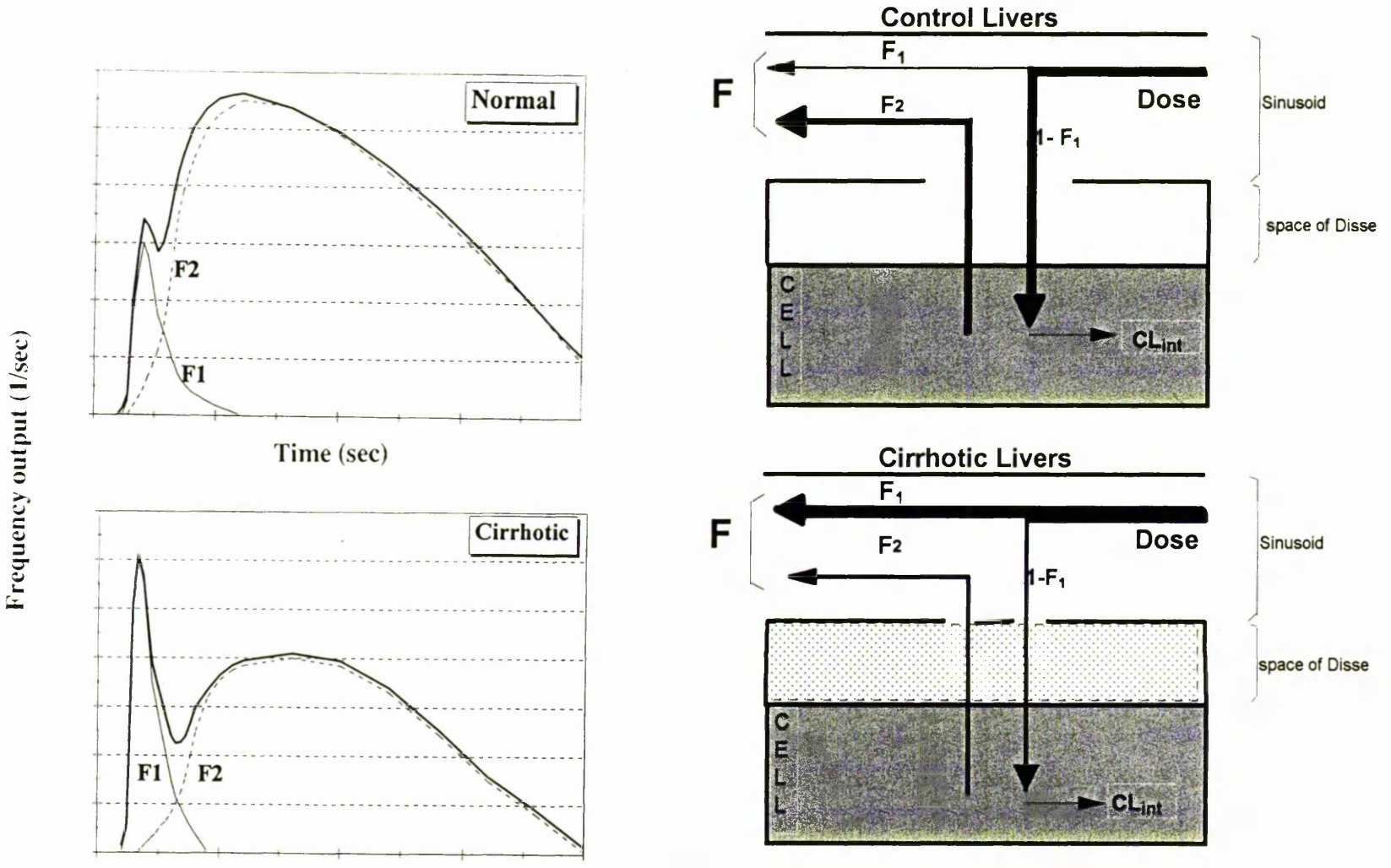

Figure 4.23 Simulation of throughput (F_1,.....) and returning (F_2 - - - -) components, and the complete profile (—) of frequency output of diazepam and diclofenac in representative normal and cirrhotic livers. Diagram illustrates the effect of cirrhosis on the hepatic distribution of the two drugs.

Reduction in *f*u (hence, the gradient of cellular uptake) leads to marked reduction in k_{12} and an increase in the throughput component [66,120]. As the clearance is also decreased, only a small change in the returning component is observed. Therefore, the survival fraction is increased. In the present studies, appearance of a permeability barrier (Section 4.5) leads to a substantial increase in throughput component and a decrease in 1-F1 value. As a consequence, the returning component is greatly decreased. The result is an unchanged survival fraction. Upon comparison of these two studies, it can be concluded that in terms of increasing the throughput component, the cirrhotic condition has acted similar to decreasing the *f*u. However, the survival fraction has remained unchanged in cirrhotic livers primarily due to its initial large value in the control livers. Using a smaller albumin concentration would have allowed for the permeability barrier to manifest its role in the survival fraction. Comparison of the two studies also reveals that the control livers in this work demonstrate the greater membrane permeability for diclofenac. The reason for this greater permeability, which was also observed for salicylate, is not quite clear.

The unchanged diclofenac survival fraction demonstrates that in cirrhotic livers the probability, "that a drug molecule which is released unchanged into the sinusoid after its initial intracellular sojourn and re-entered the cellular space on subsequent occasions," has not been changed. This is in contrast to the expectation that in cirrhotic livers, the access of albumin to the space of Disse is restricted, which may consequently reduce the rate of wash out of drug. On the other hand, the decrease in fraction $1\text{-}F_1$ in cirrhotic livers has been so marked that despite a 2.5-fold reduction in clearance in this group, the value of F_2 still has been reduced noticeably (by threefold). This implies an unchanged CL_{int}.

The initial peak of diazepam output profile in controls, though small, is not due to a hepatocyte membrane permeability limitation because the value of PS (145 ml/min/g) is nearly 100 times higher than perfusion flow rate (1.4 ml/min/g). The peak represents injected materials that do not enter the cells during passage through the liver (throughput component) because of extensive (93%) binding to HSA. The tail represents materials returning from the cellular space having escaped elimination (returning component). In cirrhotic livers, although the PS value was reduced substantially, it was still much higher (~70 times) than the flow rate. This indicates that diazepam distribution in this group is still perfusion-rate limited.

4.6.3.4 Dispersion model

For drugs undergoing hepatic elimination, the output profile is composed of the transit times of only those molecules that escape extraction, and moment analysis alone is therefore of limited use in characterising events of all drug molecules. Under such circumstances, recourse to a pharmacokinetic model may be necessary if both distribution and elimination mechanisms are to be investigated.

According to the two-compartmental dispersion model, the radial transport (by diffusion) of diclofenac and diazepam into their distribution space is non-instantaneous [228-230,319] and dis-equilibrium between the vascular and cellular spaces contributes to the variance of transit times during their passage through the liver. If this disequilibrium is ignored, that is if the organ output profiles are analysed by the one-compartment dispersion model, the estimates of dispersion due to organ heterogeneity are likely to be spurious. This has been clearly demonstrated in Figure 4.8 where the relationships predicted from the application of the one- and two-compartment forms of dispersion models are shown. The two-compartment dispersion model has been likened to a model with barrier-limited conditions [85,90]. In cirrhotic livers, the formation of a new permeability barrier further impedes the non-instantaneous cellular transport of the two drugs, reducing their MTT whilst increasing the relative spreading. Therefore, this barrier only magnifies the existing disequilibrium conditions for diclofenac and diazepam and the two-compartment dispersion model still describes adequately the output profiles of the two drugs.

The observed difference in diclofenac D_N value estimated under impulse-response conditions (0.4) [66] and that of steady-state conditions (2.5) [120] could be explained by enzymatic activity. In impulse response mode, the size and shape of the output profile is influenced by events within the entire liver, including the eliminating regions. In the steady-state mode, D_N is determined solely by events that have a direct impact on the efficiency of drug elimination and by the degree of dispersion within the elimination region [228,229,230]. Therefore, the difference in D_N of cirrhotic livers compare to control livers is attributable not only to the altered structural changes but to the potential changes in the arrangement of enzyme distribution as well. The decreased diffusion of diclofenac can also decrease the efficiency of hepatic drug elimination and possibly increase its dispersion number. However, this phenomenon has a significant impact on drug elimination only

as the extraction ratio of a compound approaches unity, whereas in the cirrhotic livers, the extraction ratio of diclofenac did not exceed 0.1.

The shape of the diclofenac output profile is partly controlled by the dispersion of its binding protein, HSA. The D_N determined for a compound which is 100% bound to a perfusate protein should be identical to that of the binding protein itself. As the degree of binding is reduced, the ligand will begin to rely less on the distribution and dispersion properties of the protein. However, only when the binding protein is removed from the perfusate (when fu becomes 1) will the true dispersion characteristics of the compound be expressed. Hence, the disparity between the D_N values estimated for diclofenac by the impulse-response [66] technique and the steady-state approach [120] is not contradictory, but does highlight the importance of using both approaches for investigating the hepatic handling of xenobiotics.

4.6.3.5 Non-hepatic region

The passage of material through "non-hepatic" regions is usually considered as a time lag (t_{lag}) and its effect is removed by subtracting t_{lag} from measured time [66,282,319]. However, even minor degrees of axial spreading within the non-hepatic regions (due to non-ideal input, turbulent flow, and discrete sampling) can profoundly influence the overall shape of the profile, particularly at the earlier time points [154]. Thus, to gain an accurate estimate of D_N in the liver, appropriate correction for the delay and dispersion in the non-hepatic part of the system is needed, as employed in this study. It was observed that when the appropriate correction is not made, then the estimate of D_N of solute within the liver is biased, the bias being particularly large for rapidly eluting materials such as albumin and albumin-bound drugs.

Although the large non-exchanging vessels positioned between the inflow and outflow cannulae and the sinusoidal bed may also influence the shape of the observed output profile, it has been assumed that the magnitude of the delay and distortion of an impulse in these regions is minor compare with that in other regions.

4.6.3.6 Membrane permeability and output profiles

In the analysis of hepatic drug clearance data, the transfer of substrate across the hepatocyte cell membrane is generally assumed to be so rapid that the unbound substrate concentrations within the extracellular and intracellular regions are equal. However, if the irreversible removal of a substrate from the intracellular site is faster than the rate at which it arrives from the extracellular compartment, extraction could become membrane permeability limited. Under such conditions, equating hepatic drug clearance to organ enzyme activity is clearly inappropriate. The current experiments, conducted under impulse-response conditions, allow the evaluation of the relative importance of intrinsic membrane permeability (PS, the unidirectional rate of transfer divided by the unbound concentration of substrate at the membrane surface) and intrinsic clearance to substrate elimination [282].

From Equations 2.16 to 2.18, the ratio of k_{21} to k_{23} can be used to estimate the relative magnitude of PS and CL_{int}. For control livers, this ratio is 5.6 and 4.8 for diclofenac and diazepam, respectively, suggesting that the elimination of these two lipophilic drugs by the perfused rat liver is not subject to membrane permeability limitation. For cirrhotic livers, although the ratio declines by twofold (to 2.6 and 2.4), the elimination is still perfusion rate-limited. It was notable that CL_{int} value of the two drugs (expressed per g of liver) did not change during cirrhosis (Tables 4.15 and 4.16). Therefore, the reduction in the uptake rate of diclofenac and diazepam in experimental cirrhosis is due to diffusional difficulties rather than the overall ability of liver to eliminate the drugs.

It is possible to calculate the R_N (the efficiency number) for diazepam and diclofenac using the equation 2.11 and 2.12. In the control livers, R_N value for diazepam was substantially greater than that for diclofenac suggesting a greater metabolic capacity for diazepam. In cirrhotic livers, the metabolic efficiency of liver for both drugs decreases slightly which indicates that despite the injury, the liver still has been able to efficiently metabolise the uptaken drug. This may be due to the effect of phenobarbitone-treatment on the cirrhotic livers. The metabolic activity of the cirrhotic livers which has been initially induced by phenobarbitone, is subsequently neutralised by the insult caused by hepatotoxin (CCl4). The result is an apparently unchanged metabolic activity.

4.6.3.7 Clearance

The clearance values of diazepam and diclofenac (13.6 and 6.7 ml/min, respectively) in the control livers are twice the values reported by others [60,120] in IPRL under similar conditions. However, when clearances are expressed per g of liver weight, their values are less different. The values of intrinsic clearance for the two drugs in the control livers are also twice those estimated by others. This may have been produced by the larger cellular volume of the control livers. The unchanged diazepam CL and CL_{int} values in cirrhotic livers, compare to the control values, once again suggests that the overall metabolic efficiency of liver in experimental cirrhosis is not disturbed. This is supported by the fact that despite the small increase in the estimated value of diazepam clearance (and CL_{int}) in cirrhotic livers, its survival fraction has been decreased by more than threefold in this group (from 57% to 19%). This decrease is equivalent to an almost two fold decrease in the fraction of diazepam initially left the vascular compartment (1-F1).

4.7 General Discussion

4.7.1 Choice of Model Substances

4.7.1.2 Reference markers

Various substances have been used as labelled marker for the indicator dilution technique. The choice depends mainly on the organ of study. For circulation studies in all organs, except the liver, erythrocytes and albumin are used as vascular markers. An erythrocyte travels slightly faster than a bolus of albumin through a circulatory bed which is impermeable to the albumin over a single passage time [88]. The labelled erythrocyte is not quite the ideal vascular reference substance, but it is comparable. In the liver, where no substance dissolved in plasma (including albumin) is confined to the microvasculature, it is the most suitable reference available for study.

As interstitial markers, different substances including albumin, sucrose, sodium, inulin, T-1824 have been used in liver studies. These are substances which are found to gain access to the space of Disse but not permeating the cellular membranes. The volume in which these substances are penetrating in the space of Disse is variable and depends on their size. The accessible space decreases as the size of the probing molecule increases. This ranges from sodium, having the largest interstitial volume of distribution, to albumin with lowest volume of distribution. The proportion of the space accessible to a molecule like albumin is of particular interest, since it can be compared to that found in other tissues. The exclusion phenomenon implies that, in the design of uptake experiments, it is necessary to use, in addition to labelled erythrocytes, a specific type of second extracellular marker which describes the behaviour the uptake substance would have if it did not enter liver cells. For non-protein bound low molecular weight model drugs (such as salicylate in the current studies) sucrose would be the appropriate second reference; for albumin bound model drugs (such as diclofenac and diazepam), labelled albumin is appropriate.

As hepatic intracellular marker, water is generally used. For the estimation of total cellular water this is naturally the first option. Urea is the other substance which has recently been suggested as alternative intracellular marker. The use of urea in conjunction with water in normal and cirrhotic liver provides an opportunity to extent the present limited information on its distribution.

4.7.1.3 Model Drugs

The pharmacokinetic considerations (Section 1.4.2) indicate the potential complexity of permeability studies in cirrhosis, if meaningful quantification of any change is to be made. A pragmatic approach would be the use of some model drugs possessing specific dispositional characteristics. In fact the aforementioned pharmacokinetic rationales have been applied to clinical situations where clearance of a particular drug is used to provide an estimate of metabolic capacity or blood flow, which were then employed as a quantitative index of the hepatic function [143]. Requirements of a model drug for permeability studies may be summarised as:

a) there should be some previous data on the drug so that comparison between the results in control and cirrhotic livers could be made.

b) drugs with different chemical properties (*ie* hydrophilic or lipophilic) should be included in the study.

c) for liver perfusion studies, its extraction should be low or lowered by some means, otherwise the clearance would depend on perfusion flow and any change in permeability could be obscured.

For liver perfusion studies, the compounds selected were salicylate, diazepam and diclofenac. Salicylate is representative of a wide class of relatively hydrophilic polar compounds and does not undergo metabolism or biliary excretion [121]. Diazepam and diclofenac represent lipophilic compounds which undergo metabolism and binding. The convenience of these two model compounds as probes for hepatic drug elimination arises from their high extraction properties when binding within perfusate is negligible, together with their high affinity for HSA that can be added to the perfusion medium to effect substantial reductions in hepatic extraction. There are many similarities between these two drugs in terms of their molecular size, shape, and chemical properties (Table 4.17). However, their permeability properties are different.

4.7.2 Choice of Animal

Most of the methods described in the literature for *in vitro* [43], *in vivo* [220] and and organ perfusion studies [294,188,291,197] are devised for use with the laboratory rat, Mus norvegicus albinus. The suitability of the rat for biochemical experimentation is widely accepted, and much data on mammalian metabolism and tissues is derived from this source. In particular, the rat liver has been studied in detail [280].

4.7.2.1 Rat and liver perfusion

Liver perfusion techniques have been devised for many species, and in earlier methods the dog, cat and larger domestic animals were used. The reasons were mainly technical; operative techniques in larger animals were more familiar and chemical methods of assay required large amounts of tissue. The ability to apply the general technique to a small and readily available animal such as the rat has enabled liver perfusion to become important in a field long dominated by incubation techniques with homogenates and tissue slices. Microchemical assays remove the requirement for large amounts of tissue. For normal laboratory purposes a small animal such as the rat is very convenient and suitable techniques using this animal is more desirable than use of well-established methods in a larger animal [168].

4.7.2.2 Rat and toxicity studies

In studies concerned with toxicity, there is no general preference for any single species or strain of research animal. The selection depends on the aim of the study, as well as on the particular functional or anatomical features of the animals' organ, plus such considerations as the planned technical approach, availability, ease of handling. Various animal species have been used for production of experimental cirrhosis including dogs, pigs, rabbits, hamsters, guinea pigs, rats and mice [276]. Today, for most purposes, the animal of choice is the rat due to the response of this animal to the hepatotoxin and also development of various techniques and microanalytical methods which may yield more insight into liver function in health and disease at the microscopic level [276]. It has been shown that male rats are more susceptible than females to CCl4 treatment in terms of several serum indicators of hepatotoxicity and elevation of liver-to-body weight ratio [3].

4.7.2.3 Other animals

A number of experiments associated with cirrhosis have been performed using rabbits. These experiments are difficult to evaluate because rabbits frequently acquire chronic hepatitis (due to Coccidiosis) [176]. In one study, only 6 out of 50 rabbits collected from different sources were not diseased [190]. Rabbit have been regarded, thus, as entirely unsuitable for hepatotoxicity experiments[176]. A group of workers [168] who produced a successful liver perfusion in the rat expressed that their success depended partly upon the choice of rat as experimental animal; the dog was a particularly uncomfortable choice of earlier workers since the canine liver has vasomotor responses that limit perfusion. Using the rat, larger number of experiments may also be performed. Furthermore, in-bred strains of rat are less variable genetically.

4.7.3 Mechanisms of Altered Outflow Profiles

The are several mechanisms that influence the hepatic outflow profiles of drugs and may account for observed changes in the profiles of drugs through cirrhotic livers. These include a) change in protein binding, b) decreased metabolism, c) decreased membrane permeability, and d) decreased diffusion. The potential contribution of each mechanism is examined.

4.7.3.1 Role of binding protein

Only unbound substances are able to transfer across cellular membranes, the protein ligand-complex being too polar and large [98]. Therefore, extensive protein binding limits the rate of uptake of substrate, proportionally [282,283]. However, there are a number of observations that cannot be fully explained by this conventional view. For example, for many extensively-bound substrates, uptake rates decline much less when albumin is added to the extracellular medium than would be expected from the decline in the equilibrium unbound concentration [265]. On the other hand, under physiological and pathological conditions, available substance has been shown to include free as well as a large portion of albumin-bound drug [98]. These observations have been attributed to the "albumin-mediated phenomenon" [20,122]. Despite many attempts to clarify this phenomenon, its mechanism is still controversial. Three types of models have been proposed: a) a model in which dissociation of albumin-ligand complexes in the stirred extracellular fluid is rate limiting the process [122], b) a model in which an interaction between protein and hepatocyte surface is thought to promote dissociation and uptake of drug [122,265], and c) a model of rate-limiting diffusion of ligand through the unstirred water layer (UWL) to the uptake site [122].

a) Dissociation rate-limited uptake: This model has been shown to adequately describe the uptake of bromosulfophthalein [265] and testosterone [98] in perfused rat liver. The model implies that if the dissociation rate of drug from albumin is low relative to the rate of the other steps (*eg* the uptake rate or the removal rate), then non-equilibrium binding exists within the sinusoids and dissociation of bound drug determines the uptake rate [98]. Therefore, drug would be carried to the outflow with the labelled albumin, as an early component of the indicator dilution curve and therefore is inaccessible at the uptake surface. In the present studies, despite the high affinity of diazepam and diclofenac for albumin (reflected in their large k_a; Section 3.3), no such component was observed in control livers. Also the unbound fraction (0.07 and 0.008 for diazepam and

diclofenac, respectively) alone cannot account for 90% cellular uptake during a single passage through the liver. Therefore, the dissociation rate must be fast, relative to the transit time through the liver, and effect of the protein binding in control livers is not the delayed dissociation case.

In the cirrhotic livers, one may argue that the presence of an early component in the profile and reduced uptake of protein bound drugs may be explained by such phenomenon. The model implies that dissociation of drug from albumin depends on the dissociation rate and the sinusoidal transit time [98]. In the cirrhotic livers, the dissociation rate and consequently the dissociation may have been changed. Numerous structural alterations that take place in the microenvironment surrounding the cell membranes in cirrhotic livers may alter the dissociation of drug-albumin [66] and exert such an effect. Assuming that the dissociation rate of drugs from albumin is rapid enough, a reduction in dissociation of drug from albumin may have resulted from a reduction in the sinusoidal transit time. It was possible to demonstrate that the sinusoidal transit time (or volume) has been decreased substantially in cirrhotic livers; a three-fold decrease in sinusoidal volume has been accompanied by three-fold decrease in the uptake ($1-F_1$) of the protein bound drugs. Other steps in uptake should not be neglected, particularly the re-binding of free drug, as has been suggested by some other workers [98].

b) Hepatocyte-albumin interaction: Some evidence exists that implies a specific albumin receptor on the liver cell surface that accelerates the uptake of albumin-bound organic compounds by promoting more rapid dissociation of their albumin-ligand complexes [20,122,265]. Cirrhosis may disturb this mechanism through two paths: Reduced access of albumin to the space of Disse would lead to a reduction in the amount of albumin reaching the hepatocyte surface and hence decreasing the uptake. Any change in the state of the hepatocyte membrane and damage to hepatocyte surface [280] could alter the interaction between the hepatocyte membrane and binding protein. In addition it has also been suggested that there are clusters of membrane proteins with high affinities for specific classes of ligands [20].

c) Reduced diffusion: see latter text.

4.7.3.2 Impaired metabolism

Clinical and experimental observations with drugs indicate a wide diversity in the effect of hepatic disease on hepatic elimination. Change in hepatic elimination in isolated perfused cirrhotic liver may be mediated by change in intrinsic clearance, CL_{int}, or change in flow perfusing the liver, Q [216].

4.7.3.2.1 Change in CL_{int}

Hepatic cirrhosis results in substantial damage to parenchymal cells. The actual effect of this hepatocellular damage on the clearance of drugs is difficult to generalise. Reduced CL_{int} of drugs of different categories (Section 1.4), which has led to the formulation of the operational models of "intact cell hypothesis" and "sick cell hypothesis", could be caused by the following mechanisms.

a) Reduction in the number of hepatocytes: The so-called "intact cell hypothesis" states that a reduced volume of liver cells with a normal enzymatic makeup (intact cell) is only perfused in part due to the hemodynamic disturbances [217,219,161]. Morphometric analysis [219] and assessment of microsomal function [217] provide support for this theory. The yield of hepatocytes are substantially reduced in cirrhotic livers (Table 4.8), and impaired mitochondrial function in cirrhosis is mainly due to loss of hepatocellular mass [216,96]. Tracer studies in this and other work confirmed the results of morphometric studies that the specific intracellular volume is reduced in cirrhotic livers.

b) Reduction in protein content of the liver cells: In many instances [216,96], replacement of liver tissues by fibrous bands can not account for 50% reduction in clearance of substances, providing support for the sick cell hypothesis. This theory postulates an abnormal function of the individual hepatocytes responsible for the overall failure of the diseased liver [217,294]. This abnormal function is caused by reduction in the amount of cytochrome P-450 (nM/mg protein) [96,219] and specific loss of microsomal enzymes [217].

c) Alteration in enzyme activity: In clinical [2,147,269] and experimental [280] cirrhosis, a change in the properties of the endoplasmic reticulum is observed which in many cases is characterised by a decline in the activity of the cytochrome P-450 system. After stopping CCl4 intoxication, while

the rats remain cirrhotic, the activity of enzymes in all zones gradually returns to normal [269]. Occasionally, enzyme activity per unit surface area of inner mitochondrial membrane may be increased to maintain mitochondrial function of the cirrhotic liver [133]. Due to liver cell necrosis, serum activity of several enzymes (*eg* hexosaminidase) is increased in cirrhosis [306].

The effect of altered CL_{int} on hepatic extraction and clearance is highly dependent upon the initial value of this parameter [306]. If $Q >> CL_{int}$, then extraction and clearance reflect drug metabolism and a change in CLint produces a proportional change in clearance. If $CL_{int} >> Q$, then the metabolic activity of the liver must be decreased quite markedly before any effects on clearance are apparent as was the case for diazepam and diclofenac in the present studies. In such cases, hepatic clearance is not a good indicator of the hepatic function. There is therefore the potential situation of hepatic disease producing significant dysfunction of the hepatocyte at the biochemical level, but the liver has sufficient "reserve capacity" that such impairment has negligible effect upon the overall hepatic clearance of the drug [306].

d) Heterogeneity: Most phase 1 metabolic reactions are localised predominantly in zone 3 [37&42-46&138/800] and this zone is extensively damaged in cirrhosis. Thus, a general metabolic disturbance is expected in cirrhosis. However, a heterogeneity of function observed in the CCl4 model of cirrhosis [217] which is analogous to that in humans [217]. This is because while metabolic zonation persists in CCl4-induced cirrhosis[269], different cytochrome P-450 isoenzymes (different functions) [217] and different hepatic microsomal sites [80] are affected to a different extents. The severity of the disease is also important. Knowledge of the anatomical location of the enzymes responsible for metabolism of various substrates and their relation to the site of the toxic lesion may appear to contribute to an understanding of the relationship between microscopic anatomy of the disease process and altered drug metabolism. Despite reports that enzymatic systems responsible for diazepam and diclofenac metabolism are damaged in cirrhosis, the CL_{int} value for these two drugs did not change in the cirrhotic livers. This could be due to the existence of a reserved capacity for hepatic metabolism. The recovery of enzymatic activity post-treatment is also possible. It also should be noted that some of the hepatic enzyme systems consists of multiple isoforms of similar molecular weights and electrophoretic mobilities with overlapping

substrate specificities (*ie* even where a particular compound is preferentially metabolised by one isoform, this preference may not be absolute [20].

4.7.3.2.2 Changes in Q

The contribution of hepatic artery to the perfusion of cirrhotic nodules is increased [217]. Occasionally, the formation of new vascular channels in fibrotic bands between parenchymal cell cords and in communication with the spaces of Disse [272] may facilitate the access of substrates to remote cell surfaces [202]. Sinusoidal capillarisation alters the access of axial flow to the sinusoids [3,161]. The most influential hemodynamic alteration during cirrhosis is shunting. Extrahepatic [161] and intrahepatic or functional shunts [252] divert a considerable fraction of blood (and blood containing substances) from hepatocytes.

4.7.3.3 Reduced permeability

The fluid state of the hydrophobic bilayer of hepatocyte plasma membrane plays an important role in regulating transport [93]. Perturbation of membrane by ethanol and calcium reduced membrane fluidity and taurocholate transport [170,251]. Pathological changes in liver tissue following CCl4 poisoning includes changes in the properties of cellular membranes [280]. A strong inverse correlation between the ratio of membrane lipids (measure of membrane fluidity [182]) and the activity of its enzymes exists which is decreased in cirrhotic livers [182]. Increase in these ratios is known to be responsible for high membrane microviscosity and therefore reduced enzyme rotational diffusion. The membranous system retracts into smooth surface tubular aggregates which are considered to be denatured membrane. Rapid, extensive lipid peroxidation of the membrane structural lipids has been proposed as the basis of CCl4 hepatocellular toxicity [280]. However, whether various uptake transport mechanisms of substances are affected by cirrhotic livers are not clear [216].

Hepatic uptake of some organic anions and cations is mediated by well-characterised transport systems [20,165,166]. For most drugs, however, such carrier-mediated transport systems have not been demonstrated and permeability occurs mainly by passive diffusion. The impact of a transmembrane barrier on the distribution and elimination kinetics of drugs and metabolites has

been evaluated in theory and practice [58,257]. However, the quantitative contribution of such factors as the microenvironment surrounding the surface of hepatocyte membrane and the physiochemical properties of the compound are still poorly understood.

The overall decreased permeability in cirrhotic livers was manifested in decreased PS value (Tables 4.14 to 4.16). Using Equation 2.12, the permeability of the hepatocyte membrane (ρ) in relation to the drugs was calculated. In cirrhotic livers, the greater reduction in the PS value (57% for diclofenac and 32% for diazepam) was accompanied by a lesser reduction in the ρ value (16% for diclofenac and 9% for diazepam) indicating that the change in the drugs outflow profiles was not simply due to membrane permeability limitations.

4.7.3.3.1 Membrane permeability and physicochemical properties

Table 4.17 summarises the PS values of a range of compounds (corrected for *fu*) obtained from isolated perfused rat liver studies, collected from literature together with some physicochemical properties. The data demonstrated a progressive increase in PS with increase in logD (pH 7.4) value.

Salicylic acid, which is a hydrophilic substance, is an example of a relatively poorly permeable model drug. It is a compound of high polarity which carries one negative charge at the acidic group and with a logP 2.26 and pK_a values of 2.97 and 13.4, salicylate is predominantly ionised at physiological pH. Based on these characteristics salicylate is expected to pass through the normal hepatocyte membrane with some difficulty, but to the contrary it showed a high membrane permeability. It has been shown that for polar and ionised substances such as salicylic acid, the unexpectedly high membrane uptake is explained by the phenomenon of 'hydrogen binding'. Hydrogen binding between oxygen or nitrogen atoms of a molecule and hydrogen atom of internal or a neighbouring molecule increases its lipophilicity and membrane permeability (Figure 4.24).

Table 4.17 Permeability-surface area product of several compounds in the isolated perfused rat liver.

Drug[a]	PS(mL/min/g)[b]	logP[c]	logD	pKa[c]	MW	Reference
AS	0.17	-1.72[d]	?	9.71	273.3	93
AMP	0.9	1.35	-3.52	2.53, 7.24	349.4	321
ATL	0.38	0.16	-2.04	9.6	266.3	54
C0	0.25	-0.35[e]	-4.20	3.55, 6.89[e]	156.2	54
C9	309	4.13[f]	4.03	7.82[f]	282.2	53
CFZ	0.51	0.58	-3.82	3?	584.7	122
DZ	137	2.80	2.80	3.3	284.8	60
DF	220	4.40	1.50	4.5	318.1	66
EP	0.35	-0.74	-5.84	2.3, 3.39, 8.02	348.3	257
LD	180	2.26	1.64	7.9	234.3	345
4-MU	66	1.58	1.58	none	176.2	172
NE	1.7	-1.06	-2.29	8.6, 9.8, 12	169.2	346
OXA	0.52	2.38	-2.30	2.72	401.4	321
SA	4.6	2.26	-2.17	2.97, 13.4	138.1	121
WF	62	2.52	0.22	5.1	308.3	282

[a] Abbreviation: AS, acetaminophen sulfate; AMP, ampicillin; ATL, atenolol; C9, 5-nonyl-5-ethyl barbituric acid; CFZ, cefodizime; DZ, diazepam; DF, diclofenac; EP, enalaprilat; LD, lidocaine; 4-MU, 4-methylumbelliferone; NE, norepinephrine; OXA, oxacillin; SA, salicylic acid; WF, warfarin.
[b] Where appropriate, corrected for unbound fraction in the perfusate. c:383, d:93, e:384, f:279, g:54.

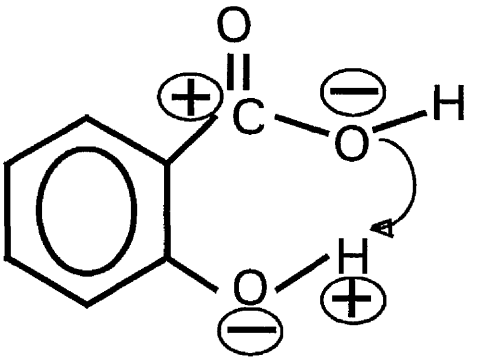

Figure 4.24 Hydrogen binding increases the lipophilicity and permeability of salicylic acid.

For very lipophilic drugs, hepatic uptake is so rapid that it is only possible to measure permeability in the presence of its binding protein. Because most drugs enter the hepatocytes by passive diffusion, hepatic uptake is expected to depend on factors such as lipophilicity, degree of ionisation, molecular size and extent of protein binding [243]. Chou who evaluated the literature data on the relationship between the partition coefficient and PS of several compounds demonstrated that PS value tends to increase with increasing lipophilicity, though no continuous relationship was found across the whole range of drugs studied [54]. However, for compounds with PS values greater than 10 ml/min/g liver and those with PS values less than 1 ml/min/g liver, a linear relationship between logPS and logP was demonstrated.

It is generally expected that small molecules diffuse more quickly than large molecules. However for a range of drugs studied, the relationship between molecular weight and PS is not clear [54]. This may be due to the relatively narrow range of molecular weights examined or to the dominant effect of logD on PS that obscures the effect of molecular weight on PS.

The partition coefficient, logD, is an index of lipophilicity that accounts for the degree of ionisation at physiological pH. The PS of unbound drug increases as logD is elevated showing a sigmoidal relationship [54,173-175]. For poorly permeable drugs, as the cellular uptake in short transit time through the liver is low, there is doubt whether PS can be estimated accurately from hepatic outflow data at low levels of PS. For highly permeable drugs, the upper limit or plateau represents a rate limitation caused by diffusion through the aqueous layer at the surface of the hepatocyte membrane [54].

4.7.3.3.2 Membrane permeability and perfusate flow

Hepatic uptake is influenced by cellular permeability, perfusate flow and drug binding. It has been proposed that uptake is permeability rate limited when the ratio of PS to flow ($\frac{fu_b.PS}{Q}$) is less than 0.06, and is perfusion rate limited when that ratio is greater than 5.7. For drugs having that ratio between 0.06 and 5.7, both permeability and flow effectively influence the uptake [54]. The estimated value of this ratio for diazepam, diclofenac and salicylate in control livers was 7.3, 2.8 and 5.9 respectively. These values reduced to 4.6, 1 and 2.1 respectively in cirrhotic livers. Thus, it may be concluded that the uptake of salicylate and diazepam is influenced by permeability while that of diclofenac is influenced by both permeability and flow. However, the role of binding and lipophilicity should not be ignored. For drugs with a logD greater than 0, uptake is flow-rate limited if the drug is not protein bound. If the drug is highly bound, the uptake shifts from flow rate-limitation towards a permeability rate-limitation. The uptake of drugs with logD values of less than –3 is usually permeability rate limited irrespective of the degree of binding. For drugs with logD values between –3 and 0, hepatic uptake is a function of both flow rate and permeability.

4.7.3.4 Reduced diffusion

The absence of correlation between the uptake of bound-drug with unbound fraction (albumin-mediated transport phenomenon) is greater for highly permeable ligands (*eg* warfarin, diazepam, diclofenac and taurocholate) than for ligands with medium membrane permeability (*eg* tolbutamide and salicylate) [122]. This effect disappears for the uptake of ligands of low membrane permeability (*eg* cefodizime). The diffusion-limited uptake model assumes that association and dissociation of ligand and albumin are fast enough to achieve equilibrium at every section of the unstirred water layer (UWL), and considers the diffusion of ligand through the UWL to be the major factor. According to this model, the apparent influx clearance for a bound-drug ($PS_{inf,app}$) is obtained using the following equation

$$\frac{1}{PS_{inf,app}} = \frac{1}{P_{diff}} + \frac{1}{fu.PS_{inf}} \qquad (4.20)$$

where P_{diff} and PS_{inf} represent the diffusion clearance through the UWL and the intrinsic influx clearance of free ligand through the plasma membrane, respectively. P_{diff} is also a function of *f*u:

$$P_{diff} = \frac{D_u \cdot A}{s.fu} + \frac{D_b \cdot A}{s.(1-fu)} \quad (4.21)$$

where D_u, D_b, A, and s represent diffusion constants for unbound and bound ligand, effective uptake area, and the thickness of UWL, respectively.

With a highly-permeable ligand (large PS_{inf}), $PS_{inf,app}$ is almost equal to P_{diff} and is unexplainable with free fraction. With a ligand of low membrane permeability (small PS_{inf}), $PS_{inf,app}$ is almost equal to $fu.PS_{inf}$, and can be explained by the free fraction. Thus, the rate-limiting step of influx clearance will change from the diffusion through the UWL to the membrane permeation as the permeability of the ligand in question decreases, resulting in the disappearance of the albumin-mediated transport phenomenon. The effect of UWL should be negligible when the permeability of the ligand is low.

The behaviour of diazepam and diclofenac in the current studies can be explained by the above theory, using a knowledge of the relative resistance of intrahepatic regions to transport [260]. In normal livers, these ligands show a high membrane permeability. Therefore, the $PS_{inf,app}$ would be controlled mainly by diffusion across the space of Disse. In cirrhotic livers, due to the massive structural changes in the space of Disse (Chapter 4), the rate of diffusion of substances from sinusoids into the hepatocyte membrane is greatly reduced, leading to a reduction in $PS_{inf,app}$ of drugs. This causes the drugs to be carried to the outflow with the labelled albumin, as an early component of the indicator dilution curve. Conversely, if the permeability of the drugs is decreased during cirrhosis, the rate-limiting step is membrane permeation (the effect of the UWL is negligible), $PS_{inf,app}$ is almost equal to $fu.PS_{inf}$, and can be explained by free fraction.

Comparison of $PS_{inf,app}$ between perfused rat livers and isolated hepatocytes using ligands of different membrane permeability, not only indicates a more pronounced UWL effect in the perfused liver, but also suggests that dissociation-limited transport cannot fully account for albumin-mediated transport and that diffusion-limited phenomenon is much involved. The effect of the dissociation rate-constant may be important in the transport of ligands with extremely high membrane permeability (*eg* warfarin) but in most ligands including even those classified as ligands of high membrane permeability (*eg* diazepam) the dissociation rate constant does not seem to be a major factor. In these cases, albumin mediated transport is mainly explained by the

effect of the UWL. Therefore, when the unbound fraction is large, the diffusion of ligands through the UWL may lead to the underestimation of the true membrane permeability and may result in the observation of albumin-mediated phenomenon.

The increased effect of UWL in cirrhotic livers is a contribution of three factors.

a) Increased deposition of collagen in the space of Disse which increases the thickness of the UWL by creating toruosity and the hepatocytes adherent water film [147,122]. Hill demonstrated that a cylinder 1 cm in diameter composed of material similar to frog's nerve, if suddenly placed in oxygen, would take 185 minutes to attain 90% of its full saturation with that gas. An actual nerve 0.7 mm thick would take 54 seconds for the same stage of saturation to be reached. A single nerve fibre 7 microns thick would take only 5 milliseconds [157]. The rapidity of diffusion obtainable in systems of small dimensions is the basis of the capillary circulation. The estimated thickness of UWL in normal perfused liver (where the thickness of the space of Disse is 1-2 μm;[122]) reported to be 10 μm [122]. This layer should be much greater in cirrhotic livers where the thickness of the space of Disse is increased by up to 5 times. Oxygen delivery, hence metabolism and secretion, could also be compromised if the critical diffusion distances are exceeded [276].

b) Since the area of fenestrae does not occupy 100% of the sinusoidal wall, the effective area (not for membrane transport but for vascular to space of Disse diffusion), hence uptake, is affected. This effect in increased in cirrhosis.

c) Hepatic intra- and extra-cellular diffusion coefficients show little dependency on the molecular weight and are much smaller than diffusion coefficients in water [122]. These diffusion coefficients are reduced in cirrhosis.

The importance of the equilibrium partition should also be noted. It has been shown that the proportion of material present in the space of Disse at any one time is governed by the equilibrium partition of material in the space of Disse and the sinusoidal space, rather than by a diffusion coefficient [83]. Chinard *et al* [44] found that the ratios of recoveries of inert gases in the pulmonary outflow approached the ratio of their solubilities rather than the ratios of their diffusion coefficient. From the larger logP value of diclofenac than that of diazepam (Table 4.17), it is conceivable that at any one time, a larger proportion of diclofenac would be present in the

Disse space than diazepam. Therefore, any disturbance in this space, would influence the clearance of diclofenac to a greater extent than diazepam, as was demonstrated in these studies (Tables 4.15 and 4.16).

4.7.4 *In vitro-in vivo* Correlation

The membrane permeability of fifteen drugs which have been estimated using isolated rat hepatocytes and perfused rat liver, have recently been re-evaluated by Miyauchi *et al* [173]. It was demonstrated that the PS of total drug obtained from hepatocyte studies correlated with that obtained from perfused liver experiments only in certain range. They suggested that this was due to the diffusional resistance of an unstirred layer within the space of Disse that limits the uptake of highly permeable solutes.

4.7.5 Shunting

Although the impact of shunting on hepatic clearance of drugs in liver disease is well recognised [381], little attempt has been made to model the shunting in these circumstances. Nevertheless, shunting should be considered when estimating the intrinsic clearance of highly extracted drugs and when attempting to discriminate among the models of hepatic elimination. This issue is particularly important in steady-state situations. The presence of shunting would result in the appearance of bimodal indicator dilution curves as demonstrated by Huet *et al* [119]. However, for functional shunts, capillary throughput components may be so intimately intermixed that unimodal dilution curves result.

In the current study, the presence of anatomical shunting based on the recovery of microspheres was rejected. However, appearance of a sharp peak in several outflow profiles of the model drugs in the cirrhotic livers (Chapter 4) may have been caused by the presence of functional shunting. Also, the observed diazepam and diclofenac extraction in the cirrhotic livers was lower than that predicted to result from a reduced enzyme activity alone, consistent with the development of functionally significant intrahepatic shunts.

Chou [54] and Oliver [382] recently proposed an operational model in which shunting was included in the dispersion model. This model was capable of explaining the apparently large D_N for diclofenac in isolated perfused rat liver when the influence of fu on F, at steady state, was evaluated. Using this model, it was also possible to offer a simple and plausible explanation for the non-linear relationship between albumin concentration and hepatic uptake of several highly-extracted-highly-bound drugs. This model, which views shunting as a special case of capillary heterogeneity and considers shunted fraction of flow as a parallel compartment, was applied to several frequency outflow data sets of model drugs where the original dispersion model did not describe the peak and tailing regions of the peak satisfactorily. As can be seen from Figure 4.25, the fit of the revised model to the observed data was satisfactory and better than the previous model. This finding indicates that functional shunting, to some extent, has been present in the cirrhotic liver.

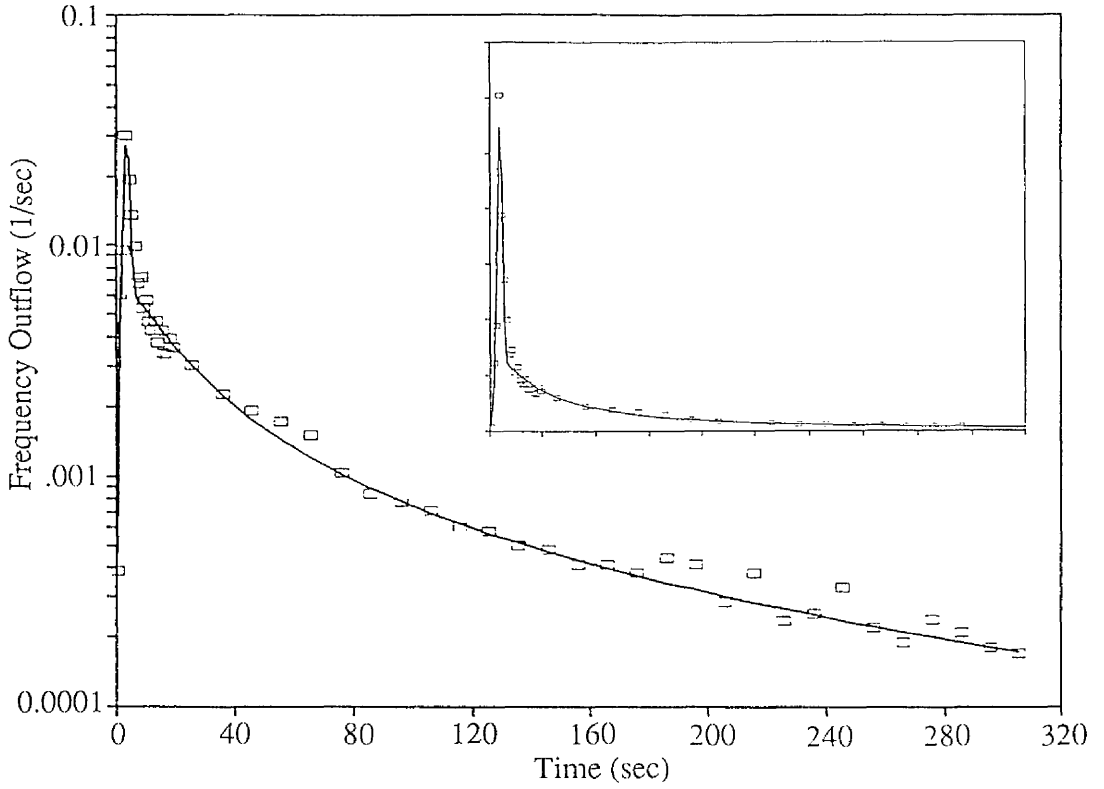

Figure 4.2.5 Semilogarithmic presentation of frequency outflow of diazepam obtained from a cirrhotic liver. The line is the fit of two-compartment dispersion model (which includes a component for shunting) to the observed data (markers).

4.7.6 Phenobarbitone-treated livers

A potential problem in using the current method for the induction of cirrhosis in rats is the use of the enzyme-inducer, phenobarbitone. This has required the use of appropriate phenobarbitone-treated (PT) controls. In the current study (Chapter 3, Tab 4.2.3), physiological and histological data in PT control livers and normal control livers are similar. Parameters of moment analysis of markers and drugs, such as MTT, CV2, and V, were also similar in the two groups. These finding has been confirmed by others [119,188,259,294]. Phenobarbitone induces most enzymes panacinarily which may cause acinar gradients to diminish or exaggerate . Pathological states may constitute a modulating factor. Cirrhosis, for instance, is known to change enzyme distribution. The increased metabolic activity of PT livers may have a significant impact on drug elimination. However, the significant increase in Cl_{int} of diazepam and diclofenac in PT livers was lower than expected. It has been shown that the maximum enzymatic activity following phenobarbotone treatment is achieved after 10 days treatment [208]. Therefore, it may be possible that during prolonged phenobarbitone administration, the liver adopt itself and hepatic metabolic activity return to a lower level.

CHAPTER FIVE: STUDIES IN EXPERIMENTAL CIRRHOSIS

Section Two: Steady-state Considerations

5.1 Introduction

The magnitude of dispersion can be estimated either by reference to the concentration-time profile of a substance from the liver after bolus input into the hepatic portal vein or by examining the influence of controlled changes in physiological determinants such as drug binding within perfusate on drug availability [228]. In the previous chapter, it was shown that the hepatic distribution of diazepam was permeability rate-limited and could be characterised by the two-compartment dispersion model with a D_N value of 0.13. The present study extends these findings by evaluating the applicability of the dispersion model to describe the hepatic elimination of this highly extracted compound under varying conditions of protein binding and estimating the degree of hepatic dispersion.

5.2 Experimental Design

The single-pass isolated perfused liver preparation used was the same as described in Section 3.3.2. The perfusate consisted of human serum albumin (HSA) (concentrations specified below) in basic Krebs bicarbonate buffer (KBB) solution, delivered at 1.22, 1.18 and 1.4 ml/min/g for normal control, PT control and cirrhotic livers, respectively. Viability of the liver was assessed as described in Section 3.3.2 and was confirmed by the steadiness of the diazepam effluent concentrations at steady state during continuous drug infusion.

5.2.1 Transient Kinetics

In order to standardise the liver preparations, a bolus (100 μl) of labelled erythrocytes, albumin and water was injected into the portal vein during constant infusion with basic perfusate and hepatic effluent was collected.

5.2.2 Steady-state Extraction

These experiments were conducted to assess the influence of albumin on the availability of diazepam at steady state. After the initial stabilisation with basic perfusate (drug-free, HSA-free), the perfusate was alternated between 0%, 0.1%, 0.5%, 1% and 2% (g/100 ml) HSA for 120 min (20 min at each HSA concentration) while the total concentration of diazepam was maintained at

1 mg/L. The inflow and outflow perfusate samples were collected at 5 min interval from the beginning to 20 min, and 1 min interval between 20 and 25 min and analysed for diazepam. The concentration of diazepam was determined using HPLC. Protein binding of diazepam in perfusate solution of varying HSA concentration was determined by equilibrium dialysis (Section 3.3.4). Preliminary experiments showed that the non-specific adsorption of diazepam to the perfusion apparatus was negligible and that the time to achieve steady-state extraction for diazepam at 0.1%, 0.5%, 1% and 2% HSA was 13, 11, 9 and 8 min, respectively. Linearity with respect to diazepam elimination was tested with HSA-free perfusate containing three different diazepam concentration (0.5, 1, and 5 mg/L) perfused in random order for 20 min each.

To assess for changes in the viability of the liver preparation with time, the initial protein-free perfusate was then used again for 20 min after the forth protein-containing test perfusate. A preparation was acceptable if the viability of diazepam during the second period of perfusion with protein-free perfusate did not differ by more than 10% from that during the first run.

5.3 HPLC Assay for the Measurement of Diazepam

The assay of diazepam is well documented. The majority of techniques employ HPLC coupled with UV detection of diazepam. The UV maximum absorbance observed for diazepam occurs at 254 nm. In this work, diazepam was assayed by HPLC using a modification of the method of Raisys *et al* [210].

5.3.1 Silanization

To prevent any risk of diazepam adsorption to glassware, a silanization step was incorporated in the method. Dichlorodimethylsilane (200 ml) was mixed with carbon tetrachloride (4 L) in a glass container. All glassware including test tubes and beakers were steeped in the container and left for 48 hours. The test tubes were examined to ensure complete silanization and the glassware was drained and washed first with methanol and then with water. The glassware was then left in an oven (50 °C) to dry. The whole procedure was performed under constant vacuum flow.

5.3.2 Mobile Phase and Buffers

The mobile phase was a mixture of acetonitrile and water (50:50, v/v) with 1% triethylamine. The mobile phase was adjusted to pH 3 with 85% orthophosphoric acid. The mobile phase was freshly prepared every day, filtered, and degassed using nitrogen.

5.3.3 HPLC Apparatus

The HPLC system consisted of a Kontron analytic LC Pump which delivered mobile phase at a flow rate of 1.5 ml/min to a C18 chromatographic column at ambient temperature. Samples were injected using a BDH HPLC syringe and diazepam was detected using an ultra-violet absorbance detector set to 254 nm and the signal was monitored by a HP integrator (integration in peak-height mode). Quantitation of diazepam was determined by the peak-height ratio of drug to internal standard with reference to an appropriate calibration curve constructed in the blank perfusate. A guard column with a disposable cartridge was used to protect the analytical column.

5.3.4 Assay Procedure

Fractional outflow samples from steady-state experiments in the isolated perfused rat liver preparation (containing KBB and HSA) were assayed for diazepam. Every day before the start of the assay, the system was left to equilibrate for 30 min. Nitrazepam solution (internal standard; 50 μl, 3.75 μg/ml) and acetonitrile (to precipitate HSA; 200 μl) were added to the sample (200 μl). Acetonitrile was added to the sample very gently and vortex mixed in order to avoid protein denaturation, which results in the entrapment of substances. After vortex mixing (1 min) and centrifugation (2 steps of 10-min; first at 1500 rpm and then at 3000 rpm), 50 μl of the supernatant was injected into the HPLC system. The retention times of diazepam and nitrazepam were 8.5 and 4.5 min, respectively (Figures 5.1 and 5.2). Known metabolites of diazepam (oxazepam, temazepam, and desmethyldiazepam) eluted at 5.2, 5.7, and 6.5 min, respectively.

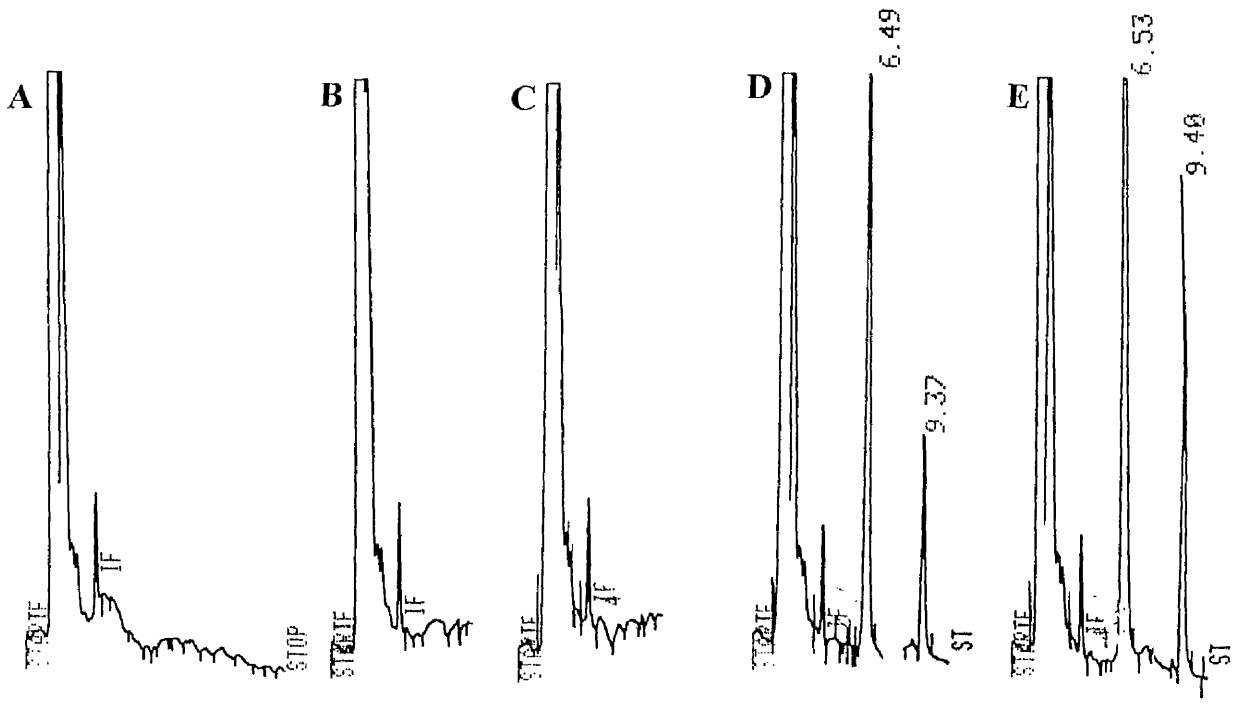

Figure 5.1 HPLC chromatograms of blank and diazepam standard solutions. **A**: Krebs blank, **B**: outflow perfusate blank with no albumin, **C**: outflow perfusate blank with 0.5% albumin, **D**: diazepam 200ng/ml, **E**: diazepam 1000ng/ml. Retention times: diazepam 9.5 min, nitrazepam 6.5 min. Mobile phase: acetonitrile:water, 50:50 v/v at 1.5 ml/min.

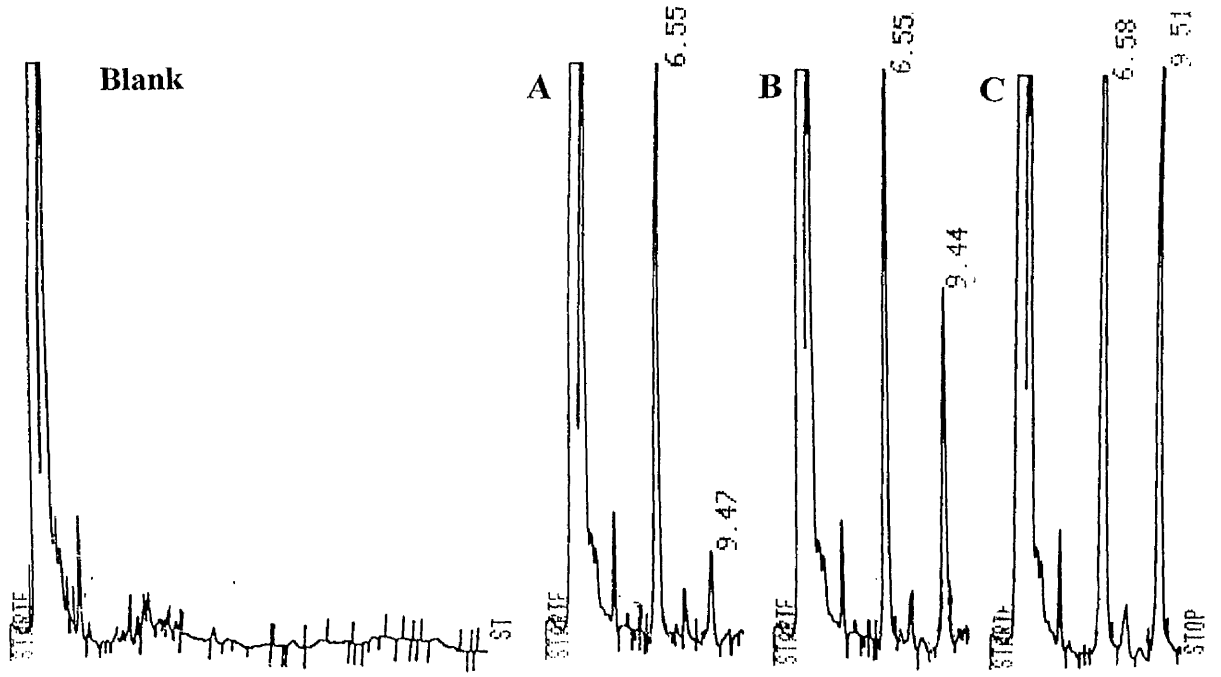

Figure 5.2 HPLC chromatograms of blank and diazepam in outflow perfusate obtained at steady state after continuous infusion to the isolated rat liver perfused with **A**: Krebs with no albumin, **B**: Krebs with 0.5% albumin, **C**: Krebs with 1% albumin. Retention times: diazepam 9.5 min, internal standard (nitrazepam) 6.5 min. Mobile phase: acetonitrile:water, 50:50 v/v at 1.5 ml/min

5.3.5 Calibration

The standard solutions of diazepam were prepared in the appropriate medium from the stock solutions (10 mg/ml in acetonitrile) which were stored in tightly sealed vials at –20°C. Calibration curves were constructed over the range of 100 to 1500 ng/ml. The lowest detection limit was 10 ng at a signal-to-noise ratio greater than 3. Regression analysis of each set of experimental results confirmed a linear relationship between peak height ratio and the quantity of diazepam analysed. The coefficient of variation ranged from 10% at a concentration of 10 ng/ml to 4% at a concentration of 1500 ng/ml. The determination coefficient (r^2) for the calibration curves was always greater than 0.9 (Figure 5.3).

5.3.6 Assay Variability

The inter- and intra-assay variability was assessed at diazepam concentrations of 100, 750 and 1500 ng/ml. For intra-assay variability each sample concentration was replicated three times. Inter-assay variation was assessed by repeating the aforementioned procedure on a further two separate occasions. Variability was calculated by one-way ANOVA. Assay variability was acceptable (Figure 5.4) and in general the inter-run (n=3) coefficient of variation varied from 4% to 10% for high and low concentrations.

5.3.7 Extraction Procedure

Hepatic outflow samples obtained during perfusion with protein-free perfusate contained concentrations of diazepam that could not be measured accurately using the method described above. Therefore, it was necessary to perform a simple extraction procedure prior to HPLC analysis of such samples. Nitrazepam solution (50 µl) and a mixture containing hexane:ethylacetate (8 ml; 8:2 v/v) were added to 4 ml of sample. After vortex mixing (1 min) and centrifugation (3400 rpm, 20 min) the upper organic layer was transferred to a clean test tube and evaporated to dryness (under nitrogen at 35°C). The residue was reconstituted in 100 µl methanol and 50 µl was injected into the HPLC system. Calibration curves were constructed over the range of 10 to 150 ng/ml and the intra- and inter-day coefficient of variation was calculated.

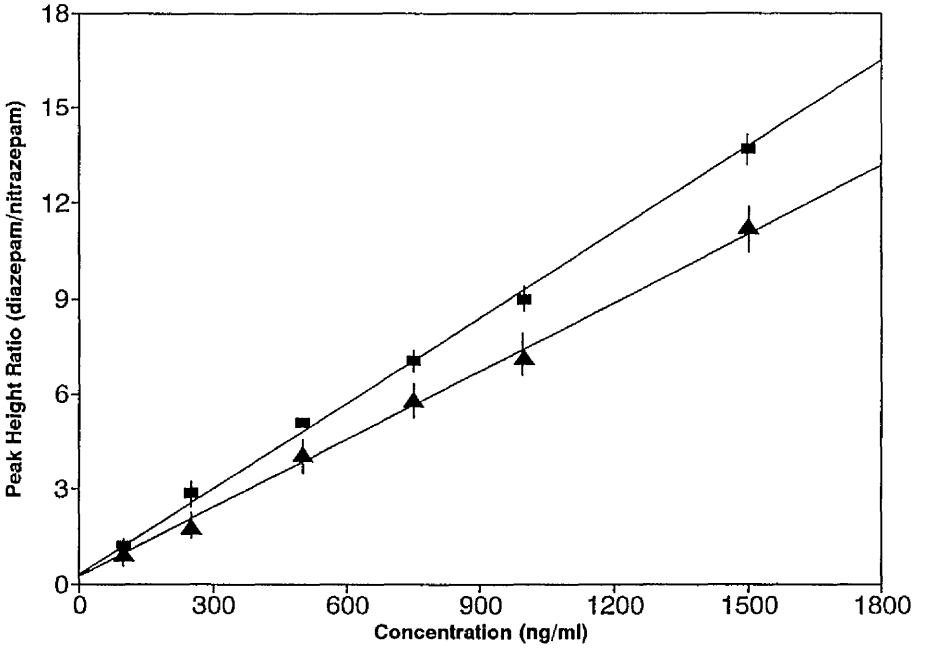

Figure 5.3 Calibration Curve for diazepam, extracted from (A): 4 ml 0.1% HSA , (B): 1 ml 0.5% HSA.

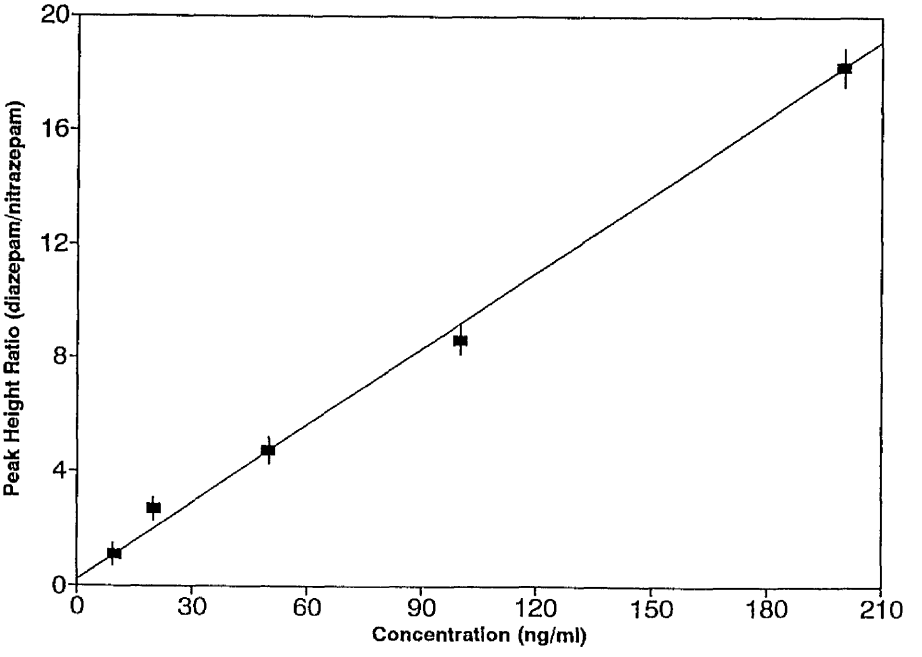

Figure 5.4 Inter-run calibration curve for diazepam (mean of 3 runs).

5.3.8 Extraction Efficiency

Recovery of diazepam from the extraction procedure was assessed at a concentration corresponding to 20 ng/ml perfusate. A triplicate sample of diazepam-free perfusate was spiked with the stock solution, then extracted by the procedure above. An aliquot of the resulting reconstituted extract (50 μl) was injected into the column. The same amount of diazepam standard solution was similarly injected into the system. Assay recovery, calculated as

$$\% \text{ of peak recovery} = \frac{\text{Peak Height Extracted Drug x } 100}{\text{Peak Height Direct Injection}}$$

The extraction efficiency of diazepam and nitrazepam was greater than 88%.

5.4 Data Analysis

5.4.1 Transient Kinetics

The outflow concentrations of labelled markers at the midpoint time of the collection interval was transformed to frequency output and statistical moments (F, MTT, and CV^2) and dispersion model parameters (D_N) of the profiles were estimated (see Section 4.4).

5.4.2 Steady-state Extraction

The steady-state availability (F) of diazepam was calculated from the ratio of outflow concentration (C_{out}) to input concentration (C_{in}). The extraction ratio (E) was calculated as 1-F, and clearance (CL) was calculated as the product of perfusate flow (Q) and E. An initial estimate for CL_{int} of diazepam was calculated from the availability data using the well-stirred (Equation 2.23) and parallel tube models (Equation 2.24). The dispersion (Equation 2.21), well-stirred and parallel tube model equations were fitted to the F versus fu_b data (weight =1/F) by non-linear least-squares regression (SIPHAR 3.3, SIMED, France). In all cases, it was assumed that $PS >> CL_{int}$. The quality of fit provided by the various models was compared with the computer-generated logarithm of the likelihood (logL) estimates and by the weighted residual sum of squared (WSS). The likelihood ratio test was used to assess whether the closed boundary dispersion model provides an improved description of the data compared with its reduced forms, the well-stirred and parallel-tube models. Probabilities (p) less than 0.01 was taken as statistical significance. All data are presented as mean±SD.

5.5 Results

5.5.1 Transient Kinetics

Figure 5.5 shows a representative frequency outflow profile of the reference markers in the control and cirrhotic livers. The outflow profiles of markers were similar to those described in the previous chapter showing one-compartment and flow-limited distribution in all livers. While the volumes of distribution (V) of markers were reduced in cirrhotic livers, the D_N and CV^2 increased in this group (Table 5.1). The recovery of markers was complete (0.98±0.03).

5.5.2 Steady-state Extraction

Figure 5.6 shows a representative plot of availability versus time, in control and cirrhotic livers, when diazepam was perfused at a constant input rate while alternating the concentration of HSA in the perfusate from 0 to 2%. In control livers, when perfused with 0.1% HSA, binding of diazepam in the perfusate was low (fu_b=0.4) and the extraction was high (F=0.11±0.03) and the clearance approached the perfusate flow rate (Table 5.2). As the perfusate concentration of HSA was increased, both fu_b and CL of diazepam decreased. At the highest HSA concentration (2%), when the $f$ub of diazepam is around 0.03, about 68% of the diazepam passed through the liver unchanged, and the clearance of diazepam was less than 0.4 ml/min/g. Hence, the binding of diazepam to HSA effectively transformed the CL of diazepam from flow-limited to capacity-limited. In the cirrhotic livers, while the above pattern was observed, the F value increased and CL decreased notably.

The relationship between F and $f$ub of diazepam for control and cirrhotic liver preparations is displayed in Figures 5.8 and 5.9. Also shown are the predicted lines by the dispersion, well-stirred, and parallel tube models. The fitted parameters of diazepam from the application of these models to the mean values of all data sets together with the coefficient of variation for the estimates are listed in Table 5.3. The WSS, logL and the likelihood ratio test for all models are listed in Table 5.4. Based on the minimum sum of squares residuals and on the plot of the residuals, the dispersion model provided a better description of the relationship between fu and F than the well-stirred and parallel-tube models. Furthermore, based on the likelihood ratio test for full and reduced models, this improvement was statistically significant ($p<0.01$) in all preparations. The CL_{int} of diazepam estimated by the dispersion model always lay between the estimates provided using the well-stirred and parallel-tube models.

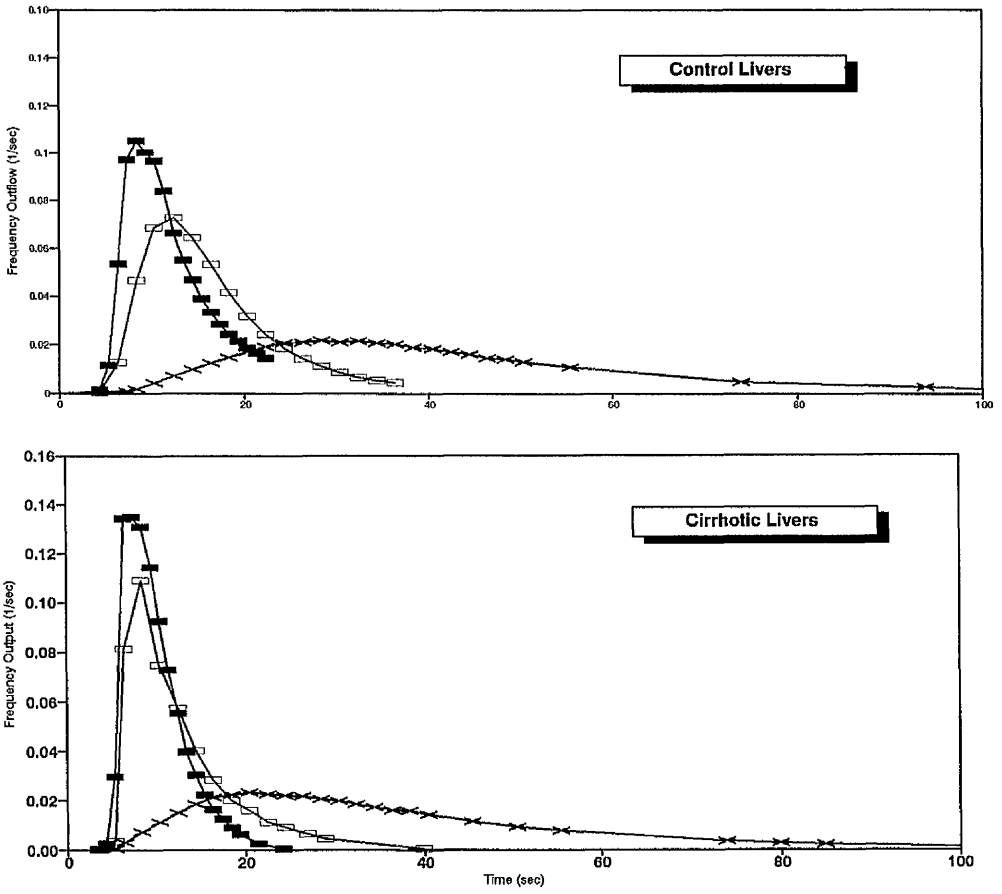

Figure 5.5 Typical frequency outflow of radiolabelled reference markers in the isolated perfused rat liver preparations. Erythrocytes ■, Albumin □, Water X.

Table 5.1

Estimated values of various parameters of radiolabelled reference markers in the isolated perfused rat liver preparations.

			Erythrocytes				Albumin				Water			
	Q ml/min/g	LW g	MTT sec	V_H ml/g	CV^2	D_N	MTT sec	V_H ml/g	CV^2	D_N	MTT sec	V_H ml/g	CV^2	D_N
Normal Livers n=5	**1.22** [0.06]	**27** [2.5]	**11** [0.6]	**0.2** [0.04]	**0.3** [0.05]	**0.1** [0.03]	**17** [1.8]	**0.3** [0.06]	**0.3** [0.06]	**0.2** [0.3]	**39** [6.2]	**0.8** [0.16]	**0.5** [0.08]	**0.2** [0.04]
PT Livers n=5	**1.18** [0.08]	**26** [3.1]	**10** [0.7]	**0.2** [0.05]	**0.3** [0.06]	**0.1** [0.03]	**16** [1.5]	**0.3** [0.06]	**0.3** [0.06]	**0.1** [0.3]	**42** [7.3]	**0.8** [0.12]	**0.6** [0.1]	**0.2** [0.04]
Cirrhotic Livers n=10	**1.4** [0.16]	**32** [4.6]	**7.6** [0.1]	**0.2** [0.03]	**0.3** [0.06]	**0.1** [0.03]	**11** [1.2]	**0.3** [0.05]	**0.4** [0.08]	**0.2** [0.3]	**32** [5.2]	**0.8** [0.13]	**0.5** [0.1]	**0.3** [0.06]

MTT and V_H calculated using moment analysis
CV^2 and D_N calculated using dispersion model
values are mean [±SD]

PT: phenobarbital-treated
Q: perfusion flow rate
LW: liver weight

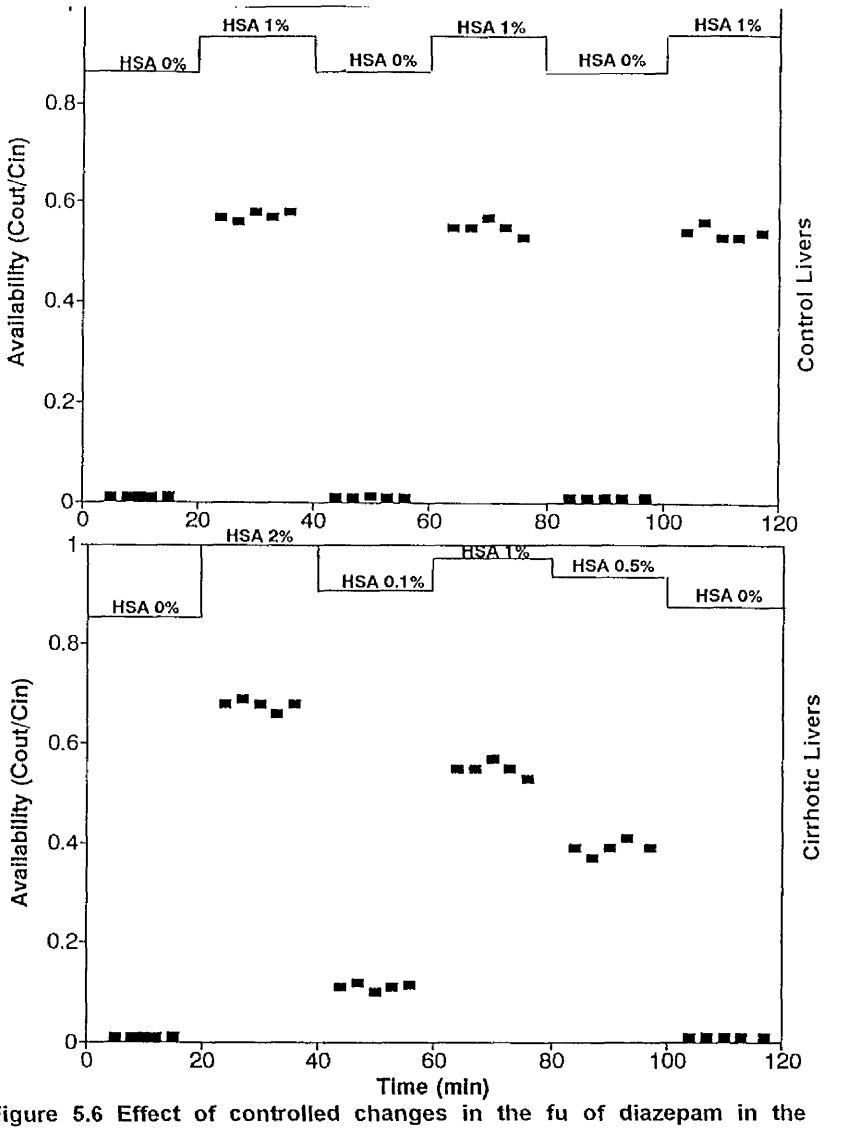

Figure 5.6 Effect of controlled changes in the fu of diazepam in the perfusate on the F of diazepam at steady state ( ) under constant rate drug infusion in a representative liver.

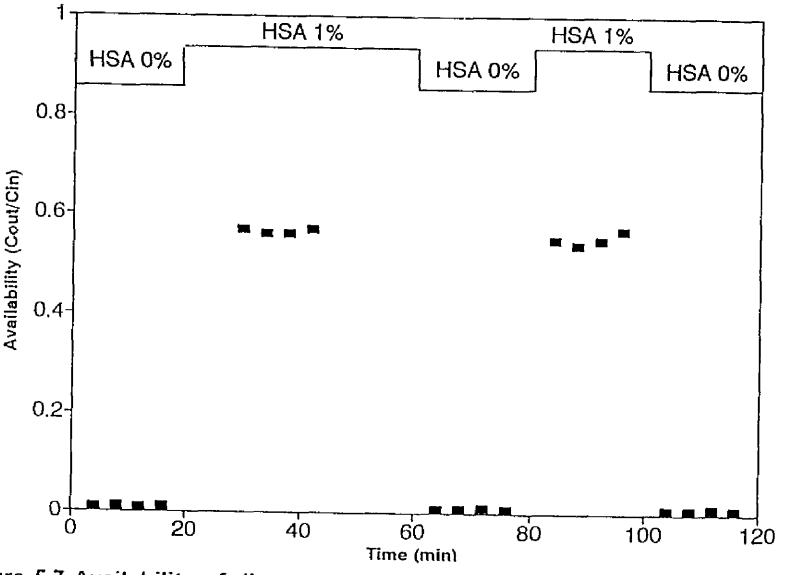

Figure 5.7 Availability of diazepam vs time in a representative liver while alternating between protein-free perfusate and perfusate containing 1% HSA with constant rate infusion.The design of experiment ia also shown.

Table 5.2

Effect of perfusate HSA concentration on availability (F) and clearance (CL) of diazepam at steady-state.

	HSA%	F	CL (ml/min/g)
Normal livers n=5	0	0.01±0.002	1.15±0.22
	0.1	0.11±0.03	1.05±0.20
	0.5	0.39±0.04	0.72±0.14
	1	0.55±0.07	0.54±0.10
	2	0.68±0.11	0.39±0.08
PT Control livers n=5	0	0.01±0.003	1.23±0.24
	0.1	0.092±0.03	1.14±0.22
	0.5	0.34±0.06	0.83±0.15
	1	0.5±0.11	0.61±0.11
	2	0.63±0.11	0.46±0.09
Cirrhotic Livers n=10	0	0.09±0.025	1.25±0.26
	0.1	0.22±0.063	0.76±0.16
	0.5	0.51±0.062	0.48±0.08
	1	0.68±0.09	0.34±0.05
	2	0.88±0.15	0.17±0.04

PT: phenobarbital-treated values are mean±SD

Table 5.3

Estimated values of intrinsic clearance (CLint) and dispersion Number (DN) for diazepam associated with the models of hepatic elimination.

	Dispersion Model		Well-stirred Model	Parallel-Tube Model
	Dn	CLint	CLint	CLint
Normal Livers n=5	0.58±0.11	10.6±0.8	15±1.4	6.4±0.2
PT Livers n=5	0.79±0.12	14.1±0.9	19.8±1.5	7.9±0.2
Cirrhotic Livers n=10	2.2±0.45	7±0.4	8±0.4	3±0.2

PT: phenobarbital-treated values are mean±SD

Table 5.4

Results of the modeling of diazepam elimination.

		Dispersion Model	Parallel-tube Model	Well-stirred Model
Normal Livers	**CV%**	8	9	3
	WSS	0.005	0.001	0.05
	-2 log L	24.5	15.2	14.4
	Likelihood Ratio Test	–	p<0.01	p<0.01
PT Livers	**CV%**	7	9	3
	WSS	0.005	0.01	0.05
	-2 log L	24.4	13.9	15.2
	Likelihood Ratio Test	–	p<0.01	p<0.01
Cirrhotic Livers	**CV%**	6	5	7
	WSS	0.005	0.01	0.05
	-2 log L	24.4	0.9	19.9
	Likelihood Ratio Test	–	p<0.01	0.01

PT: phenobarbital-treated log L: log likelihhod

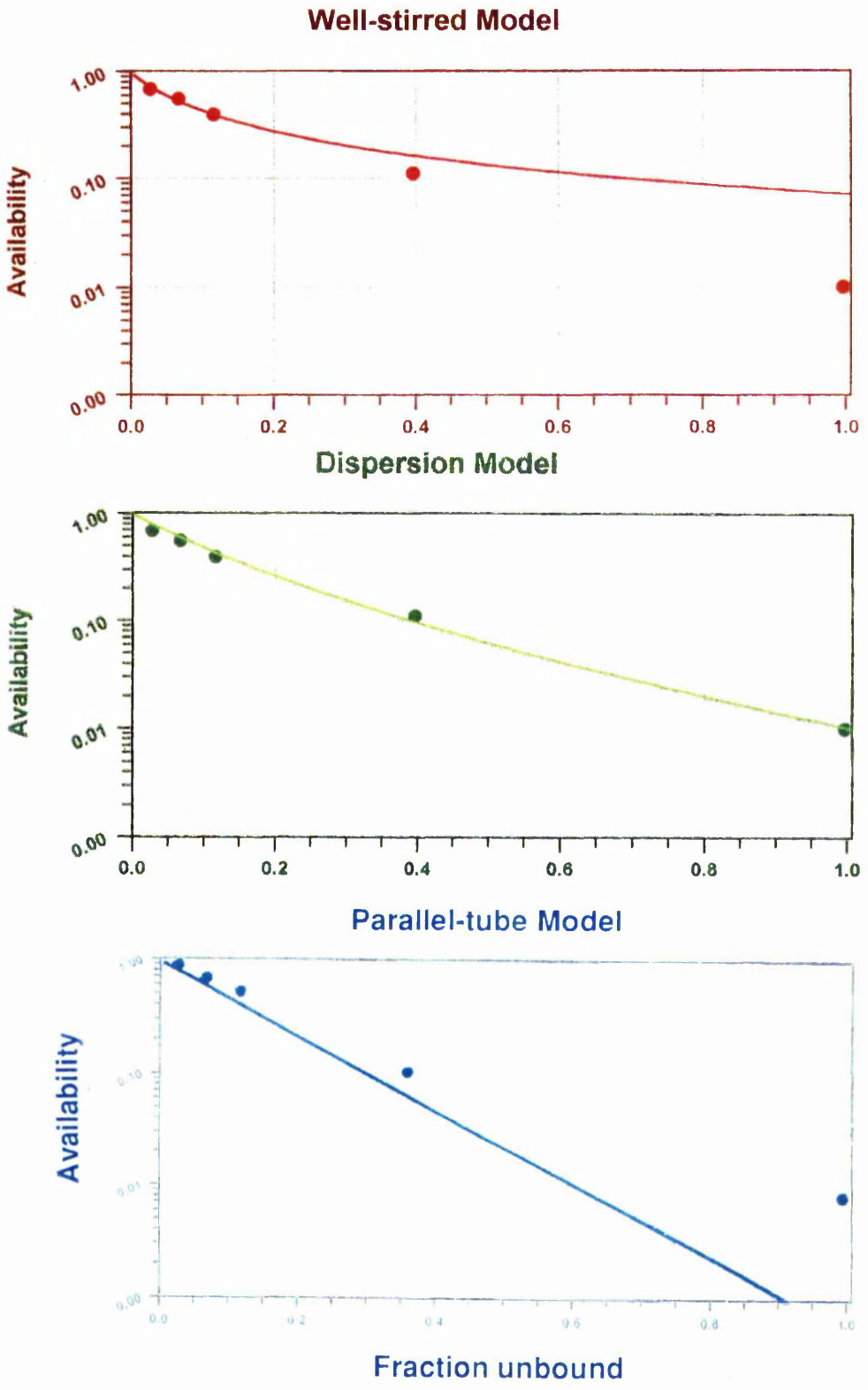

Figure 5.8 Prediction of models of hepatic elimination for the relationship between F at steady state and diazepam fu within the perfusate in a representative control liver.

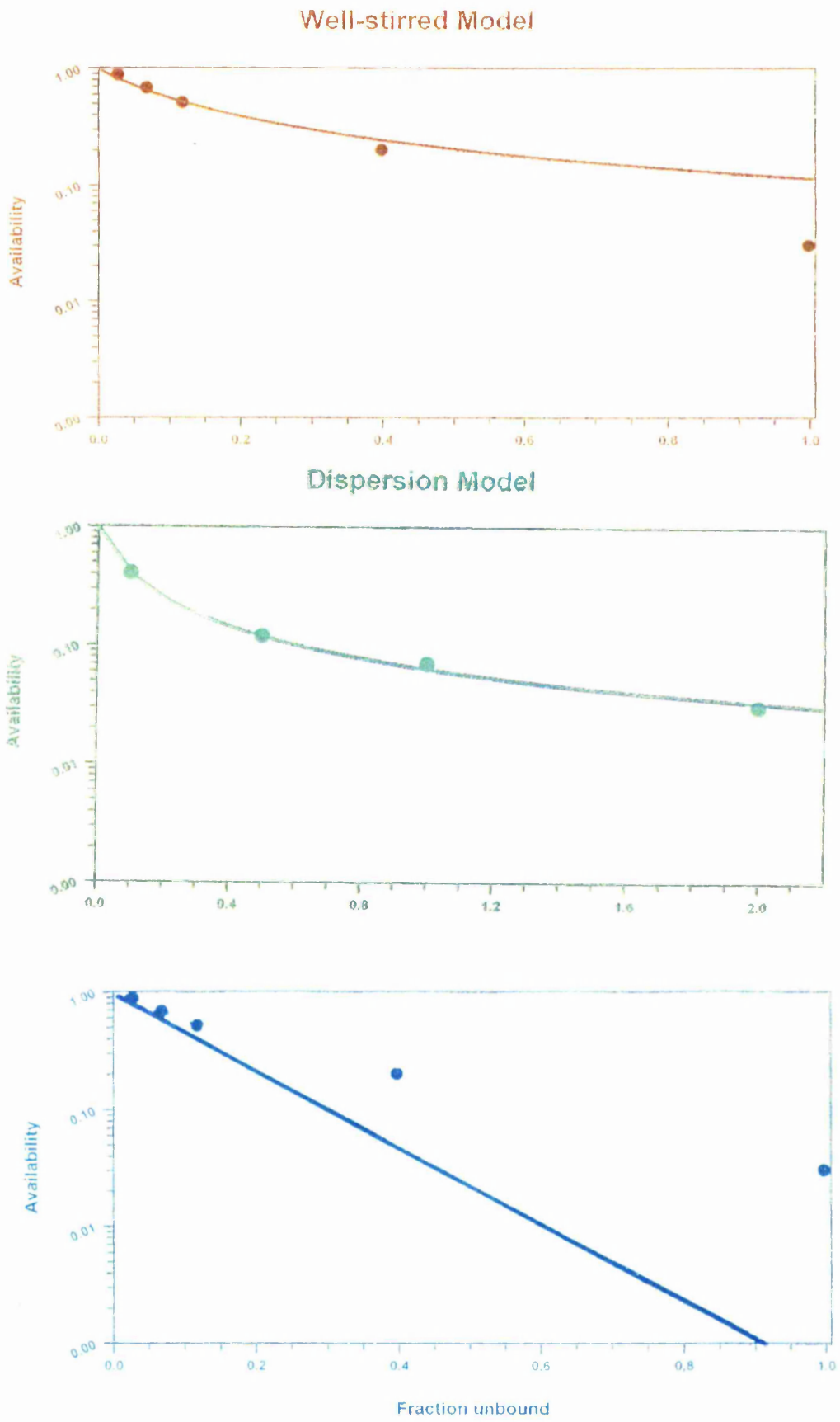

Figure 5.9 Prediction of models of hepatic elimination for the relationship between F at steady state and diazepam fu within the perfusate in a representative cirrhotic liver.

5.5.3 Viability of the Liver Preparation and Linearity

Figure 5.7 shows a representative plot of availability versus time in control liver when diazepam was perfused at a constant input rate while alternating between protein-free perfusate and perfusate containing 1% HSA. In all cases, the availability of diazepam did not change by more than 10% throughout the experiment for each condition. Experiment conducted in three perfused livers indicated that the availability of diazepam did not change with drug concentration up to 5 mg/L. The mean value of F was 0.0094 at 0.5 mg/l, 0.01 at 1 mg/l, and 0.0098 at 5 mg/l.

5.6 Discussion

5.6.1 Transient Kinetics

The reference markers were used to characterise the hepatic distribution and dispersion and provide a basis for comparison between the control and cirrhotic livers. The results of moment analysis and modelling indicated that although the hepatic spaces including vascular, interstitial and cellular spaces reduced in cirrhotic livers, the distribution of markers in this group was still flow-limited and resembled one-compartment characteristics. Similar to the data from the previous chapter, while the D_N values of markers were reduced in cirrhotic livers, the values of CV^2 increased in this group. The data indicate that the diffusional properties of livers have been altered during cirrhosis.

5.6.2 Steady-state Extraction

For drugs that are not eliminated during single-pass through the liver (*eg* salicylate), hepatic dispersion and disposition kinetics are best investigated after bolus dose. For highly extracted drugs, such as diazepam, estimating D_N from a bolus study could be difficult. The steady-state approach was adopted to examine the relationship between F and fu and investigate the effect of altered permeability on availability.

The various physiologic models of hepatic drug clearance predict identical results under conditions of low extraction [193,229,308]. However as E increases, model predictions can diverge appreciably. This divergence is because the essential difference between the models lies in the assumption applied to intrahepatic concentration gradients. For a given organ, arterio-venous concentration difference, the concentration of substrate at the elimination site and estimates of CL_{int} are model dependent. For this reason, the model differ in the predicted change in F in the

event of an alteration in organ CL_{int} or in drug protein binding (fu) under conditions of high extraction.

In the present study, changes in fu was used to alter the F of diazepam. The E value of this compound in the isolated perfused liver increases substantially as binding to protein is reduced (Table 5.2). In the absence of albumin (when fu=1), F approaches zero, reflecting a high intrinsic ability of the hepatic enzymes to metabolise the drug. This is the case in both control and cirrhotic livers. However, cirrhosis lead a greater change in F when the fu values were larger than when fu values were lower. Of the models applied to the relationship between diazepam F and fu, the dispersion model provided the best description in control and cirrhotic livers (Figure 5.7). Because the parallel-tube (PTM) and well-stirred (WSM) models are equivalent to the dispersion model with a D_N of 0 and ∞, respectively, it was possible to apply the likelihood ratio test for full and reduced models [38]. Based on this criteria, the improved fit provided by the dispersion model was statistically significant, although the relationship predicted by the WSM extreme was in all cases closer to the full model than was the PTM.

In the derivation of the dispersion model, it was assumed that the magnitude of the D_N (a result of the variation in solute residence times and the degree of axial spreading) is due almost entirely to the variation and mixing in sinusoidal path lengths and flow velocities [228,229]. Thus D_N should be a property of the organ rather than the compound. The diazepam control D_N values obtained in this work (0.58) were close the narrow range of 0.1 to 0.4 obtained for non-eliminated compounds with different hepatic distribution kinetics [64,223,224,231]. The D_N value showed a significant increase in cirrhotic livers (2.2). The diazepam D_N values in the steady-state experiment were not only higher than values estimated in the bolus experiment (where D_N truly reflects the degree of hepatic dispersion) (Table 4.15), they demonstrated a much greater increase from control to cirrhotic livers as well. While a part of this difference is due to the underestimation of D_N in bolus experiments, it suggests that factors other than the residence time distribution of blood elements influences the relationship between F and fu.

One such factor could be the transverse heterogeneity of drug metabolising enzymes. In the presence of transverse heterogeneity (when some sinusoids have a greater proportion of the total enzymatic activity), the apparent D_N estimated from steady-state experiments under first-order

conditions will be greater than the "true dispersion number" (that which is based on the residence time distribution of a non-eliminated tracer) [13]. As the CV of transverse enzyme heterogeneity increased, the predictions of the dispersion model with D_N of 0.1 tended towards those of the WSM [229]. Transverse heterogeneity of this type has previously been suggested as possible explanation for estimated D_N values of taurocholate of up to infinity [46,267]. The increased diazepam D_N in cirrhotic livers suggests that the CV of transverse enzyme heterogeneity is increased during cirrhosis.

Axial heterogeneity of enzyme systems [100,195] may also contribute to the magnitude of D_N. The relationship between F and R_N is determined by the heterogeneity of the region of the hepatic acinus where the drug is being eliminated. Hence, a drug that is eliminated in the periportal region of the hepatic acinus may have a higher D_N than one that is metabolised predominantly within the perivenous region or than one for which axial heterogeneity does not exist. This is because the degree of vascular heterogeneity appears to be greater in the periportal region than in the perivenous region [100]. Various isoenzymes which metabolise diazepam are located predominantly in the periportal region of hepatic acinus which, together with the perivenous region, are extensively damaged during cirrhosis [202,203,]. This would imply that the steady-state axial heterogeneity of enzyme systems, and hence D_N, should be decreased. However, a greater D_N in cirrhotic livers may indicate that the perivenous region has been damaged to a greater extent than the periportal zone. An alternative explanation for the increased D_N is increased variation in sinusoidal path length, flow and mixing. The contribution of these mechanisms to the increased heterogeneity in cirrhotic livers, as discussed in the previous chapter, appears to be enough for this degree of increase in D_N.

As with most models of hepatic clearance, the dispersion model assumes that the transfer of substrate to the hepatocyte surface is perfusion-rate limited. However, as was discussed in Chapter 4, in some instances drug uptake may be limited by the diffusion of substrate across an unstirred water layer (UWL) adjacent to the cell surface [2]. In these instances, interpretation of drug binding availability relationships with the dispersion model should be carried out with care. This is particularly the case in cirrhotic livers where the exact state of the UWL is not clear.

Although the axial dispersion model assumes that axial diffusion of substrate is a minor component of overall axial spreading, a model of hepatic elimination has been recently proposed that accounts for axial tissue diffusion for highly lipophilic drugs [221,347]. This arterio-venous flux which take place *via* diffusion will increase as the fu of drug increases. The so-called "tissue-diffusion axial dispersion model" has been successful in explaining several experimental data that appear to conflict with dispersion model [66]. The solution to this model can be obtained by replacing the D_N term in equation 2.21 with the expression $[D_N+D_t.K.f u]$ [221,347]. Here, D_t is the tissue diffusion number (a measure of axial spreading of solute within the tissue phase) and K is the degree of drug accumulation in the cell. Because an increase in fu will promote accumulation of drug within the tissue (hence tissue flux), the apparent D_N for a compound will increase as its binding within the perfusate is increased.

When this model applied to the mean F versus fu data presented in Table 5.2 and Figure 5.7, the estimated D_N and the term $D_t.K$ were 0.19 and 0.32, and 0.81 and 0.89 in control and cirrhotic livers, respectively. With first-order transfer rate constants determined in the previous chapter, the volume of distribution of diazepam in the liver was estimated to be 8 times greater than the anatomical volume of the liver when albumin is excluded from the perfusion medium (fu=1). Hence under conditions of high extraction, diclofenac accumulates extensively within the extravascular regions of the liver. Although a significant proportion of this partitioning may represent binding to non-diffusible cell components, the relative importance of partitioning into regions of the cell in which axial diffusion can occur should not be ignored. The fact that diazepam volume of distribution reduced substantially in cirrhotic livers (>twofold) and cellular volume decreased slightly (15%) indicates that this axial diffusion becomes more important in cirrhotic livers.

In the previous chapter, diazepam D_N was estimated from bolus experiments. However, it is important to recognise that under such conditions, the D_N estimate will be influenced by events across the entire organ, including large non-exchanging vessels. Therefore it is not surprising that D_N estimates in this work are different from those in the bolus experiments. In the impulse-response experiments, the mean values of fu and E of diazepam were 0.07 and 0.4, respectively. Metabolic events therefore had intermediate influence on the overall shape of the hepatic outflow profile in control livers and transverse enzyme heterogeneity would therefore have intermediate

influence on the so-derived D_N estimate. In cirrhotic livers this influence may be increased. Under conditions of high extraction when radial tissue diffusion become most important, diazepam outflow concentrations after a bolus injection are so low that analytical problems arises.

The influence of *f*u on diazepam availability in the isolated perfused rat liver has been examined and a wide range of values for D_N has been reported; in some of the experiments, D_N estimates were similar to the findings in this work while in others D_N had extreme values of 0 or ∞ [46]. A possible explanation for this variability may lie in the use of erythocytes in the perfusate in those experiments. Due to the partitioning of diazepam into erythocytes, *f*u did not exceed 0.6-0.7 even in protein-free perfusate and, as a consequence, the mean availability, under these conditions (0.06), was 5-6 times higher that the mean value in this work in the absence of protein of 0.011. To provide good estimates of D_N and adequate discrimination between models of hepatic elimination, F (and hence *f*u) must vary over a wide range, with F at *f*u=1 being a pivotal value [193].

Rowland *et al* [240] evaluated the influence of protein binding on diazepam availability at steady state in similar experiments to those performed in this work and concluded that the parallel-tube model fitted the data better than the well-stirred model. Reanalysis of the data [229] with the dispersion model yielded a dispersion number of 0.30±0.23, slightly smaller than the findings in these experiments.

In a similar approach, Diaz-Garcia *et al* [60] examined the applicability of the WSM, PTM, and mixed-boundary form of dispersion model to describe the relationship between *f*u and F in steady state experiment. This form of dispersion model can not be reduced to well-stirred extreme as D_N approaches ∞. Although the closed boundary conditions may be more appropriate, the choice of boundary conditions is relevant only at high dispersion numbers. In the range of D_N values determined for diazepam, the predictions of availability for the mixed and closed boundary conditions are almost identical either at steady state or after a bolus dose [60]. In fact, the parameters derived by applying the axial dispersion model to the steady-state data for all three boundary conditions considered by Roberts and Rowland [228] were almost identical, as were the log likelihood estimates.

Chou [54] highlighted the significance of optimal experimental design in estimating the dispersion model parameters. This worker compared the results of studies on barbiturates with the results of two similar published studies on diazepam [60] and diclofenac [120]. In the two latter studies, despite more preparations being used, the likelihood ratio plots demonstrated that the 95% confidence interval of D_N (and log D_N) for barbiturates was narrower and more symmetric (*ie* more precise) than that of diazepam and diclofenac. This was primarily due to the spread of the *f*u points that were not spaced in a geometric progression order. It was shown that the 95% confidence interval of D_N for diazepam was closer to the parallel-tube model, while that of diclofenac was closer to the well-stirred model. These findings are similar to those by Rowland *et al* [229,240] who showed that the relationship between steady-state F and *f*u for diazepam was better described by the parallel-tube model than by the well-stirred model and a D_N value of 0.3 was estimated from the data. Conversely, in a similar study [46], the influence of protein binding on the availability of diazepam is consistent with the prediction of the dispersion model with a much larger D_N (1.04), which is still within the 95% confidence interval estimated from the data of Diaz-Garcia *et al* [60]. In the current work, where a larger D_N was found, the relationship between steady-state F and *f*u for diazepam was better described by the well-stirred model than the parallel-tube model.

Model analysis indicated that WSM and PTM predicted a more pronounced reduction in CL_{int} value than the dispersion model (Table 5.3). The value of diazepam CL_{int} obtained in the steady-state experiments was different from that in the bolus experiment (Table 4.15). As CL_{int} is more accurately estimated from steady-state experiments, the value of Cl_{int} obtained in this work was substituted in the following equation which determines the availability in the bolus experiments [66].

$$F=\exp\left[\frac{1-\left[1+\frac{4D_N \cdot V_b \cdot k_{12} \cdot k_{23}}{Q(k21+k23)}\right]^{0.5}}{2D_N}\right] \qquad (5.1)$$

The values of availability calculated for control and cirrhotic livers were 0.58 and 0.62, respectively, which are similar to the values obtained before (Table 4.15). Therefore, the overall ability of liver to efficiently metabolise diazepam has not been decreased in experimental

cirrhosis. This is most likely due to the inducing effect of phenobarbitone treatment of the cirrhotic livers.

In conclusion, the D_N needed to explain the effects of altered perfusate binding on diazepam F was around 2, reflecting such a large degree of organ heterogeneity that the liver was effectively behaving as a well stirred system. Because this D_N estimate exceeds that determined from the RTD of non-eliminated compounds, factors in addition to flow heterogeneity must have influenced the relationship between F and fu for this model compound. Such factors could include UWL, axial and transverse enzyme heterogeneity, and axial tissue distribution of compound. Further studies are needed before the contribution of any one factor can be assessed.

CHAPTER SIX: STUDIES WITH CREATININE

Section One: *In vivo* Experiments

6.1 Introduction

Overall distribution and elimination of a drug is often estimated from the study of plasma kinetics. The data so generated provide limited information, however, on how individual tissues contribute to produce the observed plasma drug concentration-time profile. Determination of tissue drug concentration with time helps to solve this problem. In humans, tissue sampling presents practical difficulties, thus animals are commonly used to investigate the kinetics of drug distribution into tissues.

The following series of experiments were aimed primarily to investigate the kinetics of tissue distribution for creatinine in the rat. Creatinine is an attractive test substance for tissue distribution studies, since its metabolic and physiological characteristics are well established [264,298,52]. Although creatinine has been extensively used for the study of tubular and glomerular renal function [29,95], its use as an extracellular marker needs to be defined. In studies performed previously by Bumstead [358] in this laboratory, it was demonstrated that creatinine is able to traverse erythrocytes membrane *in vitro* and equilibrate into the aqueous space available for distribution.. However, the permeability was low as was evident from the time needed to achieve distribution equilibrium (~60 min). In the same studies, it was also concluded that the distribution of creatinine in single-pass isolated perfused liver preparation is compatible with the two-compartment dispersion model which assumes permeability rate-limited distribution [358]. The purpose of this study was, therefore, to further study the tissue distribution of creatinine *in vivo* and to investigate whether its cellular uptake is permeability rate-limited. Sucrose, which is believed to occupy only extracellular space, was chosen as tracer marker.

6.2 Methods

6.2.1 Surgical Procedure

6.2.1.1 Induction of anaesthesia

Each rat was anaesthetised by a combination mixture of the following composition:

Substance	Purpose	Ratio
Medazolam	Anaesthetic	1 part
Hypnorm	Muscle relaxant	1 part
Water	Base	2 parts

Medazolam (1 part) was added to water (1 part). After mixing, Hypnorm (1 part) was added and then the remaining water. The addition of components had to be in that order otherwise the mixture would precipitate. A dose of 2.7 ml/kg of this mixture was used to produce an effective anaesthesia after 10 min. The administered dose was enough to maintain the anaesthesia throughout the surgery (30 min).

6.2.1.2 Preparation of the animal

The surgical procedure was performed on a heated operating table in order to keep the body of the animal warm. The anaesthetised animal was held on the table using tape. After the hair around the neck and lower part of the abdomen was removed, a patch of skin on the right ventral surface in the neck region was cut and a midline incision of 2 cm through the skin was made. The carotid artery and jugular vein were cannulated with PE-50 tubing for blood sampling and infusion of substances, respectively.

6.2.1.3 Cannulation of the Carotid artery

After opening the neck, the overlying connective tissue was kept moist by the application of saline. The connective tissue covering the throat was separated to reveal three muscles overlying the trachea. The three muscles were carefully separated to reveal the trachea and the adjacent right common carotid artery. The right common carotid artery was located and 1-2 cm length was isolated from the surrounding tissues. The vessel was separated from the vagus nerve by gentle teasing apart the connective tissue with forceps. Extreme care was taken to prevent damage to the nerve and carotid artery.

A ligature was securely tied at the proximal end (towards the head) of the exposed artery thus occluding blood flow to the brain. A small artery clip was placed distally (towards the heart). A ligature was closely tied between the proximal ligature and the artery clip. A small incision was carefully made in the top part of the exposed artery between the two ligatures. A polyethylene cannula (PE 50) previously filled with heparinised saline (25 units/ml) and attached to a 1 ml syringe was inserted 5-10 mm into the artery. The cannula was securely tied in position with the loose ligature. Thus by opening the artery clip, blood from the heart could flow freely down the cannula for sampling purposes.

6.2.1.4 Cannulation of the Jugular vein

A small incision through the skin was made directly over the right jugular vein. A short section of the right external jugular vein was located, separated and gently cleared of the surrounding connective tissue. A ligature was securely tied at the proximal (towards the head) end of the exposed vein just after the junction of the cephalic vein to prevent venous return from the head. A second ligature was loosely tied, distally to the first, around the junction with the subclavian vein. A small incision was carefully made in the jugular vein between the ligatures. A polyethylene cannula (PE 50) filled with heparinised saline attached to a 1 ml syringe was gently threaded into the jugular vein (approximately 1 cm) and fed down into the superior vena cava. Slight adjustments were made to the position of the cannula by sliding the cannula to and from within the vein until blood could be withdraw readily up the cannula thus ensuring free flow. The cannula was flashed back with heparinised saline and secured in place with the proximal and distal ligatures. Both cannulae were exteriorised *via* the neck. After surgery, rats were left overnight to recover prior to dosing.

6.2.2 Preparation of Administered Solution

A double component mixture containing both creatinine and sucrose in phosphate pH 7.4 buffer was prepared and 200 µl of this solution (containing 50 µCi ^{3}H-sucrose and 15 µCi ^{14}C-creatinine) was administered rapidly into the jugular vein of each rat. The solution was mixed before use. Immediately after the dose, 0.1 ml heparinised saline was injected ensuring complete injection of the dose and prevention of clotting.

6.2.3 Protocol

Twenty seven healthy rats (460±55 g) were randomised in nine groups of three. It was shown in the preliminary experiments that the disposition blood profiles of both sucrose and creatinine were covered in one hour and that the peak and first phase of the curve were complete in just over 5 minutes. Hence, the total duration of the experiment was planned to be 60 min with sampling times at 1, 2, 3, 4, 5, 8, 15, 30 and 60 min. At each time point one triplicate experiment (*ie* one group of three rats) was performed. All *in vivo* protocols performed throughout these experiments were undertaken on conscious recovered rats.

The first drop of each sample was discarded due to contamination of saline residing in the cannula. Blood (0.3 ml) was drawn from the venous catheter into a heparinised syringe, and rapidly cooled to 4±1°C by placing it immediately in ice. Blood (100 µl) was transferred into a glass scintillation vial for subsequent treatment and measurement of substances. The rest of the sample was centrifuged (2000 rpm for 2 min) and the plasma separated immediately. After removal of a blood sample, the cannula was back flushed with heparinised saline (0.3 ml) to prevent clotting in the cannula and to compensate for any blood loss.

After the final blood collection in each time point, the animal was sacrificed immediately by cervical dislocation and then kept in freezer for 1 hr for immediate temperature loss. The tissues dissected immediately after the experiments. The total blood volume sampled for each rat did not exceed 2.7 ml. In order to achieve a well-defined blood profile, three other rats were used. These animals were administered 200 µl of the creatinine/sucrose stock solution as a bolus dose. Blood was sampled at 1, 2, 3, 4, 5, 8, 15, 30 and 60 min later. The rats were sacrificed by cervical dislocation at the end of experiment (60 min) and tissues harvested as before.

6.2.4 Tissue Dissolution

After the end of each *in vivo* experiment, the following main tissues were excised and analysed: Adipose, brain, gut (small intestine), heart, kidney, liver, lung, skeletal muscle (hindlimb), skin, spleen, stomach and testes. All tissues were briefly rinsed with 0.9% sodium chloride, and blotted dry. To accurately assess the activity of β-isotopes in tissue samples, it was necessary to dissolve the tissues.

The method used was based on the work of Balk *et al* [9]. A known amount of aforementioned tissues (in duplicate) were cut and transferred to a 20 ml glass scintillation vial with 1.4 ml soluene-350 and left to dissolve over night in an oven at 50°C. In each case, the tissue was precisely weighed with an accuracy of approximately 1 mg in the 0.2-0.5 g range. Soluene-350 is a toluene-based quaternary-ammonium compound which effectively solubilizes proteinaceous material, at a rate which can be increased by warming, and produces minimal chemiluminescence (CLM). On the following day, after cooling, samples were neutralised with hydrochloric acid (2M, 140 µl) prior to bleaching. The bleaching step was included in the assay procedure [27] to reduce any potential colour quenching caused by varying residual blood content of sampled tissues. Hydrogen peroxide (30%v/v, 0.6 ml) was added to the sample which was then left for 15 min at room temperature before being heated in an oven at 40°C for 2.5 hr, to reduce background CLM caused by the addition of peroxide. Since hydrogen peroxide causes frothing and produces high background counts, isopropanol (0.6 ml) was used to counteract this effect. After cooling, 12 ml scintillation fluid was added. The samples were left for one day in the dark, for further CLM reduction, and then vortex mixed and counted for 5 min on scintillation counter in dual channel.

6.2.5 Effect of Quench and Cross-over

The extent of quench and cross-over between ^{3}H & ^{14}C was assessed in spiked samples. Tissue samples (4 of each) from a rat were treated according to the method. A known amount of ^{3}H -sucrose or ^{14}C -creatinine, or combination of both labels (typically 30000 dpm and 5000 dpm, respectively) was added to each tissue sample and blank samples with dissolving fluids only. After dissolution overnight, the single- and dual-labelled samples were counted appropriately. The efficiency of counting for each isotopes in each tissue was estimated by comparison with the blank samples. For each isotope in each tissue, the efficiency of count was higher than 92% (Tables 6.1 and 6.2). However the effect of quenching in dual-labelled samples (*ie* low efficiency of the higher energy isotope, ^{14}C, and increased efficiency, due to crossover, of the lower energy isotope, ^{3}H, was considerable. These results were used to correct for the effect of quench or crossover in the *in vivo* experiments.

Table 6.1

Estimation of efficiency of count (%) in single- and double-labelled spiked tissues (n=4).

Tissue	Single-labelled		Dual-labelled	
	^{3}H-sucrose	^{14}C-creatinine	^{3}H-sucrose	^{14}C-creatinine
Adipose	102	96	117	80
Brain	106	99	119	72
Gut	100	98	123	78
Heart	102	98	125	75
Kidney	100	97	116	79
Liver	101	98	123	80
Lung	98	99	128	78
Muscle	100	93	126	76
Skin	100	93	118	73
Spleen	103	99	112	77
Stomach	99	96	119	71
Testes	105	98	120	77

For tissue dissolution see the methods

Table 6.2

The linear relationship between the dose and count efficiency (%) in different tissues (n=3).

	100% Dose		20% Dose		10% Dose		5% Dose	
Tissues	^{3}H	^{14}C	^{3}H	^{14}C	^{3}H	^{14}C	^{3}H	^{14}C
Adipose	116	89	173	71	171	70	160	66
Brain	99	73	141	71	146	68	140	68
Gut	108	70	181	68	177	65	175	66
Heart	106	71	160	68	158	65	161	66
Kidney	106	80	130	70	130	97	119	91
Liver	101	77	127	73	123	70	100	72
Lung	109	81	145	69	148	65	140	66
Muscle	108	76	127	73	123	70	100	72
Skin	111	69	135	72	132	71	132	70
Spleen	115	72	155	62	188	65	152	60
Stomach	113	75	140	71	129	68	120	69
Testes	101	71	179	65	179	68	170	65

^{3}H: ^{3}H-sucrose
^{14}C: ^{14}C-creatinine

values are mean
double-labelled spiked tissues

6.2.6 Effect of the Dose

The linearity of relationship between the quantity of isotope in a tissue and count was investigated. The combination mixture of the dose with various concentration (100%, 20%, 10%, and 5%) was added to tissue samples and treated as described before. Blank samples (no spiked dose) and standards (with dissolving fluids only) were set up and the activity for ^{3}H and ^{14}C was measured. The results indicated that changing the spiked dose produced a linear response in the measured counts (Figure 6.1).

6.2.7 Estimation of Background Counts

An estimate of background was obtained with blank tissue samples from a sham experiment. Briefly, 200 mg sample from each tissue was excised, transferred into 20 ml glass scintillation vials and treated as detailed in the method and counted for both ^{3}H and ^{14}C. Results indicated that most of the background activity arising from the tissue can be accounted for by the activity in Soluene-350, hydrochloric acid, isopropanol, hydrogen peroxide and scintillation fluid (Table 6.3). These values were subsequently used to correct all tissue samples for background activity. It should be noted that the scintillation counter used gave an estimation of CLM and automatically corrected for it.

6.2.8 Sample size Correction

In order to make sample collection quicker, an optional amount of the sample was precisely weighed and the weight recorded. The amount of measured radioactivity in each sample was then corrected by its weight and calculated for 1g of sample.

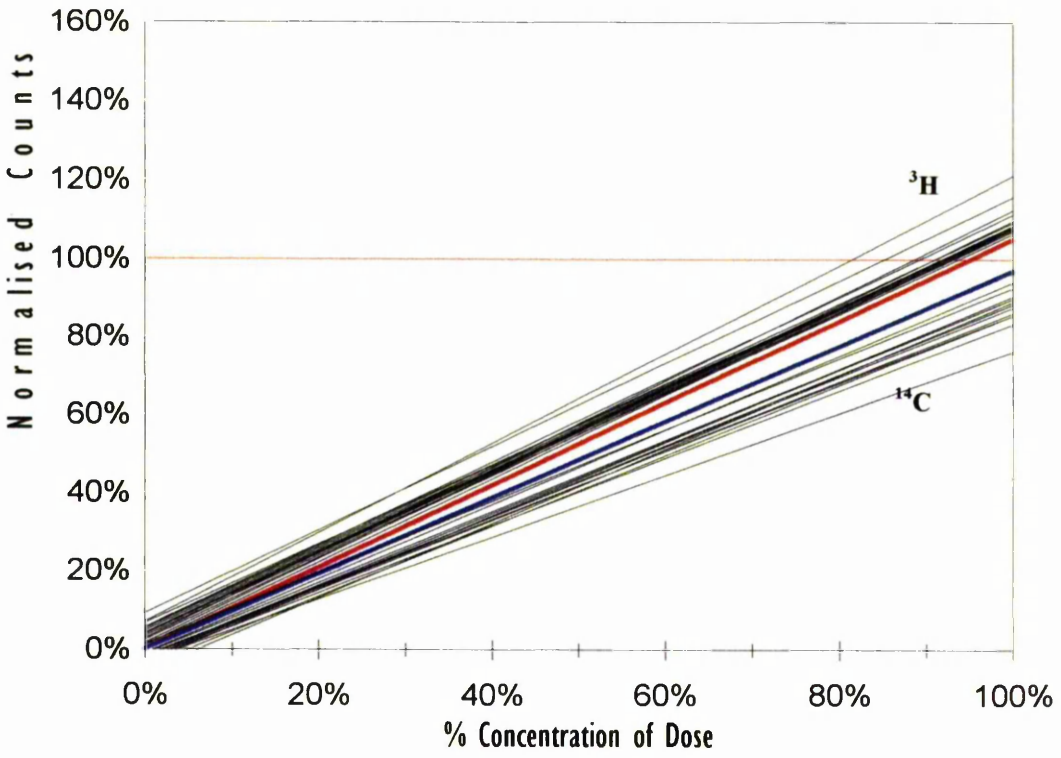

Figure 6.1 The linear relationship between the dose and measured counts in various tissues. The red and blue lines are the standard curves for ^{3}H-sucrose and ^{14}C-creatinine, respectively. Data points have been omitted for clarity.

Table 6.3

Estimation of background activity in dissolved tissues and fluids (n=3, mean±SD).

	Background Activity (dpm/200mg)	
Tissues	**^{3}H Channel**	**^{14}C Channel**
Adipose	41 ± 5	44 ± 5
Brain	40 ± 5	44 ± 5
Fluids	45 ± 6	50 ± 5
Gut	42 ± 5	41 ± 6
Heart	54 ± 8	54 ± 8
Kidney	44 ± 5	48 ± 6
Liver	55 ± 5	72 ± 8
Lung	42 ± 4	45 ± 5
Muscle	45 ± 5	56 ± 8
Spleen	53 ± 5	68 ± 7
Skin	47 ± 7	50 ± 6
Stomach	44 ± 6	48 ± 6
Testis	51 ± 6	58 ± 7

for tissue dissolution see the methods

6.3 Events Viewed from Plasma (Blood)

6.3.1 Data Analysis

6.3.1.1 Exponential Fitting

A biexponential equation (Equation 6.1) was found to best describe the blood and plasma concentration time data of both creatinine and sucrose. A computer program (Siphar; SIMED, France) was used and parameters C_1 & C_2 and λ_1 & λ_2 were obtained. A weighting factor equal to $1/y^2_{observed}$ was used.

$$C=C_1 \cdot e^{-\lambda 1 t} + C_2 \cdot e^{-\lambda 2 t} \quad (6.1)$$

Other pharmacokinetic parameters including elimination half-life ($t_{1/2}$), clearance (CL), initial volume of distribution (V_1), and steady-state volume of distribution (V_{ss}) were calculated using the following equations.

$$t_{1/2}=\frac{\ln 2}{\lambda_2} \quad (6.2)$$

$$CL=\frac{Dose}{AUC} \quad (6.3)$$

$$V_1=\frac{Dose}{(C_1+C_2)} \quad (6.4)$$

$$V_{ss}=\text{Dose}\ \frac{\frac{C_1}{(\lambda_1)^2}+\frac{C_2}{(\lambda_2)^2}}{(\frac{C_1}{\lambda_1}+\frac{C_2}{\lambda_2})^2} \quad (6.5)$$

$$V_d=\frac{CL}{\lambda} \quad (6.6)$$

6.3.1.2 Moment Analysis

Statistical moment analysis was used to calculate the area under plasma concentration versus time curve (AUC; Equation 2.2) and mean residence time (MRT; Equation 2.3).

6.3.2 Results

Blood and plasma profiles together with the biexponential fit for creatinine and sucrose are presented in Figure 6.2. The associated estimated parameters are presented in Table 6.4. As the administered dose of sucrose was larger than that of creatinine, a greater plasma concentration and C_1 and C_2 was achieved for sucrose compared to creatinine. The plasma half-life of sucrose

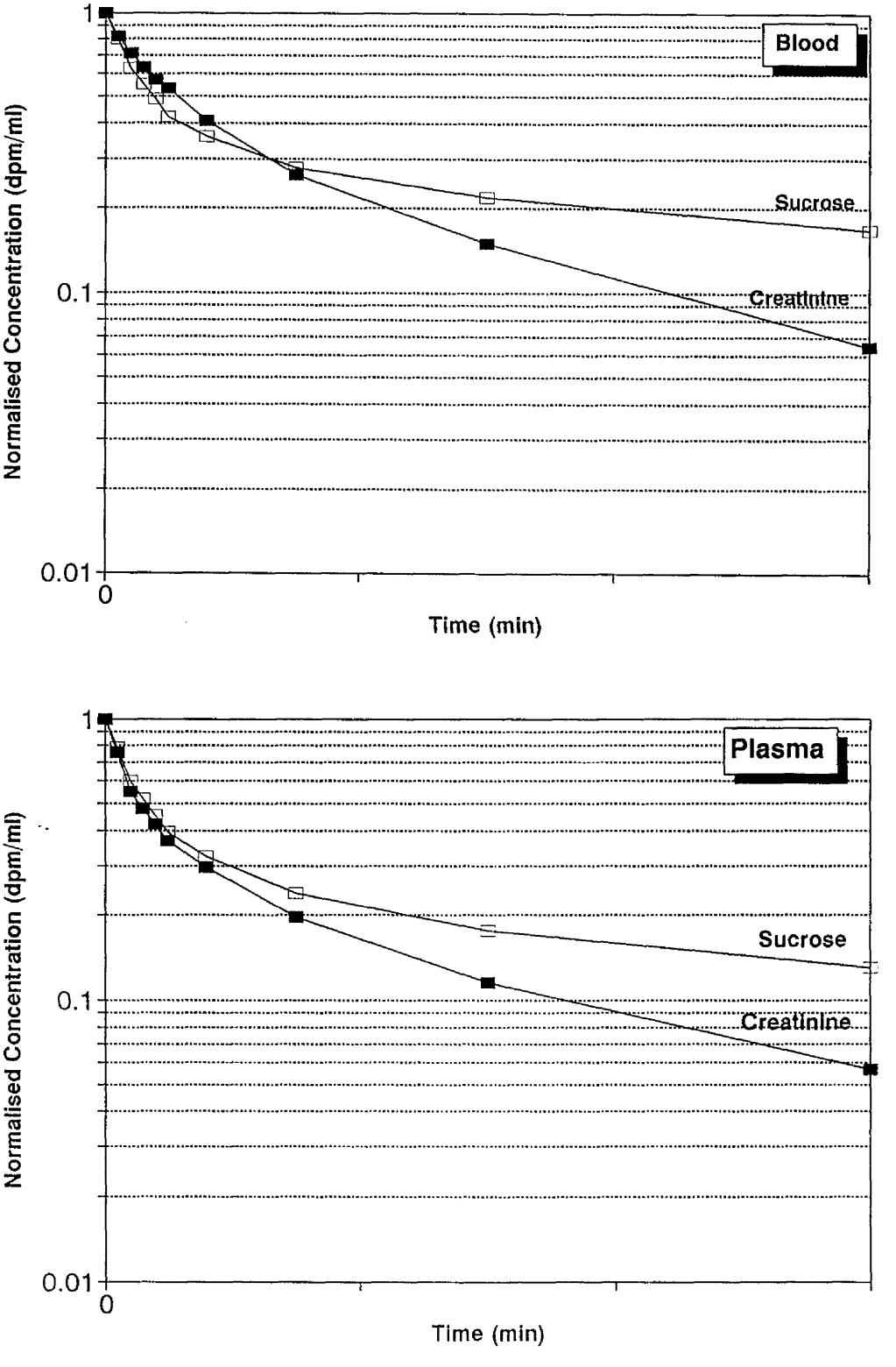

Figure 6.2 Typical semilogarithmic plot of arterial blood and plasma concentration of creatinine and sucrose in rats after an intravenous bolus dose. The concentrations have been normalised for the maximum observed concentration. The symbols are the experimental observations and the solid lines are the best-fit curves.

Table 6.4
Pharmacokinetic parameters for creatinine and sucrose after intravenous bolus administration in rats (n=3).

		Creatinine		Sucrose	
		Blood	**Plasma**	**Blood**	**Plasma**
C1 dpm/g	Mean	**14300**	**42000**	**69200**	**180000**
	±SD	1400	3500	4900	12000
	CV%	9	8	7	7
C2 dpm/g	Mean	**16200**	**25000**	**37000**	**93000**
	±SD	1500	3300	3700	8500
	CV%	0.09	13	10	9
λ1 1/min	Mean	**0.274**	**0.422**	**0.42**	**0.4**
	±SD	0.05	0.08	0.061	0.057
	CV%	18	18	14	14
λ2 1/min	Mean	**0.035**	**0.032**	**0.015**	**0.017**
	±SD	0.007	0.007	0.003	0.004
	CV%	20	20	20	22
t1/2ß min	Mean	**20**	**22**	**48**	**40**
	±SD	3	3	5	4
	CV%	14	14	10	10
CL ml/min	Mean		**5**		**1.5**
	±SD		0.6		0.25
	CV%		12		15
V1 ml	Mean		**70**		**35**
	±SD		5		3
	CV%		7		8
Vss ml	Mean		**160**		**86**
	±SD		12		7
	CV%		7		8

(40 min) was nearly twice that of creatinine (21 min). While plasma half-life of creatinine was marginally larger than its blood half-life, for sucrose blood half-life was larger than the plasma half-life. Clearance of creatinine (5 ml/min) was larger than that of sucrose (1.5 ml/min). The initial volume of distribution and volume of distribution at steady state of creatinine (70 and 160 ml, respectively) were approximately twice those of sucrose (35 and 86 ml, respectively).

6.3.3 Discussion

Most of studies on creatinine have been conducted in relationship to the evaluation of renal function and muscular metabolism. However, there are several studies in which creatinine has been examined from a pharmacokinetic view point. Some aspects of transport kinetics of creatinine including its intestinal absorption and its *in vitro* membrane permeability through erythrocytes and also the effect of temperature on its flux have been studied previously in this laboratory [358]. Creatinine has also been included in a number of other studies evaluating the Pharmacokinetics of distribution in man and animals. As the results of these studies on distribution properties of creatinine are sometimes in contradiction, the current studies conducted to extends the previous findings and elucidate the pharmacokinetics of creatinine more closely.

6.3.3.1 Volume of distribution

The apparent volume of distribution (V_d) usually has no direct physiological meaning and does not refer to a real volume. However, V_d contains the plasma (blood) volume as a real value and that V_d is related to the permeability of the biological membranes, such as blood capillary membranes to the drug. The apparent volume of distribution cannot take a smaller value than the plasma volume itself, and increases as tissue distribution of drugs increases [359]. In humans and rats the total aqueous space constitutes 60% of body weight; 40% representing the intracellular space and 20% representing the extracellular space. Acidic drugs have relatively low volumes of distribution, and basic drugs have high volumes of distribution [360]. Drugs with larger partition coefficients take the larger V_d values. The apparent partition coefficient value for creatinine in an n-heptane-pH 7.4 phosphate buffer system was estimated to be 2.9×10^{-5} [361]. The initial distribution space is generally conceived to represent drug distribution in the blood and in the tissues that rapidly come into equilibrium with the blood, relative to the sampling times [132].

Although the volume of distribution, V_d, relates amount in body to plasma concentration during the terminal phase, its value is influenced by elimination. The faster a compound is eliminated, the greater is the ratio of drug in slowly equilibrating tissues to that in plasma during the terminal phase and the larger is the volume of distribution. The need to define a volume term to reflect purely distribution has led to the introduction of volume of distribution at steady state, V_{ss}. The value of V_{ss} lies between the initial dilution volume, V_1, and the volume of distribution during the terminal phase, V_d [243]. In general, the difference between the values of V_{ss} and V_d is small. Much depends on the disposition kinetics of the compound. The greater the extent of elimination before distribution equilibrium is achieved, the larger the difference would be. For creatinine, the difference between V_d (156 ml) and V_{ss} (160 ml) is very small because negligible elimination occurs during the distribution phase (Table 6.5 and Figure 6.5).

Another view of distribution at steady state is to consider the ratio of amount in body (A_{ss}) to amount in the initial dilution volume ($A_{ss,1}$). The ratio is V_{ss} / V_1. For creatinine this ratio is approximately 2.5 indicating that at steady state, this compound is nearly equally distributed between the initial dilution volume and the rest of the body.

The body fluid space through which creatinine is distributed has been the subject of some dispute. While some workers believe it is only distributed in extracellular fluid [126,362,363], others state that it is distributed evenly in total aqueous fluid [364,365]. In order to ascertain the distribution characteristics of creatinine, it was necessary to include one reference marker in the study. As sucrose has been extensively used as an extracellular marker in this project and other work and it is available in tritiated form, it was selected as reference. If creatinine is to be distributed into only the extracellular space, its volume of distribution must approximate that of sucrose. For a non-eliminating substance which distributes only into the extracellular space, the steady-state volume of distribution (V_{ss}) should approximate 20% of body weight (80-90 ml for a 400 g rat). This was the case for sucrose with a V_{ss} of 86 ml. The estimated V_{ss} of creatinine was 160 ml (38% body weight) indicating that this compound has been distributed into a larger space than only the extracellular space, but less than the total-aqueous space (60% body weight; 240-280 ml for a 400 g rat). As creatinine has been nearly reached steady state by 60 min (time frame of the experiment) in most tissues (see the next section where tissue distribution of

creatinine is evaluated), it is conceivable that it is distributed into a part, and not all, of the total aqueous space.

The earliest determination of the volume of distribution of creatinine was carried out by Dominguez *et al* [365]. These workers studied the disappearance curve after a single intravenous injection, and estimated the volume of distribution to be 76% of body weight, a value was recognised to be greater than total body water. In the analysis of the disappearance curve, they assumed that with the passage of time, creatinine became homogeneously distributed throughout its entire volume of distribution, that is to say, that the "tissue" creatinine concentration became identical with the "plasma" creatinine concentration after sufficient time had elapsed. This assumption is invalid for two compartment systems.

The average volume of distribution of creatinine in dogs calculated by Greenberg *et al* [366] (by dividing its plasma level at steady-state into the total amount subsequently lost in the urine) was estimated to be 49% of body weight. They stated that this value was significantly larger than that of the extracellular marker (inulin) which averaged 20% of body weight.

Sapirstein *et al* [367] determined the volume of distribution of creatinine in the dog after a single intravenous injection. Mannitol was used as extracellular marker. They assumed that creatinine is distributed between two compartments and moves between the first and second in proportion to the concentration difference between them, while being excreted from the first in proportion to its concentration there. The estimated value of V_d for mannitol was 20%. Initially, creatinine distributed into a volume which corresponded to that of mannitol. However, the final volume of distribution of creatinine varied from 29% to 45% (mean 36%). These workers assumed that the compartments penetrated by creatinine are arranged in series rather than in parallel. Therefore, penetration of the second compartment could only occur by way of the first. This implies that the entire volume of distribution of creatinine becomes homogeneously mixed before the second is significantly penetrated. The V_d of creatinine found by these workers is in close agreement with that of 36-40% found in the current work or that of 33% found by others [367,368,358]. Whether this similarity indicates the existence of a true compartment (presumably including the extracellular and a restricted portion of the intracellular fluid) or is simply a coincidence, is uncertain. Sapirstein [367] also stated that the inter-compartmental clearance is related to the

permeability of the barrier between the two compartments. Since the volume of distribution of the first compartment appears to correspond to the extracellular fluid, it seems likely that inter-compartmental clearance is related to the permeability of the cell surface. However, these models are only used to describe the data and are not representative of actual anatomical spaces.

Edwards [363] found the creatinine volume of distribution to be equivalent to total body water in anuric rabbits and anuric humans. He disputed the claim of Sapirstein, that the creatinine space was similar to the thiocyanate space (extracellular space), stating that it was based on a mathematical analysis, which assumed that creatinine was distributed through only two fluid compartments.

Recently, Pappenheimer [362] calculated V_d for both males and females, with the following results: Females=0.64 L/Kg; Males=0.57 L/Kg. These values compare well with those obtained by Jones and Edwards [363]: Females=0.46 L/Kg; Males=0.62 L/Kg, and Hankins *et al* [370]: Females=0.49 L/Kg; Males=0.51 L/Kg. Goldman [371] has quoted that the average volume of distribution of creatinine is assumed to be 50 L, which is rather large compare to the total volume of body water 42 L. This implies a degree of tissue binding which is not documented in the literature.

Boroujerdi & Mattocks [372] analysed the specific activity data, obtained from both urinary and plasma samples, produced from a single intravenous injection of radiolabelled creatinine to rabbits by several means and found the best fit to be a biexponential equation, thus indicating that a two-compartment body model was required to describe the system. In a separate study, Watanabe [361], suggesting a similar model, stated that compartment 1 represented the blood and rapidly perfused tissues, and compartment 2 the less rapidly perfused tissues, which in this case was thought to be largely the muscle, where high concentrations of creatinine are present. Also, the major source of creatinine is thought to be creatinine phosphate of the muscle, thus indicating that production occurs in compartment 2. Although models are only used to described the data and cannot be used to actually identify specific physiologically recognisable compartments, it may be inferred that creatinine passes into at least some parts of cellular compartments. The extent to which this occurs obviously cannot be determined from a simple model.

A point that should be noted regarding all these reports, is the credibility of creatinine measurement. In most studies, particularly in the past, cold creatinine was being used. which is measured by a colourimetric method. The limited precision and accuracy associated with this method is not compatible with that required for disposition kinetic studies and volume estimations. In recent years, radiolabelled creatinine has become available. The great accuracy and precision associated with the radioanalysis, which was applied in the present work, puts a greater confidence on the results.

6.3.3.2 Distribution in erythrocytes (RBC)

In order to study the diffusion of organic solutes within blood, it is necessary to have an understanding of those factors which have an influence, such as plasma-erythrocyte solute distribution and diffusive transport through the erythrocyte. The diffusion of organic solutes through the erythrocyte membrane is also of fundamental importance in other circumstances such as the performance of artificial kidney [373]. Due to the relative ease of its experimental handling and its general availability, the erythrocyte has been one of the favourite study objects for the study of transport processes. In fact earlier and present plasma membrane models rely to a considerable extent on evidence obtained from the erythrocyte membrane. Most studies on solute transport in red blood cells usually use tracer solutes, which are labelled with ^{14}C. Although there has been no independent confirmation that the tracer permeability, or membrane diffusivity, evaluated in these experiments is equivalent to the permeability of the solute of interest [374]. In the present study the permeability of red cells to creatinine is evaluated. Using both radiolabelled and cold solute, it has been confirmed that the ^{14}C-radiolabelled is equivalent to the permeability of creatinine [358].

The plasma-erythrocyte solute distribution and diffusive transport through the erythrocyte can be described by measuring the solute concentration in both plasma and erythrocytes which is best conducted *in vitro*. However, it is possible to estimate the values of solute concentrations in RBCs from *in vivo* experiments using the following equation:

$$C_{RBC}=\frac{C_{blood}-(0.55\times C_{plasma})}{0.45} \qquad (6.7)$$

The above equation assumes a hematocrit value of 0.45.

As depicted in Figure 6.4, the concentration of creatinine in erythocytes rose fast and reached its maximum at approximately 5 min and declined gradually afterwards. In an *in vitro* experiment, conducted by Bumstead [358] in this laboratory, the time to reach equilibrium for creatinine in human erythocytes was found to be around 50 min. The noticeable difference between the two experiments could be due to two reasons. First, some permeability differences may exist between human and rats erythrocytes. Therefore, it would be beneficial to repeat the *in vitro* experiment using rat erythrocytes. Second, the environment of RBC in an *in vitro* experiment may be different to that *in vivo* conditions. It is possible that in an artificial environment, the permeability of erythocytes membranes, perhaps as a protective response, are reduced. Similar situation has been observed by Skalsky *et al* [264] who showed that the erythrocyte membrane permeability of uraemic cells was significantly lower than that of non-uraemic cells, but that the equilibrium partition coefficient was unaffected. The investigators attributed this decrease in permeability to an alteration in the red cell membrane associated with the uraemia. It has been concluded [141] that as the transport of creatinine across the red blood cell membrane is primarily by passive diffusion through the lipid bilayer, then any alteration in the membrane structure, especially to the lipid content, would affect creatinine transport. Thus the increase in lipid content results in a higher resistance against creatinine diffusion, which is reflected in the observed decrease in permeability. It has been demonstrated [141] that the permeability of uraemic cells could be returned to normal values by incubating the cells in normal plasma for several hours, but not if the cells were incubated in buffer (as was conducted by Bumstead [358]). The mechanism for reversing the effects of uraemia are uncertain, but it is known to be linked to the rapid exchange of lipids and cholesterol between the plasma and the erythrocyte membrane.

It should be noted that creatinine concentrations used in the current experiments were different from those used in the aforementioned *in vitro* experiment. The creatinine flux across the erythrocyte membrane is proportional to the concentration and creatinine is transported by passive diffusion (suggested by the lack of evidence of a saturable [374]. This together with the fact that arterial blood concentrations achieved in these experiments (0.5 mg/dl) were much lower than the range studied in the *in vitro* experiments (2-75 mg/dl) may indicate that plasma concentration has been not high enough to force the creatinine through the erythrocyte membrane. But the concentration of creatinine in plasma was always much greater than that in

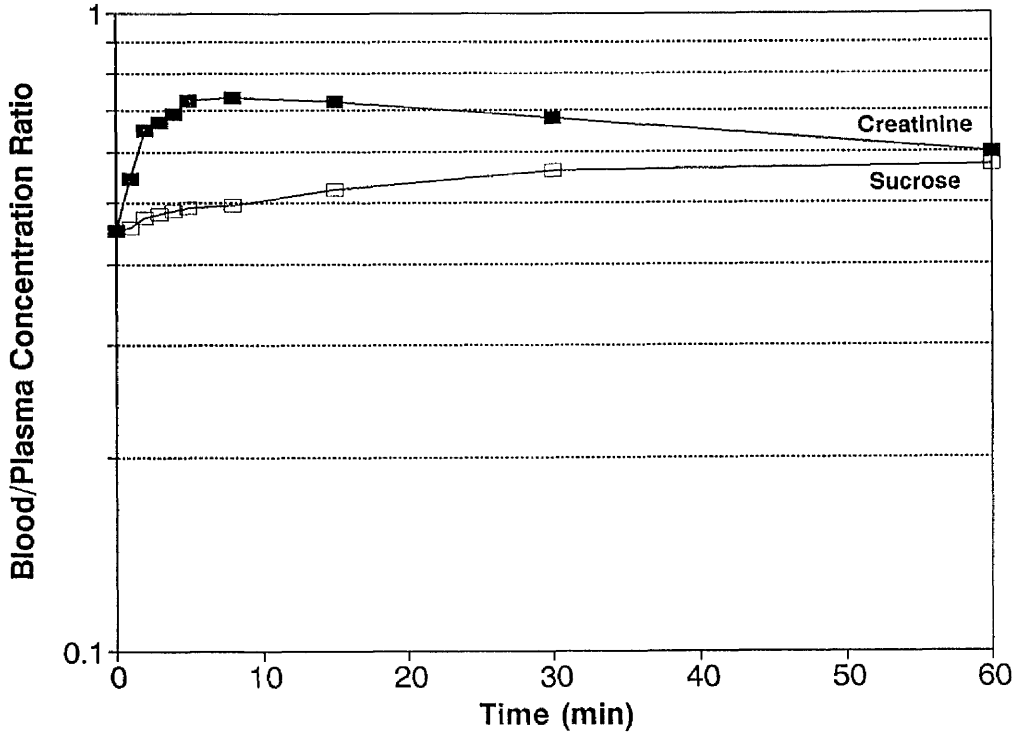

Figure 6.3 Semilogarithmic plot of blood to plasma concentration ratios of creatinine and sucrose after an intravenous bolus dose in rats.

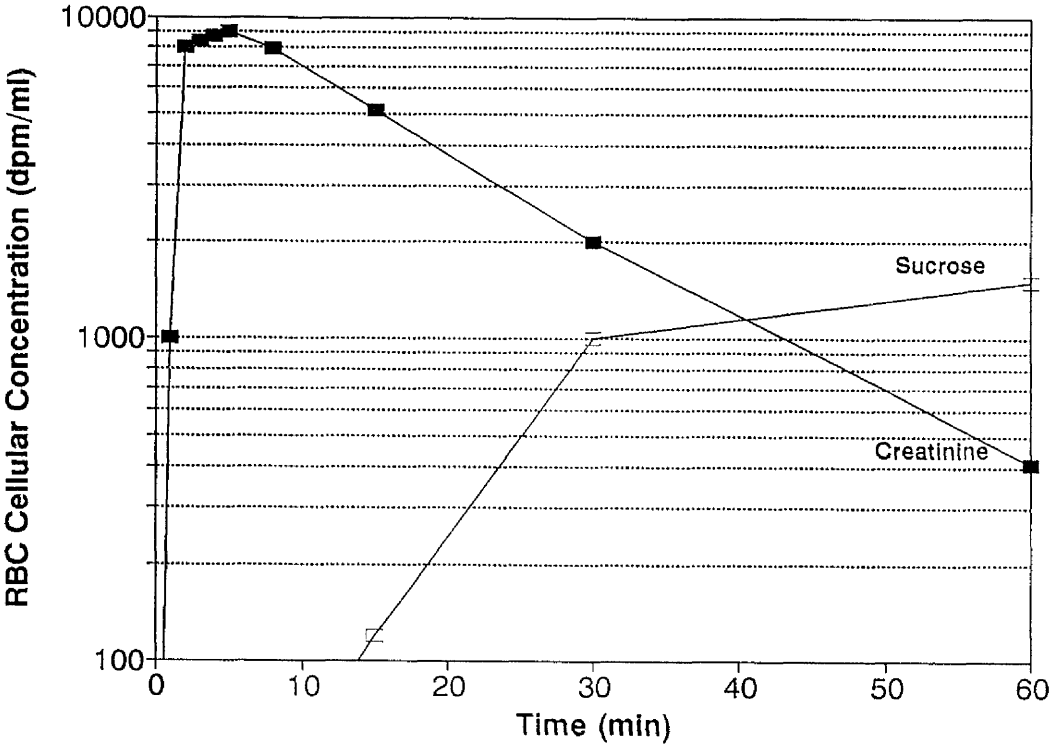

Figure 6.4 Plot of concentration of creatinine and sucrose in erythrocytes after an intravenous bolus dose in rats.

erythocytes implying a strong driving force for creatinine diffusion which is necessary for passive diffusion.

Bumstead [358] established that it is possible for creatinine to enter cells and demonstrated that it traverses the intestinal epithelium *via* the paracellular pathway rather the transcellular pathway. Their findings rejected suggestions by Lansdorf *et al* [375] that creatinine diffuses through the lipid bilayers in erythrocyte membrane. They also demonstrated that there was no significant difference in the bi-directional flux rates, which is as expected for a passively transported solute.

The creatinine flux across erythrocyte membrane is temperature-dependent [358] A relatively small change in temperature (*eg* from 37°C to 15°C) has a dramatic effect on the rate of creatinine transport across red blood cell membrane [358]. Over this temperature range the half-life increases from approximately 10 min to more than three hours, with a corresponding 20-fold decrease in the permeability coefficient. In the present work, blood samples obtained from the animals were immediately cooled so that the diffusion of creatinine between erythrocytes and plasma after blood sampling was effectively stopped. Therefore, blood and plasma profiles reflect the events in blood and plasma *in vivo*.

The equilibrium ratio of a solute concentration in erythrocytes to that in the fluid phase is determined experimentally and is defined as the equilibrium partition coefficient (K_{eq}) in which the solute concentration is based on the entire volume of each phase. In the current study for erythrocytes the K_{eq} value for creatinine was 0.45 (Figure 6.5) which is in general agreement to the values of 0.7 found for erythrocytes suspended in buffer at 37°C and the literature values [358]. The distribution of solute between the erythrocytes and buffer can also be expressed in terms of the water phase equilibrium distribution coefficient, R, in which solute concentration is based on the volume of water in each phase. If the creatinine concentration in cells is corrected for the reduced fraction available for dissolution, the system is in a state of thermodynamic equilibrium and that each phase is inert towards creatinine, *ie* there is no creatinine binding. Assuming that the water content of erythocytes available for dilution is 0.8 [358], the value of R for creatinine is expected to be 0.85 which is close to the value was found in this work (0.7).

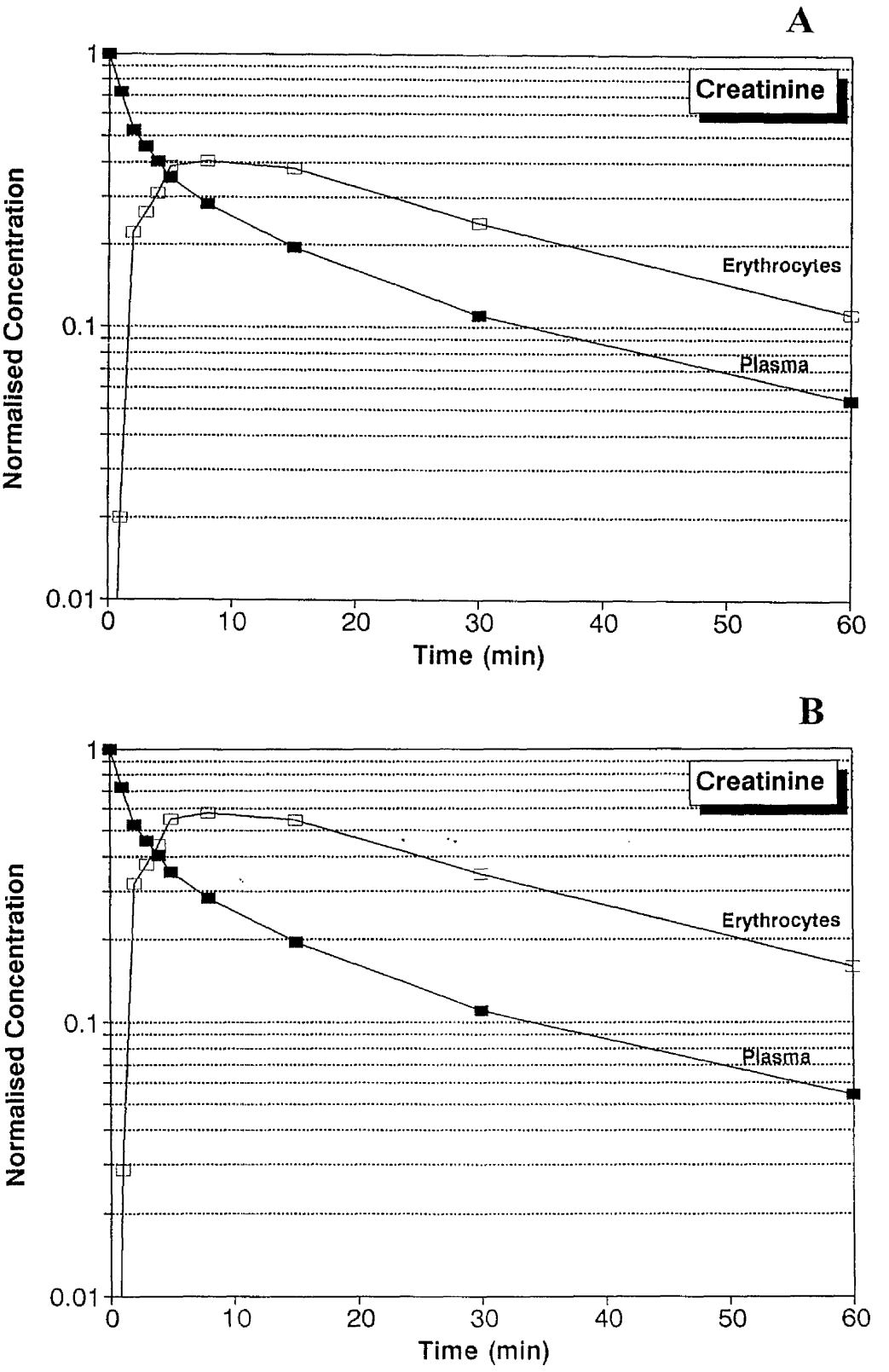

Figure 6.5 Semilogarithmic plots of the ratio of creatinine concentration in erythrocytes to that in plasma after an intravenous bolus dose in rats. Panel A: Plot of the overal concentration (representing Keq); Panel B: Plot of the concentrations corrected for water content of the erythrocytes (representing R).

The erythrocyte studies in this project and those performed by Bumstead [358] demonstrated that creatinine can traverse erythrocyte membrane. Despite the fact that the volume fraction of water in the cells was taken into consideration, the concentration in both compartments were not equal at equilibrium, suggesting that creatinine does not distributes into total available aqueous space.

Taking into account the inter-subject variability in erythrocytes and experimental error, the equilibration of creatinine between the erythocytes and the suspending medium follows the kinetics expected for a single exponential [264,358]. The mean permeability coefficient value reported by Bumstead [358] was 9.6×10^{-7} cm/min at 37°C. No correlation was found between the permeability coefficient and initial concentration, suggesting that permeability is concentration independent. Skalsky *et al* [264] demonstrated that there was a significant inter- and intra-subject variability in creatinine transfer rates across normal human erythrocytes. The influx rate for creatinine through the erythrocytes is relatively slow compare with the permeability values of other solutes such as urea (0.0252 cm/min), tritiated water (0.59 cm/min) and glucose (9×10^{-6} cm/min [358].

The difference between kinetic profiles of sucrose and creatinine in erythrocytes is noteworthy. The concentration of sucrose in erythrocytes did not attain equilibrium by 60 min. This difference in diffusional properties of the two molecules can be explained by their different chemical structures. Creatinine is an linear inert small molecule (MW=113) which can easily traverse through intercellular routes in erythrocyte membrane an achieve equilibrium quickly. In contrast, sucrose is a larger molecule (MW=330; includes two aromatic rings). Therefore, compared to creatinine, it traverse the membrane with difficulty and reaches equilibrium at a latter time. The difference in the diffusional properties of the two compounds in blood has been stressed in Figures 6.3 to 6.6. Blood to plasma concentration ratio of creatinine reached its maximum around 5 min whereas that of sucrose continued to rise and did not reach the climax by 60 min.

After intravenous administration, the fraction of dose in blood and fraction of dose eliminated for creatinine and sucrose at each time point were estimated using the following equations [243]:

$$\text{Fraction of dose in blood} = \frac{\text{blood concentration} \times \text{ total blood volume}}{\text{Dose}} \quad (6.8)$$

$$\text{Fraction of dose eliminated} = f_1[1-e^{-\lambda_1 t}] + f_2[1-e^{-\lambda_2 t}] \quad (6.9)$$

$$\text{where } f_1 = \frac{\frac{C_1}{\lambda_1}}{(\frac{C_1}{\lambda_1} + \frac{C_2}{\lambda_2})} \text{ and } f_2 = \frac{\frac{C_2}{\lambda_2}}{(\frac{C_1}{\lambda_1} + \frac{C_2}{\lambda_2})} \quad (6.10)$$

Respective values are listed in Table 6.5 and displayed in Figure 6.6. Although the profiles of cumulative amount eliminated for creatinine and sucrose were similar, at time=60 min a greater fraction of administered creatinine (0.82) was eliminated compared to sucrose (0.62). At time=1 min, a larger fraction of sucrose remained in blood (0.49) compared to creatinine (0.33). As represented in Table 6.5, at time=60 min, it appeared that compared to creatinine, a larger fraction of sucrose remained in tissues. Considering the distribution properties of sucrose, this was unexpected. This issue is further discussed subsequently. The results indicated that at time=1, the ratio of blood to plasma for sucrose approximated the hematocrit value (~0.45) while that of creatinine was greater than the hemetocrit value (~0.52). This was another indication of the rapid influx of creatinine and slow influx of sucrose into the erythrocytes.

Table 6.5

Fraction of the dose of creatinine and sucrose in blood and tissues and fraction eliminated at each time point after an i.v. bolus in rats (n=3).

Time	Fraction in Blood		Fraction in Tissues		Fraction Eliminated	
	Creatinine	Sucrose	Creatinine	Sucrose	Creatinine	Sucrose
1	0.331	0.493	0.596	0.445	0.072	0.041
2	0.281	0.389	0.559	0.517	0.131	0.071
3	0.254	0.339	0.541	0.547	0.172	0.097
4	0.231	0.302	0.522	0.583	0.208	0.119
5	0.211	0.261	0.498	0.615	0.254	0.136
8	0.162	0.216	0.471	0.609	0.328	0.175
15	0.118	0.182	0.388	0.541	0.465	0.261
30	0.061	0.134	0.291	0.425	0.648	0.419
60	0.026	0.101	0.168	0.218	0.821	0.625

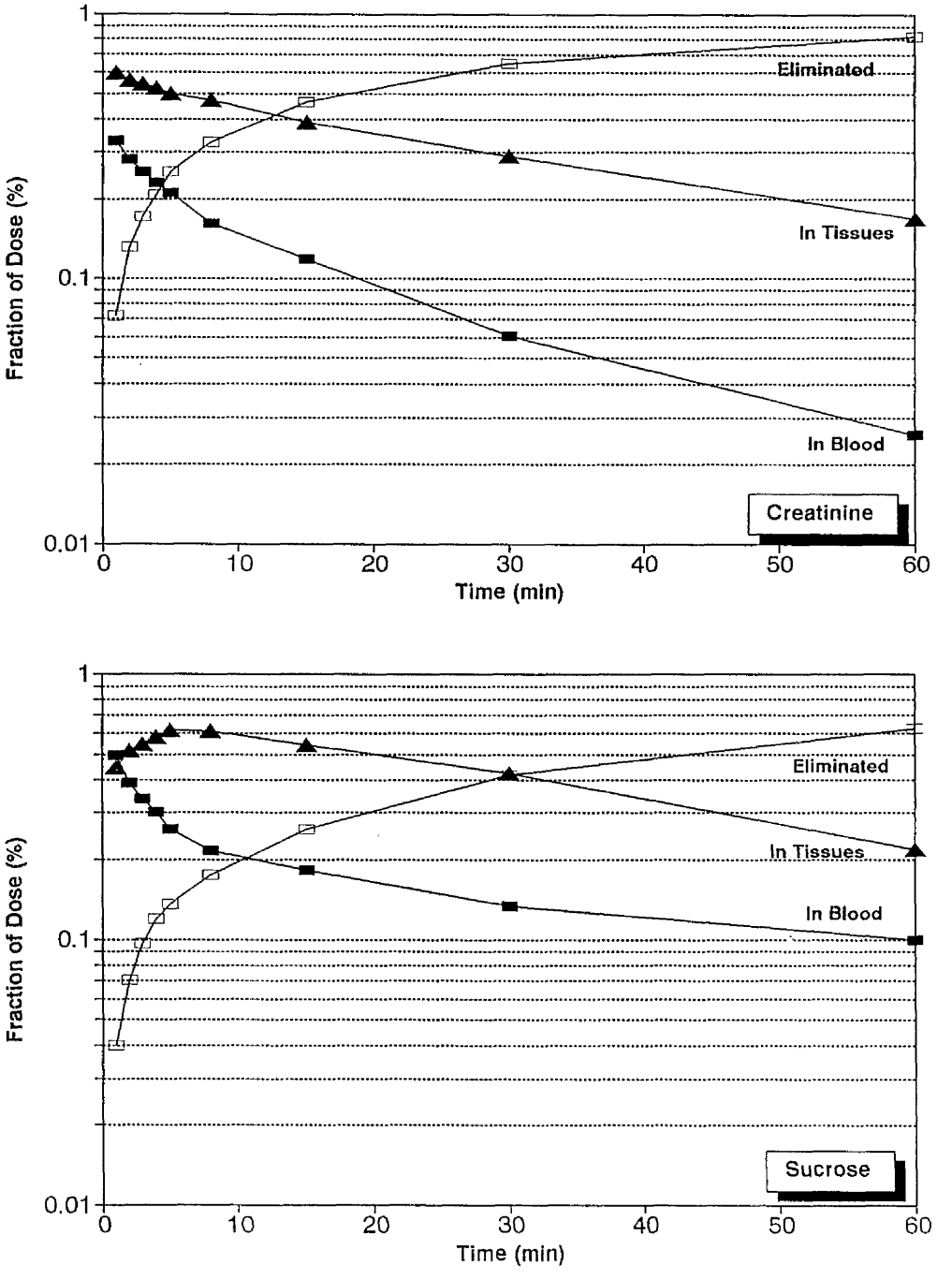

Figure 6.6 Plots of fraction of dose eliminated or remaining in tissues and blood for creatinine and sucrose after intravenous bolus administration in rats.

6.4 Events Viewed from Tissues

6.4.1 Data Analysis

The amount (A) of labelled creatinine and sucrose in each tissue was estimated using the following relationships.

Amount in g tissue =

$$\frac{\text{count}_{(\text{dpm})} \text{ per g Tissue} - (\text{fraction of blood in Tissue} \times C_{\text{blood}})}{1 - \text{fraction of blood in Tissue}} \qquad (6.11)$$

$$\text{Total amount in tissue } (A_T) = \text{Amount in g tissue} \times \text{Total Tissue Weight}_{(\text{excluding blood})} \qquad (6.12)$$

The physiological literature values in Table 6.6 were used for the estimation of total amount in tissues and other parameters.

6.4.2 Results and Discussion

The temporal profiles for creatinine in 12 tissues are presented in Figure 6.7. In well-perfused tissues such as liver, lung and spleen, while the initial concentration was high, the concentration decayed rapidly with time. Other tissues such as adipose, testes and brain showed a slower rise in concentration and a lower maximum value. The fall in creatinine tissue concentration after 15 min indicated that creatinine achieved equilibrium in all tissues fairly quickly. For sucrose, although the rise in tissue concentration was fast, the time needed to reach equilibrium was noticeably longer than for creatinine (Figure 6.8). Although the sucrose concentration in none of the tissues had fallen by 60 min (except kidney), most of the tissues were close to achieving an equilibrium. The Simulation studies demonstrated that for a two-compartmental system with elimination occurring from the central compartment, the final slope of decline in concentration of solute in tissues is in parallel to the decline in plasma concentration and this was clearly demonstrated for creatinine in these experiments (Figure 6.6). Plot of the ratio of concentration of materials in tissue to that in plasma provides an opportunity to compare the temporal tissue profiles in all the tissues. Simulation studies demonstrated that for the two-compartmental system with elimination used, as the fall in plasma and tissue concentration becomes eventually parallel, the ratio of tissue-to-plasma concentrations approaches a plateau. Plots of this ratio for various tissues have been demonstrated in Figures 6.9 and 6.10.

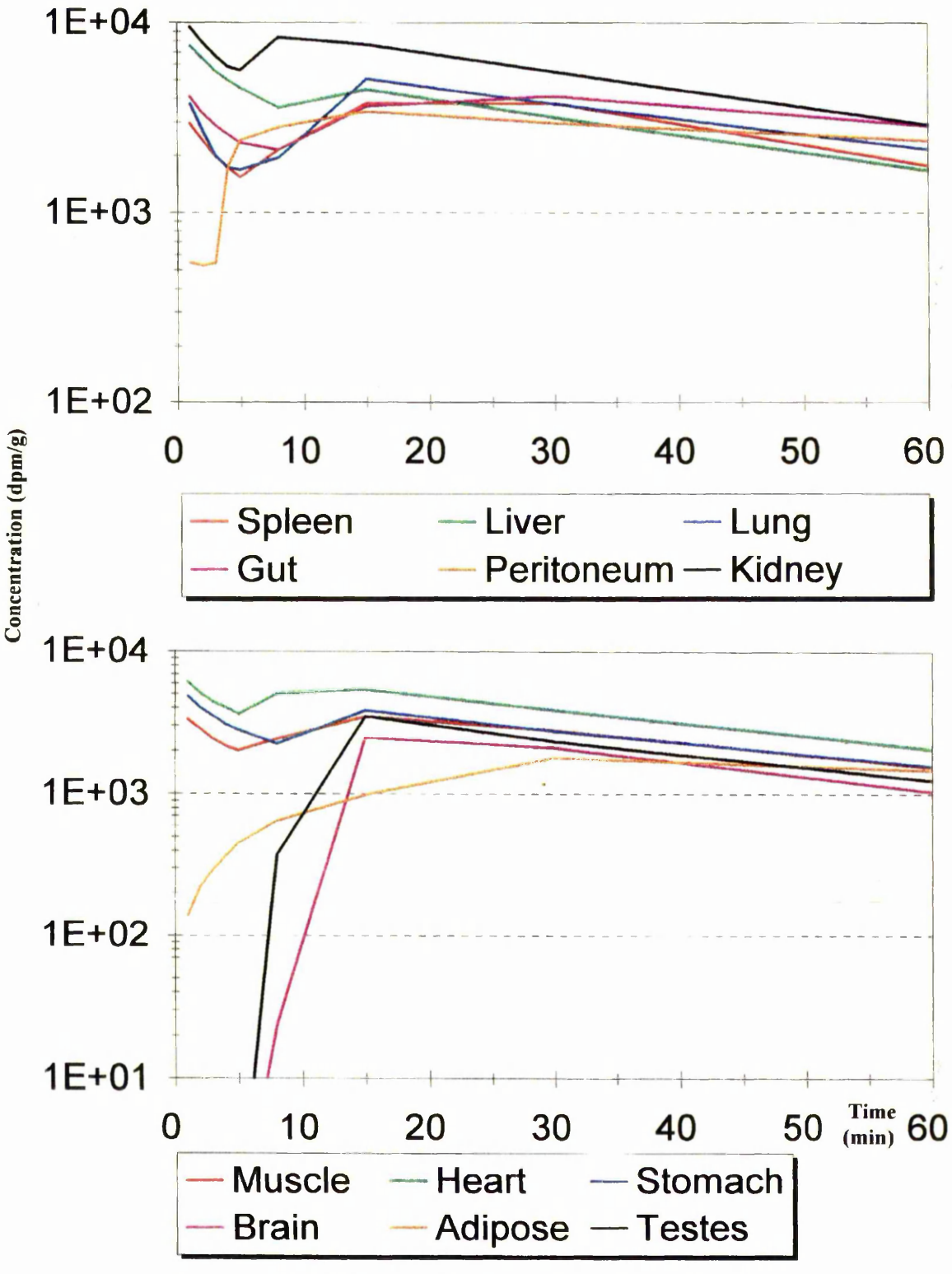

Figure 6.7 Creatinine concentration in tissues.
(mean values, n=3)

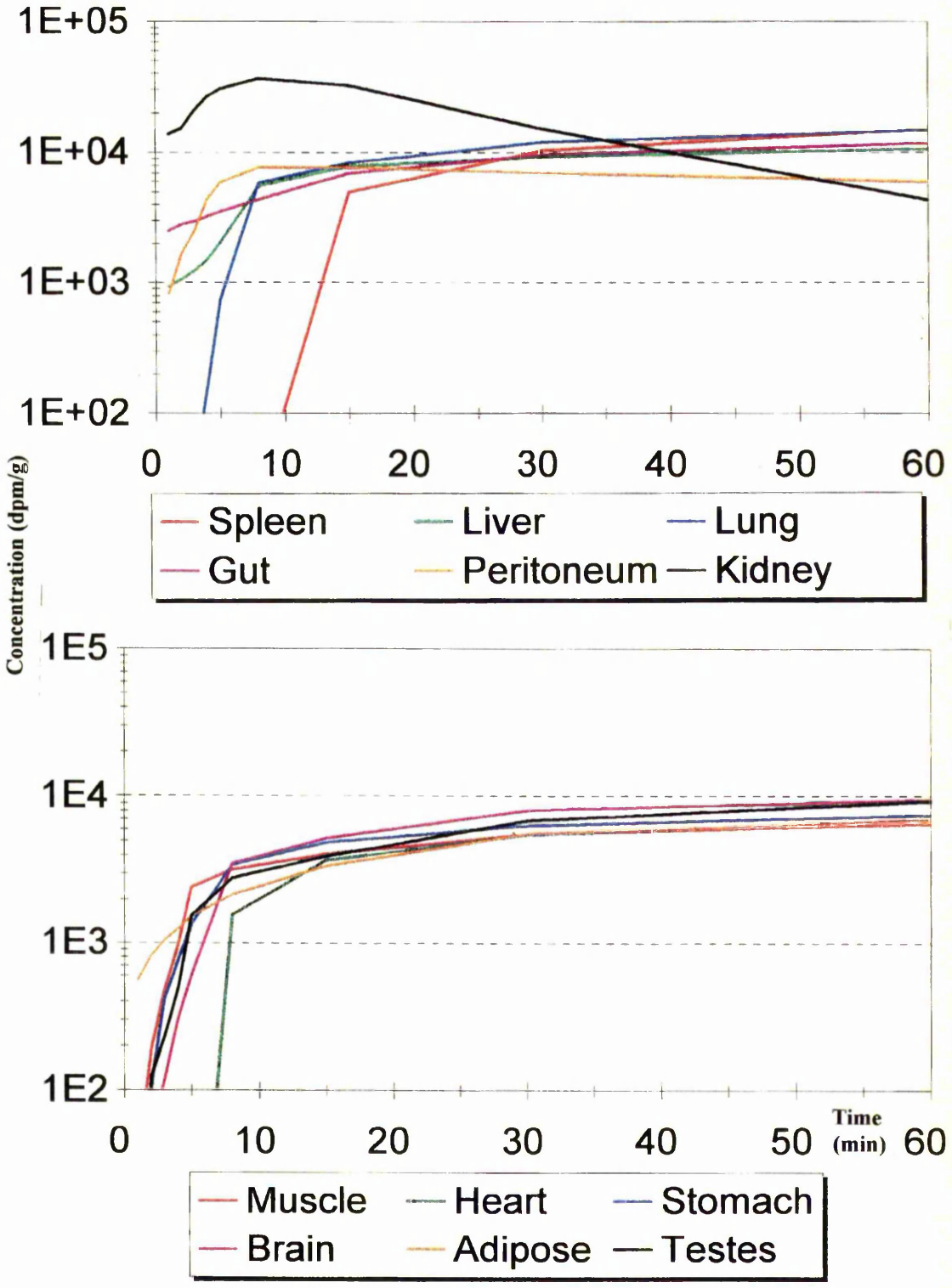

Figure 6.8 Sucrose concentration in tissues.
(mean values, n=3)

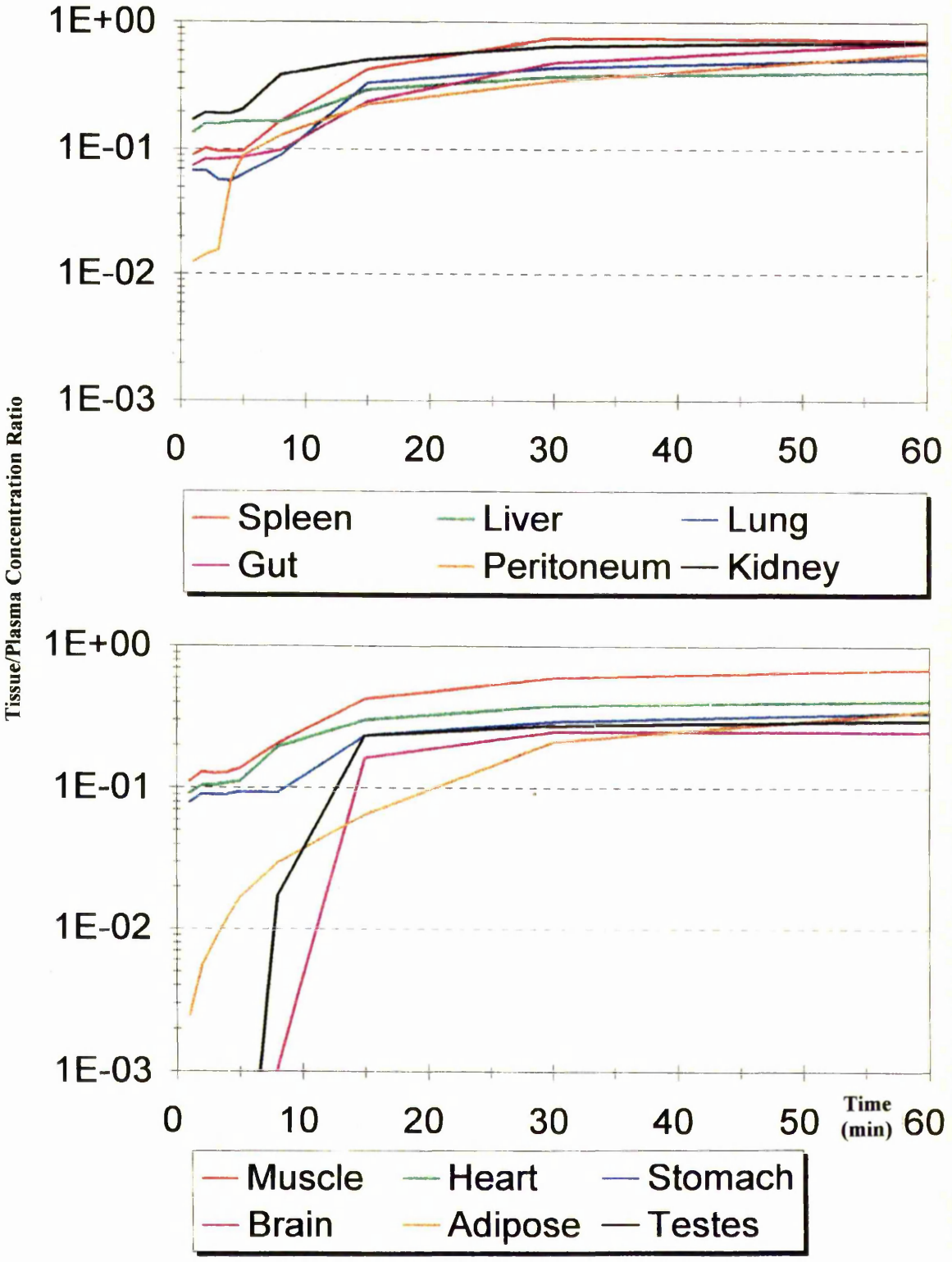

Figure 6.9 Plots of the ratio of creatinine concentration in tissues to that in plasma.

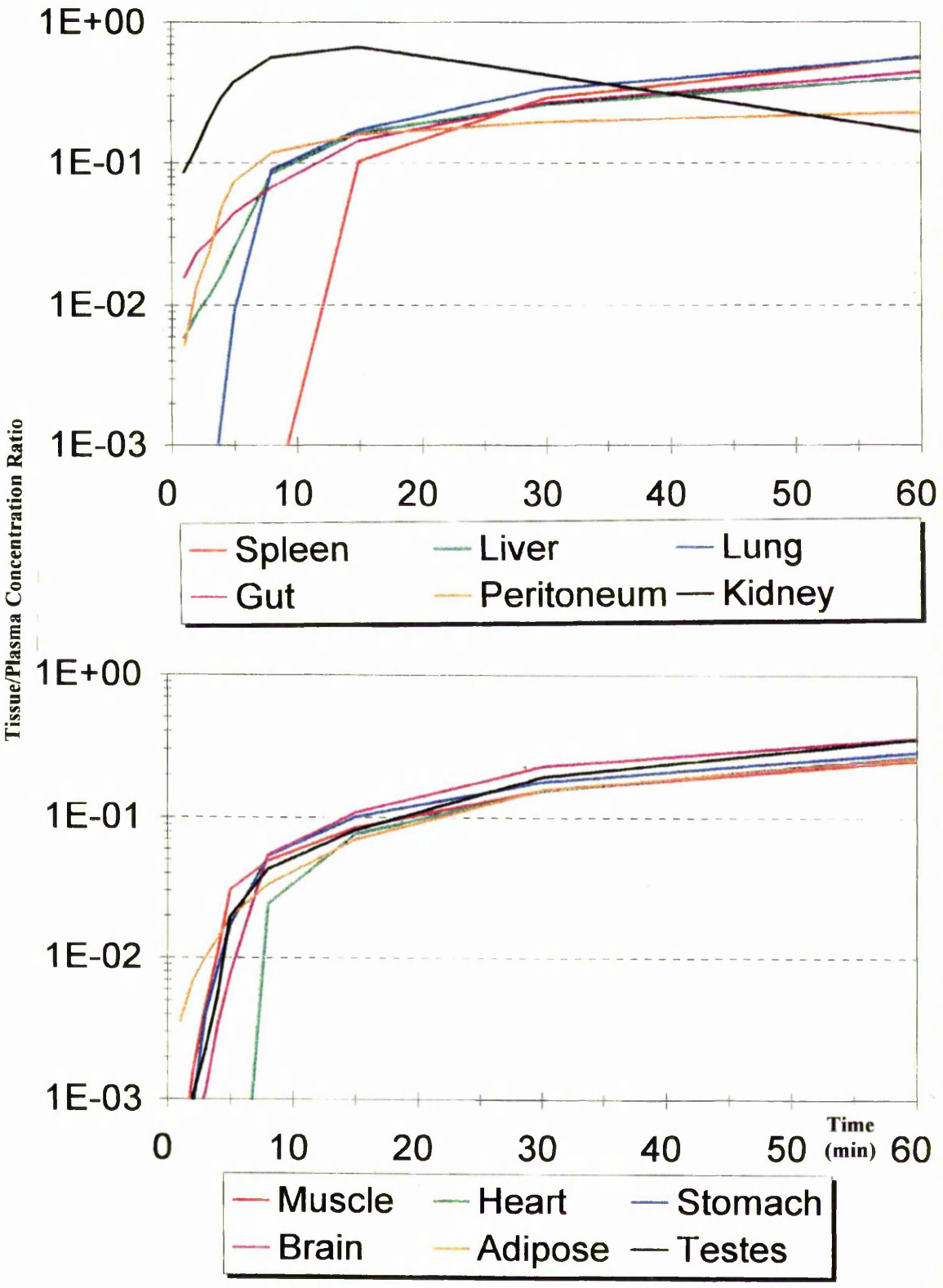

Figure 6.10 Plots of the ratio of sucrose concentration in tissues to that in plasma.

It was also possible to estimate the amount of each compound in cells using the following equation:

$$\text{Amount in cell} = A_T - (\text{fraction of interstitial volume in tissue} \times C_{plasma}) \qquad (6.13)$$

The temporal profiles of creatinine cellular concentrations are depicted in Figure 6.11. The concentration in cells in all tissues, after a considerable delay (~3-10 min) rose rapidly to a peak and then fall gradually. As for the plot of tissue concentrations, the delay for rise in cellular concentration for adipose tissue was longer (~20 min). Given the poor perfusion of adipose tissue, this observation was not surprising. For sucrose, several differences were observed in the cellular concentration profiles (Figure 6.12). First, the lag times for the appearance of sucrose in cells not only were longer compared to creatinine, more variation was observed amongst the various tissues (~5-30 min). Second, by the end-point time of the experiment (60 min) the sucrose cellular concentrations were not quite at equilibrium.

In creatinine tissue concentration profiles, apart from the large initial concentration, another peak concentration is observed. Comparison between tissue profiles and cellular profiles reveals that the large initial concentration stems from creatinine concentration in plasma perfusing the extra-cellular space of the tissues, which is high at earlier times. The second peak is due to the rise in creatinine cellular concentration. Comparison between tissue and cellular concentration profiles of creatinine with those of sucrose, where tissue profiles lack the early peak, indicates that creatinine was able to traverse the vascular membranes fairly rapidly whereas sucrose passage through vascular membranes took place with difficulty. Therefore, the permeability barrier for creatinine is located at the cellular membrane which is expected from an inert small molecule. For sucrose, however, the data indicate that in some tissues a barrier may be present at vascular membrane. Similar behaviour have been observed previously in capillaries with poor permeability to sucrose such as the coronary circulation in the dog [236]. In this capillary system there is a non-linear dissociation of sucrose molecules and even large molecules such as albumin because sucrose molecules cross the capillary membrane in a barrier-limited manner to diffuse in the extra-vascular space. Thus, when sucrose molecules reach the outflow they emerge at a latter time than albumin. This situation may be likened to the extensive capillarisation of sinusoids in hepatic cirrhosis (Chapter 4) which renders diffusion of sucrose barrier-limited.

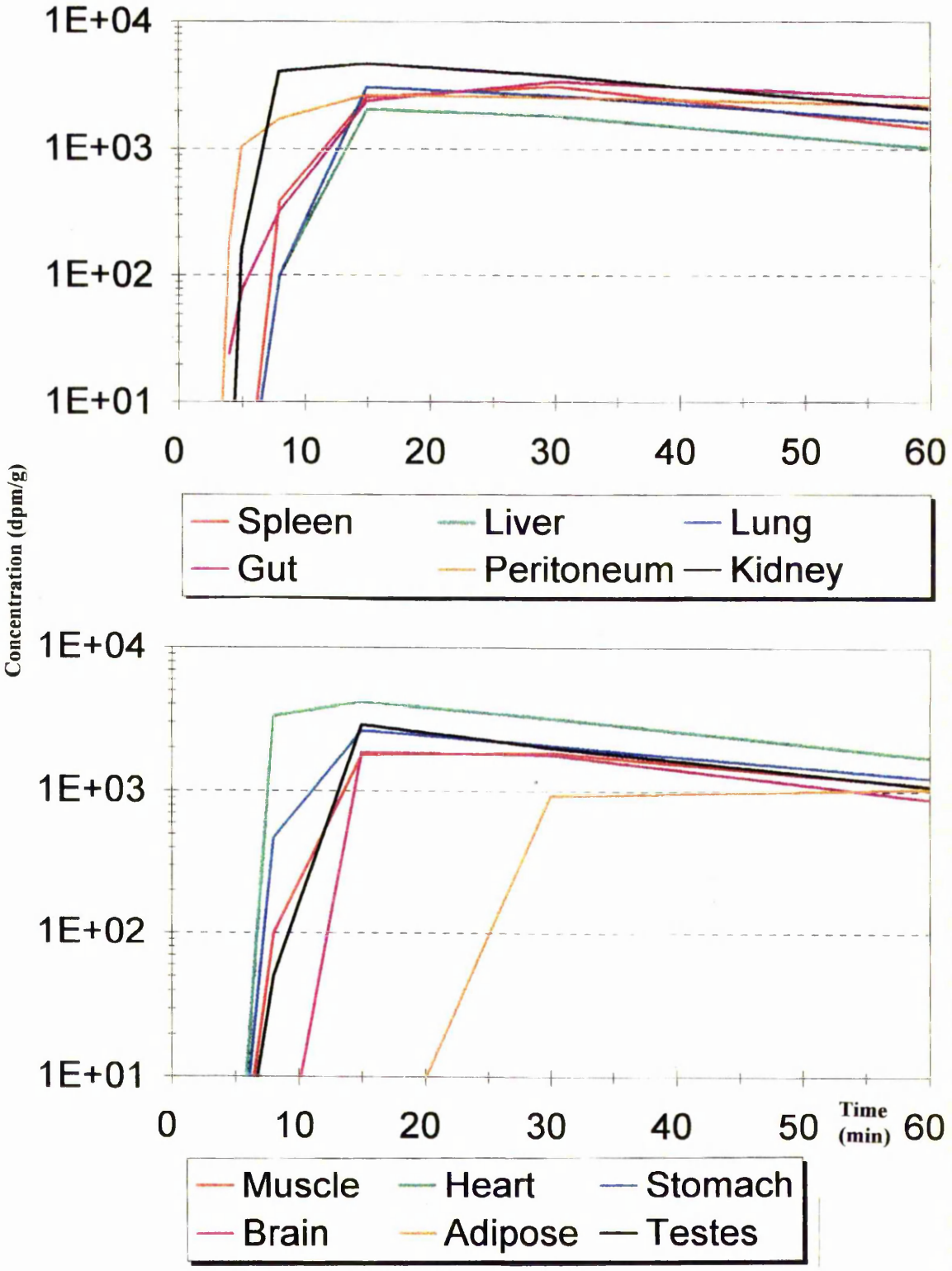

Figure 6.11 Creatinine concentration in tissue cells. (mean values, n=3)

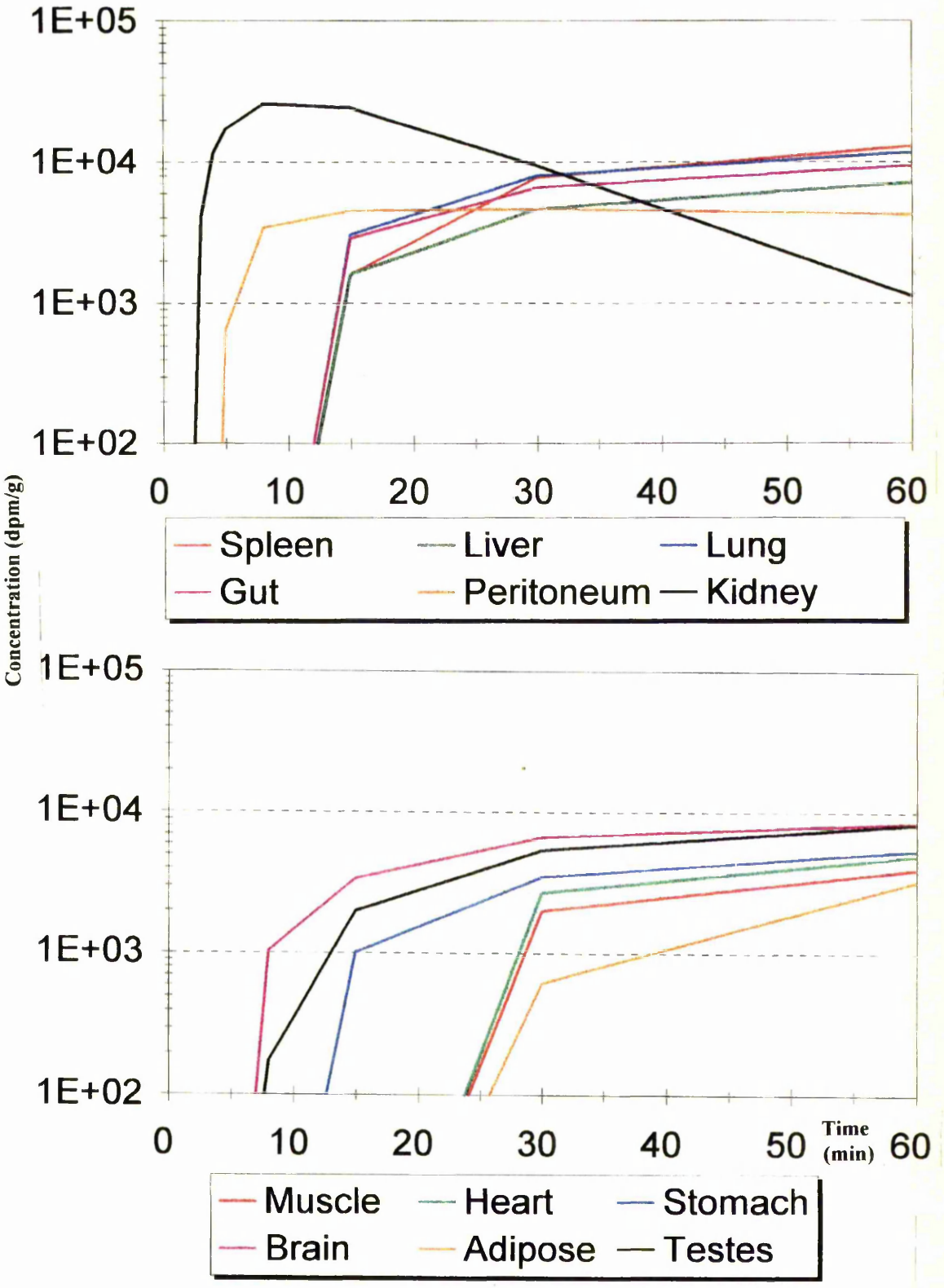

Figure 6.12 Sucrose concentration in tissue cells.

(mean values, n=3)

6.4.2.1 Estimation of equilibrium distribution ratio

The equilibrium distribution ratio, K_p, and volume of distribution at steady state (blood), V_{ss}, and the distribution rate constant, k_T, were calculated using moment analysis:

$$K_p = \frac{AUC_T}{AUC_P} \tag{6.14}$$

$$V_{b,ss} = \sum K_{p,b} \cdot V_T + V_b \tag{6.15}$$

$$k_T = \frac{Q_T / V_T}{K_p} \tag{6.16}$$

in which AUC_T, AUC_P, V_T, V_b, and Q_T are the area under tissue concentration curve, the area under plasma concentration curve, volume of tissue, blood volume, and blood flow perfusing the tissue, respectively.

The above equations assume that tissue and cellular profiles have reached a plateau (equilibrium). For creatinine, as demonstrated in Figures 6.13, where the ratios of tissue and cellular concentrations to plasma concentrations are depicted, the ratios reached a plateau for all tissues by 30 min. For sucrose, in several tissues, as the ratios did not completely reached the plateau by 60 min (Figure 6.14), the ratio at the last time was used to give an estimate of K_p. The values of K_p, $V_{b,ss}$, and K_T of creatinine and sucrose for various tissues are presented in Table 6.7. In each tissue, the K_p values of sucrose approximated the value of interstitial space in that tissue. In all tissues, the K_p values of creatinine are greater than those of sucrose indicating the entrance of creatinine into the cells.

The rate of drug uptake into the tissues depends on several parameters, including the rate of tissue perfusion with blood, the mass of tissue, and the partition characteristics of the compound between blood and tissue. The latter involves such factors as membrane permeability, intra and extracellular pH, and plasma and tissue drug binding [132]. From the physicochemical properties of creatinine and sucrose described before, it was expected that sucrose could achieve equilibrium sooner than creatinine, yet the time to reach plateau occurred much latter. The continuous rise in tissue and cell concentrations of sucrose, even after 30 min, is surprising. For a solute which distributes only in extra-cellular fluids, the equilibrium in an *in vivo* animal experiment is usually achieved within 30 min, as has been shown for inulin [358]. Recall that radiolabelled

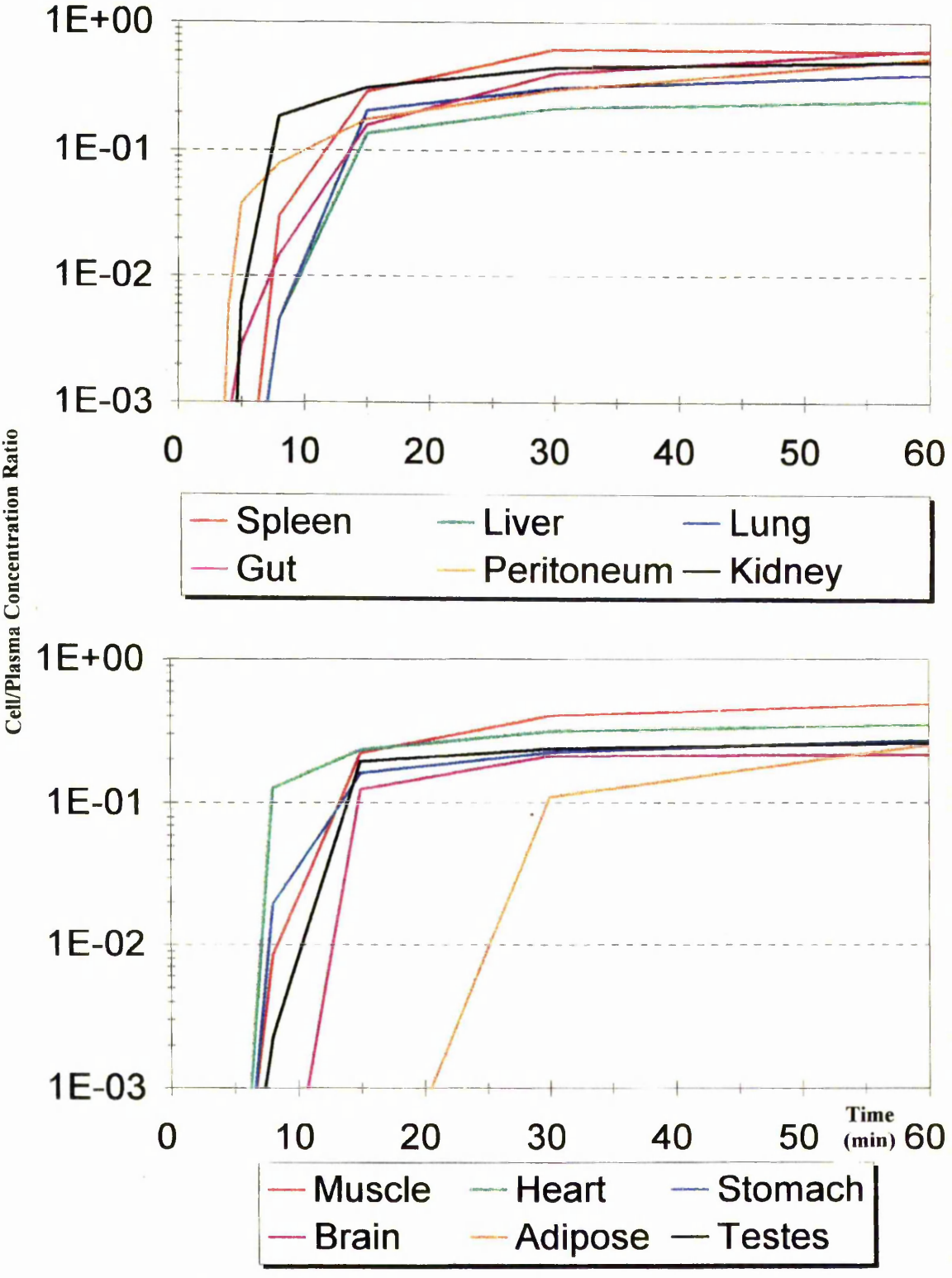

Figure 6.13 Plots of the ratio of creatinine concentration in tissue cells to that in plasma.

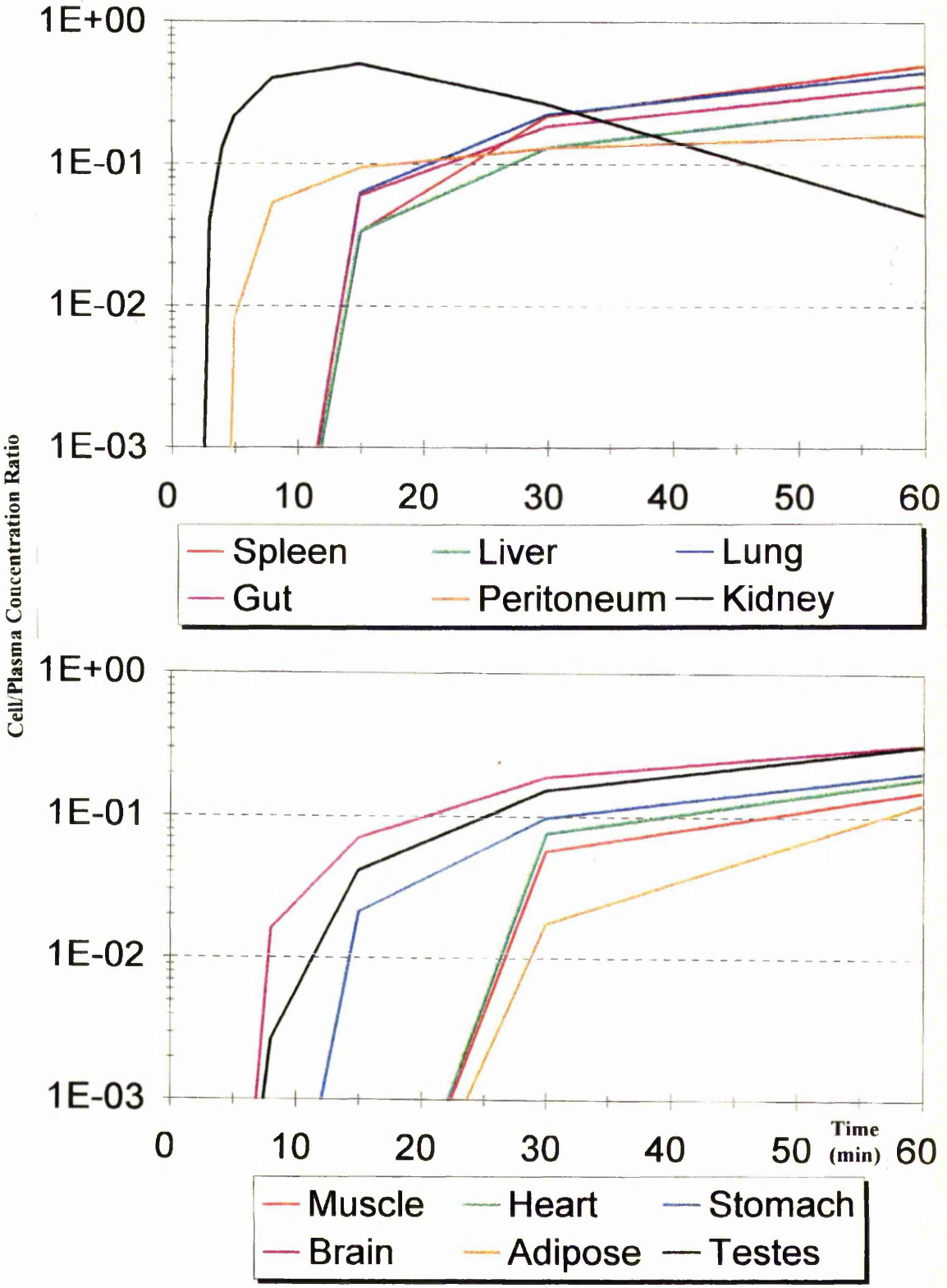

Figure 6.14 Plots of the ratio of sucrose concentration in tissue cells to that in plasma.

sucrose was used in the current experiments. Sucrose is a disaccharide comprising of two molecule glucoses. ^{14}C-atoms are situated on glucose molecules. There is strong evidence that when sucrose is administered intravenously in rats, it is metabolised in a time-related manner [377]. This metabolism most probable occurs at the brush borders in kidneys' proximal tubules, so that the glucose molecules produced are reabsorbed very quickly [378] and through the general circulation reaches the cells. This is the reason for a longer lag time and steeper rise in the concentration profiles of sucrose in tissues and cells.

The current findings that creatinine enters the cellular space of all tissues studied is contrary to the claim that creatinine does not diffuse through the cells [362,369]. However, these findings also contradict the findings of some other workers who described a volume of distribution equal to total aqueous space for creatinine [365]. In experiments conducted by Bumstead *et al* [358] in this laboratory, the mechanism by which creatinine passes the cellular membranes was investigated. It has been concluded that creatinine traverses the membranes through intercellular pathways and that no significant transcellular route for intestinal absorption of creatinine exists [358]. In conclusion, creatinine is able to enter cells and distribute into a considerable proportion of total aqueous space. Compare to sucrose, less variation is observed for the distribution of creatinine between different tissue.

6.4.2.2 Notes on experimental procedures

6.4.2.2.1 Sampling times: In the plan of the experiments, it was anticipated that the time for creatinine and sucrose to reach distribution equilibrium would vary between body tissues. It was therefore crucial to choose tissue sampling times that would allow the study of its distribution into both highly and poorly perfused tissues *in vivo*. The results indicated that such a optimum sampling times were chosen in this study.

6.4.2.2.2 Method of sacrifice: A quick method of sacrifice is essential to prevent further distribution of drug so that results collected reflect events at the sampling time. Exsanguination *via* the carotid artery takes approximately 3 minutes, making this procedure more applicable to steady state experiments [27]; it is unsuitable for kinetic tissue distribution studies due to the time

lag involved. Decapitation, although a quick method, is undesirable and eventually cervical dislocation was chosen as the method of sacrifice as it is quick and clean.

6.4.2.2.3 The administered dose: It was decided to administer to each rat a double-component mixture containing creatinine and sucrose. This should reduce the inter-rat variability and therefore improve the probability of detecting real differences in the Pharmacokinetics between the model compound and the reference substance. The associated number of sample assays required per investigation can also be reduced. The complexity of the assay is increased, however, as two different radionucleotides need to be assayed for each tissue sample at the same time.

6.4.2.2.4 Calculation of creatinine: The initial assumption made was that creatinine does not bind to plasma and tissue proteins and is freely distributed throughout the body fluids, with a volume of distribution of 60% of body weight. Thus for a 400-g rat its volume of distribution would be 240 ml. The minimum plasma concentration that could be reliably measured was considered to be 1000 dpm/250 µl. The time span of the whole *in vivo* experiment was assumed to be 1 hr. Thus, for the creatinine having an elimination half-life of ~20 min, in order to reach the concentration of 1000 dpm/250 µl within 1 hour, its bolus dose should be ~ 15 µCi. After a pilot plan experiment, the calculated dose proved to be satisfactory.

6.4.2.2.5 Calculation of sucrose: Sucrose is restricted to extracellular fluids, with a volume of distribution of approximately of 20% of body weight. This corresponds to 80 ml for a 400 g rat The minimum sucrose plasma concentration was chosen to be 1000 dpm/250 µl. With an elimination half-life of ~40 min, after 1 hr, the initial bolus dose had to be 8 µCi to produce such a minimum count. However, in order to minimise the error in measurement of ^{3}H due to energy overlap of the ^{14}C in the ^{3}H window, the amount of ^{3}H radiolabelled material should be at least 3 times higher than the amount of ^{14}C substances. For this reason, although the dose of sucrose was theoretically correct, it was increased to provide a reasonable count at later times.

6.4.2.2.6 Correction for blood drug content: ^{51}Cr-labelled erythrocytes (20 µCi, suspended in 0.5 ml normal saline; Section 3.3.7), were administered *via* the jugular vein to 4 rats. After 20 min, the rats were sacrificed by cervical dislocation and the tissues excised All dissected organs were

lightly rinsed with sodium chloride (0.9%) and dried. Systemic blood was collected *via* the carotid artery, into heparinised tubes, immediately prior to sacrifice. The volume of blood remaining in each tissue, expressed as grams of μl blood/g tissue, was calculated as the ratio between the measured activity dpm/g tissue and dpm/g blood. Values were converted into ml of blood/g tissue using 1.05 g/ml as the density of blood [22]. The residual drug in blood was subtracted from determined samples and a correction for blood volume was made, using values obtained above. There was a good agreement between values so obtained and literature values (Table 6.6).

Table 6.6 Blood volumes in various tissues in rat.

Tissue	Blood volume (μl/g)	
	This study (400g rat)	Literature (250g rat)
Adipose*	4	1-4
Brain*	22	17-24
Gut*	22	12.5-25
Heart*	180	61-300
Kidney*	90	66-100
Liver**	120	100-115
Lung**	250	220-260
Muscle*	7	7.2-25
Skin*	8	7.1
Spleen**	260	282-336
Stomach*	19	13-25
Testes*	12	6-34

* 22, 27
** Pharmaceutical Research, 1993-1994

CHAPTER SEVEN: STUDIES WITH CREATININE

Section Two: Studies in Isolated Perfused Rat Liver

7.1 Introduction

In contrast to other organs where the capillary can present a substantial barrier between the vascular and interstitial space, the hepatic capillaries possess open fenestrae. Therefore, free exchange of fluid and solute between blood and the space of Disse indicates that the first barrier encountered by a substance entering the liver is the hepatocyte membrane [313]. For lipophilic compounds, as membrane permeability is high enough to ensure rapid exchange between vascular and cellular compartments, the distribution is perfusion rate-limited. However, when the hepatocyte membrane may form an effective barrier to hydrophilic and large molecules, the distribution may become permeability rate-limited [243].

In the previous chapter, the distribution kinetics of creatinine *in vivo* was evaluated. This and other work [358] demonstrated that creatinine traverses cellular membrane and enters the cells in a permeability-limited fashion. However, the value of membrane permeability of creatinine could not be determined from such *in vivo* experiments. The *in situ* perfused liver provides an opportunity to evaluate the permeability of a cellular membrane to creatinine in an intact organ system. Originally, an impulse-response experiment alone was designed. However, for the following reasons it was decided to perform a set of steady-state experiments in the same liver preparations and study the events after stopping continuous infusion. First, it was anticipated that output profiles obtained in impulse-response mode alone would not be enough to fully evaluate the disposition kinetics of creatinine in the liver. Second, simultaneous analysis of the outflow data from bolus (calculation of DN) and steady-state (measurement of permeability) experiments would allow to achieve a greater confidence on the estimation of both permeability and dispersion.

7.2 Methods

7.2.1 *In situ* perfused liver preparations

The *in situ* perfused rat liver preparations were obtained as described in Section 3.3.2. Briefly, a group of 5 male Sprague-Dawley rats weighing 360±20 g were anaesthetised and the hepatic vein, bile duct and vena cava were cannulated. These preparations were then used for both impulse-response and steady-state experiments.

7.2.2 Impulse-response Experiments

The liver was perfused with Krebs-Henseleit buffer (pH 7.4, 37°C). After stabilisation period of 20 min, the flow rate was checked and a 50 µl sample containing 0.1 µCi ^{14}C-creatinine and 0.3 µCi ^{3}H-sucrose was rapidly injected into the hepatic portal vein and samples collected from the outflow cannula into a carousel. Initially, samples were collected every two seconds for 2 min, then every 30 sec for a further 2 min (collection time 5 sec), and a final sample collected 5 min after the injection was made (collection time 5 sec). A 200 µl aliquot from each sample was measured using a dual channel ^{3}H/^{14}C counting program (see Section 3.3.6).

7.2.3 Steady-state Experiments

After the bolus experiment, creatinine was infused into the stream perfusing the liver at the constant rate of 0.1µCi per min for 20 min using a motor-driven syringe. Samples were collected from the outflow cannula during the last 5 min of the infusion and after stopping the infusion, initially into a carousel (collected every second for 60 min) and then into the test tubes for a further 8 min (collection time 5 sec). At the end of the experiment, the flow rate was determined to ensure consistency and then the liver was immediately excised and weighed. A 200 µl aliquot from each sample was measured radiochemically (Section 3.3.6).

7.3 Data analysis

7.3.1 Impulse-response Experiments

In order to compare the outflow profiles for creatinine and sucrose, the outflow activity (dpm) were expressed as a fraction of the dose (fractional output, per ml). Statistical moment analysis (Equations 2.1-2.8) was used to calculate the area under the output activity versus time (AUC), mean transit time (MTT), relative dispersion (CV^2) and hepatic volume of distribution (V_H) of radiolabelled creatinine and sucrose. The one- and two-compartment dispersion models

(Equations 2.10-2.20), allowing for the correction of tubing effect, were fitted to the frequency output of sucrose and creatinine, respectively, and the kinetic parameters including k_{12}, k_{21}, and D_N were subsequently calculated.

7.3.2 Steady-state Experiments

The outflow concentration at steady state (C_{SS}) and after stopping the infusion was normalised for C_{SS}. The two-compartment dispersion model (Equation 7.1) was fitted to the hepatic output profiles of creatinine after stopping infusion and the relevant pharmacokinetic parameters were calculated.

$$W(s)_H = \frac{\dfrac{k_{12}}{1+k_{21}} \times \dfrac{V_b}{V_H} \times \exp\left[1 - \sqrt{Q_H \dfrac{\dfrac{1+4D_N.V_b}{s+k_{12}-k_{12}.k_{21}}}{s+k_{21}}}\Big/ 2/D_N\right]}{k_{12}} \qquad (7.1)$$

7.4 Results

7.4.1 Impulse-response Experiments

Figure 7.1 shows the output profiles of ^{3}H-sucrose and ^{14}C-creatinine from a representative liver. On a normal scale the creatinine profile appears to mirror that of sucrose. However, when viewed on a semilogarithmic plot it can clearly be demonstrated that although initially the profiles are identical, at latter time points marked differences become apparent. After the first 25 sec the sucrose concentration appearing in the outflow cannula is slightly higher relative to that of creatinine. After approximately 80 sec the sucrose concentration continues to decline steeply, whereas in contrast the creatinine concentration becomes fairly constant, with the difference between the two solutes increasing with time.

Parameters estimated from moment analysis for sucrose and creatinine are listed in Table 7.1. The recovery of radioactivity after injection of each solute was complete. (0.96+0.03 for sucrose and 0.98+0.03 for creatinine). The extrapolated fraction was negligible (3% for sucrose and 5% for creatinine). The values of MTT, CV^2, and normalised V_H of creatinine (37.1 sec, 1.2, 0.66

ml/min/g, respectively) were more than twice of those of sucrose (13.5 sec, 0.39, 0.26 ml/min/g, respectively).

Figure 7.2 demonstrates the fit of the dispersion model equations to the frequency outflow profiles of sucrose and creatinine. While the one-compartment dispersion model adequately described the outflow data for sucrose, the two-compartment form of dispersion model was needed to fit satisfactorily the outflow profiles of creatinine. The model parameter estimates for both compounds are presented in Table 7.2. The average coefficient of variation for the estimates were all less than 20%. The D_N value of creatinine (0.69+0.14) was greater than that of sucrose (0.26+0.05).

7.4.2 Steady-state Experiments

Following stopping the infusion, after approximately 12-14 sec, creatinine output activity started to decline exponentially (Figure 7.3). First there was a sharp fall in concentration and then after 50 sec, the concentration continued to decrease smoothly. The fit of the two-compartment dispersion model to the normalised output concentrations has been depicted in Figure 7.4. The related pharmacokinetic parameters have been presented in Table 7.3.

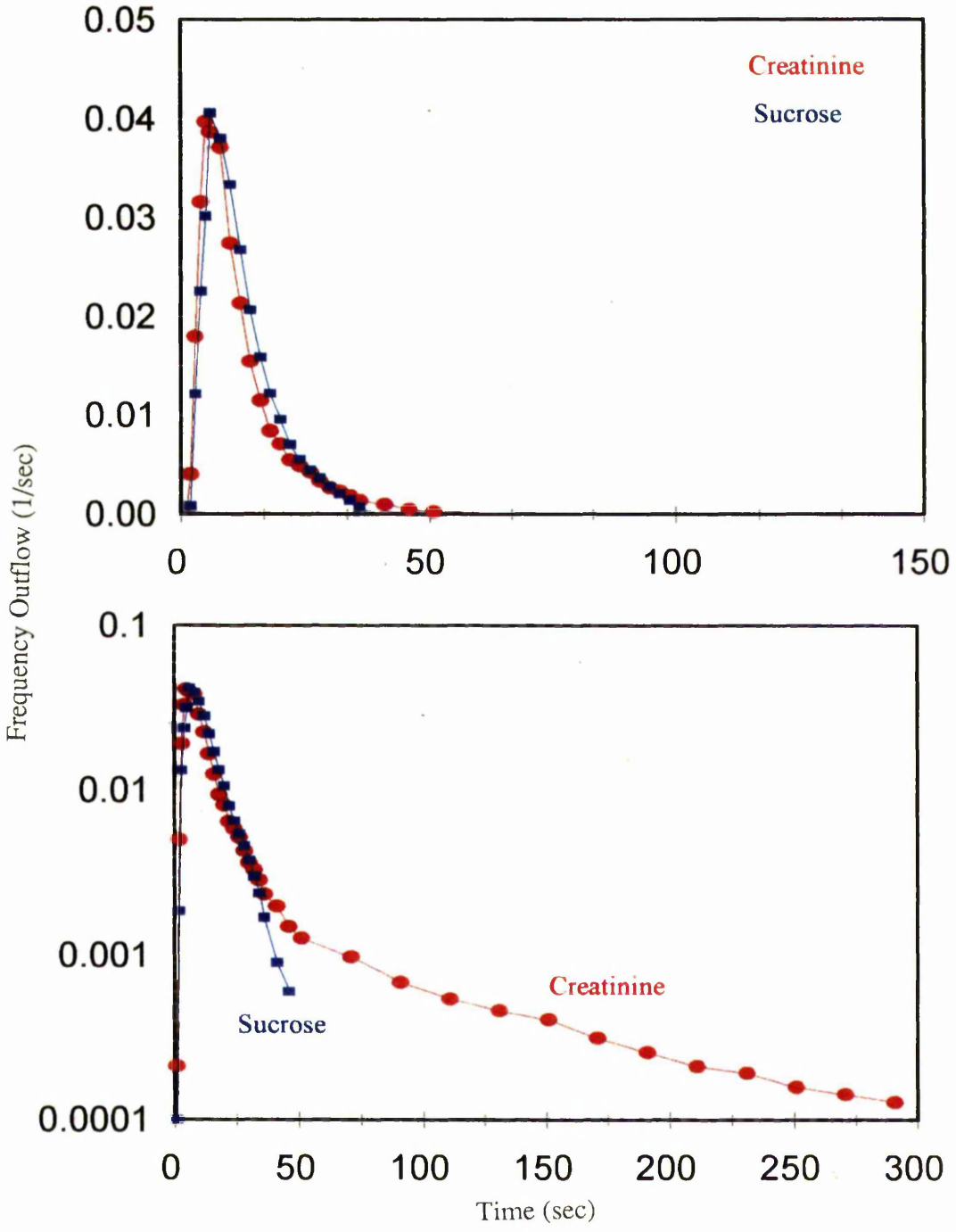

Figure 7.1 Linear and semilogarithmic frequency outflow profiles of sucrose and creatinine in a representative isolated perfused liver preparation.

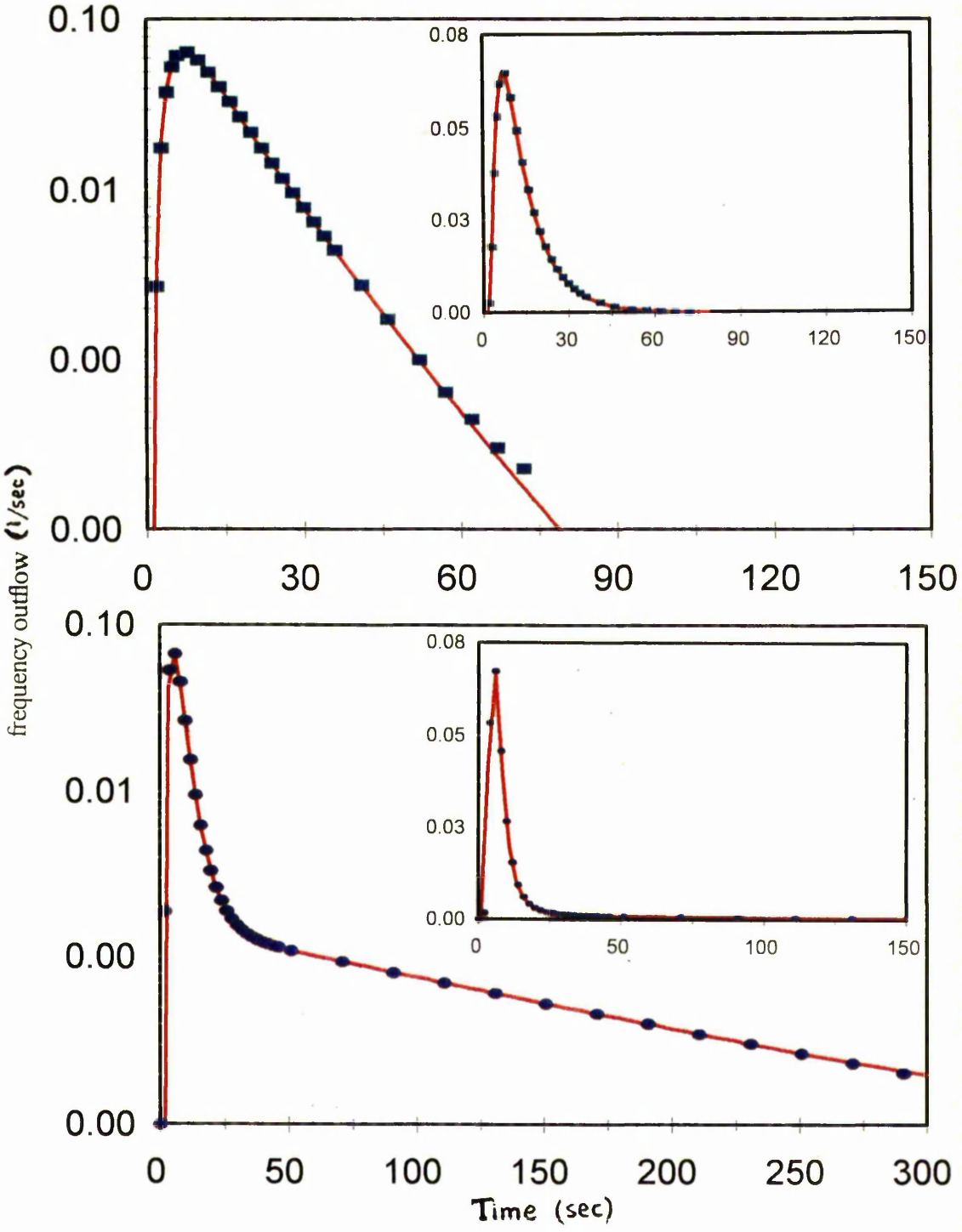

Figure 7.2 Semilogarithmic and linear (the insets) representation of frequency outflow versus midtime of the observed values (markers) and the simulated values (lines) produced using the two-compartment dispersion model. Top graph: sucrose; Bottom graph: creatinine

Table 7.1

Observational and statistical parameters of creatinine and sucrose outflow profiles in isolated perfused rat liver preparations (n=5).

		F(t)max 1/sec	tmax sec	MTT sec	V ml/g	CV^2	F %
Sucrose	mean	0.041	6.5	13.5	0.29	0.4	96
	±SD	0.007	0.7	1.1	0.05	0.06	3
	%cv	17	10	8	17	15	3
Creatinine	mean	0.04	6.5	37.1	0.66	1.4	99
	±SD	0.007	0.8	6.1	0.1	0.25	4
	%CV	17	12	16	16	17	4

Table 7.2

Parameters obtained by applying the dispersion model to the outflow profiles of sucrose and creatinine after bolus injection of each into the isolated perfused rat liver preparations (n=5).

		D_N	V_H ml/g	K_{12} 1/sec	K_{21} 1/sec	PS	K_P
Sucrose	mean	0.29	0.32				
	±SD	0.05	0.06	NA	NA	NA	NA
	%CV	17	18				
Creatinine	mean	0.55	0.68	0.071	0.044	1.05	1.7
	±SD	0.09	0.12	0.014	0.008	0.15	0.3
	%CV	17	17	18	19	14	17

NA: not applicable

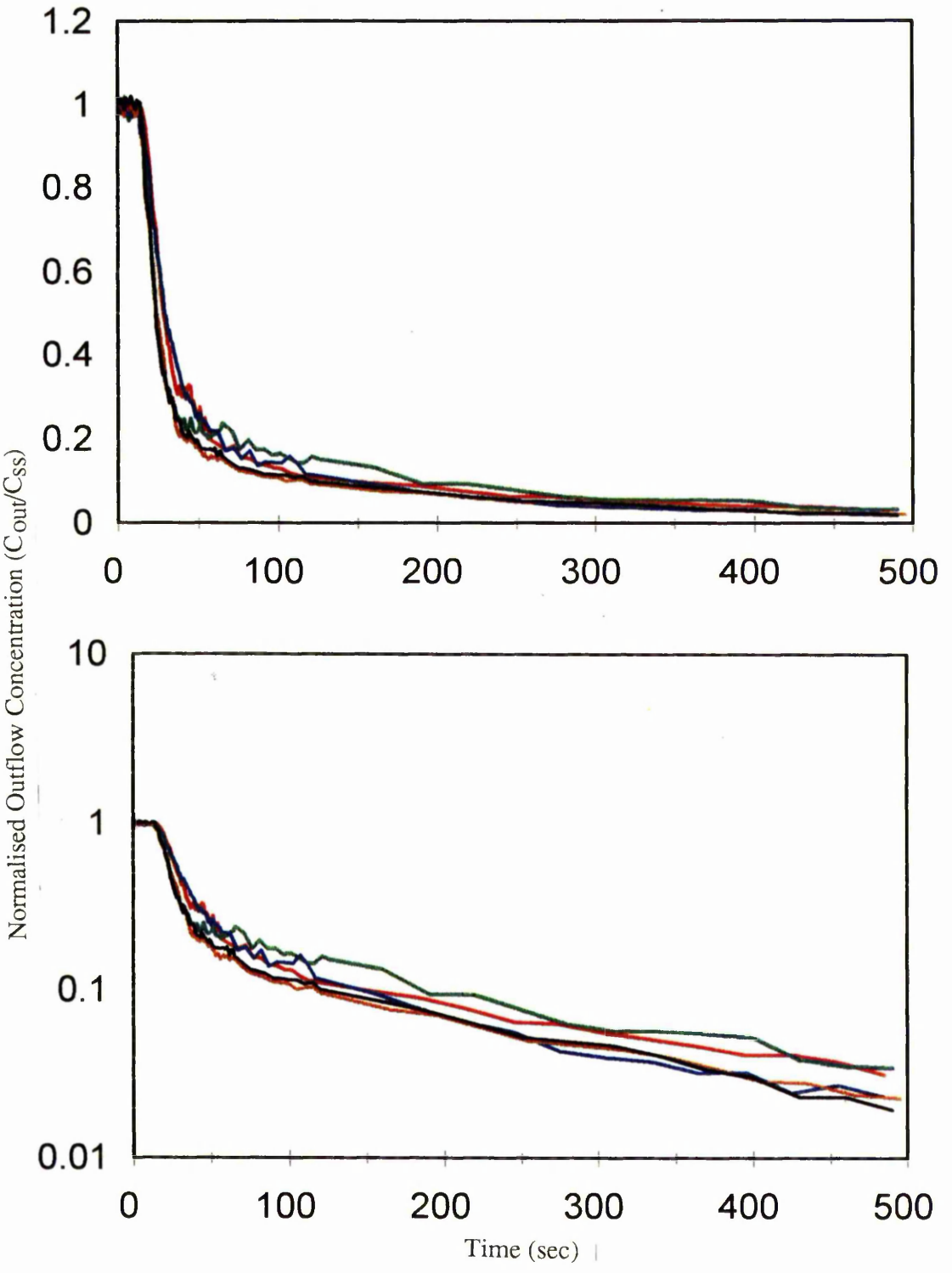

Figure 7.3 Normalised outflow concentration profiles of creatinine after continuous infusion to steady state in all liver preparations in isolated perfused rat liver.

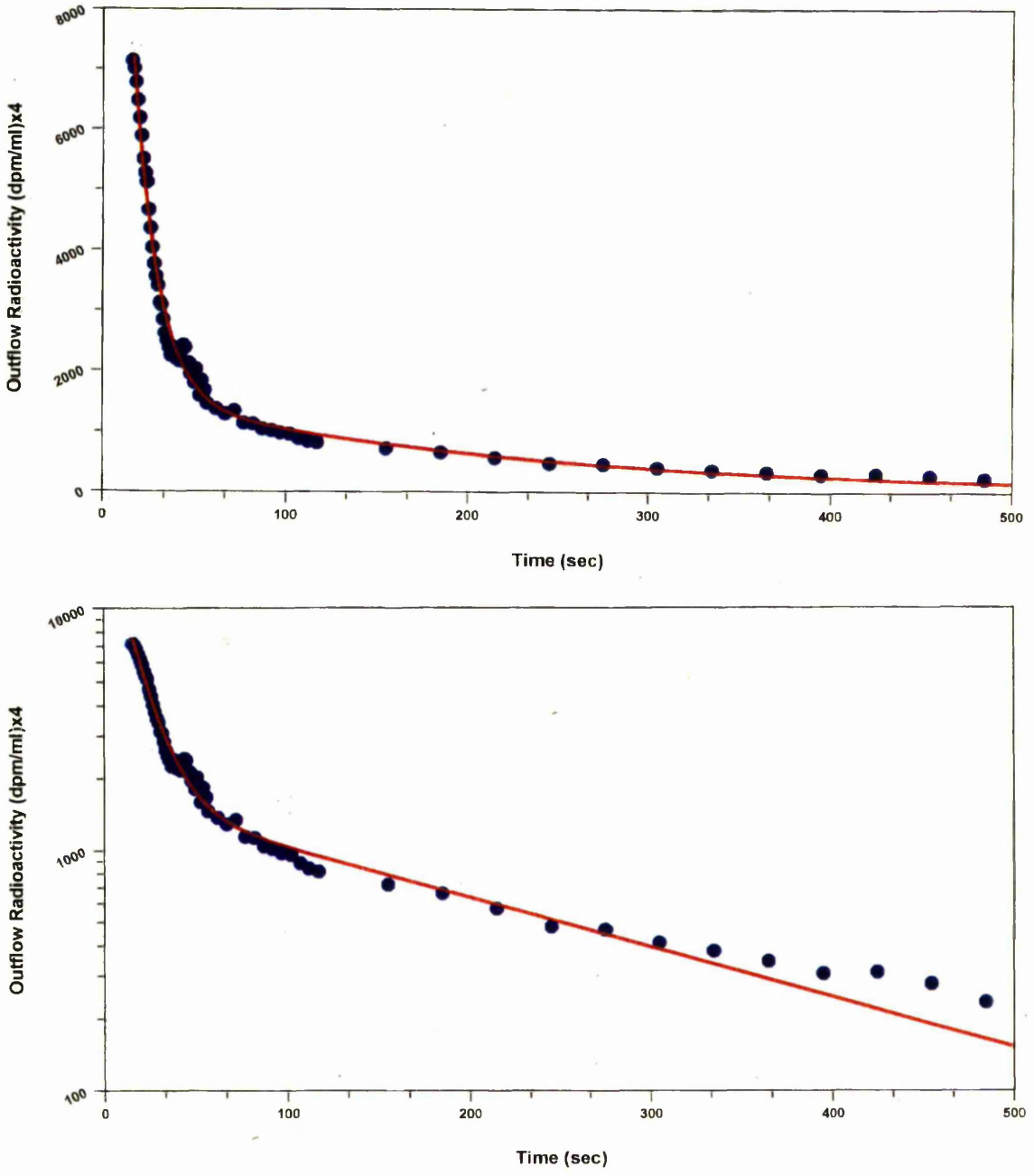

Figure 7.4 Fit of two-compartment dispersion model (lines) to the observed outflow profile of creatinine (markers) in a representative isolated perfused rat liver after stopping continuous infusion for 45 min. Top graph: linear, Bottom graph: semilogarithmic

Table 7.3

Pharmacokinetic parameters obtained by applying two-compartment dispersion model to the outflow profiles of creatinine in isolated perfused rat livers after stopping continuous infusion (n=5).

D_N	k_{12}	k_{21}	C_1	λ_1	C_2	λ_2	$t_{1/2}\beta$	CV^2
0.69	0.07	0.03	7100	0.07	1400	0	180	1.5

7.5 Discussion

7.5.1 Moment Analysis and Dispersion Model

The fact that the value of V_H of creatinine was much larger than that observed for sucrose (which is believed to access only the extracellular space) indicates that creatinine is not confined to the vascular space and is able to penetrate hepatocyte membrane. Also, the value of CV^2 of creatinine was much larger than that of sucrose suggesting the existence of non-equilibrium of creatinine distribution between the vascular and cellular spaces [54].

The D_N value of creatinine was greater than that of sucrose, indicating that creatinine has a greater relative degree of axial spreading in the liver. While both the k_{12} and k_{21} values were small, indicating a slow creatinine cellular influx and efflux, k_{21} value was considerably smaller than k_{12} value indicating a greater influx of creatinine compared to efflux. Quantitative analysis [54] has revealed that uptake is rate-limited by permeability when the ratio of effective permeability-surface product to blood flow (*ie* f_{ub}.PS/Q) is less than 0.06, and is perfusion rate-limited when f_{ub}.PS/Q is greater than 5.7. For $0.06 \leq f_{ub}PS/Q \leq 5.7$, both permeability and flow rate are important in determining uptake. In the current study, an estimate of the permeability-surface area product (PS) for creatinine was obtained from k_{12} using a rearrangement of Equation 2.16, given that f_{ub} is 1, and that V_b value equals the volume of distribution of sucrose. The value of PS/Q ratio (PS=1.05 ml/min/g and Q=1.4 ml/min/g liver) for creatinine was around 0.7 indicating

that while the hepatic uptake of creatinine is a function of both membrane permeability and perfusion flow rate, it is influenced by permeability to a greater extent than by flow rate. .

The two-compartment dispersion model which was first fitted to the creatinine bolus and steady-state data separately, described the observed data well giving confidence to the predicted rate constants and dispersion number. However, as sometimes the confidence in the estimation of dispersion model parameters, due to poor fitting, from bolus experiments alone may not be great, a modified form of dispersion model was developed to fit to both the bolus and steady-state data simultaneously. The obtained parameters were similar to those obtained from the previous fittings. This indicated that, as creatinine is not eliminated in liver, its dispersion in a single-pass journey in liver is similar to that following constant-rate infusion.

The V_H values for sucrose and creatinine (non-eliminating solutes) estimated using statistical moment analysis (Table 7.1) were similar to the values obtained using the appropriate dispersion model (Table 7.2). This gives some indication of the goodness of the fitting. Recall that model parameters can be estimated without curve fitting, using Equations 4.18 and 4.19 where the effect of a permeability barrier on the relative dispersion value (CV^2) of a non-eliminating solute was described. From various parameters that influence the CV^2 of a non-eliminating solute, CV^2 of solute within the vascular space and membrane permeability are important in the case of creatinine. The fact that creatinine PS value (1.05 ml/min/g) was smaller than the perfusion flow rate (1.4 ml/min/g) indicates that a barrier exists between the vascular and cellular compartment. Therefore, the effective permeability is sufficiently low such that transport becomes non-instantaneous, and hence the CV^2 of creatinine becomes greater than CV^2 of sucrose (vascular marker).

The values of model parameters (D_N, k_{12}, and k_{21}) determined for creatinine in this study (0.55, 0.071, and 0.044, respectively) were consistently greater than those obtained by Bumstead [358] (0.12, 0.026, and 0.039, respectively). A possible explanation for the lower estimate of D_N lies in the sensitivity of this parameter to the fitting procedure used to describe the creatinine dilution curves; the model tended to underestimate the peak and end stage tailing portions of the creatinine outflow curve. Failure to accurately characterise the throughput portion, especially the upcurve and $f(t)_{max}$, could lead to an underestimate of the true value of D_N. In practice, this

problem arises when the collection interval of liver effluent is relatively large compared to the time taken for the throughput component to eluent. More frequent sampling times by this worker, particularly at the beginning of collection, could improve the estimate of D_N.

7.5.2 Volume of Distribution

It was possible to calculate the steady-state volume of distribution of creatinine using the following relationship [243]:

$$V_{ss} = V_b \left(1 + \frac{k_{12}}{k_{21}}\right)$$

The V_{ss} value obtained from these experiments (0.7 ml/g liver) approximates the total aqueous hepatic volume. This value was larger than that obtained from the *in vivo* studies (V_{ss} =0.38 ml/g body weight). Furthermore, the volume of distribution of creatinine calculated from *in vivo* experiments (Chapter 6) was 0.36 ml/g body weight. In the present study, the mean V_H value estimated from impulse-response and steady-state experiments was about 0.67 ml/g liver which approximates the total aqueous volume of the liver. These differences could be due to two reasons. First, on calculating the steady-state volume of distribution from *in vivo* studies using plasma measurements alone (Equation 6.14), the volumes of all tissues including bones, skin and soft tissues are lumped together. Clearly, the distribution of creatinine in bones and skin is much less than that in soft tissues like liver and spleen. Second, the cellular membrane permeability may play an important role on the magnitude of the volume of distribution during the terminal phase (Equation 6.6). In the early phase of the *in vivo* experiments, creatinine is distributed primarily in its initial volume of distribution, which is the extracellular space. At later times, it is distributed further into the cellular space at a rate which is influenced by λ_2. The rate constant for the uptake of creatinine into the hepatocyte membrane (k12=0.071 1/sec) is greater than the overall rate of cellular membrane penetration of creatinine in the whole body (λ_2=0.032 1/sec). This finding reject claims that the distribution volume estimated from a single-pass bolus injection would be less than that of *in vivo* studies [54].

7.5.3 Distribution Kinetics after Steady-state

In the impulse-response experiments, the activity (concentration) of creatinine in samples in the tailing region of output profiles was low. Thus, the confidence in the pharmacokinetic parameters

obtained from this region was not great. Furthermore, as there was little difference between the output profiles of sucrose and creatinine obtained in these experiments, the hepatic distribution of creatinine could not be fully explained from bolus experiments alone, using the distribution kinetics of sucrose. Occasional poor description of the observed data by modelling also lessened the confidence in calculated parameters. Therefore, to overcome these problems, it was necessary to do a second set of experiments in the same liver preparations in which the events after constant rate infusion and upon stopping infusion was evaluated. Simultaneous evaluation of both sets of data should get more insight into the mechanisms that influence the hepatic dispersion of creatinine.

7.5.4 Creatinine Binding Properties

The intracellular hepatic volume of distribution of creatinine (the difference between creatinine total hepatic volume of distribution and the volume of extracellular marker sucrose) was calculated to be 0.45 ml/g liver, which is similar to the values found for water in normal livers (Chapter 4). This indicates that creatinine is not bound to intracellular components of hepatocytes and confirms the general view about creatinine, that this compound does not bind to plasma proteins [373,379]. Hirate [114], who developed a theoretical model to describe creatinine mass transfer through erythocytes, stated that his model was based upon the assumption of negligible creatinine-protein binding in either the erythrocytes or plasma. However, others (Bickel 62) have stated that in view of the reported binding of guanidine, nitrate, urethane, and uric acid (all nitrogen compounds), one may infer that a fraction of plasma creatinine is protein bound.

7.5.5 Membrane Transport of Creatinine

Hepatic uptake of some organic anions and organic cations is mediated by well-characterised transport systems [20,165,166]. For most compounds, however, such carrier-mediated transport systems have not been demonstrated, and permeability occurs mainly by passive diffusion. The impact of a transmembrane barrier on the distribution kinetics of various solutes has been evaluated both theoretically and experimentally [58,249,257]. However, the quantitative contribution of such factors as the microenvironment surrounding the surface of the hepatocyte membrane and the physicochemical properties of the compound are still poorly understood.

Various pathways have been proposed for the uptake of creatinine. According to the results obtained from human intestinal epithelial monolayer experiments [358], creatinine appears to traverse the intestinal epithelial barrier *via* the paracellular pathway. *In vitro*, creatinine can pass from the suspending medium into the erythrocytes *via* water-filled pores, albeit at a relatively slow rate compared with the permeability values of other solutes such as urea (P=0.0252 cm/min), tritiated water (P=0.59 cm/min, and glucose ($P=9\times10^{-6}$ cm/min) [380]. The *in vitro* efflux experiments [358] has indicated that a bi-directional flow exists and that the two rate constants and permeability coefficients are equal. The permeability of erythrocyte membrane to creatinine is much greater *in vivo* experiments compare to *in vitro* conditions which may be due to the difference between human and rat erythocytes properties. In normal conditions of renal function, creatinine is only filtered through glomerulous and is neither secreted nor reabsorbed [184]. In renal insufficiency, it is secreted into the proximal tubules, which is a sign of active transport [184]. Passage *via* cellular membrane lipid bilayers has also been suggested [375]. The route of creatinine transport across an epithelial barrier would therefore depends on which pathway provides the least resistance to diffusion.

7.5.6 Comparison with Extracellular Marker (Sucrose)

The distribution of creatinine within the liver was examined to determine whether it can enter hepatocytes, in order to ascertain if erythrocytes can be taken as representative of the majority of cell types. Marked differences were observed when the sucrose and creatinine output profiles from the single-pass liver experiment were compared suggesting that the two solutes are not interchangeable as volume markers. The fractional outflow of each solute appearing in the output cannula were initially identical, although after approximately 25 sec the sucrose concentration began to increase relative to that of creatinine, giving the impression that a small proportion of the creatinine was retained in the liver. This view was further substantiated by the fact that although the creatinine concentration initially declined in an exponential manner, as expected for an extracellular marker, at later time points the profile began to level out to a fairly constant value, consistent with a slow release of the previously retained creatinine. These differences reflect the ability of creatinine to traverse hepatocyte membranes: the initial decrease in the outflow concentration of creatinine, relative to sucrose, can be explained in terms of creatinine uptake into the hepatocytes along a concentration gradient. However, as the creatinine

concentration in the vasculature begins to decline the concentration gradient is reversed and therefore creatinine is slowly released from the cells, thus accounting for the maintenance of a reasonably constant output level at the later time points. These differences are reflected in the mean transit times (MTT) for each solute.

Several investigators have used creatinine together with other compounds such as inulin as extracellular markers. Itoh *et al* [126] who studied the ratio of extracellular space to the plasma space for creatinine and inulin in the rat kidney found that, on average, inulin distributed to only 62% of the volume which is available for creatinine, suggesting that the distribution volume for creatinine is greater than that for inulin. They stated that the difference may not be due to cellular uptake of creatinine, but to the small excluded volume of creatinine in the interstitial space (reflective of the fibrillar structure of the extracellular space which is related to the molecular weight [83,90] compared with inulin. Consequently, they stated that the distribution of creatinine may be restricted to the plasma and interstitial space similar to inulin. From these findings Itoh *et al* [126] concluded that creatinine was a better extracellular marker than inulin. Bumstead [358] who studied the distribution of creatinine and inulin in the isolated perfused rat liver and found that, in agreement to the findings in the present study and findings of Itoh *et al* [126] in kidney, sucrose is only distributed into approximately 45% of the space available to creatinine. Although this worker rejected the interpretation of Itoh *et al*, stated that "whether this volume represents creatinine uptake into hepatocytes or distribution into extracellular spaces that are inaccessible to sucrose cannot be determined from a single experiment". This doubt has probably been caused by the *in vitro* erythrocyte experiments of this worker in which creatinine showed a relatively low equilibrium rate constant and led to the conclusion that within the period of the single pass experiment, equilibration of creatinine into its total volume of distribution would not be expected. However, as this worker stated, there should be signs of uptake into the hepatocytes as shown by the hepatic volume of distribution of creatinine being greater than that of inulin. The greater values of V_H and CV^2 in the current studies indicated that creatinine is distributed into a much larger volume of distribution than extracellular space. The results of the steady-state experiments clearly demonstrated that creatinine does enter hepatocytes and is distributed into the total water space.

7.5.7 Calculation of Rate and Time of the Infusion

From the bolus experiments, the t½ of creatinine ($0.693/k_{21}$) was calculated to be approximately 15 min. Thus, the time needed to reach 90% of plateau would be around 45 min. The minimum acceptable count (at the tailing of the profile) was chosen to be at least 10 times of the background activity (usually 150–200 dpm/ml) and at least 5% of the maximum count. Therefore, the steady-state concentration to be achieved was 40000 dpm/ml. Having the perfusate flow rate (Q), the concentration at plateau (C_{ss}), and duration of the infusion (τ), the dose was calculated. Assuming creatinine is distributed into total cellular space (70% of liver weight), then the concentration of creatinine eluting from cells after the infusion stopped, was anticipated to be approximately 25000–30000 dpm/ml. The observed concentration was 26000±2000 dpm/ml which was within the anticipated range.

The plateau is reached when rate of drug elimination matches rate of infusion, R_0. The plasma concentration, C_{ss}, is given by this relationship:

$$C_{ss}=\frac{R_0}{\text{Clearance}}$$

Thus, having the clearance, the rate of infusion needed to produce a given steady-state concentration can be calculated. In the present work, given that creatinine is not metabolised in the liver, the clearance is equal to the rate of perfusion, Q.

From bolus experiments, the fraction of creatinine associated with the terminal phase can be calculated using the following equation.

$$AUC = \frac{C_0}{k}$$

As the frequency concentration at the beginning of the terminal phase (C_0) and k were approximately 0.0014 1/sec and 0.009 1/sec, respectively, the fraction of creatinine that entered into the cells is about 16%. Obviously this mass was not enough to maintain an acceptable outflow concentration in terms of measurement and hence confidence. Therefore, was necessary to increase the fraction of dose entering the cells by constant-rate infusion.

From steady-state experiments, the fraction of creatinine dose that enters the cell can be calculated using the following relationship.

$$AUC_{total} = \frac{C_1}{\lambda_1} + \frac{C_2}{\lambda_2}$$

From values quoted in Table 7.3, fraction of dose that enters the cells and fraction that remains in the extracellular space were approximately 76% and 24%, respectively. Therefore, using the continuous infusion protocol, a high level of intracellular creatinine was achieved which was enough to maintain an acceptable outflow concentration for the duration of the experiments.

REFERENCES

1 Agnisola C, Foti L, Genoino IT. (1980). Influence of age on nucleotidase in plasma membranes isolated from rat liver. Mech Ageing Rev. 13:227-239.

2 Ahamad AB, Bennett PN, Rowland M. (1984). Influence of route of hepatic administration on drug availability. J Pharmacol Exp Therap. 230(2):718-725.

3 Allis JW, Ward TR, Seely JC, Simmons JE. (1990). Assessment of hepatic indicators of subchronic carbon tetrachloride injury and recovery in rats. Fundament Appl Toxicol 15:558-570

4 Antoniello S, Auletta M, Cerini R, Cacciatore P, Magri P. (1990). Beta-Hexoaminidase activity in the acute phase of CCl4 poisoning in the rat. Enzyme 43:151-154

5 Anundi I, Hhogberg J, Stead AH. (1979). Glutathione depletion in isolated hepatocytes: Its relation to lipid peroxidation and cill damage. Acta Pharmacol Toxicol. 45:45-51.

6 Babb AL, Popovich RP, Farrel PC, Blagg CR. (1972). The effects of erythrocyte mass transfer rate on solute clearance measurements during hemodialysis. Proc Eur Dial Transplant Assoc. 9:303-319

7 Baglioni S (1910) Stoffwechseluntersuchungen an uberlebenden organen. Handb Biol Arb Meth. 3:364-351

8 Baldus WP, Hoffbauer FW. (1963). Vascular exchange in the cirrhotic liver as studied by the injection technique. Am J Dig Dis 8:689-700

9 Balk L, Meijer J, DePierre JW, Applegren LE. (1984). the uptake and distribution of benzo[a]pyrene in the northern pike (Esox lucinus). Examination by whole-body autoradiography and scintillation counting. Toxicol Appl Pharmacol. 74(3):430-449

10 Barona E, Leo M, Borowky SA et al. (1977). Pathogenesis of alcohol-induced accumulation of protein in the liver. J Clin Invest. 60:646-554

11 Barrowman JA, Perry MA, Kvietys PR, Granger DN. (1982). The exclusion phenominon in the liver interstitium. Am J Physiol. 243:G410-4.

12 Bass L, Robinson P, Bracken AJ. (1978). Hepatic elimination of flowing substrate: The distributed model. J Theor Biol 126:457-482

13 Bass L, Roberts MS, Roinson PJ. (1987). On the relation between the extended forms of the sinusoidal perfusion and of the convection dispersion models of hepatic elimination. J Theor Biol 126:457-482

14 Bass L, Keiding S. (1988). Physiologically based models and strategic experiments in hepatic pharmacology. Biochem Pharmacol 37:1425-1431

15 Bass L, Pond SM. (1988). The puzzel of rates of cellular uptake of protein-bound ligands. In: Pharmacokinetics: Mathematical and statistical approaches to metabolism and distribution of chemicals and drugs. Eds Pecile A, Rescigno A. London:Plenum Press pp245-269

16 Bassingthwaighte JB, Goresky CA. (1984). Modeling in the analysis of solute and water exchange in the microvasculature. In: Handbook of physiology, Section 2: The cardiovascular system, Vol IV, Eds RenkinEM, Michel CC. pp 549-626, Baltimore: Waveely Press.

17 Bennett HS, Luft JH, Hampton JC. (1959). Morphological classification of Vertebrate blood capillaries. Am J Physiol. 196:381

18 Benowitz N, Forsyth RP, Melmon KL, Rowland M. (1974a). Lidocain disposition kinetics in monkey and man. 1 Prediction by a perfusion model. Clin Pharmacol Ther 16:87-98

19 Benowitz N, Forsyth RP, Melmon KL, Rowland M. (1974b). Lidocain disposition kinetics in monkey and man. 2 Effects of hemorrhage and sympathomimetic drug administration. Clin Pharmacol Ther 16:99-109

20 Berk PD, Potter BJ, Stremmel W. (1987). Role of plasma membrane ligand-binding proteins in the hepatocellular uptake of albumin-bound organic anions. Hepatology 7:165-176

21 Berkersky I, Colburn WA, Fishman L, Kaplan SA. (1980). Metabolism of salicylic acid in the isolated perfused rat kidney. Drug Metab Dispos. 8:319-324.

22 Bernareggi A, Rowland M. (1990). Physiologic modeling of cyclosporin kinetics in rat and man. J Pharmacokinet Biopharm. 19(1): 21-50

23 Bill A. (1977). Plasma protein dynamics: Albumin and IgG capillary permeability, extravascular movement and regional blood flow in unanesthetised rabits. Acta Physiol Scand 101(1):28-42

24 Blashke TF. (1977). Protein binding and kinetics of drugs in liver disease. Clin Pharmacokinet. 2:32-44

25 Blendis LM, Orrego H, Crossley IR, Blake JE, Medline A. (1982). The role of hepatocyte enlargement in hepatic pressure in cirrhotic and noncirrhotic alcoholic liver disease. Hepatology. 2(5):539-546

26 Bjorkman S, Stanski DR, Verotta D, Harashima H. (1990). Comparative tissue concentration profiles of fentanyl and alfentanil in humans predicted from tissue/blood partition data obtained in rats. Anesthesiology. 72(5):865-873

27 Blakey GE. (1995). Tissue kinetics for a series of barbiturates. Ph D Thesis. Department of Pharmacy, The University of Manchester. p.109

28 Bollman JL, Mann FC. (1931). Experimentally induced legions of the liver. Ann Intern Med. 5:699-712

29 Boroujerdi M. (1982). The comparability of pharmacokinetics of creatinine in rabbit and man: a mathematical approach. J Ther Biol. 95:369-380

30 Boudinot FD, Jusko WJ. (1984). Fluid shifts and other factors affesting plasma protein binding of prednisolone by equilibrium dialysis. J Pharm Sci 73: 774-780

31 Boxenbaum HG, Riegelman S, Elashoff RM. (1974). Statistical estimations in pharmacokinetics. J Pharmacokinet Biopharm. 2:123-148.

32 Branch RA, Shand DG. (1976). Propranolol disposition in chronic liver disease: A physiological approach. Clin Pharmacokinet1:264-279

33 Brodie TG (1903) The perfusion of surviving organs. J Physiol Lond. 29:266-271

34 Brother AD. (1964). Pharmacologic aspects of aging: study on the effect of increasing age on drug accumulation in adults. J Am Geriatr Soc. 12:114-134

35 Brother AD. (1965). The effect of increasing age on the distribution of peripheral blood flow in man. J Am Geriatr Soc 13:192-198

36 Brother AD. (1967). Pharmacodynamic consequences of hepatic diseases and their implication in the treatment of cirrhotic patients. Med Ann D C. 36:267-271

37 Bruckner JV, McKenzie WF, Muralidhara S, Luthra R, Kyle GM, Acosta D. (1986). Oral toxicity of carbon tetrachloride: Acute, subacute, and subchronic studies in rats. Fundament Appl Toxicol 6:16-35

38 Buse A. (1982). Am Statistian 36:153-157

39 Byrne AJ, Morgan DJ, Harrison PM, McLean AJ. (1985). Variation in hepatic extraction rate with unbound drug fraction:discrimination between models of hepatic drug elimination. J Pharm Sci. 74:205-207

40 Cameron GR, Karunaratne WAE. (1936). Carbon tetrachloride cirrhosis in relation to liver regeneration. J Pathol Bacteriol 42:1-21

41 Chen R. (1967). Removal of fatty acids from serum albumin by charcoal treatment. J Biol Chem 242(2):178-182

42 Chen HS, Gross JF. (1979). Estimation of tissue-to-plasma partition coefficients used in physiological pharmacokinetic models. J Pharmacokinet Biopharm. 7(1):117-125

43 Chenery RJ, Ayrton A, Oldham HG, Standring P, Norman SJ, Seddon T, Kirby R. (1987). Diazepam metabolism in cultured hepatocytes from rat, rabbit, dog, guinea pig, and man. (1987). Drug Metab Dispos.

44 Chinard FP, Vosburgh GJ, Enns T. (1955). Transcapillary exchange of water and of other substances in certain organs of the dog. Am J Physiol 183:221-234

45 Chinard FP, Enns T, Nolan MF. (1962). Pulmonary extravascular water volumes from transit-time and slope data. J Appl Physiol. 17:179-183.

46 Ching MS, Morgan DJ, Smallwood RA. (1989). Models of hepatic elimination: implications from studies of the simultaneous elimination of taurocholate and diazepam by isolated rat liver under varying conditions of binding J Pharm Exp Ther 250:1048-1054

47 Chiou WL. (1978). Critical evaluation of the potential error in pharmacokinetic studies of using the linear trapezoidal rule method for the calculation of the area under the plasma level-time curve. J Pharmacokinet biopharm. 6(6): 539-546.

48 Chojkier M, Groszmann RJ. (1981). Measurement of portal-systemic shunting in the rat by using gama-labelled microspheres. Am J Physiol. 240:G371-G375

49 Cohn EJ, Hughes WL, Weare JH. (1947). J Am Chem Soc. 69:1753-1761

50 Comper WD, Laurent TC. (1978). Physiologic function of connective tissue polysaccharides. Physiol Rev. 58:255-315.

51 Condie LW, Laurie RD, Mills T, Robinson M, Bercz P. (1986). Effect of gavage vehicle on hepatotoxicity of carbon tetrachloride in mice: corn oil versus Tween-60 aqueous emulsion. Fundament Appl Toxicol. 7:199-206

52 Cope CL. (1930). The excretion of creatinine by the human kidney in health and in nephritis. Q J Med. 24:567-571

53 Chou CS, Evans AM, Fornasini G, Rowland M. (1993). Relationship between lipophilicity and hepatic dispersion and distribution for a homologous series of barbiturates in the isolated perfused in situ rat liver. Drug Metab Dispos 21:933-938

54 Chou CH. (1995). Physiological modelling of hepatic elimination: A quantitative approach with an axial dispersion model. Ph D Thesis. The University of Manchester.

55 Cousineau D, Goresky CA, Rose CP. (1985). Blood flow and norepenephrine effects on liver vascular and extravascular volumes. Am J Physiol. 248(17):H186-192.

56 Curry SH, Hu OYP. (1984). Evaluation of equilibrium dialysis volume shifts: a comment. J Pharmacokinet Biopharm 12: 463-564.

57 Dedrick RL. (1986). Interspeacies scaling of regional drug delivery. J Pharm Sci 75:1047-1052

58 De Lanoy IA, Pang KS. (1987). Effect of difussional barriers on drug and metabolite kinetics. Drug Metab Dispos. 15: 51-58.

59 Dewey WC. (1958). AEC Research and Development Report UR-524. University of Rochester ,Rochester, New York.

60 Diaz-Garcia J.M, Evans A.M, Rowland M. (1992). Application of the axial dispersion model of hepatic drug elimination to the kinetics of diazepam in the isolated perfused rat liver. J Pharmacokinet Biopharm. 20:171-193.

61 Diaz-Garcia JM, Oliver-Botana J, Fos-Galve D. (1992). Pharmacokinetics of diazepam in the rat:influence of a carbon tetrachloride-induced injury. J Pharm Sci. 81(8):768-772

62 Dyer A. (1980). Liquid scintilation counting practice. London: Heyden.

63 Evans A.M, Hussein Z, Rowland M. (1991). Application of the axial dispersion model describes the hepatic drug outflow profile of diclofenac in the presence of its binding protein. J. Pharm. Pharmacol. 43:709-714.

64 Evans AM, Hussein Z, Rowland M. (1991). A two-compartment dispersion model describes the hepatic outflow profile of diclofenac in the presence of its binding protein. J Pharm Pharmacol 43:709-714

65 Evans AM, Hussein Z, Rowland M. (1993) Influence of albumin on the distribution and elimination of diclofenac in the isolated perfused rat liver. J Pharmacokinet Biopharm. 20:171-193

66 Evans A.M, Hussein Z, Rowland M. (1993). Influence of albumin on the distribution and elimination of diclofenac in the isolated perfused rat liver: Analysis by impulse-response technique and the dispersion model. J.Parm. Sci. 82:421-428.

67 Farrell GC, Cooksley WGE, Powell LW. (1979). Drug metabolism in liver disease: activity of hepatic microsomal metabolising enzymes. Clin Pharmacol Ther. 26(4):483-492

68 Fawcett DW. (1955). Observation on the cytology and electron microscopy of hepatic cells. J Nat Cancer Inst 15 (suppl):1475-1955

69 Fernandez-Munzo D, Caramelo C, Blanchart A. (1985). Systemic and splanchnic hemodynamic disturbances in concious rats with experimental liver cirrhosis without ascites. Am J Physiol 249:G316-G320

70 Fiessinger N, Wolf M, Blum G. (1922). Les hepatites experimentales de la Souris apres inhalation de tetrachloride deethane. Compt Rendu Soc Biol 87:19-20

71 Forker EL, Luxon BA. (1978). Hepatic transport kinetics and plasma disappearance curves: distributed modeling versus conventional approach. A J Physiol 235:E648-E660

72 Forker EL, Luxon BA. (1981). Albumin helps mediate removal of taurocholate by rat liver. J Clin Invest 67:1517-1522

73 Forker EL, Luxon BA. (1983). Albumin binding and hepatic uptake: The importance of model selection. J Pharm Sci 72:1232-1233

74 Forker EL, Luxon BA. (1985). Lumpers vs distributors. Hepatology 5:1236-1237

75 Foster JF. (1960). In: The plasma proteins. Eds Putnam FW. New-york:Academic Press.

76 Freeman LM. (1975). Clinical scintilation imaging. London: Grune and straton.

77 Frink EJ, Digiovanni DA, Davis JR, Brown BR. (1989). Serun albumin levels in response to glycin infusion in normal and cirrhotic rats. Anesth Analg. 69:776-782

78 Gannong WF. (1991). Review of medical physiology. New Jersey: Prentice-Hall.

79 Garrick RA, Chinard FP. (1980). Permeability of dog erythrocytes to urea. Microvasc Res. 20:88-91.

80 Geoffrey M. (1984). Different effects of carbon tetrachloride toxicity and cirrhosis on substrate binding to rat hepatic microsomal cytochrome P450. Clin Pharmacol 33(4):687-689

81 Gillette JR. (1971). Factors affecting drug metabolism. Ann N Y Acad Sci 179:43-66

82 Glasinovic JC, Dumont M, Duval M, Erlinger s. (1975). Hepatocellular uptake of taurocholate in the dog. J Clin Invest 55:419-427

83 Goresky CA. (1963). A linear method for determining liver sinusoidal and extravascular volume. Am J Physiol 626-640

84 Goresky CA, Silverman M. (1964). Effect of correction of catheter distortion on calculated liver sinusoidal volumes. Am J Physiol. 207:883.

85 Goresky CA, Ziegler WH, Bach GG. (1970). Circ Res. 27:739-764.

86 Goresky CA, Bach GG, Nadeau BE. (1973). On the uptake of materials by the intact liver: the transport and net removal of galactose. J Clin Invest 52:991-1009

87 Goresky CA, Warnica JW, Burgess JH, Nadeau BE. (1975). Effect of exercise on dilution estimates of extravascular lung water and on the carbon monoxide diffusing capacity in normal adults. Circ Res 37:379-389.

88 Goresky CA, Warnica JW, Burgess JH, Cronin RF. (1978). Microvasc Res. 15:149-168.

89 Goresky CA. (1981) Tracer behaviour in the hepatic microcirculation. in Hepatic circulation in health and disease. Eds Lautt WW. Raven Press. 25-39

90 Goresky CA. (1983). Kinetic interpretation of hepatid multiple-indicator dilution studies. Am J Physiol. 245:G1-G12.

91 Goresky CA, Gordon ER, Bach G. (1983). Uptake of minohydric alcohols by liver: demonstration of a shared enzymic space. Am J Physiol. 244(7):G198-G214.

92 Goresky CA, Cousineau D, Rose CP, Lee S. (1986) Lack of liver vascular response to carotid occlusion in mildly acidotic dogs. Am J Physiol. 251(20):H991-H999.

93 Goresky CA, Pang KS, Schwab AJ, Barker F, Cherry WF, Bach GG. (1992). Uptake of a protein-bound polar compound, acetaminophen sulphate, by perfused rat liver. Hepatology 16(1):173-191

94 Greenway CV, (1989). Effect of hepatic blood flow on hepatic ethanol kinetics measured in cats and predicted from the parallel-tube model. Can J Physiol Pharmacol 67:728-733

95 Griscon LG, Giacomini KM. (1988). Inhibition of cimetidine transport by creatinine in luminal membrane vesicles prepared from rabbit kidney. Drug Metab Dispos. 16:331-332

96 Gross JB, Reichen J, Zeltner TB, Zimmermann A. (1987). The evolution of changes in quantitative liver function tests in a rat model of biliary cirrhosis: Correlation with morphometric measurement of hepatocyte mass. Hepatology. 7(3):457-463

97 Groszmann RJ, Vorovioff J, RileyE. (1982). Splanchnic hemodynamics in portal-hypertensive rats: measurement with g-labeled microspheres. Am J Physiol . 1:365-374.

98 Guechot J, Loric S, Vaubourdolle M, Chretien Y, Giboudeau J, Poupon R. (1989). Effect of protein binding on testosterone extraction by human cirrhotic liver: evidence for a dissociation-limited uptake. J Clin Endocrin Metabol. 69(1):200-204

99 Gumucio JJ, Miller DL, Krauss MD, Zanoli CC. (1981). Transport of flurescent compounds into hepatocyte and the resultant zonal labelling of the hepatic acinus in the rat. Gastroenterol 80:639-646

100 Gumucio JJ. (1983). Functional and anatomical heterogeneity in the liver acinus: impact on transport. Am J Physiol 244:G578-G582

101 Gumucio JJ. (1989). Hepatic heterogeneity: The coming of age from the description of a biological curiosity to a partial understanding of its physiological meaning and regulation. Hepatology 9:154-160.

102 Haft DE, Miller DJ. (1958) Alloxan diabetes and demonstrated direct action of insulin on metabolism of isolated perfused rat liver. Am J Physiol. 192: 33-36

103 Hamilton WF, Moore JW, Kinsman JM, Spurling RG. (1932). Studies on the circulation: IV further analysis of the injection method and of changes in hemodynamics under physiological and pathological conditions. Am J Physiol 99:534-551

104 Haraldsson B. (1986). Physiological studies of macromolecular transport across capillary walls. Studies on continous capillaries in rat skeletal muscle. Acta Physiol Scand 128(Suppl 553):1-40

105 Haraldsson B, Rippe B. (1984). Higher albumin clearance in rat hindquarters perfused with pure albumin solution than with serum as perfusate. Acta Physiol Scand 122(1):93-95

106 Haratake J, Hisaoka M, Yamamoto O, Horie A. (1990). Morphological changes of hepatic microcirculation in experimental rat cirrhosis: a scanning electron microscopic study. Hepatology. 13(5):952-956

107 Hartroft WS. (1964). Experimental cirrhosis. In: The liver: morphology, biochemistry, physiology. Eds Rouiller C. New york:Academic Press. pp477-514

108 Heatherington A.C (1994). A physiological based pharmacokinetic model for drug distribiution. Ph.D Thesis, The University of Manchester.

109 Hechter, O.; Zaffaroni, R.; Jacobsen, R.P.; Levy, H.; Pincus, G. (1951) The nature and biogenesis of the adrenal secretory product. Rec. Prog. Horm. Res. 6.215

110 Hechter, O.; Solomon, M.M.; Capsi, E. (1953) Corticosteroid metabolism in liver. Studies on perfused rat livers. Endocrinology 53:202

111 Hems, R.; Ross, B.D.; Berry, M.N.; Krebs, H.A. (1966) Gluconeogenesis in the perfused rat liver. Biochem. J. 101:284

112 Herz R, Cueni B, Bircher J, Paumgartner. (1973). The excretory capacity of the isolated rat liver. An in vitro-in vivo comparison. Naunyn-Schmiedeberg's Arch Pharmacol. 277:297-304.

113 Heukelom VS. (1896). Beitr Z Path Anat U Z Allg Path 20:221-228

114 Hirate J, Horikoshi I, Watanabe J, Ozeki S. (1984). Effect of hyperthermia and anaesthesia on the disposition of creatinine and urea in mice. J Pharmacobiodyn. 7:883-890

115 Hirate J, kato Y, Horikoshi I, Nagase S, Ueda CT. (1989). Further observations on the disposition characteristics of salicylic acid in analbuminemic rats. Biopharm Drug Dispos. 10:299--309.

116 Hirooka N, Iwasaki I, Horie H, Ide G. (1986). Hepatic microcirculaton of liver cirrhosis studied by corrosion cast/scanning electron microscope examination. Acta pathol Jpn. 36(3): 375-387.

117 Hu OYP, Curry SH. (1986). Calculation of fraction bound in equilibrium dialysis with special reference to drug losses by decomposition and adsorption. Biopharm Drug Dispos. 7: 211-214.

118 Huang JD. (1983). Error in estimating unbound fraction of drug due to the volume shift in equilibrium dialysis. J Pharm Sci 72: 1368-1369.

119 Huet PM. Goresky CA, Villeneuve JP, Marleau D, Lough J.O. (1982). Assessment of liver microcirculation in human cirrhosis. J Clin Invest. 70:1234-1244.

120 Hussein Z, Evans AM, Rowland M. (1993). Physiologic models of hepatic drug clearance. Influence of altered protein binding on the elimination of diclofenac in the isolated perfused rat liver. J Pharm Sci 82:880-885

121 Hussein Z. McLachlan A.J. Rowlamd M. (1994). Distribution kinetics of salicylic acid in the isolated perfused rat liver assessed using moment nalysis and the two-Compartment axial dispersion Model .J. Pharmaceutical Research. 11(No.9):1337-1347.

122 Ichikawa M, Tsao SC, Lin TH, Miyauchi S, Sawada Y, Iga T, Hanano M, Sugiyama Y. (1992). Albumin-mediated transport phenomenon observed for ligands withe high permeability: Effect of unstirred water layer in the disse's space of the rat liver. Hepatol. 16:38-49.

123 Ishise S. Pegram BL, Yamamoto J, Kitamura Y, Frohlich ED. (1980). Reference sample microsphere method cardiac output and blood flows in conscious rat. Am J Physiol. 239:H443-H449.

124 Igari Y, Sugiyama Y, Awazu S, Hanano M. (1982). Comparative physiologically based pharmacokinetics of hexobarbital, phenobarbital and thiopental in the rat. J Pharmacokinet Biopharm. 10(1):53-75.

125 Igari Y, Sugiyama Y, Sawada Y, Iga T, Hanano M. (1983). Predicton of diazepam disposition in the rat and man by a physilogically based pharmacokinetic model. J Pharmacokinet Biopharm. 11:577-593.

126 Itoh W, Sawada Y, Sugiyama Y, Iga T, Hanano M. (1985). Permeability of materials in postglomerular capillary bed and distribution to interstitium of kidney in rats. Jap J Physiol. 35:291-299

127 Jacquez JA. (1985). Physiological systems with flow: The modeling of flow and exchange in capillary beds. In Compartment analysis in biology and medicine, 2nd eds, pp 167-207, Ann Arbor: The University of Michigan Press.

128 Kaplan SA, Jack ML, Alexander K, Weinfeld RE. (1973). Pharmacokinetic profile of diazepam in man following single intravenous and oral and chronic oral administrations. J Pharm Sci. 62(11):1789-1796

129 Kassissia I, Rose CP, Goresky CA, Schwab AJ, Bach GG, Guirguis F. (1992). Flow-limited tracer oxygen distribution in the isolated perfused rat liver:effect of temperature and hematocrit. Hepatology 16(3):763-775.

130 Kassissia I, Brault A, Huet PM. (1994). Hepatic artery and portal vein vascularization of normal and cirrhotic rat liver. Hepatology. 19(5):1189-1197.

131 Klots U, Antonin KH, Brugel MD, Bieck PR. (1976). Disposition of diazepam and its major metabolite desmethyldiazepam in patients with liver disease. Clin Pharmacol Ther. 21(4):430-436

132 Klotz AC, Avant GR, Hoyumpa A, Wilkinson GR. (1975). The effect of age and liver disease on the disposition and elimination of diazepam in adult man. Clin Invest. 55:347-359

133 Krahlenbuchl S, Reichen J, Zimmermann A, Gehr P, Stucki J. (1990). Mitochondrial structure and function in CCl4-induced cirrhosis in the rat. Hepatology 12(3):526-532

134 Krebs, H.A.; Henseleit, K. (1932) Untersuchungen uber die harnstoffildung im tierkorper. Hoppe-Seyler's Z. physiol. chem. 210:33

135 Kretz-Rommel A, Boelsterli UA. (1993). Diclofenac coovalent protein binding is dependent on acyl glucronide formation and is inversely related to P450-mediated acute cell injury in cultered rat hepatocytes. Toxicol Appl Pharmacol. 120:155-161.

136 Kuehl GV, Harkness DR, Skraubut EM, Bechthold DA, Emerson CP, Valeri R. (1981). In vitro intractions of 51Cr in human red blood cells and hemolysates. Vox Sang 40:260-272

137 Lacquet AM. (1932). Experimental pathology of the liver: effects of carbob tetrachloride on the normal and restored liver often partial hepatectomy. Arch Pathol 14:164-174

138 Lam G, Chen ML, Chiou WL. (1982). Determinationof tissue to blood partition coefficients in physiologically based pharmacokinetic studies. J Pharm Sci. 71(4):454-456

139 Lamson PD, Wing R. (1926). Early cirrhosis of the liver produced in dogs by carbon tetrachloride. J Pharmacol Exp Therap 29:191-202

140 Landahl HD. (1954). Transient phenomana in capillary exchange. Bull Math Biophy 16:55-58

141 Langsdorf LJ, Zydney AL. (1993). Effect of uraemia on the membrane transport characteristics of red blood cells. Blood. 81:820-827

142 Lapis K. (1979). Cirrhosis. In: Electron microscopy in Human medicine. The liver, the Gallblader, and the Biliary ducts. Ed Johannessen JV. New york:MacGraw-Hill. 8:158-189

143 Lauterburg BH, Preisig R. (1981). Quantitation of liver function. In: Oxford textbook of clinical hepatology. Ed McIntyre N et al. Oxford University Press. 309-314

144 Law R.O. (1982). Techniques and applications of extracellular space determination in mammalian tissues. Experientia. 38:411-520.

145 Layden TJ, Schwarz J, Boyer JL. (1975). Scanning electron microscope of the rat liver: studies of the effects of taurolithcholate and other models of cholestasis. Gastroenterology 69: 724-738.

146 Laznicek M, Kvetina J. (1988). The effect of molecular structure on the distribution and elimination of some organic acids in rats. Quant Struct Act Relat. 7:234-239.

147 Laznicek M, Laznickova A. (1994). Kidney and liver contributions to salicylate metabolism in rats. Euro J Drug metab. Pharmacokinetics. 19(1):21-26.

148 Leehey DJ, Betzelos S, Daugirdas JT. (1987). Arteriovenous shunting in experimental liver cirrhosis in rats. J Lab Clin Med 109(6):687-692

149 Leemann T, Transon C, Dayer P. (1993). Cytochrome P450TB (CYP2C): A major monooxygenase catalysing diclofenac 4-hydroxylation in human liver. Life Sci 52: 29-34.

150 Levy G. (1965). Pharmacokinetics of salicylate elimination in man. J Pharm Sci. 54:959-967.

151 Leevy CM, Popper H, Sherlock S. (1976). Diseases of the liver and biliary tract: standardisation and nomenclaturee, diagnostic criteria, and diagnostic methodology. Fogarty International Centre Proceedings, No 22 DHEW Publication Number (NIH) 76-725. Washington DC. Printing Office.

152 Levy G. (1979). Phaarmacokinetics of salicylate in man. Drug Metab Rev 9:3-19.

153 Lieber CS. (1984). Alcohol and the liver: 1984 update. Hepatology. 4(6):1243-1260

154 Luxon BA, Forker EL. (1982). Simulation and analysis of hepatic indicator dilution curves. Am J Physiol 243:G76-G89

155 Mak K. M. Lieber C. S (1984). Alterations in endothelial fenestrations in liver sinusoids of baboons fed alcohol: a scanning electron microscopy study. Hepatology. 4:386-391.

156 Malik AB, Kaplan JE, Sava TM. (1976) Reference sample method for cardiac output and regional blood flow determinations in the rat. J Appl Physiol. 40:472-475.

157 Marshall WJ, McLean EM (1969). The effect of cirrhosis of the liver on microsomal detoxications and cytochrome P450. Br J Exp Path. 50:578-583

158 Mastai R, Huet PM, Brault A, Belgiorno J. (1989). The rat liver microcirculation in alcohol-induced hepatomegaly Hepatology. 10(6): 941-945.

159 McIndoe AH. (1928). Portal cirrhosis. Arch Pathol Lab Med. 22:23-30.

160 McLean EK, McLean AE, Sutton PM. (1969). An improved method for producing cirrhosis of the liver in rats by simultaneous administration of carbon tetrachloride and phenobarbitone. Br J Exp Path. 50:502-509

161 McLean AJ, Morgan DJ. (1991). Clinical pharmacokinetics in patients with liver disease. Clin Pharmacokinet 21(1):42-69

162 McNamara PJ, Bogardus JB (1982). Effect of initial conditions and drug protein binding on the time to equilibrium in dialysis systems. J Pharm Sci 71: 1066-1067.

163 McNamara PJ, Fleishaker JC, Hayden TL. (1987). Mean residence time in peripheral tissue. J Pharmacokinet Biopharm. 15(4): 439-451

164 Meier P, Zierler KL (1954) On the theory of the indicator dilution method for measurement of flow and volume. J Appl Physiol 6:631-744.

165 Meijer DF. (1987). Current concepts on hepatic transport of drugs. J Hepatol 4:259-268

166 Meijer DKF, Mol WEM, Muller M, Kurz G. (1990). Carrier-mediated transport in the hepatic distribution and elimination of drugs, with special reference to the category of organic cations. J Pharmacokinet Biopharm 18: 35-70.

167 Meijer DF, Groothuis GM (1991). Hepatic transport of drugs and proteins. In: Oxford textbook of clinical hepatology Ed McIntyre et al. Oxford University Press 40-78

168 Miller LL, Bly CG, Watson ML. (1951) The dominant role of the liver in plasma protein synthesis. J Exp Med. 94:431-435

169 Mills GC. (1959). The purification and propertees of glutathione peroxicase of erythrocytes. J Biol Chem. 234:502-506.

170 Mills PR, Meier PJ, Smith DJ, Ballatori N, Boyer LJ, Gordon ER. (1987). The effect of changes in the fluid state of rat liver plasma membrane on the transport of taurocholate. Hepatology. 7(1):61-66

171 Minami T, Cutler DJ. (1992). A kinetic study of the role of band 3 anion transport protein in the transport of salicylic acid and other hydroxylbenzoic acid across human erythrocyte membrane. J Pharm Sci 81:424-427

172 Miyauchi S, Sawada Y, Iga T, Hanano M, Sugiyama Y, Morita K, Iga T, Hanano M. (1987). Kinetics of hepatic transport of 4-methylumblliferone in rats. Analysis by multiple indicator dilution method. J Pharmacokinet Biopharm. 15:25-38

173 Miyauchi S, Sawada Y, Iga T, Hanano M, Sugiyama Y. (1993a). Comparison of the hepatic uptake clearance of fifteen drugs with a wide range of membrane permeabilities in isolated rat hepatocyte and perfused rat livers. Pharm Res 10:434-440

174 Miyauchi S, Sawada Y, Iga T, Hanano M, Sugiyama Y. (1993b). The influence of glucagon on the hepatic transport of taurocholate in isolated perfused rat liver: Kinetic analysis by the multiple indicator dilution technique. Biol Pharm Bull 16:791-795

175 Miyauchi S, Sawada Y, Iga T, Hanano M, Sugiyama Y. (1993c). Dose-dependent hepatic handling of propranolol determined by multiple indicator dilution method. Influence of tissue binding of propranolol on its hepatic elimination. Biol Pharm Bull. 16:1019-1024

176 Moon VH. (1934). Experimental cirrhosis in relation to human cirrhosis. Archives of Pathology. 381-423

177 Morgan, H.E.; Henderson, M.J.; Regen, D.M. (1961) Regulation of glucose uptake in muscle. I. The effect of insulin and anoxia on glucose transport and phosphorylation in the isolated perfused heart of normal rat. J. Biol. Chem. 236:253

178 Morgan DJ, Smallwood R.A. (1990). Clinical significance of pharmacokinetic models of hepatic elimination Clin Pharmacokinet 18:61-70

179 Morris ME. (1990). Pharmacokinetics and protein binding of salicylate metabolites in rats. Drug Metab Dispos 18(5): 809-811.

180 Mortimore GB (1961) Effect of insulin on potassium transfer in isolated rat liver. Am J Physiol. 200:1315-1320

181 Moschcowitz E. (1948). Laennec cirrhosis: Its histogenesis, with special reference to the role of angiogenesis, Arch Path. 45: 187.

182 Muriel P, Mourelle M. (1990) The role of membrane composition in ATPase activities of cirrhotic ra liver: effect of silymarin. J Appl Toxicol. 10(4):281-284

183 Murray JF, Dawson AM, Sherlock S. (1958). Circulatory changes in chronic liver disease. Am J Med. 24:358-367

184 Nasseri K. (1990). Estimation of renal tubular function using n-methyl nicotinamide. Msc Thesis. Department of Pharmacy, The University of Manchester.

185 Needs CJ, Brooks PM (1985). Clinical pharmacokinetics of salicylates. Clin Pharmacokinet. 10:164-177

186 Nelson E, Hanano M Levy G. (1966). Comparative pharmacokinetics of salicylate elimination in man and rats. J Pharmacol Exp Ther. 153:159-166.

187 Neville CF, Ninomiya SI, Shimada N, Funae Y. (1993). Characterisation of specific cytochrome P450 enzymes responsible for the metabolism of diazepam in hepatic microsomes of adult male rats. Biochem Pharmacol 45:59-65.

188 Fischer-Nielsen A, Poulsen HE, Hansen BA, Hage E, Keiding S. (1991). CCl4-cirrhosis in rats: irreversible histological changes and differentiated functional impairement. J Hepatol. 12:110-117

189 Ogston AG, Phelps CF (1961) Biochem J 78:827-833.

190 Ophuls W. (1910). Proc Soc Exper Biol Med 8:75-83

191 Orrego HL, Blendis LM, Crossley A, McDonald A. (1981). Correlation of intrahepatic pressure with collagen in the Disse space and heatomegally in humans and in the rat. Gastroenterology. 80:546-556

192 Paaske WP. (1980). Permeability of capillaries in muscle, skin, and subcutaneous tissue. Physiologist 23(1):75-78

193 Pang KS, Rowland M. (1977a). Hepatic clearance of drugs. I theoretical considerations of a "well-stirred" model and a "parallel-tube" model. Influence of hepatic blood flow, plasma and blood cell binding, and the hepatocellular enzymatic activity on hepatic drug clearance. J Pharmacokinet Biopharm. 5:625-653

194 Pang KS, Rowland M. (1977b) Hepatic clearance of drugs. 2 Experimental evidence for acceptance of "well-stirred" model over the "parallel-tube"model using lidocain in the perfused rat liver in situ preparation. J Pharmacokinet Biopharm 5:655-680.

195 Pang KS, Stillwell RN. (1983). Journal of Pharmacokinetics and Biopharmaceutics. 11:451-468.

196 Pang KS, Cherry WF, Terrell JA, Ulm EH. (1984). Disposition of enalapril and its diacid metabolite, enalaprilat, in a perfused rat liver preparation: Presence of a diffusional barrier for enalaprilat into hepatocytes. Drug Metab Dispos 12:309-313

197 Pang KS, Lee WF, Cherry WF, Yuen V, Accaputo J, Schwab AJ, Goresky CA. (1988). Effects of perfusate flow rate on measured blood volume, Disse space, intracellular water space, and drug extraction in the perfused rat liver preparation: characterization by the technique of multiple indicator dilution. J Pharmacokinet Biopharm. 16:595-533.

198 Pang KS, Barker F, Schwab AJ, Goresky CA. (1990). Urea and EDTA as reference indicators in hepatic multiple indicator dilution studies. Am J Physiol. 259:G32-G40.

199 Parks HF. (1957). The hepatic sinusoidal endothelial cells and its histological relationships, In: Electron microscopy , proceeding of the stockholm Conference, Eds Sjostrand FS, Rhodin S. New york: Academic Press. 151

200 Peng CT. Liquid scintilation counting. (1980). London: Academic Press.

201 Perl W, Chinard FP. (1968). A Convection-diffusion model of indicator transport through an organ. Circ Res. 22:273-298.

202 Philips MJ, Steiner JW. (1965) Electron microscopy of liver cells in cirrhotic nodules. Am J Clin Pathol. 46(6):985-1005

203 Popper H, Ellias H, Petty DE (1952). Vascular pattern of the cirrhotic liver. Am J Clin Pathol. 22:717-729

204 Popper H, Undenfriend S. (1970). Hepatic fibrosis. Correlation of biochemical and morphologic investigations. Am J Med 49:707-721

205 Popper H, Becker K. (1975) Collagen metabolism in the liver. New York: Stratton.

206 Popper H. (1977) Pathologic aspects of cirrhosis. Am J Pathol 87:228-258

207 Popper H, Piez K. (1978). Collagen metabolism in the liver. Dig Dis 234:641-659

208 Proctor E, Chatamra K. (1982). High yield micronodular cirrhosis in the rat. Gastroenterology 83:1183-1190

209 Proctor E, Chatamra K. (1983). Controlled induction of cirrhosis in the rat. Br J Exp Path. 64:320-331

210 Raisys VA, Friel PN, Graaff KE, Wilensky AJ. (1980). High performance liquid chromatographyic and Gas-liquid chromatographic determination of diazepam and nordiazepam in plasma. J Chromatography. 183:441-448

211 Rappaport AM, Borowy ZJ, Longheed WM, Lotto WN. (1954). Subdivision of hexagonal liver lobules into a structural and functional unit: role in hepatic physiology and pathology. Anat Rec. 119:11-34

212 Rauterbeg J, Voss B, Pott G. et al. (1981). Connective tissue components of the normal and fibrotic liver. Klin Wochenscher. 59:767-779

213 Reichen J, Paumgartner. (1975). Kinetics of taurocholate uptake by the perfused rat liver. Gastroenterol. 68:132-136

214 Reichen J, Paumgartner G (1976). Uptake of bile acids by perfused rat liver. Am J Physiol. 231(3):734-742.

215 Reichen J, Lee M. (1983). Sinusoidal capillarization is more important than intrahepatic shunting to explain decreased propranolol clearance in liver cirrhotic rats. Gastroenterology. 84:1283 (Abstr)

216 Reichen J, Hoilien C, Le M, Jones R. (1987). Decreased uptake of taurocholate and Ouabain by hepatocytes isolated from cirrhotic rat liver. Hepatology. 7(1):67-70

217 Reichen J, Arts B, Schafroth U, Zimmermann A, Zeltnerr B, Zysset T. (1987). Aminopyrine N-demethylation by rats with liver cirrhosis: Evidence for the intact cell hypothesis. A morphometric- functional sutdy. Gastroenterology. 93:719-26.

218 Reichen J. (1988). Role of the hepatic artery in canalicular bile formation by the perfused rat liver; Amultiple indicator dilution study. J Clin Invest 81:1462-1469.

219 Reichen J, Ohara B, Zeltner TB, Zysset T, Zimmermann A. (1988). Determinants of hepatic functionin liver cirrhosis in the rat Multivariate analysis. J Clin Invest. 82:2069-2076

220 Reilly PE, Thompson DA, Mason SR, Hooper WD. (1990). Cytochrom P450IIIA enzymes in rat liver microsomes: involvement in C3-hydroxylation of diazepam and nordazepam but not N-dealkylation of diazepam and temazepam. Molecul Pharmacol. 37:767-774

221 Rivory LP, Roberts MS, Pond SM. (1992). Axial tissue diffusion can account for the disparity between current models of hepatic elimination for lipophilic drugs. J Pharmacokinet Biopharm. 20(1):19-61

222 Roberts MS, Rowland M (1986). A dispersion model of hepatic elimination. 1 Formulation of the model and bolus considerations. J Pharmacokinet Biopharm. 14(3):227-260.

223 Roberts MS, Donaldson JD, Rowland M. (1988). Models of hepatic elimination: comparison of stochastic models to describe residence time distribution and to predict the influence of drug distribution, enzyme heterogeneity, and systemic recycling on hepatic elimination. J Pharmacokinet Biopharm. 16:41-83

224 Roberts MS, Fraser S, Wagner A, McLeod L. (1990a). Residence time distribution of solutes in the perfused rat liver using a dispersion model of hepatic elimination. J Pharmacokinet Biopharm 18 209-234

225 Roberts MS, Fraser S, Wagner A, McLeod L. (1990b). Residence time distribution of solutes in the perfused rat liver using a dispersion model of hepatic elimination. 2 Effect of pharmacological agents, retrograde perfusions and enzyme inhibition on evans blue, sucrose, water and taurocholate. J Pharmacokinet Biopharm. 18.235-250

226 Roberts GW, Larson KB, Spaeth EE. (1973). The interpretation of mean transit time measurements for multiple tissue systems. J Theor Biol 39: 447-475.

227 Roberts MS, Rowland M. (1985). Hepatic elimination. Dispersion model. J Pharm Sci. 74:585-587

228 Roberts MS, Rowland M (1986a). A dispersion model of hepatic elimination:1 Formulation of the model and bolus consideration. Jpharmacokinet Biopharm 14:227-260

229 Roberts MS, Rowland M. (1986b). A dispersion model of hepatic elimination:2 Steady-state consideration. Influence of hepatic blood flow, binding within blood, and hepatocellular enzyme activity. Jpharmacokinet Biopharm 14:261-288

230 Roberts MS, Rowland M (1986c). A dispersion model of hepatic elimination:3 Application to metabolite formation and elimination kinetics. Jpharmacokinet Biopharm 14:289-307

231 Roberts MS, Fraser S, Wagner A, McLeod L. (1990). Residence time distribution of solutes in the perfused rat liver using a dispersion model of hepatic elimination: 1 Effect of changes in perfusate flow rate and albumin concentration on sucrose and taurocholate. J Pharmacokinet Biopharm 18:209-234.

232 Rojkind M, Kershenobich D (1976). Hepatic fibrosis. In: Progress in liver disease, Eds Popper H, Schaffner F. New york: Grune&Stratton. 294-310.

233 Rojkind M, Dunn MA. (1979). Hepatic fibrosis. Gastroenterol 76:849-863

234 Rojkind M, Kershenobich D. (1981). Hepatic fibrosis. In:The liver, vol 1. Eds Arias IM, Frenkel M.Amsterdam: Excerpta Medica

235 Rojkind M, Kershenobich D. (1981). Hepatic fibrosis. Clinical Gastroenterol. 10:737-754

236 Rose CP, Goresky CA, Bach GG. (1977). The capillary and sarcolemmal barriers in the heart: an exploration of labeled water permeability. Circ Res. 41:515-533.

237 Ross, B.D.; Hems, R., Krebs, H.A. (1967) The rate of gluconeogenesis from various precursors in the perfused rat liver. Biochem. J. 102: 942

238 Ross, B.D. (1972) Perfusion techniques in biochemistry; a laboratory manual. Clarendon Press. Oxford.

239 Rowland M, Benet LZ, Graham GG. (1973). Clearance concepts in pharmacokinetics. J Pharmacokinet Biopharm 1:123-136

240 Rowland M. Leitch D. Fleming G. Smith B. (1984). Protein binding and hepatic clearance: discrimination between models of hepatic clearance with diazepam, a drug of high intrinsic clearance, in the isolated perfused rat liver prepration. J. Pharmacokinet. Biopharm. 12:129-147.

241 Rowland M. (1984b). Protein binding and drug clearance. Clin Pharmacokinet 9(suppl 1):10-17

242 Rowland M, Evans AM. (1991). Physiologic models of hepatic elimination. In: New trends in pharmacokinetics Ed Rascigno A, Thakur K. New york:Plenum Press83-102

243 Rowland M, Tozer TN. (1995). Clinical pharmacokinetics: concepts and applications, William & Wilkins, Media, PA.

244 Rubin E, Hutterer F, Popper H. (1963). Cell proliferation and fiber formation in chronic carbon tetrachloride intoxication. Am J Pathol. 42:715-724

245 Ryoo JW, Buschmann RJ (1983). Amorphmetric analysis of the hypertrophy of experimental liver cirrhosis. Virchows Arch Pathol Anat Histopathol. 400:173-186.

246 Sahin S. (1996) Effect of route of input on the hepatic disposition kinetics of compounds Ph D Thesis. The University of Manchester, Pharmacy Department.

247 Sangen WC, Sheppard CW. (1953). A mathematical derivation of the exchange of a labelled substance between a liquid flowing in a vessel and an external compartment. Bull Math Biophys 15:387-394

248 Sasaki Y, Wagner HN. (1971). Measurement of distribution of cardiac output in unanaesthetised rats. J Appl Physiol. 30(6): 879-884.

249 Sato H, Sugiyama Y, Miyauchi S, Sawada Y, Iga T, Hanano MA. (1986). A simulation study on the effect of a uniform diffusional barrier across hepatocytes on drug metabolism by evenly or unevenly distributed uni-enzyme in the liver. J Pharm Sci 75:3-8

250 Sawada Y, Sugiyama Y, Miyamoto Y, Iga T, Hanano M. (1985). Hepatic drug clearance model: comparison among the distributed, parallel-tube and well-stirred models. Chem Pharm Bull 33 319-326

251 Schachter D. (1984). Fluidity and function of hepatocyte plasma membranes. Hepatology. 4(1):140-151

252 Schaffner F, Popper H (1963). Cappilarisation of hepatic sinusoids in man.Gastroentro. 44(3):239-242

253 Schimassek H. (1962) Perfusion of isolated rat liver with a semisynthetic medium and control of liver function. Life Sci. 11:629-636

254 Schimassek (1963) Metabolite des kohlenhydratstoffwechsels der isoliert perfundierten rattenleber. Biochem. Z. 336:460

255 Schenker S, Hoyumpa AM, Wilkinson AD. (1975) J Med Clin North Am. 59:887

256 Schucker DL, Gilbert R, Jones AL, Hradek GT, Bazin H. (1985). Effect of aging on the hepatobiliary transport of dimeric immunoglobulin A in the male Fischer rat. Gastroenterology 88:436-443.

257 Schwab AJ, Barker F, Goresky CA, Pang KS. (1990). Transfer of enalaprilat across rat liver cell membranes is barrier limited. Am J Phsiol 258:G461-G475

258 Seydel JK, Schaper KJ. (1982). Quantitative structure-pharmacokinetic relationship and drug design. Pharmac Ther 15:131-182

259 Sherman IA, Pappas SC, Fisher MM. (1990). Hepatic microvascular changes associated with development of liver fibrosis and cirrhosis. Am J Physiol. 258:H460-H465

260 Shultz J, Armstrong W. (1978). Permeability of interstitial space of muscle (rat diaphragm) to solutes of different molecular weights. J Pharm Sci 67(5):696-700

261 Shetty BV, Badr M, Melethil S. (1994). Evaluation of hepatic metabolism of salicylic acid in perfused rat liver. J Pharm Sci. 83: 607-608.

262 Sies H, Wahllader A, Waydhas C, Soboll S, Haberle D. (1980). Functions of intracllular glutathione in hpatic hydroperoxide and drug metabolism and the role of extracellular glutathione. Adv Enzyme Regul. 18:303-320.

263 Sikuler E, Groszmann RJ. (1986). Interaction of flow and resistance in maintenance of portal hypertension in a rat model. Am J Physiol. 250:G205-G212

264 Skalsky M, Schindhelm K, Farrell PC. (1978). Creatinine transfer between red cell and plasma: a comparison between normal and uraemic subjects. Nephron. 22:514-522

265 Sluijs PV, Postema B, Meijer DK. (1987). Lactosylation of albumin reduces uptake rate of dibromosulfophthalein in perfused rat liver and dissociation rate from albumin in vitro. Hepatology. 7(4):688-695

266 Smallwood RH, Mihaly GW, Smallwood RA, Morgan DJ. (1988a). Propranolol elimination as described by the venous equilibrium model using flow perturbations in the siloated perfused rat liver. J Pharm Sci 77:330-333

267 Smallwood RH, Mihaly GW, Smallwood RA, Morgan DJ, Jones DB. (1988b). Effect of plasma protein binding on elimination of taurocholate by isolated perfused rat liver. Comparison of venous equilibrium, undistributed and distributed sinusoidal and dispersion models. J Pharmacokinet Biopharm 16:377-396

268 Smallwood RH, Mihaly GW, Smallwood RA, Morgan DJ. (1988c). Lack of linear correlation between hepatic ligan uptake rate and unbound ligand concentration does not necessarily imply receptor-mediated uptake. J Pharmacokinet Biopharm 16:397-412

269 Sokal EM, Trivedi P, Portmann B, Mowat AP. (1990). Adaptative changes of metabolic zonation during the development of cirrhosis in growing rats. Gastroenterology. 99:785-792

270 Steiver JW, Carruthers JS, Kalifat SR. (1962). Vascular alterations in the liver of rats with extrahepatic billary obstruction: an electron and fluorescent microscopic study. Exp Molec Path.1:427.

271 Stenger RJ. (1965). Fibrogenesis along the hepatic sinusoids in carbon tetrachloride-induced cirrhosis: An electron microscopic study. Exp Molec Path 4:357

272 Stenger RJ. (1966). Hepatic sinusoids in carbon tetrachloride-induced cirrhosis. Arcg Path. 81:439-447

273 Stewart GN. (1921). The pulmonary circulation time, the quantity of blood in the lungs and the output of the heart. Am J Physiol. 58:20-44

274 Stierlin H, Faigle JW, Sallmann A, Kung W, Richter WJ, Kriemler HP, Alt KO. (1979). Biotransformation of diclofenac sodium (Voltaren) in animals and in man. 1 Isolation and identification of principal metabolites. Xenobiotica.

275 St-Pieere MV, Lee WF, Goresky CA, Pang KS. (1988). The multiple indicator dilution technique for characterisation of normal and retrograde perfusion in the once-through rat liver preparation. Hepatology 9(3):133-141

276 Tamayo RP. (1983). Is cirrhosis of the liver experimentally produced by CCl4 an adequate model of human cirrhosis. Hepatology. 3(1): 112-120

277 Tanigavara Y. (1992). Moment (version 3.0): Calculation of moments by trapezoidal integration method

278 Taylor G. (1967). The dispersion of soluble matter in solvent flowing slowly through a tube. Proc Roy Soc Ser 219.186-203

279 Toon S, Rowland M. (1983). Structure-pharmacokinetic relationships among the barbiturates in the rat. J Pharmacol Exp Ther 225:752-763

280 Tribble DL, Aw TY, Jones DP. (1987). The pathophisiological significance of lipid peroxidation in oxidative cell injury. Hepatology. 7(2):377-387

281 Trowell OA. (1942) Urea formation in the isolated perfused liver of the rat. J Physiol Lond. 100: 432-437

282 Tsao SC, Sugiyama Y, Sawada Y, Nagase S, Iga T, Hanano M. (1986). Effect of albumin on hepatic uptake of warfarin in normal and albuminoric mutant rats: analysis by multiple indicator dilution method. J Pharmacokinet Biopharm 14:51-64

283 Tsao SC, Sugiyama Y, Sawada Y, Nagase S, Iga T, Hanano M. (1988). J Pharmacokinet Biopharm. 16 165-181

284 Trump BF, Goldblatt PJ, Stowell RE. (1962). An electron microscopyic study of early cytoplasmic alterations in hepatic parenchymal cells of mouse liver during necrosis in Vitro. Lab Invest. 11:986

285 Tsuji A, Yoshikawa T, Nishide K, Minami H, Yamana T. (1983). Physiologically based pharmacokinetic model for beta-lactam antibiotics 1: Tissue distribution and elimination in rats. J Pharm Sci 72(11) 1239-1252.

286 Tsukamoto H, Towner SJ, Ciofalo LM, French SW. (1986). Ethanol-induced liver fibrosis in rats fed high fat diet. Hepatology 6(5): 814-822

287 Tucker GT. (1981). Empirical vs compartment vs physiological models. In: Topics in pharmaceutical sciences, Ed Breimer DD, Speiser P. Elsever. 33-48

288 Ungar H. (1951). Transformation of the hepatic vasculature of rats following protracted experimental poisoning with carbon tetrachloride: Its possible relationship to the formation of urate calculi in the urinary tract. Amer J Path. 27: 871.

289 Upton RN. (1990). Regional pharmacokinetics. 1 Physiological and physicochemical basis. Biopharm Drug Dispos 11(8):647-662.

290 Upton RN, Runciman WB, Mather LE. (1990). Regional pharmacokinetics. 2 Experimental methods Biopharm Drug Dispos. 11(9): 741-752.

291 Varin F, Huet PM (1985 Hepatic microcirculation in the perfused cirrhotic rat liver. J Clin Invest 76.1904-1912

292 Verbeeck RK, Blackburn JL, Loewen GR. (1983). Clinical pharmacokinetics of non-steroidal anti-inflamatory drugs. Clin Pharmacokinet. 8:297-331.

293 Vidins EL, Britton RS, Medline A, Blendis LM, Orrego H. (1985). Sinusoidal caliber in alcoholic and nonalcoholic liver disease: diagnostic and pathogenic implications. Hepatology. 5(3):408-414

294 Villenuve JP, Wood AJ, Shand DG, Rogers L, Branch RA. (1978). Impaired drug metabolism in experimental cirrhosis in the rat. Biochem Pharmacol. 27:2577-2581

295 Vorobioff J, Bredfeldt JE, Grozmann RJ. (1983). Hyperdynamic circulation in portal-hypertensive rat model: a primary factor for maintenance of chronic portal hypertension. Am J Physiol. 244:G52-G57

296 Vorbobioff J, Bredfeldt J, Groszmann RJ. (1984). Increased blood flow through the portal system in cirrhotic rats. Gastroenterol. 87:1120-1126

297 Wan SH, Riegelman S. (1972). Renal contribution to overall metabolism of drugs. II. Biotransformation of salicylic acid to salicyluric acid. J Pharm Sci. 61:1284-1287.

298 Watanebe J, Hayashi Y, Iwamoto K, Ozeki S. (1985). Salivary excretion of 5-fluorouacil. I. Fluctuation of the salivary/plasma concentration ratio and salivary clearance in beagle dogs following a bolus intravenous administration. Chem Pharm Bull. 33:1187-1194

299 Weibel ER, Staubli W, Gnagi HR, Hess FA. (1969). Correlated morphometric and biological studies on the liver cell. J Cell Biol 42:68-91

300 Weisiger RA, Golan J, Ockner R (1981). Science. 211:1048-1051

301 Weisiger RA, Mendel CM, Cavalieri RR. (1986). The hepatic sinusoid is not well-stirred: Estimation of the degree of axial mixing by analysis of lobular concentration gradient formed during uptake of tyroxin by the perfused rat liver. J Pharm Sci 75:233-237

302 Weiss M. (1983b). Hemodynamic influences upon the variance of disposition residence time distribution of drugs. J Pharmacokinet Biopharm 11: 63-75.

303 Wettstein M, Gerok W, Haussinger D. (1990). Hypoxia and Ccl4-induced injury, but not acidosis, impair metabolism of cysteinyl leukotrienes in perfused rat liver. Hepatology. 11(5):866-873

304 Wiederhielm CA, Black LL (1976). Am J Physiol. 231:638-641.

305 Wilkinson GR, Shand DG (1975). A physiological approach to hepatic drug clearance. Clin Pharmacol Ther 18:377-390

306 Wilkinson GR, Schenker S (1976) Drug disposition and liver disease. 139-194

307 Wilkinson GR. (1986). Influence of hepatic disease on Pharmacokinetics. In:Applied Pharmacokinetics: Principles of therapeutic drug monitoring. Eds Evans et al. 2nd ed, Spokane:Applied Therapeutics pp116-138

308 Wilkinson GR. (1987). Clearance concepts in pharmacology. Pharm Rev 39:1-47

309 Williams PL, Riviere JE. (1989). Estimation of physiological volumes in the isolated perfused porcine skin flap. Res Communict Chem Path Pharmacol. 66(1):145-158.

310 Wilson JB. (1951). Vascular patterns in cirrhotic liver. Edinburgh. Med. J. 58:537.

311 Winkler K, Bass L, Keiding S. Tygstrup N. (1974). The effect of hepatic perfusion on the assessment of kinetic constants. In: Regulation of hepatic metabolism. Eds:Lundqvist F, Tygstrup N. Copenhagen Munksgaard. pp:797-807

312 Winkler K, Bass L, Keiding S. Tygstrup N. (1979). The physiologic basis for clearance measurements in hepatology Scand J Gastroenterol. 14:439-448

313 Wisse E. De Zanger RB, Charels K, Van Der Smissen P, McCuskey RS. (1985). The liver sieve: Considerations concerning the structure and function of endothelial fenestrae, the sinusoidal wall and the space of Disse. Hepatology 5:683-692.

314 Withrington PG, Richardson PDI. (1986). Hepatic dynamics and microcirculation. In:Regulation of hepatic metabolism-intra and intercellular compartments. Eds Thurman. New-York:Plenum Press. pp27-53

315 Wolkoff AW, Johansen KL, Goeser T. (1987). The isolated perfused rat liver: preparation and application Anal Biochem 167:1-14

316 Wolkoff AW, Goresky CA. Sellin J, Gatmaitan Z, Arias IM. (1979). Role of ligandin in transfer of bilirubin from plasma into liver. Am J Physiol. 236(6):E638-E648.

317 Wood AJ, Villeneuve JP, Branch RA, Rogers LW, Shand DG. (1979). Intact hepatocyte theory of impaired drug metabolism in experimental cirrhosis in the rat. Gastroenterology. 76:1358-1362

318 Yamaoka K, Nakagawa T. Uno T. (1978). Statistical moments in Pharmacokinetics. J Pharmacokinet Biopharm. 6(6):547-558

319 YanoY. Yamaoka K, Tanaka H (1987). J Pharmacokinet Biopharm. 17:179-202

320 YanoY, Yamaoka K, Tanaka H. (1989). A non-linear least squares program. (MULTI-FILT), based on fast inverse Laplace transforms for microcomputers. Chem. Pharm. Bull. 37:1535-1538

321 Yano Y, Yamaoka K, Aoyama Y, Tanaka H. (1989). Two-compartment dispersion model for analysis of organ perfusion system of drugs by fast inverse laplace transform (FILT). J Pharmacokinet Biopharm 17:179-202

322 Yano Y, Yamaoka K, Minamide T, Nakagawa T, Tanaka H. (1990). Evaluation of protein binding effect on local disposition of oxacillin in rat liver by a two-compartment dispersion model. J Pharm Pharmacol 42:632-636

323 Yano Y, Yamaoka K, Yasui H, T, Nakagawa T. (1991). Effect of perfusion rate on the local disposition of cefixime in liver perfusion system based on two-compartment dispersion model. Drug Metab Dispos 19:1022-1027

324 Yano Y, Yamaoka K, Yasui H, Nakagawa T, (1991). Effect of perfusion rate on the local disposition of cefixime in liver perfusion system based on two-compartment dispersion model. Drug Metab. Dispos. 19:1022-1027.

325 Yoshikawa T, sugiyama Y. sawada Y, Iga T, Hanano M. (1984). Effect of pregnancy on tissue distribution of salicylate in rats. Drug Metab Dispos. 12:500-505.

326 Yutaka K. (1974). Biological application of liquid scintilation counting. London: Academic Press.

327 Ziegler H, Goresky CA. (1971). Transcapillary exchange in the working left ventricle of the dog. Circ Res 29:181-207

328 Casley-Smith JR. (1976) The functioning and interrelationships of blood capillaries and lymphatics. Experientia 32(1):1-12

329 Renkin EM, Kramer GC (1986). Measurement of vascular and microvascular permeability to large molecules. In:Microcirculatory technology. Physical techniques in biology and medicine. Eds:Baker CH, Nastuk WL. London: Academic Press 471-487

330 Sejrsen P, Paaske WP, Henriksen O. (1985). Capillary permeability of albumin in skeletal muscle Microvasc Res 29(3):265-281

331 Ponder E. (1971). Hemolysis and related phenomena. New york:Grune&Stratto

332 Robinson PJ. (1991). Effect of microcirculatory heterogeneity on the determination of pharmacokinetic parameters Implication for risk assessment. Drug Metab Rev. 23:43-64

333 Gallo JM, Lam FC, Perrier DG. (1987). Area method for the estimation of partition coefficients for physiological pharmacokinetic models. J Pharmacokinet Biopharm. 15(3):217-280

334 Kedderis GL, Carfagna MA. Held SD, Batra R, Murphy JE, Gargas ML. (1993). Kinetic analysis of furan biotransformation by F-344 rats in vivo and in vitro. Toxicol Appl Pharmacol. 123(2):274-282

335 Sultatos LG. Kim B, Woods L. (1990). Evaluation of estimations in vitro of tissue/blood distribution coefficients for organothiophosphate insecticides. Toxicol Appl Pharmacol. 103(1):52-55

336 Schary WL, Rowland M. (1983). Protein binding and hepatic clearance: studies with tolbutamide, a drug of low intrinsic clearance, in the isolated perfused rat liver preparation. J Pharmacokinet Biopharm. 11(3):225-243

337 Hase JR, Brim CD. (1966).

338 Shetty BV, Badr M, Melethil S. (1994). Evaluation of hepatic metabolism of salicylic acid in the liver. J Pharm Sci. 83:607-608

339 Goodman DS. (1957). Science. 125:1296-1301

340 Williams EJ, Foster JF. (1959). J Am Chem Soc. 81:865-870

341 Allen TH, Reeve EB. (1953) Am J Physiol. 175:219-226

342 Newton BE, Simmons B, Losher EP. (1956). Circulation Res. 4:419-423

343 Miyauchi S, Sugiyama Y, Iga T, Hanano M. (1988). Membrane-limited hepatic transport of the conjugative metabolites of 4-methylumbliferone in rats. J Pharm Sci. 77:688-692

344 Goresky CA, Schwab AJ, Rose CP. (1988). Xenon handling in the liver:red cell c apacity effect. Cir Res. 63:767-778

345 Saville BA, Gray MR, Tam YK. (1992b). Experimental studies of transient mass transfer and reaction in the liver:Interpretation with a heterogenous compartment model. J Pharm Sci. 81:265-271

346 Goresky CA, Bach GG, Cousineau D, Schwab AJ, Rose CP, Goresky S. (1989). Handling of tracer norepinephrine by the dog liver. Am J Physiol. 256:G107-G123

357 Rivory LP, Roberts MS, Pond SM. (1990). Clinical Pharmacology and Toxicology Preprint, Department of Medicine, University of Queensland. 1:1-73

358 Bumstead SJ. (1993). Intestinal paracellular drug absorption. Msc Thesis. Department of Pharmacy, the University of Manchester.

359 Watanabe J, Kozaki A. (1978). Relationship between partition coefficients and apprent volumes of distribution for basic drugs II. Chem Pharm Bull. 26:3463-3470

360 Martin AN, Swarbrick J, Cammarata A. (1969). "Physical Pharmacy", 2nd ed. Lea and Feibiger, Philadelphia. pp 403-404

361 Watanabe J, Hirate J, Iwamoto KI, Ozeki S. (1981). Distribution of creatinine following intravenous and oral administration to rats. J Pharm Dyn. 4:329-335

362 Pappenheimer JR, Madara JL. (1987). Structural basis for physiological regulation of paracellular pathway in intestinal epithelia. J Memb Biol. 100:149-164

363 Edwards D, Jones CJ, Sibley CP, Nelson DM. (1993). Paracellular permeability pathways in the human placenta: a quantitative and morphological study of maternal-fetal transfere of horseradish peroxide. Placenta. 14:63-67

364 Miller RK, Berndt WO. (1975). Mechanisms of transport across the placenta: an in vitro approach. Life Sciences. 16 7-30

365 Dominguez R, Pomerene E. (1945). Recovery of creatinine after ingestion and after intravenous administration in man. Proc Soc Exp Biol Med. 58:26-28

366 Greenberg J, Schwartz IL, Spinner M, Silver L, Starr N. (1952). Apparent volumes of distribution of P-aminohippurate and creatinine in the dog. Am J Physiol. 168:86-92

367 Sapirstein LA, Vidt DG, Mandel MJ, Hanusek G. (1955). Volumes of distribution and clearance of intravenously injected creatinine in the dog. Am J Physiol. 181:330-336

368 Guadino M, Levitt MF. (1949). Inulin space as a measure of extracellular fluid. Am J Physiol. 157:387-391

369 Pappenheimer JR. (1990). Paracellular intestinal absorption of glucose, creatinine, and mannitol in normal animals: relation to body size. Am J Physiol. 259: G290-G299

370 Hankis GR. (1981)

371 Goldman R. (1954). Creatinine excretion in renal failure. Proc Soc Exp Biol Med. 85:446-448

372 Boroujerdi M, Mattocks AM. (1979). Creatinine kinetics in the rabbit. J Pharmacol Biopharm. 7:291-301

373 Babb AL, Popovich RP, Farrell PC, Blagg CR. (1972). The effects of erythrocyte mass transfer rates on solute clearance measurements during hemodialysis. Proc Eur Dial Transplant Assoc. 9:303-319

374 Buzdygon KJ, Zydney AL. (1989). Effect of storage time on red blood cell membrane permeability to creatinine and uric acid. ASAIO Trans. 35:393-696

375 Langsdorf LJ, Zydney AL. (1993). Effect of uraemia on the membrane transport characteristics of red blood cells. Blood. 81:820-827

376 Ritschel WA. (1986) Binding of drug to biological material, In Handbook of basic Pharmacokinetics. 2rd ed. Illinois Hamilton Press pp:127-141

377 White HL, Rolf D. (1957). Whole body and tissue inulin and sucrose spaces in the rat. Am J Physiol. 188(1):151-155

378 White HL, Rolf D. (1956). Tissue distribution of sucrose and inulin in the rat. Am J Physiol. 185(2):152-156

379 Chio WL, Hsu FH. (1975). Pharmacokinetics of creatinine in man and its implications in the monitoring of renal function and in dosage regimen modifications in patients with renal insufficiency. J Clin Pharm. 15:427-434

380 Paganelli CV, Solomon AK. (1957). Unpublished data. Quoted in J Gen Physiol. 4:259-262

381 Pond SM, Tozer TT. (1984). First-pass elimination. Basic concepts and clinical consequences. Clin Pharmacokinet. 9:1-25

382 Oliver RE. (1995). Development of a whole-body physiological model based on dispersion concepts to describe the pharmacokinetics of drug in the body. PhD Thesis. Department of Pharmacy. The University of Manchester.

383 Hansch C, Schmmes PG, Taylor JB (Eds) (1990). Comprehensive medical chemistry. Vol. 6, Cumulative Subject Index and Drug Compendium. Pergamon Press, Oxford.

384 Mayer JM, Rowland M. (1984). Determination of aquous solubilities of a series of 5-ethyl-5-alkylbarbituric acids and their correlation with LogP and melting points. Drug Dev Ind Pharm. 10:69-83